INCORPORATION OF BIO-BASED MOLECULES IN SILICONES THROUGH MICHAEL ADDITIONS

By GUANHUA LU H.B.Sc

McMaster University DOCTOR OF PHILOSOPHY (2023) Hamilton, Ontario

Chemistry

TITLE: Incorporation of Bio-Based Molecules in Silicones Through Michael Additions

AUTHOR: Guanhua Lu H.B.Sc (McMaster University)

SUPERVISOR: Professor Michael A. Brook.

NUMBER of Pages: xx, 212

Abstract

Silicone stands as an indispensable material for numerous applications; however, its high energy-cost synthesis poses significant environmental challenges. To address these concerns, bio-based silicone has gained considerable attention, showcasing its potential to dilute energy density while offering inherent functional benefits. Despite promising prospects, existing incorporation methods often involve protecting groups, rare metal catalysts, and multistep synthesis, which contradict green chemistry principles. The aza-Michael reaction emerges as a superior choice due to its high atom economy and mild reaction conditions. However, it still suffers from prolonged reaction times, hindering its overall efficiency and sustainability. This thesis utilizes self-activated beta-hydroxy acrylates to greatly enhance aza-Michael kinetics, achieving a 3-fold rate enhancement in solvent-free silicone synthesis. This fast aza-Michael reaction acts as the platform for the incorporation of Vitamin C and amino acids into silicone materials. Vitamin C-modified silicone demonstrates the potential for controlled antioxidant activity release, while amino acid-functionalized silicones are synthesized using choline amino acid ionic liquids, presenting a protecting-group-free and solvent-free synthesis method. Moreover, the synthesized choline amino acid-functional polymers and elastomers are investigated for their dielectric properties revealing promising potential for dielectric elastomer actuator applications. These innovative methods offer green alternatives for incorporating hydrophilic biomolecules into hydrophobic silicone systems, providing new functionalities that address both environmental and functional requirements.

Acknowledgement

My PhD journey is a few years of time that I grew academically, but far more important I grow as a person, gaining understand of what it means to be a researcher, an educator, and a human. Through this journey, far most I would like to thank Mike for his example of a researcher I want to become. His great passion for science and curiosity has undoubtedly affected me. His patience and understanding for students also show he is a mentor for the growth of young minds. I would also like to thank Anne for making my PhD placement a truly life altering event, and I have learned so much with the help of Luna as well. I have been in McMaster for a long time, and there are many people influenced my growth. I would like to thank Bob, Hilary, and Megan for their support during my time working in NMR facility, that was a truly happy time and a highlight of my career. I would like to thank my lovely group members, especially Dan for his constant support as the backbone of the lab, Akop for being not only a lifelong friend but also mentor to my Chemistry career. Cody for his constant companion and true friend in many many times of needs, also had to mention the symbol of our friendship – cross-the-street. Miguel, Sijia, Mengchen and Shuai had been my role model throughout their time in the group. And the rest of my current lovely peers, all the care, laughter, and anxious times. The memories made with all of you are invaluable.

To my beloved partner Zilin:

I am grateful for the steps I took arriving here.

Meeting you made everything make sense.

You guided me in this maze of life.

至父母:

你们给予我的信任是我成长到今日最重要的东西。
谢谢你们让我在他乡没有漂泊的感觉，
谢谢你们一直以来的爱，使我无所畏惧。
望我可以回报千分之一的恩情。

Declaration of Academic Achievement

Published Manuscript

6. Tamim, K.; Gale, C.; Silverthorne, K.; Lu, G.; Lao, C.; Brook, M. A. *ACS Sustain. Chem. Eng.* 2023, 11 (18), 7062–7071.
5 Khattak, H.; Lu, G.; Brook, M.A, Dalnoki-Veress, K. *Eur Phys J E.* 2023, 46 (5), 33.
4. Lu, G.; Yepremyen, A.; Tamim, K.; Chen, Y.; Brook, M. A. *Polymers* 2022, *14* (22), 5040.
3. Brook, M. A.; Yepremyan, A.; Lu, G.; Melendez-Zamudio, M.; Hrabowyj, D. J.; Gale, C. B. *Green Chem*. 2022, *24* (22), 8751-8759.
2. Lu, G.; Yepremyan, A.; Godfrey, S.; Mohr, C.; Herrlein, M.; Brook, M. A. *J. Polym. Sci.* 2021, *59* (17), 1935-1941.
1. Lu, G.; Schneider, A. F.; Vanderpol, M.; Lu, E. K.; Wong, M. Y.; Brook, M. A. *Ind. Eng. Chem. Res.* 2021, *60* (42), 15019-15026.

Submitted Manuscript or Manuscript in Preparation

2. Lu, G; Li, L; Ladegaard Skov, A; Brook, M.A. Cholinium Amino Acid Ionic Liquid Grafted Silicone for Dielectric Elastomer Actuator Applications.
(Manuscript in preparation)
1. Lu, G.; Brook, M. A. Protecting group-free modification of amino acids through the aza-Michael reaction and its utilization in amino acid-functionalized polymer synthesis. *Polym Chem.* 2023. (Submission ID: PY-ART-08-2023-000939)

Author Contributions

Chapter 2: The author was responsible for all experimental work. Akop Yepremyan contributed to manuscript preparation.

Chapter 3: The author was responsible for all experimental work.

Chapter 4. The author was responsible for all experimental work, Liyun Li and Anne Skov contributed to dielectric characterization strategy and support.

Chapter 5: The author was responsible for all experimental work. Akop Yepremyan contributed to synthetic strategy and experimental support.

Table of Contents

Table of Figures

Table of Tables

Chapter 1. Introduction

1.1 Silicone and Its Role in Sustainability

1.1.1 Introduction of Silicone and Its Applications

Silicone, as a common household material found in everyone's home, has a history that dates back many decades. Its development can be traced to the early 20th century, when J. F. Hyde and Frederick Stanley Kipping first discovered and studied this remarkable material.[1,2] The process of creating silicones involves transforming sand, a readily available resource, into a group of compounds with exceptional properties.

Silicone is normally a short form for polydimethylsiloxane (PDMS), the most common type of silicone, which consists of a Si-O backbone surrounded by a methyl group-rich shell. This unique structure is very different than any traditional carbon-based polymers, which gave it several unique characteristics. Firstly, the greasy methyl groups around the chain give the polymer hydrophobic properties, making it highly resistant to water, which allows it to be used in sealants. Secondly, the stable, and high energy Si-O bonds, as well as relatively low thermal conductivity make the polymers oxidation resistant; they can withstand extreme temperatures without deformation or degradation. This quality makes silicones an ideal choice for applications for kitchenware and thermal encapsulation.[1–3]

Beyond conventional uses, silicone has found its way into advanced applications. In the field of biomaterials, its overall hydrophobicity and stable structure and the fact it does not induce a significant foreign body response renders silicone to be considered biocompatible. Silicones are thus invaluable components for medical implants, such as breast implants, catheters and prosthetic devices and for topical wound dressings.[4–7] The

soft robotics field has also harnessed the dielectric properties of silicone, using it to create actuators that mimic natural movements. These soft robotic systems offer potential applications in disparate fields such as artificial muscles and energy harvesting.[8–14]

1.1.2 The Preparation of Silicones

To synthesize the useful silicone elastomers from sand, a few necessary steps need to happen. Sand is first purified and heated with a reducing agent to approximately 1800 ℃ to convert it into pure silicon metal. Conversion of the silicon in the presence of methyl chloride and catalysts – the Direct Process - generates chloromethylsilanes. After extensive distillation to separate chlorosilanes that could become: chain termini, chain extenders, and crosslink sites, SiO bonds are introduced through the addition of water. Linear and cyclic siloxanes can be synthesized to include different functionalities including Si-Cl, Si-OH, Si-H, Si-$CHCH_2$, Si-OCH_3, to name a few.[1–3] These polymers can then be converted to elastomers using well-established industrial processes and, increasingly, to more advanced organic chemistry approaches. These methods enable the creation of silicone products with tailored properties, serving diverse applications across industries including construction, manufacturing, and biomedical fields.[1,15–19]

One widely employed industrial method for silicone synthesis is room-temperature vulcanization (RTV) curing using a tin catalyst. In this process, a condensation type of reaction occurs between silanol functional siloxane and alkoxysilanes, in the presence of tin-based catalysts and water, resulting in the formation of a three-dimensional network. This method is commonly used in the production of silicone sealants, where the cured silicone provides excellent adhesion and flexibility, making it suitable for various

construction and industrial applications (Figure 1.1B).[1,20,21] Hydrosilylation using Karstedt's catalyst is another prominent crosslinking process in research and industry. The platinum-based Karstedt's catalyst facilitates the reaction between a vinyl-terminated silicone and a hydrosilane, leading to the formation of cross-linked silicones (Figure 1.1C). This method is widely used in the production of silicone-based rubber products, such as gaskets, O-rings, and medical devices, as well as the curing method for Sylgard which is widely used in different fields of research involves PDMS. [1,22,23]

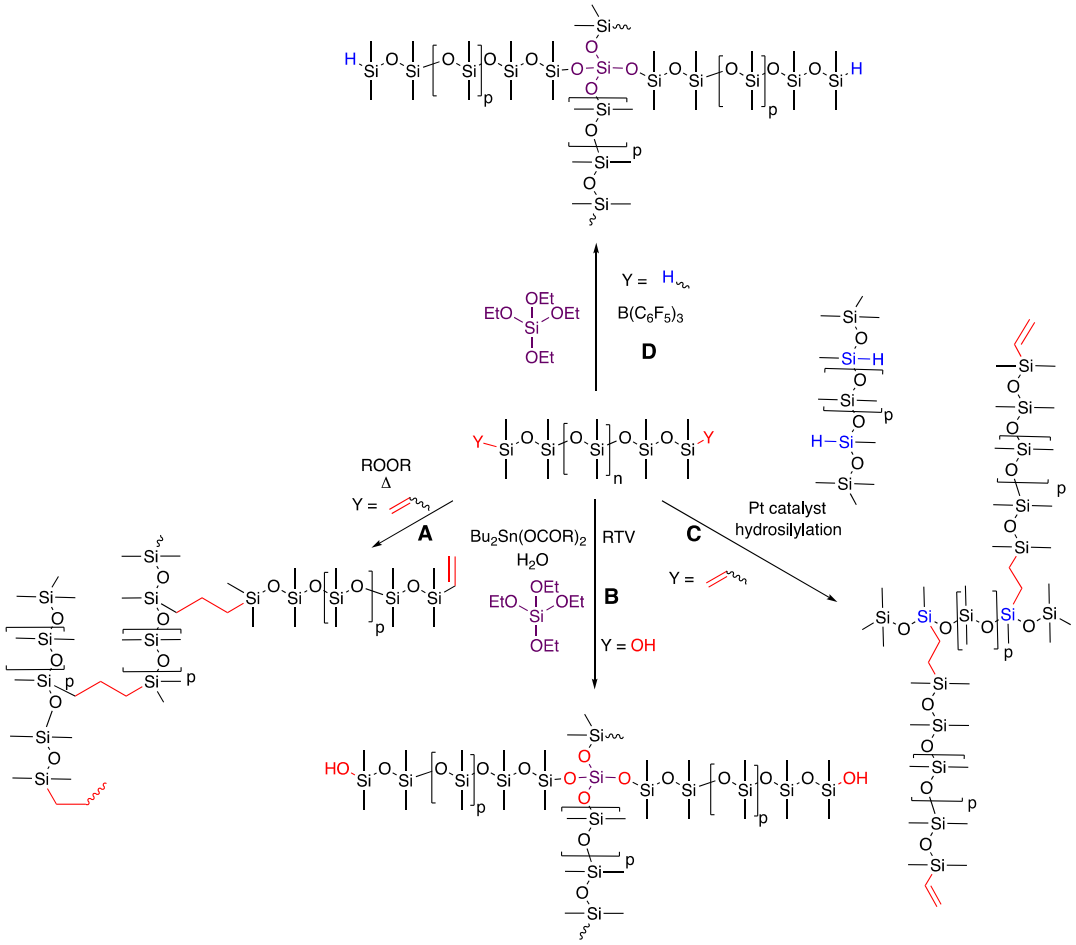

Figure 1.1. Preparation methods of silicone elastomers.

Beyond industrial methods, many other organic chemistry methods are also utilized for the modification and crosslinking of silicone to provide it higher functionality and enables more engineerability. One such method is the Piers-Rubinsztajn (PR) reaction, which utilizes tris(pentafluorophenyl)borane catalyst. This reaction involves the reaction of a silane with a silanol or alkoxysilane compound, resulting in the formation of a silicone polymer or crosslinked network (Figure 1.1D). Although less common in industrial processes, the PR reaction offers unique possibilities for tailored, structurally complex functional silicones and elastomers.[24–30]

A plethora of different common organic chemistry methods are also used for silicone polymer synthesis and crosslinking that provide different synthetic advantages and added properties. A few popular choices are, Schiff base reactions,[31] thiol-ene chemistry,[32,33] and aza-Michael additions (Figure 1.2).[34] These organic processes can occur faster than most traditional silicone curing with processes. Selected applications include hair cosmetics, underwater sealants, and dynamic (optionally thermoplastic) elastomers.[31,33,35–40]

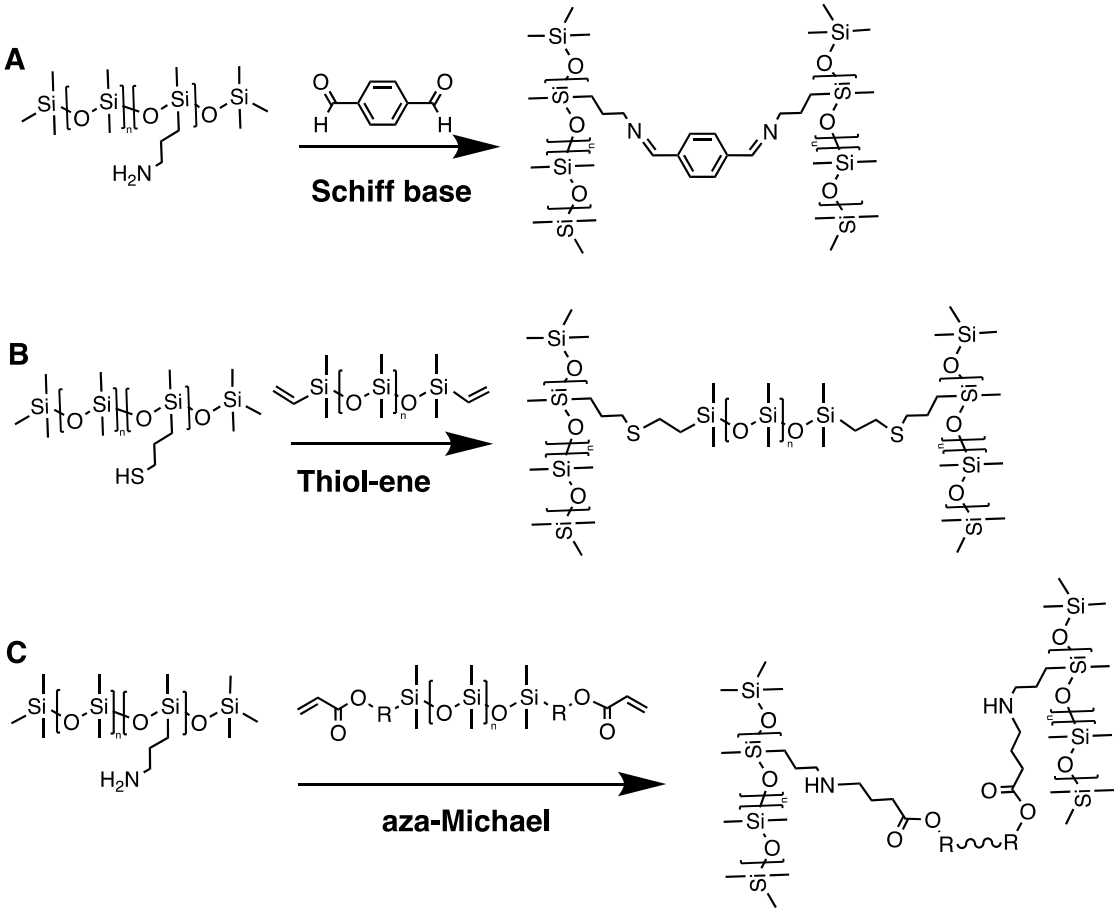

Figure 1.2. Common organic chemistry used for silicone crosslinking. A) Schiff base reaction, B) Thiol-ene reaction, C) aza-Michael reaction.

1.1.3 Introduction of Green Chemistry in Materials

With increasing concern about climate change driven by fossil fuel consumption, and environmental concerns about the accumulation of plastic waste, among others, there is a new momentum towards designing green synthetic routes that lead to sustainable materials. As seen in the previous section, silicones are widely used in the world across many different fields. While the synthetic design for silicone elastomers traditionally focused on the convenience of cure and extracting economic value from the product, the

synthesis strategies and material designs neglected many aspects of Green Chemistry. Green Chemistry refers to the practice of designing chemical processes and products in a way that minimizes their negative impact on human health and the environment. At its core are the 12 principles of Green Chemistry proposed by Paul Anastas and John Warner in the 1990s, which provide a framework for incorporating sustainability into chemical design.[41] These principles emphasize concepts such as waste prevention, renewable feedstocks, and energy efficiency. The original literature on the 12 principles, along with the broader concept of a circular economy, has shaped the way new generation materials are synthesized. It has prompted researchers and industry professionals to consider the environmental implications of their material design choices and strive for more sustainable alternatives.[42–45]

One of the most important concepts of sustainable material is to design for degradation, ensuring that at the end of the material lifecycle, at end of use, they can be safely and efficiently broken down into environmentally benign waste products. A viable alternative is to encode the ability to recycle or reuse the starting materials to achieve "complete the circle" goal.[46,47] Another major research front is how to best utilize natural feedstocks, which means the use of renewable resources as alternatives to finite fossil fuel-based materials. This shift towards bio-based feedstocks has led to the development of materials derived from plant-based sources, animal-based sources, or waste byproducts, which not only eliminate the use of fossil fuel feedstocks per se, but also increase the efficiency of degradability of products in the environment.

Energy efficiency is another key aspect of green chemistry in material synthesis. By optimizing reaction conditions, minimizing energy-intensive steps, or diluting energy dense material with other feedstocks while retaining the properties of the final product, the overall energy consumption and environmental impact of material production can be reduced. Finally, by designing high atom economy synthesis methods and employing synthetic routes that avoid the use of multistep synthesis, solvents, and rare metal catalysts, one can minimize the waste generated and avoid using rare metals (as catalysts). These issues are particularly challenging in the preparation of advanced materials, including those used in healthcare where regulatory requirements dictate that few impurities may be present. The traditional multi-step syntheses and extensive purifications generate large amounts of waste, particularly solvents.[42–45]

1.1.4 Evaluating the Sustainability of Silicones Using These Principles

The sustainability of silicones is often compared to plastic products; however, the sustainability of silicone is not immediately obvious and needs to be evaluated through multiple factors including feedstocks, end of life products, energy efficiency and waste generation. Sand, the feedstock of silicone is consisted of two of the most abundant elements on earth, namely oxygen and silicon.[48] Thus, by definition, the use of this natural resource to which silicones are converted at end of life, is sustainable.[49–52]

One of the most troublesome aspects of silicone sustainability is the energy intensive process required silicone manufacturing. The high temperature required to convert sand to silicon is already problematic. Further processing to chlorosilanes and the extensive

distillation processes required separate starting materials make silicones a very energy dense material.[1,3,19]

The crosslinking methods used in silicone production must also be examined when considering sustainability. Often, rare metals like platinum or toxic catalysts based on tin are used to create silicone elastomers. Research efforts to explore alternative crosslinking methods that minimize reliance on both types of metals are required to to reduce the ecological footprint associated with silicone production.[53,54]

The degradation of silicone in the presence of acids or bases is quite efficient, but it is much slower under general environmental conditions. Depolymerization can take weeks of months, but complete degradation to sand, carbon dioxide and water, all of which are all environmentally benign, can take years.[55–58] It is also important to consider the limited existing recycling infrastructure for silicone elastomers. Commercial processes are in their infancy and are more complicated than those used for thermoplastics that can be thermally recycled (note that organic elastomers are likely much less degradable than silicone elastomers; examine automobile tires). In many cases, silicone elastomers used in small volumes will not be separated at end of life and will end up in landfills.[59,60]

Enhancing silicone recycling techniques will be one strategy to improve silicone sustainability, while a different strategy will involve improved spontaneous degradation in the environment even should then end up in landfills.

After carefully evaluating the sustainability of silicone in today's industry, a few important research fronts are noted. While being more sustainable than plastic in terms of a renewable feedstock and more environmentally benign at end-of-life, new crosslinking

methods that can avoid the use of rare or toxic metal catalysts, as well as improved recyclability of silicone must be developed. An additional strategy to mitigate the high energy density of silicones is to dilute them with new innovative silicone copolymers or fillers that draw from natural products; innovative methods are required to enhance the sustainability of silicone.

1.2 Bio-based Molecules in Sustainable Silicone Material

1.2.1 Overview of Natural Feedstocks Used in Material Research

As environmental issues surge in the today's world, the importance of exploring bio-based materials and polymers as a sustainable and functional alternative to traditional petroleum-derived materials is becoming increasingly evident. Extensive research is being conducted in this area, evident from the growing number of studies and publications exploring renewable biomass resources.[61–68] The utilization of natural feedstocks as constituents in materials has proven effective in reducing their carbon footprint and environmental impact. Studies demonstrate that bio-based materials and bioenergy have significantly lower greenhouse gas emissions compared to their fossil fuel-based counterparts; every metric ton of bio-based materials that replaces petroleum saves 55 ± 34 gigajoules of energy and 3 ± 1ton CO_2 equivalents of greenhouse gas.[64,66,69,70]

While it is important to utilize bio-based compounds to improve sustainability, there is always the challenge of making sure the newly developed bio-based materials match the existing industrial material's performance and properties. To bridge the gap between innovative sustainable materials and practical/ economical value, it will be necessary to

guarantee access to reliable sources of natural feedstocks and utilize more efficient chemistry. From a practical perspective, one must design for functionality using processes that balance the cost of preparation with the intrinsic economical value of the material. This includes optimization of synthetic strategy to minimize energy cost, multistep syntheses, and waste generation, conducting thorough performance characterizations of the materials to gain a comprehensive understanding of their properties and functionality, and finally demonstrating realistic end-of-life options for bio-based materials. All of these are essential to the creation of a viable closed-loop system that makes the utilization of sustainable material more feasible.[64,69,70]

When selecting bio-based compounds for incorporation into bio-based materials, several key factors must be carefully considered to ensure sustainability and functionality. Firstly, the availability and cost of the bio-based compound are critical aspects that influence the feasibility of large-scale production and commercialization.[71–76] Secondly, degradability plays a crucial role in the life cycle of bio-based materials. For instance, esters containing soybean oil-based materials can be easily depolymerized under controlled conditions, allow them to reduce the environmental impact.[77–81] Finally, inherent functionality is essential for achieving specific properties or functionalities in bio-based materials. As an example, incorporating bio-based antioxidants like vitamins or phenols into polymers enhances their resistance to oxidation and provides it antimicrobial properties in certain cases. Such materials may be them suitable for food packaging.[82–86] More sophisticated compounds where peptides are grafted to synthetic materials may deliver biological functionality, making them suitable for biomedical applications. Considerations of these

factors during the material design process ensures the development of sustainable and high-performance bio-based materials with diverse applications across various industries.

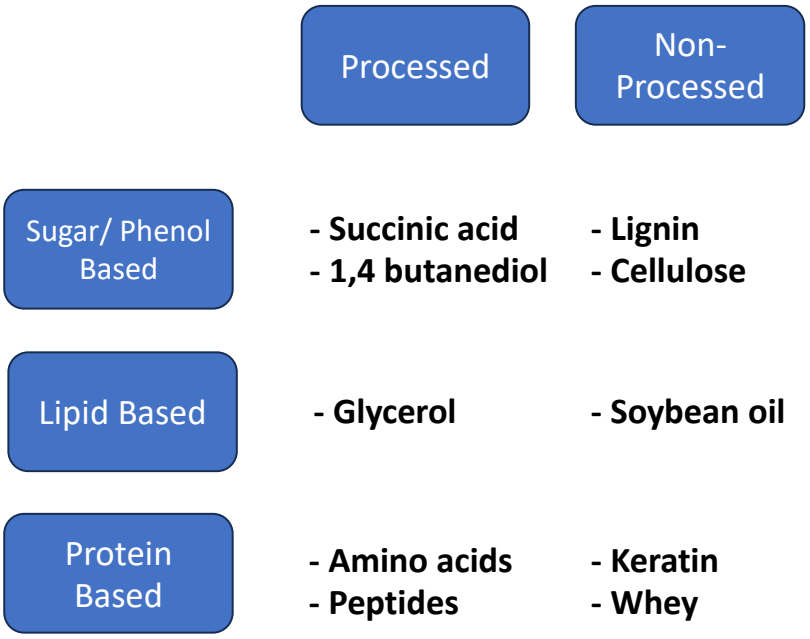

Figure 1.3. Scheme for Bio-mass classification.

Bio-based polymers can be classified in various ways, considering the processing methods employed and the sources of biomass used. One classification is based on the utilization of non-processed biomass,[72,74,87–89] as well as processed biomass to obtain monomers that replace fossil fuel-based polymers. (Figure 1.3)

The direct use of non-processed biomass, such as lignin from plant biomass or waste agricultural products, are favorable choices due to their cost-effectiveness and reduced environmental impact. These types of materials serve as an eco-friendly fillers or structural copolymer for bioplastics or materials, effectively diluting the energy density of other material. However, non-processed biomass may contain impurities, affecting the overall material properties and consistency, particularly over different growing seasons or

when sourced from different parts of the planet. On the other hand, processed biomass extracts, obtained as by-products of biomass processing, offer greater control and design flexibility. Instead of being generated from petroleum, monomers like ethylene glycol (EG), terephthalic acid (TPA), 1,4-butanediol (BD), succinic acid (SA), and 2,5-furandicarboxylic acid (FDCA) can be derived from processed biomass to create bio-based polymers (the Biorefinery).[90–98] This approach has the potential to allow one to maintain the use of traditional polymer structures while utilizing renewable starting materials. While their processing is accompanied by a higher cost, it can ensure the original polymer properties are met and more consistently matched. Despite the advantages and disadvantages, both approaches play a vital role in the sustainable materials research, offering a versatile array of options to material design. [64,99]

The source of natural compounds is also a way to classify bio-based materials. (Figure 1.3) In addition to lignocellulosic biomass described above, [72,74,87–89,100,101] lipids from plant or microbial sources have gained attention for their potential in bio-based polymers. Lipids, including waste biomass like soybean oil and other vegetable oils, can be used in processed or non-processed form, can be converted into monomers like glycerol, which can then be used in the production of bio-based polyesters or polyurethanes,[102,103] or applications including food packaging, coatings, and adhesives.[78,80,104–106] Animal-based, non-processed sources such as proteins and keratin, also are abundant and are used in bioplastics and fillers.[107–110] Fine processed or synthetic peptides are used in more advanced applications like biomaterial or regenerative medicine.[111–115]

1.2.2 Bio-based Silicones

Silicones require a lot of energy for their production, as discussed in a previous section. The incorporation of bio-based compounds to silicone can dilute its environmental impact, provided that the properties of the diluted material match those of the pure silicone. The wide use of silicone in biomedical fields, as well as many other industries including the food industry, and as sealants, and coatings, can benefit from some of properties bio-based compounds provide including antioxidant, anti-microbial, anti-fouling, and overall increased degradability.[116–122] One must, however, ensure that undesirable biological properties are not introduced.

The incorporation of bio-based molecules into silicone involves a wide range of compounds derived from different biomass sources. These sources include what is widely used in other types of material like lignocellulose compounds, lipid-based compounds and protein-based compounds, as well as antioxidants like eugenol and tannins.[119–127]

Depending on the class of bio-based compound and the targeted properties, three key strategies are used to incorporate them into silicone: utilizing them as natural fillers and reinforcements, as co-polymers, and for surface modification to enhance their functional properties.

Lignocellulose compounds, like softwood lignin, have been utilized as both crosslinkers and reinforcing agents in silicone elastomers. This approach has resulted in materials with good mechanical properties, solvent resistance, and high-temperature stability. Moreover, lignin can be used to create silicone foams that can act as a flame retardant in specific applications.[128–131] Microcellulose, when used as a reinforcing agent in silicone

elastomers, enhances their mechanical and thermal properties.[132] Additionally, cellulose when covalently incorporated into silicone, improves surface properties and dielectric properties.[133] These examples demonstrate the potential of lignocellulose compounds in advanced silicone materials for various applications.

Starch, another sugar-based compound, has been incorporated into silicone elastomers and foams up to 50% to increase its natural contents making it more sustainable. In another case, with clever synthetic design, highly controlled worm-like nanotubes with tunable porosity were synthesized. This approach provides a pathway to produce silicone-based materials with desirable properties for specific applications.[134,135]

Sugars, being highly versatile biomolecules, have found diverse applications in silicone systems. Energy-dissipating polymeric silicone surfactants have been developed, resulting in gluconamidosilicones with shear thickening properties. Another approach involves using naturally derived silicone surfactants based on saccharides and cysteamine. Moreover, saccharides can be utilized for both crosslinking and reinforcement in silicones through boric acid-sugar interactions. Although a smaller percentage of sugar is incorporated into silicone compared with starch or lignocellulose compounds, simple saccharides can provide material with more controlled functionalities. [136–138]

Phenols and antioxidants like tannins and eugenol have been utilized for their innate antioxidant activity and potential anti-microbial activity, which is relevant for many silicone applications like antimicrobial coatings. Eugenol, a natural compound in essential oils, is highly functional and has been extensively utilized for its antioxidant activity. It is

incorporated into dynamic materials with disulfide bridges, used for 3D printing with acrylates, and plays a role in robust water-absorbing polyurethane copolymers.[119–127] Soybean oil, as a lipid-based widely available bio-based compound, has been employed as copolymer into silicone at high percentages as natural filler, as well as produce flame retardant coatings and foams.[139–142]

Proteinaceous molecules like peptides are usually incorporated into silicone through physical absorption or surface grafting, with few cases of direct synthesis methods. Usually, only a small percentage of protein is incorporated, with the focus being on peptide's innate biological functionality that needs to reside at an interface, like enhanced fibroblast adhesion, anti-microbial and anti-fouling. These materials are particularly attractive for biomedical applications such as catheters.[143–154] One exception to this trend it keratin, which is widely available protein found in hair or wool, and has proven effective as a physical filler and reinforcing agent in silicone systems. This application improves the mechanical properties of the materials, and when used in combination with ionic liquids, it enhances pressure sensing capabilities.[155,156] Amino acids would be interesting constituents of silicones, but there is a lack of a general incorporation method; a few early examples exist with carefully designed chemistry, or the exception provided by lysine, which is highly reactive due to the extra amine functional group which leads to a surfactant in a recent study.[157]

The incorporation of diverse bio-based compounds into silicone systems offers a promising pathway to develop sustainable materials with enhanced properties for various applications. By utilizing biobased molecules, the environmental impact of materials can

be diluted, fostering eco-friendly alternatives with reduced carbon footprint. Moreover, integrating different functional molecules into bio-based silicone materials unlocks advanced functionalities for soft robotics, biomedical devices, and more. To fully exploit the potential of bio-based silicone, research must focus on advanced functionality, as well as energy-efficient and sustainable synthetic methodologies. The synergy of sustainability and advanced functionality will allow bio-based silicone materials to move towards commercial viability and a greener future.

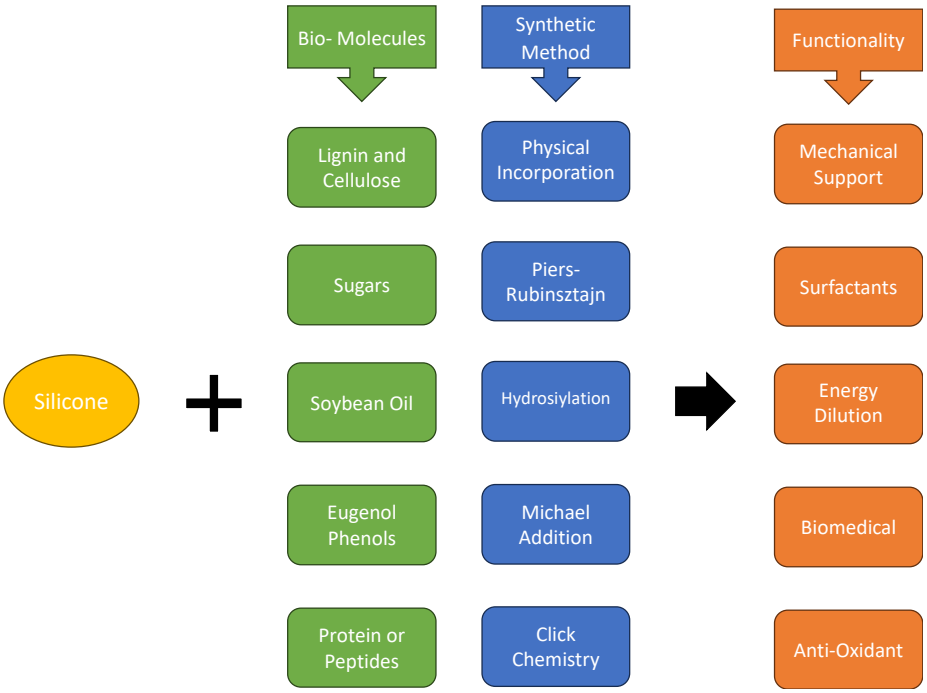

Figure 1.4. Scheme showing types of biomolecules incorporated into silicone, common synthetic methods, and target functions of bio-based silicone.

1.3 Synthetic Strategies of Bio-based Silicone

1.3.1 Synthetic Challenges

Bio-based silicone materials have demonstrated immense potential and significance in various applications, owing to their unique properties and sustainable nature. However, the complex functional groups inherent in bio-based molecules present synthetic challenges. To overcome these difficulties and fully exploit the advantages of bio-based silicone, a wide variety of methodologies have been employed (Figure 1.4). This section provides an overview of synthetic challenges of incorporation of bio-based molecules into silicone and the diverse methodologies currently being used, as well as highlights the importance of innovative approaches to further advance this promising field.

1.3.2 Overview and Classification of Synthesis Strategies

Incorporating bio-based compounds into polymer systems, particularly in silicone-based systems, presents significant synthetic challenges, with hydrophobicity being a key obstacle. Silicone materials are inherently hydrophobic, making it difficult to achieve effective dispersion/dissolution in media that are compatibility with many bio-based compounds, which often exhibit hydrophilic characteristics. This difference in polarity leads to phase separation and poor interfacial interactions, hindering the homogenous distribution of bio-based compounds within the silicone matrix.

Overcoming these challenges requires a careful selection of more compatible biomolecules, efficient chemistry, or innovative approaches, such as designing chemistry “at the interface” of silicones to make them more hydrophilic, or functionalization of bio-based compounds to make them more hydrophobic, and the development of novel

reactive coupling agents.[119,124,127,131,139,155] With respect to the synthetic sequence, it can be broadly categorized into grafting or post-polymerization modifications, and direct synthesis or monomer modification approaches.(Figure 1.5) In grafting, biomolecules are attached to pre-formed polymers or functional polymers. Direct synthesis entails the incorporation of biomolecules during or after the polymerization process. While direct synthesis and monomer modification allow for the creation of highly functional biomolecule-polymer hybrids, it limits one to smaller molecules and it can be difficult to reach high molar mass polymers.[151] Grafting or post-polymerization modification provides flexibility in tailoring existing polymers with biomolecules. Although this approach provides less control, it provides a simpler synthesis strategy and often avoids extensive purification and processing. In this section, a few direct synthesis examples will be provided, with a focus on current post-polymerization methods.

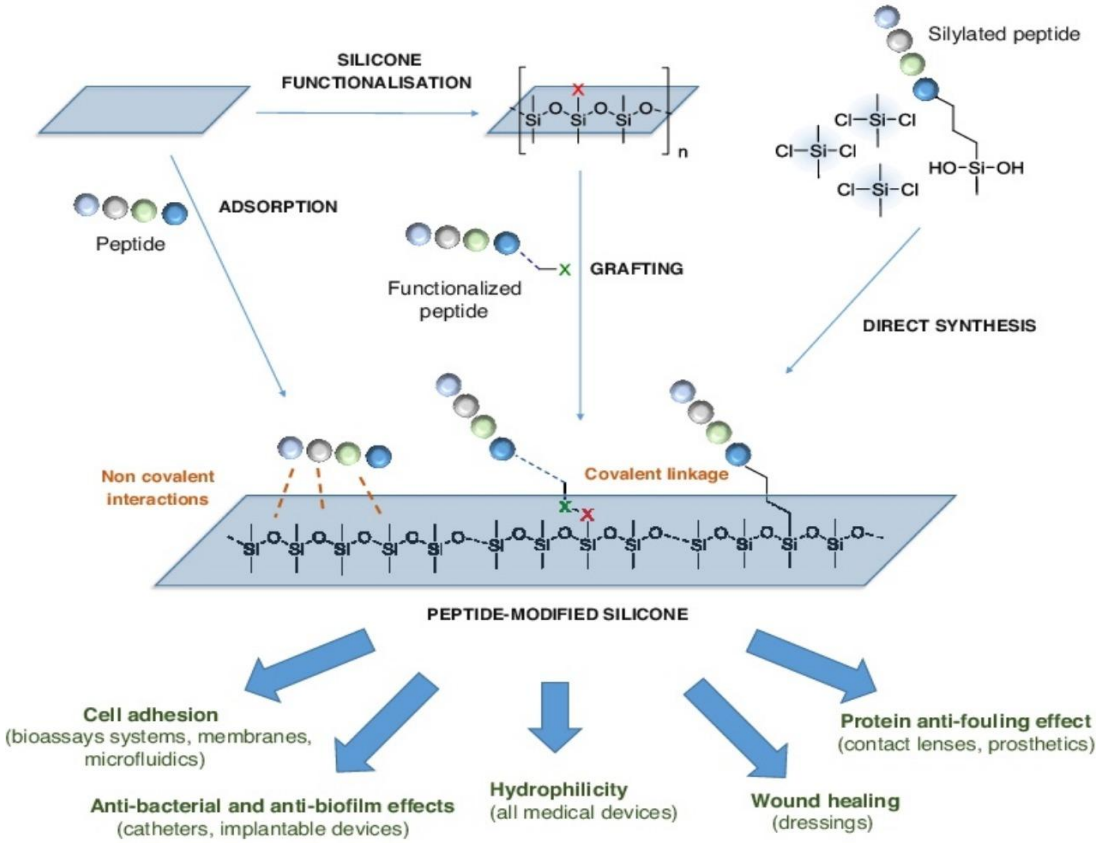

Figure 1.5. Showing different ways of grafting peptides onto silicone, demonstrating physical absorption, grating, and direct synthesis methods (adapted from Martin et al.).[151]

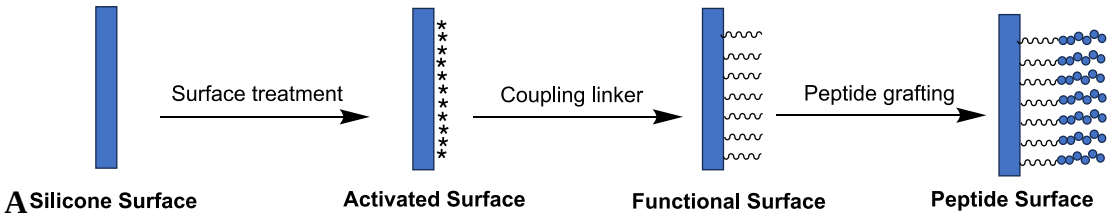

B

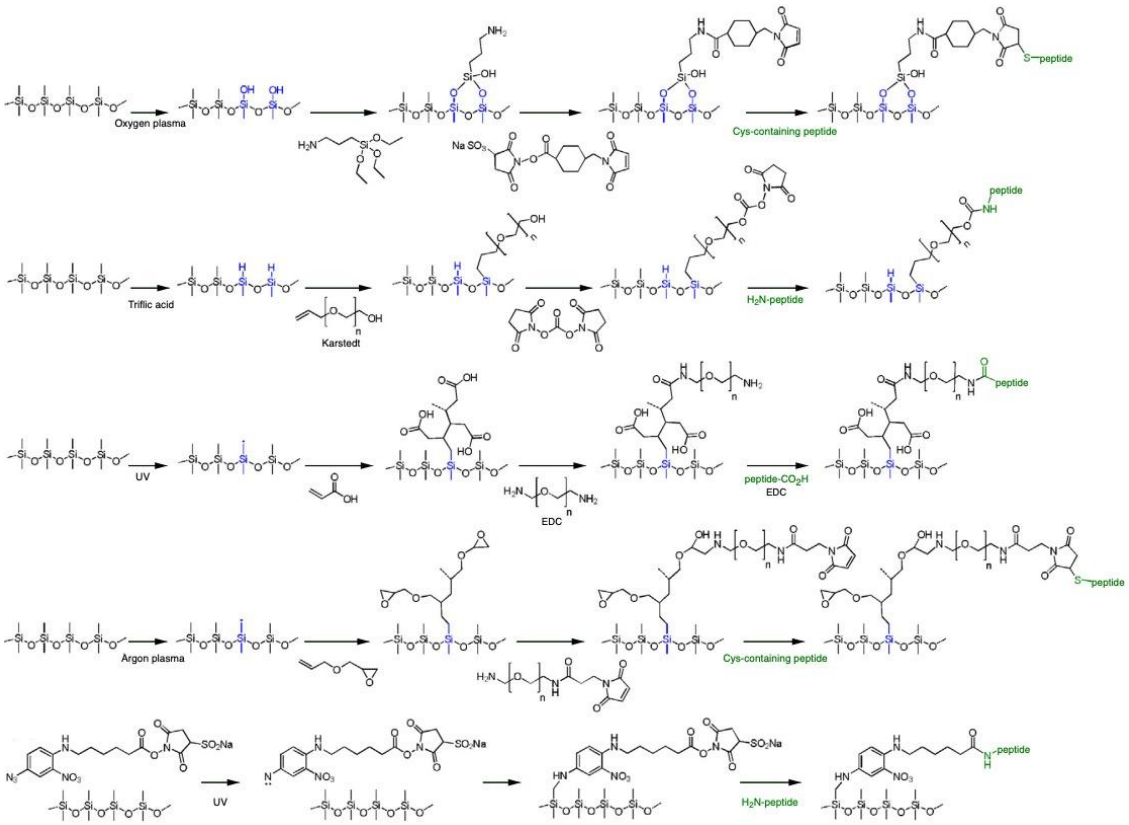

Figure 1.6. A) General scheme for peptide grafting strategy. B) Examples of the different grafting strategy (adapted from Martin et al.).[151]

1.3.3 Physical Incorporation

In the quest for bio-based silicone synthesis, various methodologies are explored, each offering unique advantages and challenges. The physical incorporation approach involves reinforcing bio-based silicone with natural biomolecules like keratin and microcellulose,

utilizing their inherent structural properties to enhance material mechanical performance. Additionally, clever designs utilizing supramolecular interactions also can enable elastomer formation through physical mixing. Di-, tri- and polyphenols can act as non-covalent crosslinkers for aminosilicone through ionic and hydrogen bonding interactions. The resulting silicone elastomers have great mechanical and antioxidant properties. Boronic acid-modified silicones can form complexes with sugars via hydrogen bonding, which also enabled supramolecular crosslinking with tunable properties.[131,132,155,156]

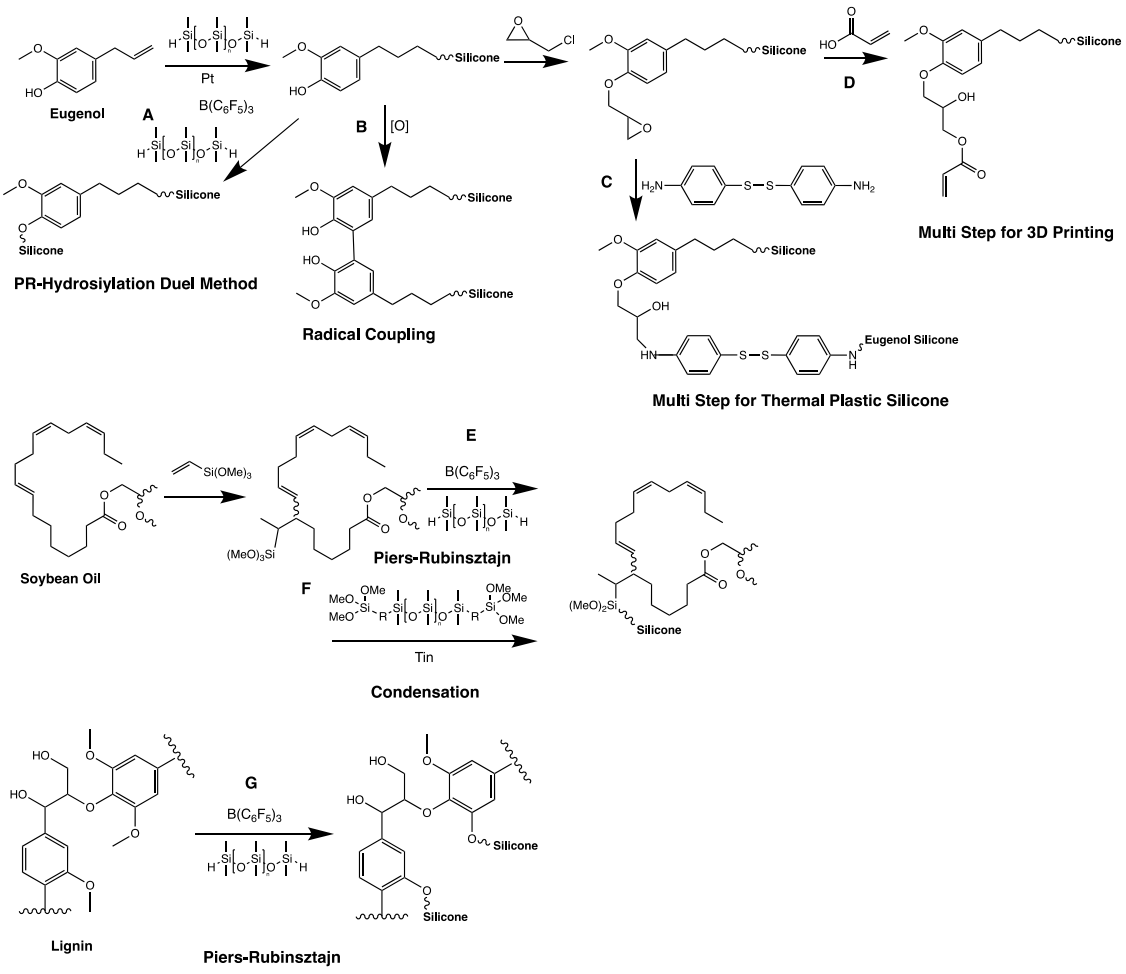

Figure 1.7. Traditional synthetic methods for incorporation of eugenol, soybean oil and

lignin in silicone system. A) Incorporation of eugenol as a duel crosslinker using hydrosilylation and the Piers-Rubinsztajn reaction. B) Incorporation of eugenol through first hydrosilylation followed by phenolic radical coupling, while preserving antioxidant activity. C) Multistep synthesis consisted of hydrosilylation, epoxy functionalization and disulfide functionalization, used for eugenol based thermal plastic silicone. D) Multistep synthesis consisted of hydrosilylation, epoxy functionalization and acrylate functionalization, used for eugenol-based 3D printing applications. E) Incorporation of soybean oil using Piers-Rubinsztajn reaction for foam synthesis. F) Incorporation of soybean oil using RTV condensation reactions. G) Incorporation of lignin through the Piers-Rubinsztajn reaction.

1.3.4 Traditional Silicone Chemistry

Traditional silicone chemistry, including condensation reactions, can be used to synthesize bio-based silicone. For instance, silylated soybean oil can be incorporated into silicone systems by reacting with hydroxy functional silicone in the presence of a tin catalyst (Figure 1.7E).[141] Another traditional method is the PR reaction, which has found application in incorporating lignin and starch, respectively, into silicone. Despite lignin's relatively lower compatibility with silicone, it serves as a valuable crosslinker and filler, while PR reactions offer a great option for foam synthesis, albeit with hydrogen and methane gas generation as by-products to consider (Figure 1.7G).[128–131,134,135] Soybean oil is also incorporated in silicone through PR in similar fashion to form silicone foam or elastomers when first compatibilized with alkoxysilane, then reacting with hydride silicones (Figure 1.7F). [27] Hydrosilylation, the most widely used reaction for silicone

polymer synthesis, is often used to create intermediate molecules for bio-based silicones through hydride siloxanes and vinyl compounds. For instance among many peptide grafting method reviewed by Martin et al.,[151] hydrosilylation has been used in grafting peptides as coupling bridges by adding allyl poly ethylene glycol to triflic acid-treated silicone surface in order to create surfaces for further functionalization (Figure 1.7B).[158–162] Eugenol is a special case, at it possesses a vinyl group and can undergo hydrosilylation directly. Eugenol also possesses a phenol group that, in combination with hydrosilylation, can be used to install highly reactive groups like epoxy that, in turn, allow incorporation of additional functional groups like sulfide groups. These products have been used for their dynamic behavior, and for 3D printing, respectively. Note that blocking the phenolic group in these latter examples hinders the antioxidant activity. In order to utilize the antioxidant properties of eugenol, phenolic coupling processes of eugenol have been developed, preserving the antioxidant activity while enabling the crosslinking of the material (Figure 1.7A-D).[119–121,123–127]

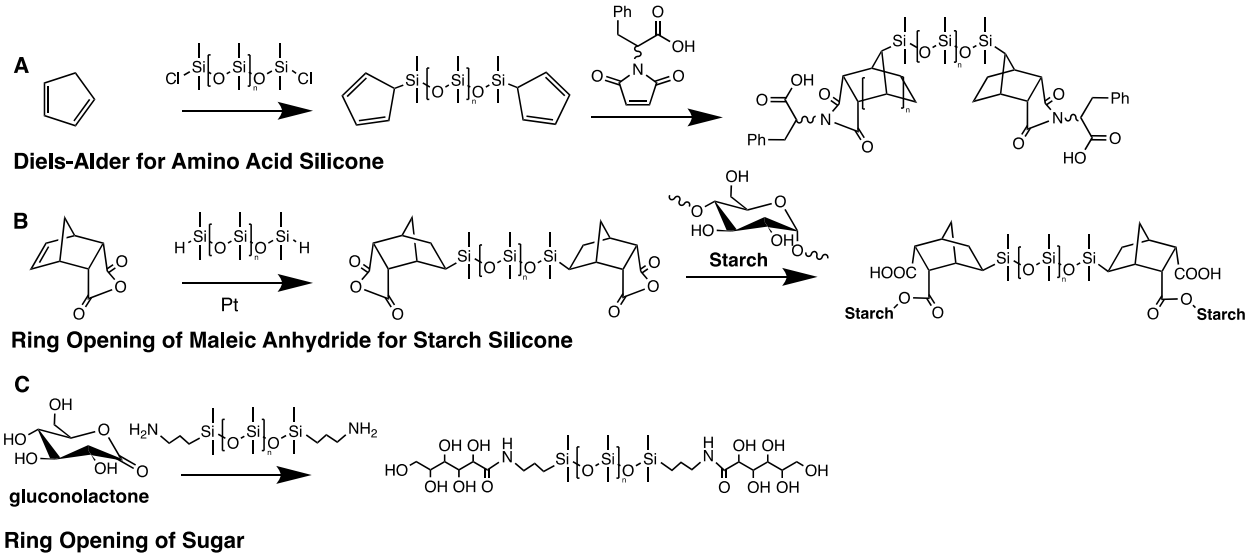

Figure 1.8. Click Chemistry used for incorporation of A) amino acid through Diels-Alder using di-ene functionalized silicone and maleimide functional amino acids, B) Starch through anhydride ring opening using maleic anhydride functional silicone, C) Sugar through lactone ring opening using amino silicone.

1.3.5 Click Chemistry

Moving beyond traditional silicone chemistry, innovative and sustainable click reactions are attractive in the bio-based silicone synthesis field. Click reactions, including ring-opening reactions and the Diels-Alder, are favored for their high atom economy, which promotes greener and more sustainable synthesis. For example, the Diels-Alder reaction can be employed for the direct synthesis of amino acid or peptide functional silicone (Figure 1.8A).[144] Other reactions, for instance, anhydride ring-opening reactions facilitate the incorporation of starch into silicone by pre-functionalizing silicone with malic anhydride also follow this concept (Figure 1.8B),[134,135] as does the reaction between sugar and amino silicone leads to amide linkages through a sugar lactone ring-opening reaction,

yielding mono or disaccharide-functional silicones suitable for energy dissipation and surfactant use (Figure 1.8C).[137,138] Epoxy opening is a versatile approach to polymer modification and is widely used to introduce various functional groups with oxygen or amine nucleophiles, such as linkers for peptide functionalization through lysine ring opening.[123,125,143,145,146,150–154] Michael addition is another powerful reaction that is gaining significant attention for the incorporation of bio-based molecules into silicone in recent years, and it is also the focus of this thesis, therefore will be discussed in more detail in the next section.

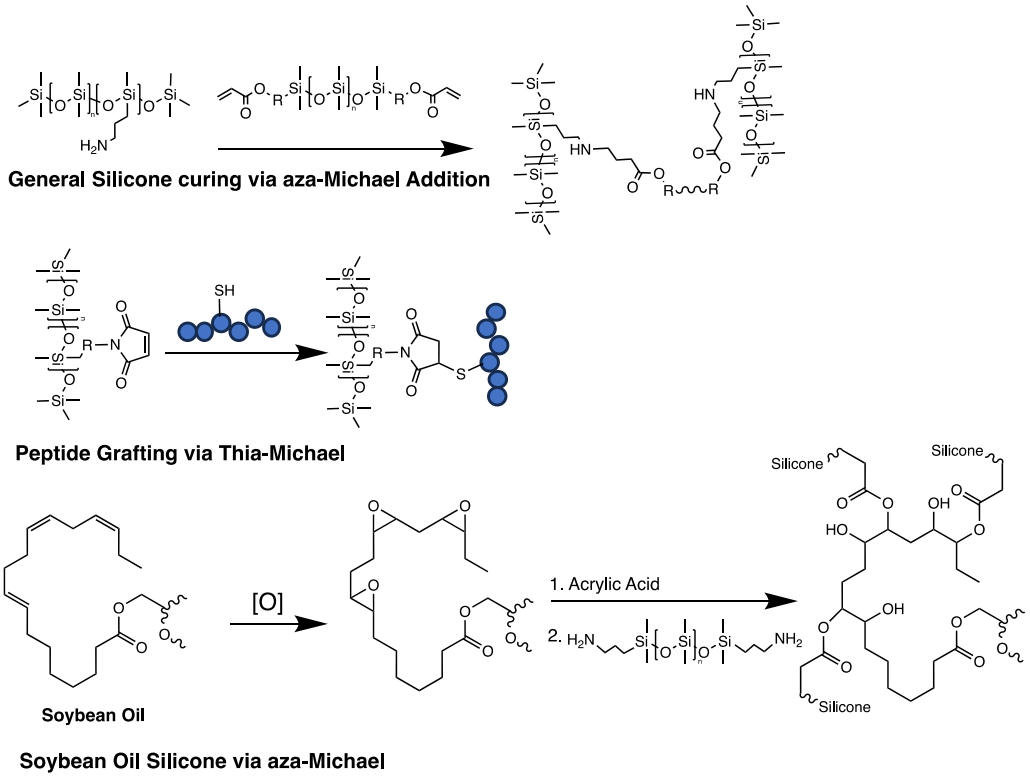

Figure 1.9. Michael addition used in A) General silicone curing, B) Peptide grafting through maleimide functional silicone surface and cysteine on peptide chain through thia Michael reaction, C) Incorporation of soybean oil into silicone system through acrylated

soybean oil and amino silicone via aza-Michael addition.

1.3.6 Michael Additions Used in Silicone Materials

The Michael reaction holds significant promise as an alternative strategy for generating advanced silicone polymers and materials. The prototypical Michael reaction involves the addition of cuprates to a,b-unsaturated systems. These reactions have many compromises due to the metal per se and the solvents that are required. However, alternative Michael reactions involve addition of a soft nucleophile, typically an amine or thiol (Michael donor), and an electron-deficient alkene molecule (Michael acceptor) like acrylates; This reaction offers numerous advantages, including mild reaction conditions, high atom efficiency, compatibility with various reagents, and absence of toxic metal catalysts, aligning well with the principles of green chemistry. Moreover, the aza-Michael reaction fits the concept of "click chemistry" enabling the synthesis or modification of polymers in an environmentally friendly manner.[34,163,164]

In the context of bio-based silicone synthesis, most traditional chemistry methods involve metal-catalyzed reactions, which often suffer from drawbacks such as catalyst sensitivity to certain compounds (i.e., inhibition), the toxicity of catalysts also limit its use in some advanced biomedical applications. The aza-Michael reaction presents a promising alternative, and could be especially powerful for incorporating amino acids, peptides, and proteins due to the availability of amines and thiols present in these molecules. For example, the thia-Michael reaction, complementary to the aza-Michael reaction, allows the linkage of proteins or peptides to polymers through cysteine side chains and maleimide pre-functionalized silicones (Figure 1.9B).[143,145,146,149–154,157] Soybean oil is

also incorporated into silicone through acrylated soybean oils as discussed previously (Figure 1.9C). Although not in silicone, another strategy involves the aza-Michael addition enables the linking of other amine-containing molecules to amino acids modified with acryloyl chloride.[165] However, the zwitterionic nature of native amino acids presents challenges, as their poor solubility and reactivity towards acrylates without the use of protecting groups need to be addressed. Developing innovative strategies to overcome these limitations is crucial to fully exploit the potential of bio-based materials in silicone systems and advance the field of sustainable and functional materials.

The incorporation of bio-based compounds into silicone systems unlocks remarkable advantages, such as enhanced functionality and improved sustainability. However, the complexity of functional groups present in bio-based molecules poses challenges during the synthesis processes, like functional group compatibility and solvency (differences in hydrophobicity between silicone and natural material). Therefore, it is necessary to apply a diverse array of methodologies, ranging from physical mixing and supramolecular interactions to traditional silicone chemistry, click reactions and powerful Michael type reactions, employed to tackle these challenges, and exploit the full potential of bio-based silicone materials across various applications. In some cases, it has not yet been possible to avoid protecting groups, multistep functionalization, extensive purification, and long reaction times. However, for most of the work in this thesis, advancements in new and optimized chemistry are reported that facilitate sustainable bio-based material synthesis and making more advanced polymer design more feasible.

1.4 Thesis Objectives

1.4.1 Overview of Thesis

The main objective of this thesis was to develop sustainable synthetic strategies to incorporate bio-based molecules into silicone systems and explore the potential functionalities of the resulting bio-based silicone materials. This section aims to address two key themes of the thesis: firstly, innovations and mechanistic understanding of bio-based silicone synthetic methodologies that target solvent-free, catalyst-free, protection-free processes and more efficient chemistry, and, secondly expanding bio-based silicone libraries by incorporating vitamin C and amino acids into silicones and exploiting their antioxidant activity and dielectric actuator potential, respectively.

1.4.2 Methodology Improvement in Sustainability

Although there are many advantages to silicone synthesis through Michael addition, it often still requires long reaction times or elevated temperatures due to relatively poor kinetics, especially when paired with hydrophilic molecules.[34,163,164] To overcome this, protecting groups on bio-based molecules or multistep syntheses are required. In chapter 2 of this thesis, an accelerated aza-Michael reaction is introduced, where β-hydroxyalkyl acrylate ester-functionalized silicone were shown to exhibit significantly higher reactivities towards amine-containing compounds or polymers compared with simple acrylate silicones. After a thorough kinetic and mechanistic study, an acceleration mechanism was proposed that reflects the higher azaMichael silicone reaction rates under solvent free conditions. This finding serves as the basis synthetic strategy platform which is then utilized in all other chapters for improved reaction efficiency and compatibility.

Chapter 3 targets the development of efficient synthetic strategies to incorporate amino acids into silicone. Amino acids offer inherent biocompatibility, zwitterionic character, and diverse functional groups, making them attractive for various applications. However, their zwitterionic functionality also presents challenges during incorporation, often requiring the use of protecting groups to facilitate solubility and harsher reaction conditions, which undermines green chemistry principles.[166–169] The accelerated aza-Michael reaction described in chapter 2 was used in combination with cholinium amino acid ionic liquids (ChAAILs) to achieve solvent free and protecting group free synthetic conditions. This method has the potential to become a general method to incorporate any amino acid into silicones and, possibly, other (polymeric) materials. A kinetic study of aza-Michael reactions between ChAAILs and various acrylates demonstrated that different amino acids can be efficiently incorporated into hydrophilic and hydrophobic polymer systems, respectively.

These chapters paved the way for more the more efficient preparation of sustainable, and functional bio-based silicone materials, bridging the gap between sustainability and advanced functionality. The reduction in waste and energy cost by employing solvent free and protection group free conditions, coupled with the ability to introduce diverse functional groups, has laid a foundation for the development of more sustainable and versatile bio-based silicone materials.

1.4.3 Expand Bio-based Silicone Research

Chapter 4 explores the potential applications of ChAAIL functionalized polymers and elastomers synthesized in Chapter 3. One of the applications studied in detail is as

silicone dielectric elastomer actuators (DEAs). While silicones exhibit many desirable properties for DEAs such as high response rate, low viscous loss, and durability, its relatively lower dielectric permeability poses challenges in artificial muscle applications.[170–172] To address this, polar ChAAILs were incorporated into silicone networks and demonstrate potential both by increasing the dielectric permittivity of silicone DEAs, and also achieving controlled dielectric permittivity tunability, offering new prospects for soft-robotic applications. These findings provide valuable insights into the potential of ChAAILs as sustainable crosslinkers for ionic liquid-containing silicone actuators, leading to the development of advanced functional materials with enhanced properties.

Chapter 5 presents the synthesis of ascorbic acid-modified silicones through accelerated aza-Michael reactions. Although protecting groups were used for this synthesis due to the high functionality of ascorbic acid, the study focuses on exploring the antioxidant capacity provided by ascorbic acid. The introduction of an acrylate ester at C1 of ascorbic acid was achieved through benzyl protection of the vinyl alcohols, enabling beta hydroxy accelerated aza-Michael to generate elastomers with tunable modulus. Exposure to a reducing environment removes the benzyl ether protecting groups and releases antioxidant activity of the elastomers in a controlled manner. These pro-antioxidant elastomers demonstrate the potential of exploiting natural materials as co-constituents of silicone polymers, offering advanced functional properties for silicone materials. The successful integration of vitamin C into silicone matrices expands the range of

applications for these materials, particularly in the field of antioxidants coatings and biomedical applications.

1.5 References

(1) Brook, M. A. *Silicon in Organic, Organometallic, and Polymer Chemistry*; Wiley, 1999.
(2) Daudt, W. H.; Hyde, J. F. *Synthesis of Methylphenyldisiloxanes*. ACS Publications.
(3) Rochow, E. G. *An Introduction Chemistry of the Silicones*; Read Books Ltd, 2011.
(4) Colas, A.; Curtis, J. 2.3 SILICONE BIOMATERIALS: HISTORY AND CHEMISTRY.
(5) Medicine, I. of; Implants, C. on the S. of S. B. *Safety of Silicone Breast Implants*; National Academies Press, 2000.
(6) Nacey, J. N.; Tulloch, A. G. S.; Ferguson, A. F. Catheter-Induced Urethritis: A Comparison Between Latex and Silicone Catheters in a Prospective Clinical Trial. *Br. J. Urol.* **1985**, *57* (3), 325–328.
(7) Zare, M.; Ghomi, E. R.; Venkatraman, P. D.; Ramakrishna, S. Silicone-Based Biomaterials for Biomedical Applications: Antimicrobial Strategies and 3D Printing Technologies. *J. Appl. Polym. Sci.* **2021**, *138* (38), 50969.
(8) Bruschi, A.; Donati, D. M.; Choong, P.; Lucarelli, E.; Wallace, G. Dielectric Elastomer Actuators, Neuromuscular Interfaces, and Foreign Body Response in Artificial Neuromuscular Prostheses: A Review of the Literature for an In Vivo Application. *Adv. Healthc. Mater.* **2021**, *10* (13), 2100041.
(9) Gale, C. B.; Brook, M. A.; Skov, A. L. Compatibilization of Porphyrins for Use as High Permittivity Fillers in Low Voltage Actuating Silicone Dielectric Elastomers. *RSC Adv.* **2020**, *10* (31), 18477–18486.
(10) Gong, M.; Song, F.; Li, H.; Lin, X.; Wang, J.; Zhang, L.; Wang, D. Optimizing Energy Harvesting Performance of Silicone Elastomers by Molecular Grafting of Azobenzene to the Macromolecular Network. *RSC Adv.* **2021**, *11* (31), 19088–19094.
(11) Han, M.; Liu, L.; Yuan, J.; Zhang, L. Ternary Silicone Dielectric Elastomer Micro‐nanocomposites with Enhanced Mechanical and Electromechanical Properties. *Polym. Compos.* **2021**, *42* (1), 126–140.
(12) Prechtl, J.; Kunze, J.; Nalbach, S.; Seelecke, S. S.; Rizzello, G. Soft Robotic Module Actuated by Silicone-Based Rolled Dielectric Elastomer Actuators: Modeling and Simulation. In *Electroactive Polymer Actuators and Devices (EAPAD) XXII*; Bar-Cohen, Y., Anderson, I. A., Shea, H. R., Eds.; SPIE: Online Only, United States, 2020; p 79.
(13) Krpovic, S.; Dam‐Johansen, K.; Skov, A. L. Importance of Mullins Effect in Commercial Silicone Elastomer Formulations for Soft Robotics. *J. Appl. Polym. Sci.* **2021**, *138* (19), 50380.
(14) Rosset, S.; Araromi, O. A.; Schlatter, S.; Shea, H. R. Fabrication Process of Silicone-Based Dielectric Elastomer Actuators. *J. Vis. Exp.* **2016**, No. 108, 53423.

(15) Chruściel, J. J. Modifications of Textile Materials with Functional Silanes, Liquid Silicone Softeners, and Silicone Rubbers—A Review. *Polymers* **2022**, *14* (20), 4382.
(16) Eduok, U.; Faye, O.; Szpunar, J. Recent Developments and Applications of Protective Silicone Coatings: A Review of PDMS Functional Materials. *Prog. Org. Coat.* **2017**, *111*, 124–163.
(17) Han, R.; Li, Y.; Zhu, Q.; Niu, K. Research on the Preparation and Thermal Stability of Silicone Rubber Composites: A Review. *Compos. Part C Open Access* **2022**, *8*, 100249.
(18) Robeyns, C.; Picard, L.; Ganachaud, F. Synthesis, Characterization and Modification of Silicone Resins: An "Augmented Review." *Prog. Org. Coat.* **2018**, *125*, 287–315.
(19) Shit, S. C.; Shah, P. A Review on Silicone Rubber. *Natl. Acad. Sci. Lett.* **2013**, *36* (4), 355–365.
(20) Hamadi, S. H. K.; Isa, M.; Hashim, S. N. M. A.; Othman, M. Review on RTV Silicone Rubber Coatings Insulator for Transmission Lines. *IOP Conf. Ser. Mater. Sci. Eng.* **2020**, *864* (1), 012188.
(21) Wang, G.; Li, A.; Zhao, W.; Xu, Z.; Ma, Y.; Zhang, F.; Zhang, Y.; Zhou, J.; He, Q. A Review on Fabrication Methods and Research Progress of Superhydrophobic Silicone Rubber Materials. *Adv. Mater. Interfaces* **2021**, *8* (1), 2001460.
(22) Asymmetric Hydrosilylation of Prochiral Alkenes and Their Derivatives. In *Hydrosilylation: A Comprehensive Review on Recent Advances*; Marciniec, B., Ed.; Advances In Silicon Science; Springer Netherlands: Dordrecht, 2009; pp 125–156.
(23) Putzien, S.; Nuyken, O.; Kühn, F. E. Functionalized Polysilalkylene Siloxanes (Polycarbosiloxanes) by Hydrosilylation—Catalysis and Synthesis. *Prog. Polym. Sci.* **2010**, *35* (6), 687–713.
(24) Brook, M. A. New Control Over Silicone Synthesis Using SiH Chemistry: The Piers–Rubinsztajn Reaction. *Chem. – Eur. J.* **2018**, *24* (34), 8458–8469.
(25) Brook, M. A.; Grande, J. B.; Ganachaud, F. New Synthetic Strategies for Structured Silicones Using B(C6F5)3. In *Silicon Polymers*; Muzafarov, A. M., Ed.; Advances in Polymer Science; Springer: Berlin, Heidelberg, 2011; pp 161–183.
(26) Chen, X.; Yi, M.; Wu, S.; Tan, L.; Ge, X.; He, M.; Yin, G. Synthesis of Structurally Precise Polysiloxanes via the Piers–Rubinsztajn Reaction. *Materials* **2019**, *12* (2), 304.
(27) Gale, C. B.; Chin, B.; Tambe, C.; Graiver, D.; Brook, M. A. Silicone Structurants for Soybean Oil: Foams, Elastomers, and Candles. *ACS Sustain. Chem. Eng.* **2019**, *7* (1), 1347–1352.
(28) Li, J.; Zhang, Z.; Zhu, T.; Li, Z.; Wang, J.; Cheng, Y. Multi-Benzocyclobutene Functionalized Siloxane Monomers Prepared by Piers-Rubinsztajn Reaction for Low-k Materials. *Eur. Polym. J.* **2020**, *126*, 109562.
(29) Schneider, A. F.; Brook, M. A. High-Throughput Synthesis and Characterization of Aryl Silicones by Using the Piers–Rubinsztajn Reaction. *Chem. – Eur. J.* **2019**, *25* (67), 15367–15374.

(30) Wakabayashi, R.; Kuroda, K. Siloxane-Bond Formation Promoted by Lewis Acids: A Nonhydrolytic Sol–Gel Process and the Piers–Rubinsztajn Reaction. *ChemPlusChem* **2013**, *78* (8), 764–774.
(31) Bui, R.; Brook, M. A. Dynamic Covalent Schiff-Base Silicone Polymers and Elastomers. *Polymer* **2019**, *160*, 282–290.
(32) Cole, M. A.; Bowman, C. N. Evaluation of Thiol-Ene Click Chemistry in Functionalized Polysiloxanes. *J. Polym. Sci. Part Polym. Chem.* **2013**, *51* (8), 1749–1757.
(33) Zheng, S.; Zlatin, M.; Selvaganapathy, P. R.; Brook, M. A. Multiple Modulus Silicone Elastomers Using 3D Extrusion Printing of Low Viscosity Inks. *Addit. Manuf.* **2018**, *24*, 86–92.
(34) Genest, A.; Portinha, D.; Fleury, E.; Ganachaud, F. The Aza-Michael Reaction as an Alternative Strategy to Generate Advanced Silicon-Based (Macro)Molecules and Materials. *Prog. Polym. Sci.* **2017**, *72*, 61–110.
(35) Bui, R.; Brook, M. A. Thermoplastic Silicone Elastomers from Divanillin Crosslinkers in a Catalyst-Free Process. *Green Chem.* **2021**, *23* (15), 5600–5608.
(36) Li, N.; Ming, J.; Yuan, R.; Fan, S.; Liu, L.; Li, F.; Wang, X.; Yu, J.; Wu, D. Novel Eco-Friendly Flame Retardants Based on Nitrogen–Silicone Schiff Base and Application in Cellulose. *ACS Sustain. Chem. Eng.* **2020**, *8* (1), 290–301.
(37) Yang, X.; Song, Y.; Jiang, Y.; Wang, X.; Yang, Y.; Wang, J.; Wang, X.; He, N.; Lai, G.; Yu, Y. Fabrication and Performance of UV–Curable Schiff Base–Containing Antibacterial Silicone Modified Materials. *Prog. Org. Coat.* **2023**, *174*, 107313.
(38) Magennis, E. P.; Hook, A. L.; Williams, P.; Alexander, M. R. Making Silicone Rubber Highly Resistant to Bacterial Attachment Using Thiol-Ene Grafting. *ACS Appl. Mater. Interfaces* **2016**, *8* (45), 30780–30787.
(39) Nguyen, K. D. Q.; Megone, W. V.; Kong, D.; Gautrot, J. E. Ultrafast Diffusion-Controlled Thiol–Ene Based Crosslinking of Silicone Elastomers with Tailored Mechanical Properties for Biomedical Applications. *Polym. Chem.* **2016**, *7* (33), 5281–5293.
(40) Zhang, J.; Chen, Y.; Brook, M. A. Facile Functionalization of PDMS Elastomer Surfaces Using Thiol–Ene Click Chemistry. *Langmuir* **2013**, *29* (40), 12432–12442.
(41) Anastas, P. T.; Warner, J. C. *Green Chemistry: Theory and Practice*; Oxford University Press: Oxford [England] ; New York, 1998.
(42) Anastas, P.; Eghbali, N. Green Chemistry: Principles and Practice. *Chem. Soc. Rev.* **2010**, *39* (1), 301–312.
(43) Anastas, P. T.; Kirchhoff, M. M. Origins, Current Status, and Future Challenges of Green Chemistry. *Acc. Chem. Res.* **2002**, *35* (9), 686–694.
(44) Horváth, I. T.; Anastas, P. T. Innovations and Green Chemistry. *Chem. Rev.* **2007**, *107* (6), 2169–2173.
(45) Zimmerman, J. B.; Anastas, P. T.; Erythropel, H. C.; Leitner, W. Designing for a Green Chemistry Future. *Science* **2020**, *367* (6476), 397–400.
(46) Davis, S. C.; Anderson-Teixeira, K. J.; DeLucia, E. H. Life-Cycle Analysis and the Ecology of Biofuels. *Trends Plant Sci.* **2009**, *14* (3), 140–146.

(47) Ayres, R. U. Life Cycle Analysis: A Critique. *Resour. Conserv. Recycl.* **1995**, *14* (3), 199–223.
(48) Taylor, S. R.; McLennan, S. M.; Armstrong, R. L.; Tarney, J. The Composition and Evolution of the Continental Crust: Rare Earth Element Evidence from Sedimentary Rocks [and Discussion]. *Philos. Trans. R. Soc. Lond. Ser. Math. Phys. Sci.* **1981**, *301* (1461), 381–399.
(49) Al-Ansary, M.; Pöppelreiter, M. C.; Al-Jabry, A.; Iyengar, S. R. Geological and Physiochemical Characterisation of Construction Sands in Qatar. *Int. J. Sustain. Built Environ.* **2012**, *1* (1), 64–84.
(50) Archer, D. Fate of Fossil Fuel CO2 in Geologic Time. *J. Geophys. Res. Oceans* **2005**, *110* (C9).
(51) Berner, R. A. The Long-Term Carbon Cycle, Fossil Fuels and Atmospheric Composition. *Nature* **2003**, *426* (6964), 323–326.
(52) Retallack, G. J. 5.18 - Soils and Global Change in the Carbon Cycle over Geological Time. In *Treatise on Geochemistry*; Holland, H. D., Turekian, K. K., Eds.; Pergamon: Oxford, 2003; pp 1–28.
(53) Chen, Y.; Zheng, B. What Happens after the Rare Earth Crisis: A Systematic Literature Review. *Sustainability* **2019**, *11* (5), 1288.
(54) Tanzi, M. C.; Verderio, P.; Lampugnani, M. G.; Resnati, M.; Dejana, E.; Sturani, E. Cytotoxicity of Some Catalysts Commonly Used in the Synthesis of Copolymers for Biomedical Use. *J. Mater. Sci. Mater. Med.* **1994**, *5* (6), 393–396.
(55) Carpenter, J. C.; Cella, J. A.; Dorn, S. B. Study of the Degradation of Polydimethylsiloxanes on Soil. *Environ. Sci. Technol.* **1995**, *29* (4), 864–868.
(56) Griessbach, E. F. C.; Lehmann, R. G. Degradation of Polydimethylsiloxane Fluids in the Environment — a Review. *Chemosphere* **1999**, *38* (6), 1461–1468.
(57) Lehmann, R. G.; Miller, J. R.; Kozerski, G. E. Degradation of Silicone Polymer in a Field Soil under Natural Conditions. *Chemosphere* **2000**, *41* (5), 743–749.
(58) Lehmann, R. G.; Varaprath, S.; Annelin, R. B.; Arndt, J. L. Degradation of Silicone Polymer in a Variety of Soils. *Environ. Toxicol. Chem.* **1995**, *14* (8), 1299–1305.
(59) Ali, M.; Courtenay, P. Evaluating the Progress of the UK's Material Recycling Facilities: A Mini Review. *Waste Manag. Res.* **2014**, *32* (12), 1149–1157.
(60) Assuah, A.; Sinclair, A. J. Solid Waste Management in Western Canadian First Nations. *Waste Manag.* **2021**, *129*, 54–61.
(61) Babu, R. P.; O'Connor, K.; Seeram, R. Current Progress on Bio-Based Polymers and Their Future Trends. *Prog. Biomater.* **2013**, *2* (1), 8.
(62) Atta, O. M.; Manan, S.; Shahzad, A.; Ul-Islam, M.; Ullah, M. W.; Yang, G. Biobased Materials for Active Food Packaging: A Review. *Food Hydrocoll.* **2022**, *125*, 107419.
(63) Avella, M.; Buzarovska, A.; Errico, M. E.; Gentile, G.; Grozdanov, A. Eco-Challenges of Bio-Based Polymer Composites. *Materials* **2009**, *2* (3), 911–925.
(64) Cywar, R. M.; Rorrer, N. A.; Hoyt, C. B.; Beckham, G. T.; Chen, E. Y.-X. Bio-Based Polymers with Performance-Advantaged Properties. *Nat. Rev. Mater.* **2022**, *7* (2), 83–103.

(65) Helanto, K. E.; Matikainen, L.; Talja, R.; Rojas, O. J. Bio-Based Polymers for Sustainable Packaging and Biobarriers: A Critical Review. *BioResources* **2019**, *14* (2), 4902–4951.
(66) Hottle, T. A.; Bilec, M. M.; Landis, A. E. Sustainability Assessments of Bio-Based Polymers. *Polym. Degrad. Stab.* **2013**, *98* (9), 1898–1907.
(67) Pan, Y.; Farmahini-Farahani, M.; O'Hearn, P.; Xiao, H.; Ocampo, H. An Overview of Bio-Based Polymers for Packaging Materials. **2016**.
(68) RameshKumar, S.; Shaiju, P.; O'Connor, K. E.; P, R. B. Bio-Based and Biodegradable Polymers - State-of-the-Art, Challenges and Emerging Trends. *Curr. Opin. Green Sustain. Chem.* **2020**, *21*, 75–81.
(69) Weiss, M.; Haufe, J.; Carus, M.; Brandão, M.; Bringezu, S.; Hermann, B.; Patel, M. K. A Review of the Environmental Impacts of Biobased Materials. *J. Ind. Ecol.* **2012**, *16* (s1), S169–S181.
(70) Walker, S.; Rothman, R. Life Cycle Assessment of Bio-Based and Fossil-Based Plastic: A Review. *J. Clean. Prod.* **2020**, *261*, 121158.
(71) Chen, H.-Z.; Liu, Z.-H. Steam Explosion and Its Combinatorial Pretreatment Refining Technology of Plant Biomass to Bio-Based Products. *Biotechnol. J.* **2015**, *10* (6), 866–885.
(72) H. Isikgor, F.; Remzi Becer, C. Lignocellulosic Biomass: A Sustainable Platform for the Production of Bio-Based Chemicals and Polymers. *Polym. Chem.* **2015**, *6* (25), 4497–4559.
(73) Deutschmann, R.; Dekker, R. F. H. From Plant Biomass to Bio-Based Chemicals: Latest Developments in Xylan Research. *Biotechnol. Adv.* **2012**, *30* (6), 1627–1640.
(74) Jiang, B.; Jiao, H.; Guo, X.; Chen, G.; Guo, J.; Wu, W.; Jin, Y.; Cao, G.; Liang, Z. Lignin-Based Materials for Additive Manufacturing: Chemistry, Processing, Structures, Properties, and Applications. *Adv. Sci.* **2023**, *10* (9), 2206055.
(75) Ma, C.; Kim, T.-H.; Liu, K.; Ma, M.-G.; Choi, S.-E.; Si, C. Multifunctional Lignin-Based Composite Materials for Emerging Applications. *Front. Bioeng. Biotechnol.* **2021**, *9*.
(76) Mobilizing Chemistry Expertise To Solve Humanitarian Problems Volume 2. *ACS Symp. Ser.*
(77) Chen, M.; Li, R.; Runge, T.; Feng, J.; Hu, S.; Shi, Q.-S. Degradable Polymeric Package from Whole Cell Wall Biomass. *Mater. Today Sustain.* **2019**, *3–4*, 100008.
(78) Fang, X.; Tian, N.; Hu, W.; Qing, Y.; Wang, H.; Gao, X.; Qin, Y.; Sun, J. Dynamically Cross-Linking Soybean Oil and Low-Molecular-Weight Polylactic Acid toward Mechanically Robust, Degradable, and Recyclable Supramolecular Plastics. *Adv. Funct. Mater.* **2022**, *32* (46), 2208623.
(79) Jiang, Z.; Ho, S.-H.; Wang, X.; Li, Y.; Wang, C. Application of Biodegradable Cellulose-Based Biomass Materials in Wastewater Treatment. *Environ. Pollut.* **2021**, *290*, 118087.
(80) Tanrattanakul, V.; Saithai, P. Mechanical Properties of Bioplastics and Bioplastic–Organoclay Nanocomposites Prepared from Epoxidized Soybean Oil with Different Epoxide Contents. *J. Appl. Polym. Sci.* **2009**, *114* (5), 3057–3067.

(81) Wang, F.; Xie, T.; Zhong, W.; Ou, J.; Xue, M.; Li, W. A Renewable and Biodegradable All-Biomass Material for the Separation of Oil from Water Surface. *Surf. Coat. Technol.* **2019**, *372*, 84–92.
(82) Guo, L.; Li, M.; Xu, Q.; Jin, L.; Wang, Y. Bio-Based Films with High Antioxidant and Improved Water-Resistant Properties from Cellulose Nanofibres and Lignin Nanoparticles. *Int. J. Biol. Macromol.* **2023**, *227*, 365–372.
(83) Hejna, A. Coffee Silverskin as a Potential Bio-Based Antioxidant for Polymer Materials: Brief Review. *Proceedings* **2020**, *69* (1), 20.
(84) Kim, J.-Y.; Lee, H. W.; Lee, S. M.; Jae, J.; Park, Y.-K. Overview of the Recent Advances in Lignocellulose Liquefaction for Producing Biofuels, Bio-Based Materials and Chemicals. *Bioresour. Technol.* **2019**, *279*, 373–384.
(85) Modjinou, T.; Versace, D.-L.; Abbad-Andallousi, S.; Bousserrhine, N.; Dubot, P.; Langlois, V.; Renard, E. Antibacterial and Antioxidant Bio-Based Networks Derived from Eugenol Using Photo-Activated Thiol-Ene Reaction. *React. Funct. Polym.* **2016**, *101*, 47–53.
(86) Woranuch, S.; Yoksan, R. Eugenol-Loaded Chitosan Nanoparticles: II. Application in Bio-Based Plastics for Active Packaging. *Carbohydr. Polym.* **2013**, *96* (2), 586–592.
(87) Jiang, Z.; Ho, S.-H.; Wang, X.; Li, Y.; Wang, C. Application of Biodegradable Cellulose-Based Biomass Materials in Wastewater Treatment. *Environ. Pollut.* **2021**, *290*, 118087.
(88) Purnama, P.; Samsuri, M.; Iswaldi, I. A Review on Fully Bio-Based Materials Development from Polylactide and Cellulose Nanowhiskers. *Polymers* **2022**, *14* (19), 4009.
(89) Wood, T. M.; Saddler, J. N. Increasing the Availability of Cellulose in Biomass Materials. In *Methods in Enzymology*; Biomass Part A: Cellulose and Hemicellulose; Academic Press, 1988; Vol. 160, pp 3–11.
(90) Akhtar, J.; Idris, A.; Abd. Aziz, R. Recent Advances in Production of Succinic Acid from Lignocellulosic Biomass. *Appl. Microbiol. Biotechnol.* **2014**, *98* (3), 987–1000.
(91) Beagan, N.; O'Connor, K. E.; Del Val, I. J. Model-Based Operational Optimisation of a Microbial Bioprocess Converting Terephthalic Acid to Biomass. *Biochem. Eng. J.* **2020**, *158*, 107576.
(92) De Bari, I.; Giuliano, A.; Petrone, M. T.; Stoppiello, G.; Fatta, V.; Giardi, C.; Razza, F.; Novelli, A. From Cardoon Lignocellulosic Biomass to Bio-1,4 Butanediol: An Integrated Biorefinery Model. *Processes* **2020**, *8* (12), 1585.
(93) Lu, J.; Li, J.; Gao, H.; Zhou, D.; Xu, H.; Cong, Y.; Zhang, W.; Xin, F.; Jiang, M. Recent Progress on Bio-Succinic Acid Production from Lignocellulosic Biomass. *World J. Microbiol. Biotechnol.* **2021**, *37* (1), 16.
(94) Minh, D. P.; Besson, M.; Pinel, C.; Fuertes, P.; Petitjean, C. Aqueous-Phase Hydrogenation of Biomass-Based Succinic Acid to 1,4-Butanediol Over Supported Bimetallic Catalysts. *Top. Catal.* **2010**, *53* (15), 1270–1273.
(95) Motagamwala, A. H.; Won, W.; Sener, C.; Alonso, D. M.; Maravelias, C. T.; Dumesic, J. A. Toward Biomass-Derived Renewable Plastics: Production of 2,5-Furandicarboxylic Acid from Fructose. *Sci. Adv.* **2018**, *4* (1), eaap9722.

(96) Pang, J.; Zheng, M.; Sun, R.; Song, L.; Wang, A.; Wang, X.; Zhang, T. Catalytic Conversion of Cellulosic Biomass to Ethylene Glycol: Effects of Inorganic Impurities in Biomass. *Bioresour. Technol.* **2015**, *175*, 424–429.
(97) Pang, J.; Zheng, M.; Sun, R.; Wang, A.; Wang, X.; Zhang, T. Synthesis of Ethylene Glycol and Terephthalic Acid from Biomass for Producing PET. *Green Chem.* **2016**, *18* (2), 342–359.
(98) Zhou, H.; Xu, H.; Wang, X.; Liu, Y. Convergent Production of 2,5-Furandicarboxylic Acid from Biomass and CO2. *Green Chem.* **2019**, *21* (11), 2923–2927.
(99) Monterumici, C. M.; Rosso, D.; Montoneri, E.; Ginepro, M.; Baglieri, A.; Novotny, E. H.; Kwapinski, W.; Negre, M. Processed vs. Non-Processed Biowastes for Agriculture: Effects of Post-Harvest Tomato Plants and Biochar on Radish Growth, Chlorophyll Content and Protein Production. *Int. J. Mol. Sci.* **2015**, *16* (4), 8826–8843.
(100) Adewale, P.; Yancheshmeh, M. S.; Lam, E. Starch Modification for Non-Food, Industrial Applications: Market Intelligence and Critical Review. *Carbohydr. Polym.* **2022**, *291*, 119590.
(101) Falua, K. J.; Pokharel, A.; Babaei-Ghazvini, A.; Ai, Y.; Acharya, B. Valorization of Starch to Biobased Materials: A Review. *Polymers* **2022**, *14* (11), 2215.
(102) Zhang, W.; Barone, J. R.; Renneckar, S. Biomass Fractionation after Denaturing Cell Walls by Glycerol Thermal Processing. *ACS Sustain. Chem. Eng.* **2015**, *3* (3), 413–420.
(103) Zhang, W.; Sathitsuksanoh, N.; Barone, J. R.; Renneckar, S. Enhanced Enzymatic Saccharification of Pretreated Biomass Using Glycerol Thermal Processing (GTP). *Bioresour. Technol.* **2016**, *199*, 148–154.
(104) Wang, Z.; Yuan, L.; Tang, C. Sustainable Elastomers from Renewable Biomass. *Acc. Chem. Res.* **2017**, *50* (7), 1762–1773.
(105) Ding, L.; Chen, Y. F.; Zhong, Z.; Lu, F.; Du, Y.; Liu, L.; Huang, Y. Preparation of the Flexible Soybean Oil-Based Material via [2 + 2] Cycloaddition Photo-Polymerization. *J. Appl. Polym. Sci.* **2021**, *138* (9), 49925.
(106) Tay, T.; Ucar, S.; Karagöz, S. Preparation and Characterization of Activated Carbon from Waste Biomass. *J. Hazard. Mater.* **2009**, *165* (1), 481–485.
(107) Rouse, J. G.; Van Dyke, M. E. A Review of Keratin-Based Biomaterials for Biomedical Applications. *Materials* **2010**, *3* (2), 999–1014.
(108) Konop, M.; Rybka, M.; Drapała, A. Keratin Biomaterials in Skin Wound Healing, an Old Player in Modern Medicine: A Mini Review. *Pharmaceutics* **2021**, *13* (12), 2029.
(109) Hill, P.; Brantley, H.; Van Dyke, M. Some Properties of Keratin Biomaterials: Kerateines. *Biomaterials* **2010**, *31* (4), 585–593.
(110) Sierpinski, P.; Garrett, J.; Ma, J.; Apel, P.; Klorig, D.; Smith, T.; Koman, L. A.; Atala, A.; Van Dyke, M. The Use of Keratin Biomaterials Derived from Human Hair for the Promotion of Rapid Regeneration of Peripheral Nerves. *Biomaterials* **2008**, *29* (1), 118–128.

(111) Chakraborty, P.; Oved, H.; Bychenko, D.; Yao, Y.; Tang, Y.; Zilberzwige-Tal, S.; Wei, G.; Dvir, T.; Gazit, E. Nanoengineered Peptide-Based Antimicrobial Conductive Supramolecular Biomaterial for Cardiac Tissue Engineering. *Adv. Mater.* **2021**, *33* (26), 2008715.
(112) Holmes, T. C. Novel Peptide-Based Biomaterial Scaffolds for Tissue Engineering. *Trends Biotechnol.* **2002**, *20* (1), 16–21.
(113) Chen, Z.; Lv, Z.; Sun, Y.; Chi, Z.; Qing, G. Recent Advancements in Polyethyleneimine-Based Materials and Their Biomedical, Biotechnology, and Biomaterial Applications. *J. Mater. Chem. B* **2020**, *8* (15), 2951–2973.
(114) B. Matson, J.; I. Stupp, S. Self-Assembling Peptide Scaffolds for Regenerative Medicine. *Chem. Commun.* **2012**, *48* (1), 26–33.
(115) Rubert Pérez, C. M.; Stephanopoulos, N.; Sur, S.; Lee, S. S.; Newcomb, C.; Stupp, S. I. The Powerful Functions of Peptide-Based Bioactive Matrices for Regenerative Medicine. *Ann. Biomed. Eng.* **2015**, *43* (3), 501–514.
(116) Rauner, N.; Mueller, C.; Ring, S.; Boehle, S.; Strassburg, A.; Schoeneweiss, C.; Wasner, M.; Tiller, J. C. A Coating That Combines Lotus-Effect and Contact-Active Antimicrobial Properties on Silicone. *Adv. Funct. Mater.* **2018**, *28* (29), 1801248.
(117) Lam, M.; Migonney, V.; Falentin-Daudre, C. Review of Silicone Surface Modification Techniques and Coatings for Antibacterial/Antimicrobial Applications to Improve Breast Implant Surfaces. *Acta Biomater.* **2021**, *121*, 68–88.
(118) Zare, M.; Ghomi, E. R.; Venkatraman, P. D.; Ramakrishna, S. Silicone-Based Biomaterials for Biomedical Applications: Antimicrobial Strategies and 3D Printing Technologies. *J. Appl. Polym. Sci.* **2021**, *138* (38), 50969.
(119) A. Brook, M.; Yepremyan, A.; Lu, G.; Melendez-Zamudio, M.; J. Hrabowyj, D.; B. Gale, C. Antioxidant Silicone Oils from Natural Antioxidants. *Green Chem.* **2022**, *24* (22), 8751–8759.
(120) Dai, J.; Yang, S.; Teng, N.; Liu, Y.; Liu, X.; Zhu, J.; Zhao, J. Synthesis of Eugenol-Based Silicon-Containing Benzoxazines and Their Applications as Bio-Based Organic Coatings. *Coatings* **2018**, *8* (3), 88.
(121) Li, A. Y.; Melendez-Zamudio, M.; Yepremyan, A.; Brook, M. A. Learning from the Trees: Biomimetic Crosslinking of Silicones by Phenolic Coupling. *Green Chem.* **2023**, *25* (13), 5267–5275.
(122) Tamim, K.; Gale, C. B.; Silverthorne, K. E. C.; Lu, G.; Iao, C. H.; Brook, M. A. Antioxidant Silicone Elastomers without Covalent Cross-Links. *ACS Sustain. Chem. Eng.* **2023**, *11* (18), 7062–7071.
(123) Zheng, J.; Cai, Y.; Zhang, X.; Wan, J.; Fan, H. Eugenol-Based Siloxane Acrylates for Ultraviolet-Curable Coatings and 3D Printing. *ACS Appl. Polym. Mater.* **2022**, *4* (2), 929–938.
(124) Chen, P.; Ge, X.; Liang, W.; Lv, J.; Zhang, Z.; Yin, S.; Li, C.; Chen, Y.; Liu, W.; Ge, J. Eugenol-Containing Siloxane Synthesized Via Heterogeneous Catalytic Hydrosilylation and Its Application in Preparation of Superb Viscoelastic Low Modulus Gels. *Silicon* **2023**, *15* (3), 1123–1131.

(125) Li, W.; Xiao, L.; Wang, Y.; Chen, J.; Nie, X. Self-Healing Silicon-Containing Eugenol-Based Epoxy Resin Based on Disulfide Bond Exchange: Synthesis and Structure-Property Relationships. *Polymer* **2021**, *229*, 123967.
(126) Laengert, S. E.; Schneider, A. F.; Lovinger, E.; Chen, Y.; Brook, M. A. Sequential Functionalization of a Natural Crosslinker Leads to Designer Silicone Networks. *Chem. – Asian J.* **2017**, *12* (11), 1208–1212.
(127) Zhang, X.; Cai, Y.; Zhang, X.; Aziz, T.; Fan, H.; Bittencourt, C. Synthesis and Characterization of Eugenol-Based Silicone Modified Waterborne Polyurethane with Excellent Properties. *J. Appl. Polym. Sci.* **2021**, *138* (22), 50515.
(128) Zhang, J.; Fleury, E.; Chen, Y.; Brook, M. A. Flame Retardant Lignin-Based Silicone Composites. *RSC Adv.* **2015**, *5* (126), 103907–103914.
(129) Zhang, J.; Fleury, E.; Brook, M. A. Foamed Lignin–Silicone Bio-Composites by Extrusion and Then Compression Molding. *Green Chem.* **2015**, *17* (9), 4647–4656.
(130) Zhang, J.; Chen, Y.; Brook, M. A. Reductive Degradation of Lignin and Model Compounds by Hydrosilanes. *ACS Sustain. Chem. Eng.* **2014**, *2* (8), 1983–1991.
(131) Zhang, J.; Chen, Y.; Sewell, P.; Brook, M. A. Utilization of Softwood Lignin as Both Crosslinker and Reinforcing Agent in Silicone Elastomers. *Green Chem.* **2015**, *17* (3), 1811–1819.
(132) Deng, S.; Binauld, S.; Mangiante, G.; Frances, J. M.; Charlot, A.; Bernard, J.; Zhou, X.; Fleury, E. Microcrystalline Cellulose as Reinforcing Agent in Silicone Elastomers. *Carbohydr. Polym.* **2016**, *151*, 899.
(133) Stiubianu, G.; Racles, C.; Cazacu, M.; Simionescu, B. C. Silicone-Modified Cellulose. Crosslinking of Cellulose Acetate with Poly[Dimethyl(Methyl-H)Siloxane] by Pt-Catalyzed Dehydrogenative Coupling. *J. Mater. Sci.* **2010**, *45* (15), 4141–4150.
(134) Chen, Y.; Brook, M. A. Starch-Directed Synthesis of Worm-Shaped Silica Microtubes. *Materials* **2023**, *16* (7), 2831.
(135) Chen, Y.; Valentini, D. A.; Brook, M. A. Starch/Silicone Elastomers and Foams. *Sustainability* **2023**, *15* (13), 9941.
(136) Macphail, B.; Brook, M. A. Controlling Silicone-Saccharide Interfaces: Greening Silicones. *Green Chem.* **2017**, *19* (18), 4373–4379.
(137) Faiczak, K.; Brook, M. A.; Feinle, A. Energy-Dissipating Polymeric Silicone Surfactants. *Macromol. Rapid Commun.* **2020**, *41* (11), 2000161.
(138) Lusterio, A.; Brook, M. A. Naturally Derived Silicone Surfactants Based on Saccharides and Cysteamine. *Molecules* **2021**, *26* (16), 4802.
(139) Melendez-Zamudio, M.; Donahue-Boyle, E.; Chen, Y.; A. Brook, M. Acrylated Soybean Oil: A Key Intermediate for More Sustainable Elastomeric Materials from Silicones. *Green Chem.* **2023**, *25* (1), 280–287.
(140) Yang, X.; Cheng, F.; Fan, Y.; Song, Y.; He, N.; Lai, G.; Gong, Z.; Shen, J. Highly Transparent Acrylate Epoxidized Soybean Oil Based UV–Curable Silicone–Modified Coatings with Good Thermal Stability and Flame Retardancy. *Prog. Org. Coat.* **2022**, *165*, 106769.

(141) Tambe, C.; Kaufmann, J.; Graiver, D.; Narayan, R. Reactive Blends Derived from Modified Soybean Oil and Silicone. *J. Polym. Sci. Part Polym. Chem.* **2016**, *54* (19), 3086–3093.
(142) Gale, C. B.; Chin, B.; Tambe, C.; Graiver, D.; Brook, M. A. Silicone Structurants for Soybean Oil: Foams, Elastomers, and Candles. *ACS Sustain. Chem. Eng.* **2019**, *7* (1), 1347–1352.
(143) Sakai, K.; Ikeda, R.; Sharma, S. C.; Shrestha, R. G.; Ohtani, N.; Yoshioka, M.; Sakai, H.; Abe, M.; Sakamoto, K. Active Interfacial Modifier: Stabilization Mechanism of Water in Silicone Oil Emulsions by Peptide−Silicone Hybrid Polymers. *Langmuir* **2010**, *26* (8), 5349–5354.
(144) LaRonde, F. J.; Brook, M. A.; Hu, G. Amino Acid and Peptide Chemistry on Silicones. *Silicon Chem.* **2002**, *1* (3), 215–222.
(145) Li, X.; Li, P.; Saravanan, R.; Basu, A.; Mishra, B.; Lim, S. H.; Su, X.; Tambyah, P. A.; Leong, S. S. J. Antimicrobial Functionalization of Silicone Surfaces with Engineered Short Peptides Having Broad Spectrum Antimicrobial and Salt-Resistant Properties. *Acta Biomater.* **2014**, *10* (1), 258–266.
(146) Dutta, D.; Kamphuis, B.; Ozcelik, B.; Thissen, H.; Pinarbasi, R.; Kumar, N.; Willcox, M. D. P. Development of Silicone Hydrogel Antimicrobial Contact Lenses with Mel4 Peptide Coating. *Optom. Vis. Sci.* **2018**, *95* (10), 937.
(147) Martin, J.; Wehbi, M.; Echalier, C.; Hunger, S.; Bethry, A.; Garric, X.; Pinese, C.; Martinez, J.; Vezenkov, L.; Subra, G.; Mehdi, A. Direct Synthesis of Peptide-Containing Silicones: A New Way to Bioactive Materials. *Chem. – Eur. J.* **2020**, *26* (56), 12839–12845.
(148) Sakunkittiyut, Y.; Kunanopparat, T.; Menut, P.; Siriwattanayotin, S. Effect of Kraft Lignin on Protein Aggregation, Functional, and Rheological Properties of Fish Protein-Based Material. *J. Appl. Polym. Sci.* **2013**, *127* (3), 1703–1710.
(149) Lateef, S. S.; Boateng, S.; Hartman, T. J.; Crot, C. A.; Russell, B.; Hanley, L. GRGDSP Peptide-Bound Silicone Membranes Withstand Mechanical Flexing in Vitro and Display Enhanced Fibroblast Adhesion. *Biomaterials* **2002**, *23* (15), 3159–3168.
(150) Lim, K.; Chua, R. R. Y.; Saravanan, R.; Basu, A.; Mishra, B.; Tambyah, P. A.; Ho, B.; Leong, S. S. J. Immobilization Studies of an Engineered Arginine–Tryptophan-Rich Peptide on a Silicone Surface with Antimicrobial and Antibiofilm Activity. *ACS Appl. Mater. Interfaces* **2013**, *5* (13), 6412–6422.
(151) Martin, J.; Martinez, J.; Mehdi, A.; Subra, G. Silicone Grafted Bioactive Peptides and Their Applications. *Curr. Opin. Chem. Biol.* **2019**, *52*, 125–135.
(152) Xu, C.; He, R.; Xie, B.; Ismail, M.; Yao, C.; Luan, J.; Li, X. Silicone Hydrogels Grafted with Natural Amino Acids for Ophthalmological Application. *J. Biomater. Sci. Polym. Ed.* **2016**, *27* (13), 1354–1368.
(153) Pinese, C.; Jebors, S.; Echalier, C.; Licznar-Fajardo, P.; Garric, X.; Humblot, V.; Calers, C.; Martinez, J.; Mehdi, A.; Subra, G. Simple and Specific Grafting of Antibacterial Peptides on Silicone Catheters. *Adv. Healthc. Mater.* **2016**, *5* (23), 3067–3073.

(154) Mishra, B.; Basu, A.; Yuan Chua, R. R.; Saravanan, R.; Anantharajah Tambyah, P.; Ho, B.; Wook Chang, M.; Jan Leong, S. S. Site Specific Immobilization of a Potent Antimicrobial Peptide onto Silicone Catheters: Evaluation against Urinary Tract Infection Pathogens. *J. Mater. Chem. B* **2014**, *2* (12), 1706–1716.
(155) Zheng, S.; D'Angelo, A.; Zell, U.; Chen, Y.; Silverthorne, K. E. C.; Brook, M. A. Naked Alpaca Wool Works Better with Silicone Elastomers. *Green Chem.* **2021**, *23* (19), 7692–7700.
(156) Liu, X.; Yu, L.; Zhu, Z.; Nie, Y.; Skov, A. L. Silicone-Ionic Liquid Elastomer Composite with Keratin as Reinforcing Agent Utilized as Pressure Sensor. *Macromol. Rapid Commun.* **2021**, *42* (5), 2000602.
(157) Camacho Ramirez, A.; Melendez-Zamudio, M.; Guerra Contreras, A.; Brook, M. A. Lysine-Based Silicone Surfactants. *Sustain. Chem.* **2023**, *4* (2), 197–208.
(158) Alauzun, J. G.; Young, S.; D'Souza, R.; Liu, L.; Brook, M. A.; Sheardown, H. D. Biocompatible, Hyaluronic Acid Modified Silicone Elastomers. *Biomaterials* **2010**, *31* (13), 3471–3478.
(159) Mikhail, A. S.; Jones, K. S.; Sheardown, H. Dendrimer-Grafted Cell Adhesion Peptide–Modified PDMS. *Biotechnol. Prog.* **2008**, *24* (4), 938–944.
(160) Mikhail, A. S.; Ranger, J. J.; Liu, L.; Longenecker, R.; Thompson, D. B.; Sheardown, H. D.; Brook, M. A. Rapid and Efficient Assembly of Functional Silicone Surfaces Protected by PEG: Cell Adhesion to Peptide-Modified PDMS. *J. Biomater. Sci. Polym. Ed.* **2010**, *21* (6–7), 821–842.
(161) Chen, H.; Brook, M. A.; Sheardown, H. D.; Chen, Y.; Klenkler, B. Generic Bioaffinity Silicone Surfaces. *Bioconjug. Chem.* **2006**, *17* (1), 21–28.
(162) Martin, J.; Martinez, J.; Mehdi, A.; Subra, G. Silicone Grafted Bioactive Peptides and Their Applications. *Curr. Opin. Chem. Biol.* **2019**, *52*, 125–135.
(163) Genest, A.; Binauld, S.; Pouget, E.; Ganachaud, F.; Fleury, E.; Portinha, D. Going beyond the Barriers of Aza-Michael Reactions: Controlling the Selectivity of Acrylates towards Primary Amino-PDMS. *Polym. Chem.* **2017**, *8* (3), 624–630.
(164) Genest, A.; Portinha, D.; Pouget, E.; Lamnawar, K.; Ganachaud, F.; Fleury, E. Zwitterionic Silicone Materials Derived from Aza‐Michael Reaction of Amino‐Functional PDMS with Acrylic Acid. *Macromol. Rapid Commun.* **2021**, *42* (5), 2000372.
(165) Bertrand, E.; Gonçalves, C.; Billiet, L.; Gomez, J. P.; Pichon, C.; Cheradame, H.; Midoux, P.; Guégan, P. Histidinylated Linear PEI: A New Efficient Non-Toxic Polymer for Gene Transfer. *Chem. Commun.* **2011**, *47* (46), 12547–12549.
(166) Leiske, M. N.; Kempe, K. A Guideline for the Synthesis of Amino-Acid-Functionalized Monomers and Their Polymerizations. *Macromol. Rapid Commun.* **2022**, *43* (2), e2100615.
(167) Ryadnov, M.; Hudecz, F. *Amino Acids, Peptides and Proteins: Volume 42*; Royal Society of Chemistry, 2017.
(168) *Ring opening polymerization of α-amino acids: advances in synthesis, architecture and applications of polypeptides and their hybrids - Chemical Society Reviews (RSC Publishing).*

https://pubs.rsc.org/en/content/articlelanding/2020/cs/c9cs00738e (accessed 2023-07-31).

(169) Bao, Y.; He, J.; Li, Y. Synthesis of Novel Hyperbranched Poly(Ester-Amide)s Based on Acidic and Basic Amino Acids via "AD + CBB′" Couple-Monomer Approach. *Polymer* **2012**, *53* (1), 145–152.

(170) Michel, S.; Zhang, X. Q.; Wissler, M.; Löwe, C.; Kovacs, G. A Comparison between Silicone and Acrylic Elastomers as Dielectric Materials in Electroactive Polymer Actuators. *Polym. Int.* **2009**, *59* (3), 391–399.

(171) Yu, L.; Madsen, F. B.; Hvilsted, S.; Skov, A. L. Dielectric Elastomers, with Very High Dielectric Permittivity, Based on Silicone and Ionic Interpenetrating Networks. *RSC Adv* **2015**, *5* (61), 49739–49747.

(172) Kussmaul, B.; Risse, S.; Kofod, G.; Waché, R.; Wegener, M.; McCarthy, D. N.; Krüger, H.; Gerhard, R. Enhancement Of Dielectric Permittivity And Electromechanical Response In Silicone Elastomers: Molecular Grafting Of Organic Dipoles To The Macromolecular Network. *Adv. Funct. Mater.* **2011**, *21* (23), 4589–4594.

Chapter 2. Aza-Michael Silicone Cure is Accelerated by β-Hydroxyalkyl Esters

2.1 Abstract

The aza-Michael reaction is proving to be a practical, catalyst free method by which a variety of polymers, including silicones, can be cured. However, its adoption may be compromised by slow cure rates; for many applications is it not practical to accelerate cure by heating. OH groups on the amine, acrylate partner or solvent are known to lead to accelerated rates of aza-Michael reactions. The impact of the location of OH groups on reaction partners is demonstrated using both small molecules and small molecules plus telechelic silicones. While all OH groups are shown to increase reaction rates, a special enhancement is provided by β-hydroxyalkyl acrylate esters, which have significantly higher rates of reaction than simple acrylates per se, and yet higher reactivities in hydroxylic media. Using this motif, in the absence of solvents, silicone elastomer cure based on the β-hydroxyalkyl acrylate motif is facile and complete in less than an hour at room temperature.

2.2 Introduction

Silicones, particularly in the form of elastomers,[1] have many beneficial properties including heat resistance, hydrophobicity and gas permeability. Their biocompatibility and desirable skin-feel have led to their wide use in medical applications and personal care products, including cosmetics and hair care products.[2] There is desire to better exploit the principles of Green Chemistry[3] in chemical processes, including for silicone

polymer synthesis. Most silicone cure technologies involve high temperature radical conditions, expensive noble metal or potentially toxic tin catalysts.[4]

Increasingly, the use of organic cure, particularly greener processes that can be done in the absence of metal catalysts, has attracted attention as an alternative to these traditional processes. Several click reactions, including the Huisgen reaction,[5] photodimerization,[6] thermal cyclization,[7] and Michael additions are of particular interest because of high atom economy and, in some cases, no requirement for catalysts.

The aza-Michael reaction has become an increasingly popular choice for the modification and curing of silicones. It benefits from catalyst-free conditions at room temperature using inexpensive and readily accessible starting materials. In addition, there are many strategies available to fine tune the efficiency of the reaction, including solvents, basicity of the amine partner, electrophilicity of Michael acceptors, and temperature.[8] A seminal review paper published by Ganachaud et al. captured the highlights of the aza-Michael reaction in silicones along with a comprehensive review of various ways of controlling the rates of aza-Michael reactions.[9]

Aza-Michael additions are known to be significantly faster in polar protic media, especially water,[10,11] which is hypothesized to result from increased electrophilicity of the acrylate carbonyl group due to hydrogen bonding with protic solvents, making them more electrophilic via a cyclic trimolecular transition state (Figure 2.1A).[12] However, the use of a solvent – that must be removed – is not ideal when an elastomer is the desired product. We sought to develop strategies that would exploit rapid, facile aza-Michael reactions for silicone elastomer cure in the absence of solvents. We compare the ability of proximal

hydroxy groups, located either on amine or acrylate partners, to accelerate aza-Michael silicone cure via intramolecular interactions (Figure 2.1B, C).

2.3 Experimental Section

2.3.1 Materials

Butyl acrylate (**BAcr**), hydroxyethyl acrylate (**HEA**), butyl amine (**BA**), ethanol amine (**EA**), 4-hydroxybutyl acrylate (**HBAcr**), 5-amino-1-pentanol (**AP**), deuterated methanol, deuterated chloroform and all other solvents were purchased from Sigma Aldrich. Acrylate-terminated PDMS (Silmer ACR **D11**, M_n ~1200 g mol^{-1} and Silmer ACR **D30**, M_n ~2600 g mol^{-1}), 3-[2-(hydroxy-3-[(1-oxo-2-propenyl)oxy]propoxy)propyl group-terminated PDMS (Silmer ACR OH **D9_OH**, M_n ~1200 g mol^{-1}, and Silmer ACR OH **Di28_OH**, M_n ~2600 g mol^{-1}) were kindly supplied by Siltech Corporation. **A4-8k** (AMS-152, 4–5% mol aminopropylmethylsiloxane, M_n ~ 7000–9000 g mol^{-1}) and **A23-20k** (AMS-1203, 20–25% mol aminopropylmethylsiloxane, M_n ~ 20000 g mol^{-1}) were purchased from Gelest. High speed mixing utilized a FlackTek speedmixer (Dual Asymmetric Centrifuge (DAC) Model DAC 150.1 FV7-K) and FlackTek cups purchased from FlackTek Inc.

2.3.2 Methods

^{1}H NMR were recorded on a Bruker Advance 600 MHz nuclear magnetic resonance spectrometer. Pre-elastomer mixtures (Figure 2.5) were mixed using a FlackTek speedmixer (Dual Asymmetric Centrifuge (DAC) Model DAC 150.1 FV7-K). A Shore OO durometer (Rex Gauge Company, Inc. US), which measures resistance to indentation, was used to characterize the hardness of the elastomer.

2.3.3 Model reaction NMR studies:

The acrylate (0.39 mmol) was dissolved in the selected deuterated solvent (0.5 mL), a stoichiometric amount of amine (0.39 mmol) was dissolved in the same deuterated solvent (0.2 mL) and added. The equivalence was established based on number of H_2C=C protons to that of NH_2. If MeOD was used, one equivalent of MeOD was added to the amine component before mixing, then the two components were added to an NMR tube and mixed to homogeneity just before the NMR measurement. ^{1}H NMR spectra were collected every 1.5 min for 30 min, and then at 1h, 2h, 4h, 8h and 12 h. (Table S7.1)

2.3.4 Reactions of silicones with small amines

The same protocol was used as for the previous model reactions: silicone acrylate (0.39 mmol) was dissolved in $CDCl_3$ (0.5 ml); stoichiometric amount of amine (BA and EA) was dissolved in $CDCl_3$ (0.2 ml). The final ^{1}H NMR was taken at 12 h for all reactions. (Table S7.1).

2.3.5 Elastomer Curing

Amino silicone (2.0 g, 0.42 mmol NH2) and acrylic silicone (1 equiv. based on 1H NMR) were added to a FlackTek propylene cup (10 g). The sample was hand mixed for 10 s and then speed mixed at 3000 rpm for 1.5 min. The cup was removed from the speed-mixer. Gellation time was determined by absence of flow upon inversion of the sample. The materials were characterized by Shore OO hardness at <2 min after start of mixing and routinely (~5 min) for the first 30 min (Table S7.2), then at 6, 12 and 18 h and each day or so until no further change was observed in the hardnesses of the 1 cm thick transparent elastomers, and a final Shore OO measurement was then recorded. No measurements

were made after 1 week. The entire process was performed at room temperature. For cure times and hardnesses, see Figure 2.5, Table S7.2.

2.4 Results and Discussion

A series of model organic compounds were used to survey the impact of proximal OH groups on the reaction rates of aza-Michael additions (Figure 2.2A). Round-Robin reactions between acrylates and amines, with and without OH groups, were followed using: ^{1}H NMR in $CDCl_3$; $CDCl_3$ + 1 molar equivalent MeOD based on the acrylate; or pure MeOD; the use of deuterated methanol permitted an assessment of the importance of polar media per se vs explicit intramolecular interactions.

Significant rate enhancements in non-hydroxylic solvents were provided by intramolecular hydrogen bonding of proximal OH groups. However, the impact on rate acceleration by OH groups on the 2 different reaction partners was not found to be equal. The presence of OH on the acrylate led to a large acceleration of the rate: **BAcr** v **HEA**, while the effect of an OH group on the amine was modest: **BA** v **EA** (Figure 2.3A). Overall reaction rates were much faster in the polar hydroxylic solvent MeOH-d, compared to $CDCl_3$ as solvent, and the effect of internal OH groups was significantly decreased. However, even in methanol the presence of β-OH groups on the acrylic partner led to an enhanced rate compared to simple acrylates, consistent with some type of intramolecular catalysis (Figure 2.1C). Note that the nitrogen atom can add to one, or two, acrylates. In $CDCl_3$, 14% of the diadduct was observed, while this level increased to 23% in pure methanol. That is, reaction of the primary amine is faster than the secondary, but with lower selectivity in more polar solvents.

The catalytic effects of different OH sources are clearly seen in a log plot of the initial rates of reaction (Figure 2.3B, Table S7.1). The best reaction, combining hydroxyethyl acrylate **HEA** with butyl amine **BA** in methanol, was 70% complete at 15 minutes, a rate that is very convenient for silicone cure. Note that many of the other reactions were not complete until much later. We elected to use the 15-minute data point because the rate plot was in the (more or less) linear region for all compounds, and it was possible to follow the most interesting reactions – those which are rapid at room temperature.

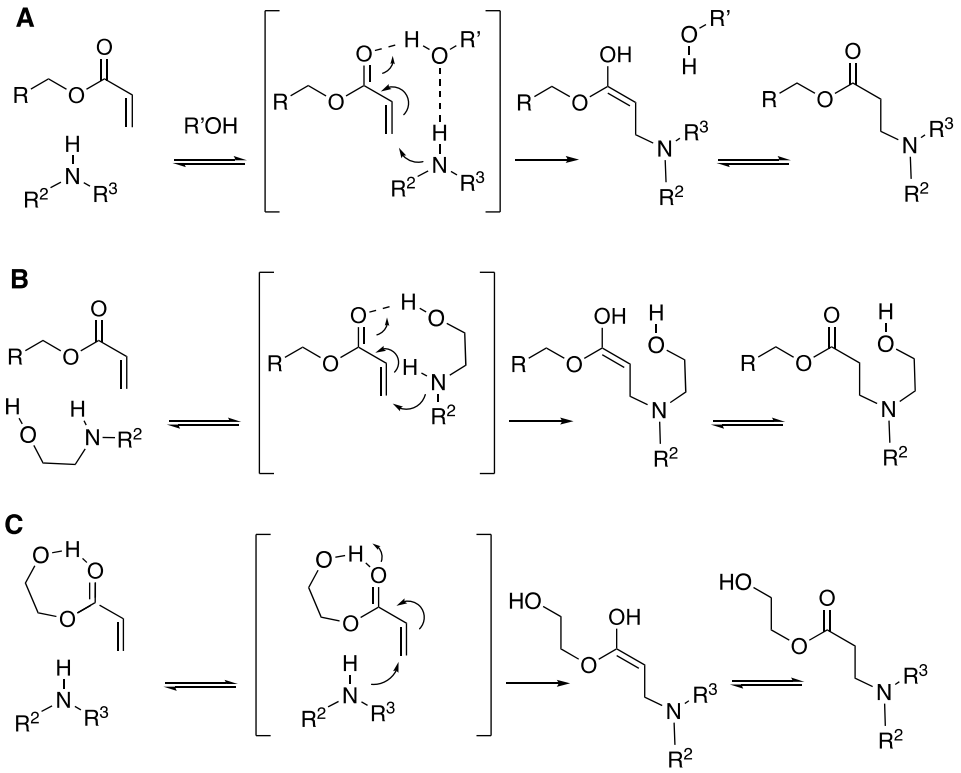

Figure 2.1. Proposed aza-Michael acceleration mechanisms by hydroxy groups. A) solvent catalyzed; intramolecular hydroxy coordination of B) β-hydroxy-modified amine; C) β-hydroxy acrylate.

One plausible explanation for the acceleration observed involves H-bonding via an internal seven-membered ring to increase the electrophilicity of the carbonyl group (Figure 2.1C). To test this idea, the spacing between the carbonyl and hydroxy groups was increased. This included a chain extension on the acrylate side by 2 carbons with **HBAcr**, and, on the amine side, by 3 carbons, **AP** (Figure 2.2B). While there was a rate enhancement if the amine possessed a hydroxy group, it was relatively insensitive to the location of the OH group with respect to the amine; the outcomes, for example, of a β- or ε-hydroxy group on the amine partner, were comparable, and similar to rates when one equivalent of methanol / acrylate was used in $CDCl_3$ solvent (Figure 2.3C). This type of acceleration is reminiscent of general acid catalysis. By contrast, on the acrylate moiety the β-position of the OH was key to its ability to accelerate the reaction. A significant decrease in the rate was observed when the hydroxy group was more remote from the carbonyl group (Figure 2.3C). That is, the contribution to the reaction rate of **HBAcr**, with a remote OH group, was comparable to having an OH group somewhere on the amine partner, **EA** and **AP**. These data suggest that the surprising intramolecular acceleration, even in an alcoholic solvent, arose via the proposed 7-membered transition state (Figure 2.1C vs A, B). Could this selective activation in the absence of polar solvents also operate and facilitate solvent-free silicone cure?

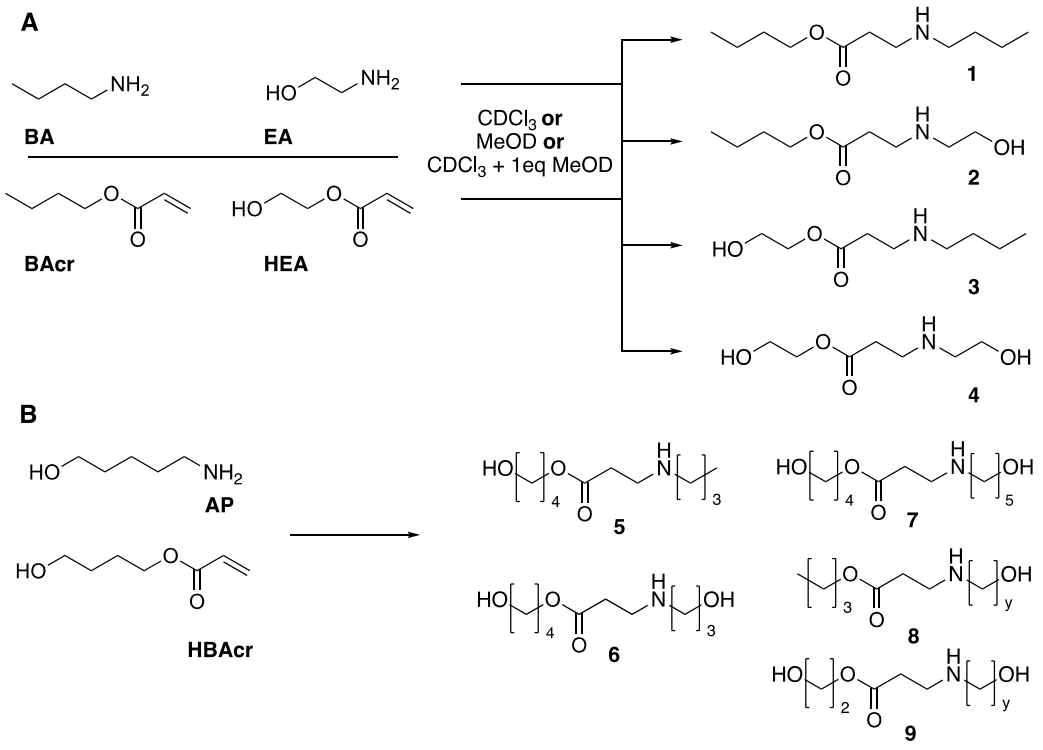

Figure 2.2. Model compounds A) Competition reactions with non- or β-hydroxylated amines with acrylates. B) Michael reactions with reagents bearing more remote internal hydroxy groups.

Silicones possess much lower surface energies – 13-19 mN m^{-1} – than alkanes.[13] Silicone acrylates and β-hydroxyacrylates are commercially prepared from telechelic hydrosilicones. The processes to make simple acrylates involve platinum-catalyzed hydrosilylation followed by an esterification of the alcohol, whereas an analogous route via epoxy compounds leads to β-hydroxyacrylates (Figure 2.4A vs B). A lower polarity environment was expected to amplify any acceleration resulting from internal H-bonding. The relative rates of aza-Michael reactions between simple amines **BA** vs β-hydroxyamines **EA** and silicone polymers possessing simple acrylates **Di11** vs β-

hydroxyacrylates **Di9_OH** were examined (Figure 2.4C,D). The patterns of reactivity shown for simple organic molecules were reflected in the reactions of analogous silicones. Slow reaction was observed for the silicone acrylate/amine pair, with only a slight enhancement for the reaction with ethanolamine. By contrast, the same reaction with the silicone β-hydroxyacrylate was significantly faster than with the simple acrylate (Figure 2.4E).

The main objective of this research was to accelerate catalyst-free silicone curing without the use of solvents. Commercially available pendent aminopropylsilicones with different amine densities and molar masses: **A4-8k** (M_n = 8000 g mol^{-1}, 4% amine) and **A23-20k** (M_n = 20,000 g mol^{-1}, 23% amine) were used as the curing agents for telechelic acrylates vs β-hydroxypropyl acrylates of two different molar masses: 1000 and 2500 g mol^{-1}, respectively. The rates of cure were followed by both time to gel, and evolution of Shore OO hardnesses (Figure 2.5, Table S7.2). As with the small molecules, cure with the β-hydroxyl acrylates was faster than simple acrylates. However, based on gel time (no flow upon sample inversion), the magnitude of the rate difference was much higher than with the small molecules, about 2 orders of magnitude. Full cure followed the same relationship and could be completed at room temperature in about 30 minutes, which is much faster than typical cure rates for platinum-catalyzed hydrosilylation (Sylgard 184 typically cures over 24 hours at room temperature) or tin-catalyzed moisture cure (skin over – cure at the interface – takes about 5 minutes, but complete cure also normally takes about 24 hours depending on humidity) at that temperature. It will be further noted that the OH group that facilitates the reaction also provides a small contribution to final Shore

OO hardness, presumably through H bonding (Figure 2.5C). We note that in addition to measurements at 30 minutes, further measurements taken in the first 24 hours and then almost daily until no further change was observed, or one week had passed. Full cure is considered the value of the highest hardness achieved after 30 minutes. We focused on the most interesting, faster reactions.

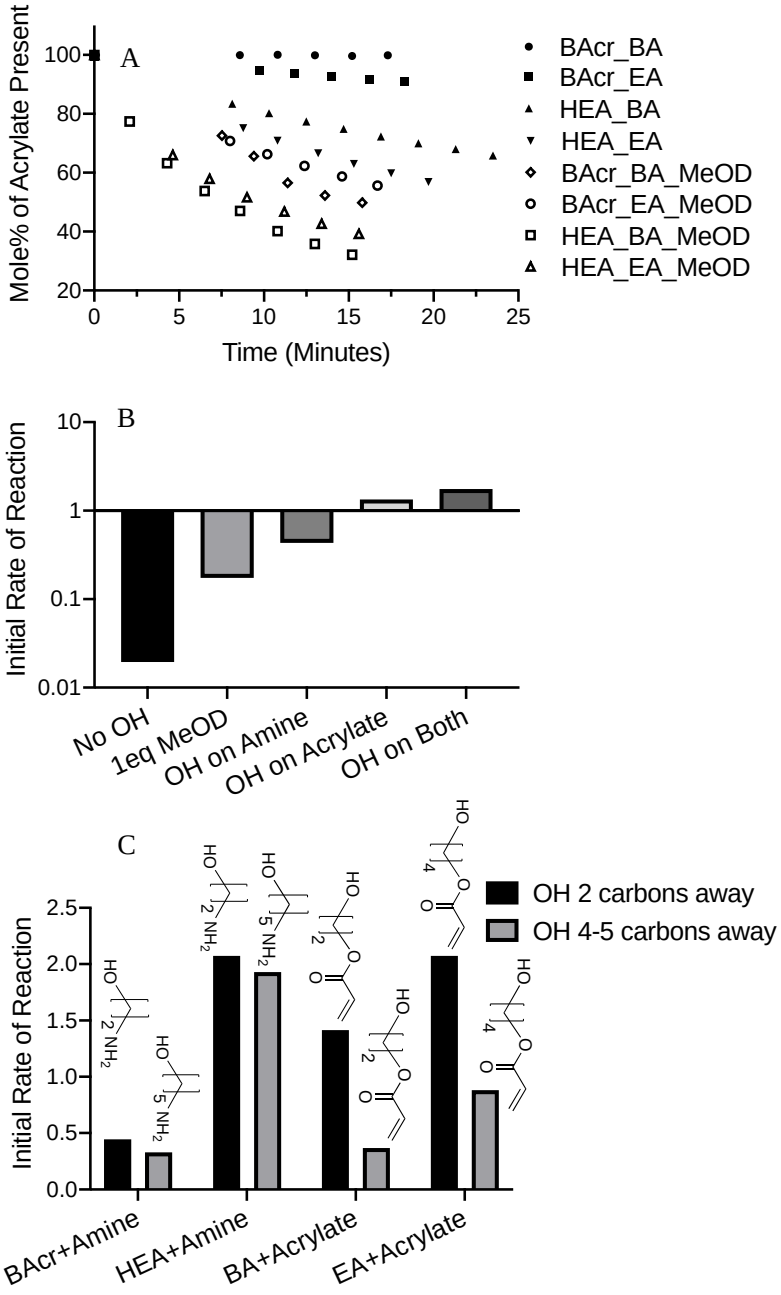

Figure 2.3. Reaction rates for model compounds (Figure 2.2, **Table S7.1**). The units for the rate of reactions were % mole/ min decrease of acrylate ^{1}H NMR signal. A) Rates plotted as loss of starting material for model compounds. B) log plot of initial rates of

reaction with the same OH group concentration. C) Initial rate of reaction comparison with different OH group positions on Michael donors and accepters.

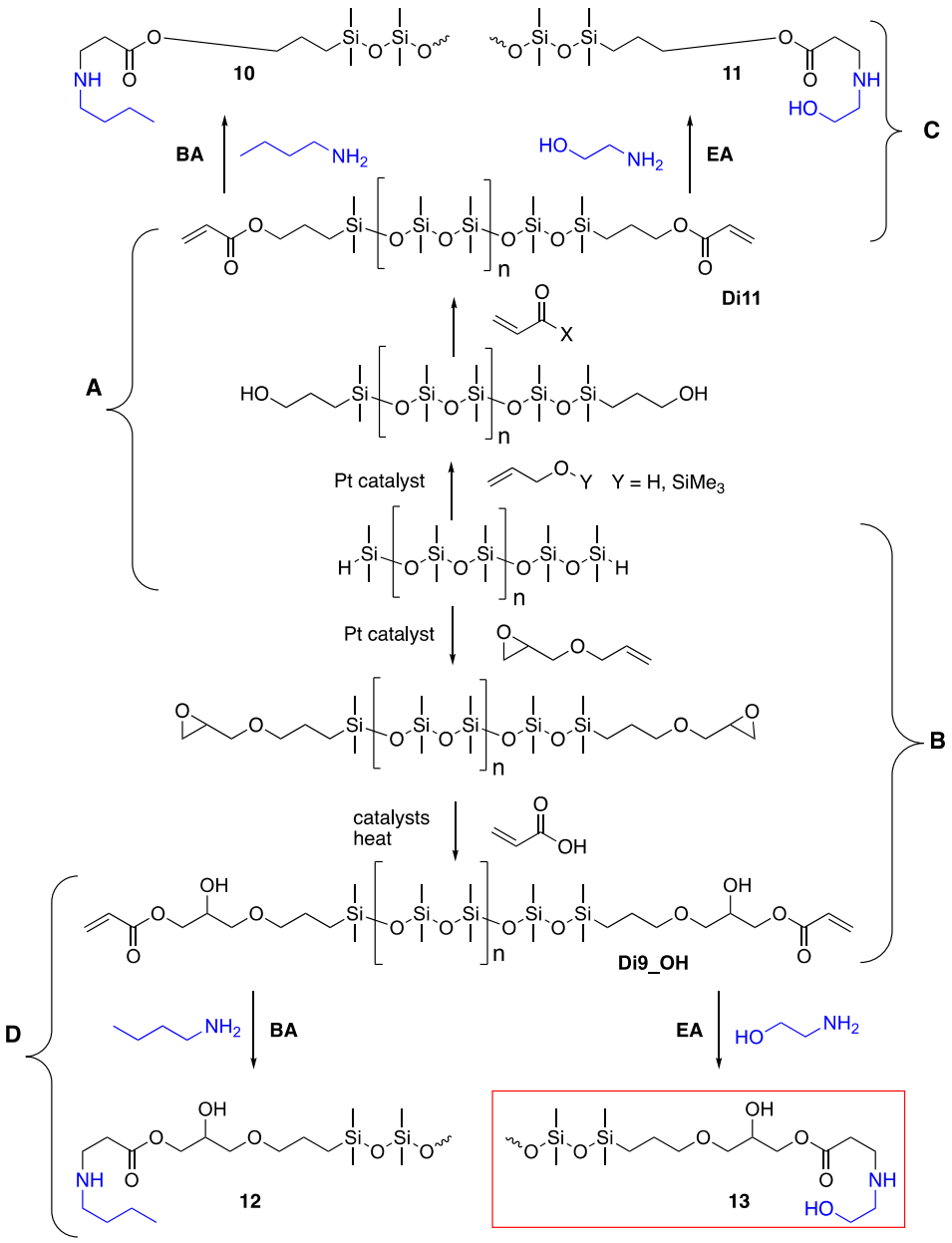

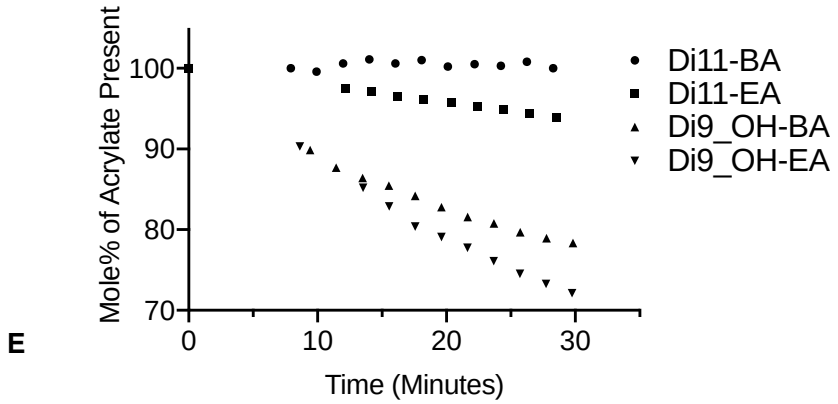

Figure 2.4. Typical preparation of A) simple silicone acrylates, and B) silicone β-hydroxyacrylates starting from telechelic SiH silicones. Reactions of small molecule amines with C) silicone acrylates and D) silicone β-hydroxyacrylates. E) Rates plotted as loss of starting material for silicone acrylates plus small model amines

Aza-Michael reactions are accelerated by proton sources, both intermolecular and intramolecular. The reactions were very fast even in a silicone medium that contains a scarcity of polar groups. Rates of cure in solvent free silicone pre-elastomer systems were particularly enhanced by β-OH groups on the acrylate partner, likely through transition states similar to Figure 2.1C. Silicone acrylates with this functionality are readily prepared by the ring opening of epoxy-modified silicones with acrylic acid and, thus, are commercially available. The use of these precursors dramatically and conveniently reduces silicone cure times at room temperature and leads to useful silicone elastomers by combining the tenets of practicality and Green Chemistry: high atom economy; no solvents; and no expensive catalysts, the products of which may leach from the elastomer.[14]

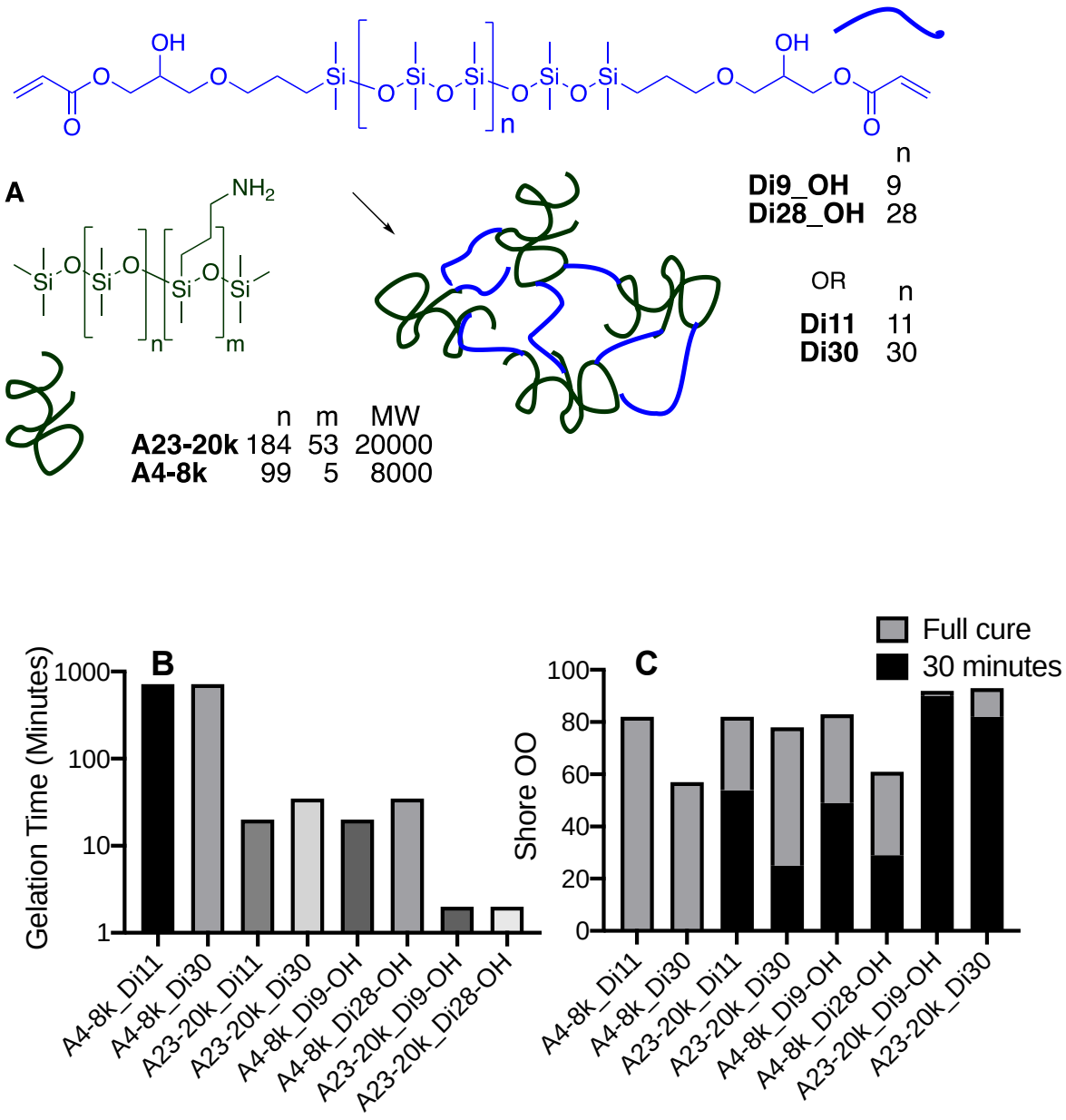

Figure 2.5. A) Solvent-free crosslinking of aminopropylsilicones and silicone acrylates, shown for **D9_OH/Di28_OH**. For the elastomers shown in B) Gelation times. C) Degree of cure at 30 min compared to full cure (measurements were taken at 12, 18, 24 h and then each day or so up to 1 week until hardness remained constant; the latter hardness

taken as full cure). In all cases the β-OH acrylates ("OH" suffix) cured significantly faster than other acrylics of comparable molar masses.

2.5 Conclusion

Silicones modified with acrylate groups are readily available as simple acrylates, typically derived from silicone carbinols, and β-hydroxyacrylates formed by ring-opening of epoxides with acrylic acid. The aza-Michael reaction with aminoalkylsilicones, used to cure silicones to elastomer proceeds in both cases to cleanly give silicone elastomers in the absence of catalysts. However, the aza-Michael reaction with silicone β-hydroxyacrylate esters was found to occur much more rapidly than with simple acrylates. Model studies show this is a feature of the geometric proximity of the OH group, rather than a generic effect of increased hydrophilicity.

2.6 References

(1) Varnava, C. K.; Patrickios, C. S. Polymer Networks One Hundred Years after the Macromolecular Hypothesis: A Tutorial Review. *Polymer* **2021**, *215* (September 2020), 123322–123322.
(2) O'Lenick, A. J. *Silicones for Personal Care, 2nd Edition*; 2008.
(3) Anastas, P. T.; Warner, J. C. *Green Chemistry: Theory and Practice*; Oxford University Press: Oxford, New York, 2000.
(4) Brook, M. A. *Silicon in Organic, Organometallic, and Polymer Chemistry*; Wiley, 1999.
(5) Rambarran, T.; Gonzaga, F.; A. Brook, M. Generic, Metal-Free Cross-Linking and Modification of Silicone Elastomers Using Click Ligation. *Macromolecules* **2012**, *45* (5), 2276–2285.
(6) Fawcett, A. S.; Hughes, T. C.; Zepeda-Velazquez, L.; Brook, M. A. Phototunable Cross-Linked Polysiloxanes. *Macromolecules* **2015**, *48* (18), 6499–6507.
(7) Zuo, X.; Chen, J.; Zhao, X.; Yang, S.; Fan, L. Synthesis and Characterization of Siloxane Resins Derived from Silphenylene-Siloxane Copolymers Bearing Benzocyclobutene Pendant Groups. *J. Polym. Sci. Part Polym. Chem.* **2008**, *46* (23), 7868–7881.

(8) Bandyopadhyay, D.; Mukherjee, S.; Turrubiartes, L. C.; Banik, B. K. Ultrasound-Assisted Aza-Michael Reaction in Water: A Green Procedure. *Ultrason. Sonochem.* **2012**, *19* (4), 969–973.
(9) Genest, A.; Portinha, D.; Fleury, E.; Ganachaud, F. The Aza-Michael Reaction as an Alternative Strategy to Generate Advanced Silicon-Based (Macro)Molecules and Materials. *Prog. Polym. Sci.* **2017**, *72*, 61–110.
(10) Ranu, B. C.; Banerjee, S. Significant Rate Acceleration of the Aza-Michael Reaction in Water. *Tetrahedron Lett.* **2007**, *48* (1), 141–143.
(11) Joshi, J. H.; Saiyed, A. S.; Bedekar, A. V. Aqueous Aza-Michael Reaction of Conjugated Alkenes: Toward Spermine. *Synth. Commun.* **2010**, *40* (19), 2857–2863.
(12) Koverzanova, E. V.; Levina, I. I.; Gridnev, A. A. Kinetics of the Aza-Michael Reaction at Room Temperature. *Russ. J. Phys. Chem. B* **2018**, *12* (1), 46–52.
(13) Zeigler, J. M.; Fearon, F. W. G.; International Topical Workshop "Advances in Silicon-Based Polymer Science"; American Chemical Society Division of Polymer Chemistry. Silicon-Based Polymer Science a Comprehensive Resource; Advances in chemistry series; American Chemical Society: Washington, DC, 1990.
(14) Lancaster, M. *Green Chemistry: An Introductory Text, Royal Society of Chemistry, 3 Edn*; Royal Society of Chemistry, 2016.

Chapter 3. Protecting group-free introduction of amino acids to polymers through the aza-Michael reaction[1]

3.1 Abstract

Amino acids are natural and versatile building blocks that offer inherent biocompatibility, zwitterionic character, and diverse functional groups, making them attractive for a range of applications. Integrating amino acids into materials can enhance biodegradability and biocompatibility - thus enhancing sustainability - due to their natural origin and also allows one to tailor material properties. However, their rich functionality presents challenges during incorporation, often requiring the use of protecting groups and harsher conditions that undermine green chemistry principles. In this study, we present a straightforward strategy for amino acid incorporation using the aza-Michael reaction with cholinium amino acid ionic liquids (ChAAILs). ChAAILs provide a self-solvating and catalyzing environment, eliminating the need for protecting groups and promoting solvent-free synthesis. A kinetic study of aza-Michael reactions between ChAAILs with various small acrylates demonstrated the range of amino acids that can be incorporated and their product stability. ChAAILs exhibit excellent reactivity not only with simple acrylates, but also hydrophilic polyethers and hydrophobic silicones, offering a promising, generic green approach for amino acid-functional polymer modification.

[1] This chapter was submitted to journal of Polymer Chemistry on 11 August 2023. Submission ID: PY-ART-08-2023-000939

3.2 Introduction

Amino acids, the building blocks of proteins, are attracting attention in many fields of research including pharmaceuticals,[1] biocatalysis,[2-5] sustainable surfactants,[6-7] as well as functional/sustainable polymers and materials.[8-14] They are attractive because of their innate biocompatibility and biodegradability as natural materials,[8, 11, 15] zwitterionic nature and versatility as multifunctional molecules.[16] Several reviews have highlighted the importance of amino acid-functional materials and described different synthetic methods for their creation.[8-14] Some interesting examples of properties of selected materials include anti-biofouling and stimuli-responsive behavior,[13] biomedical materials,[17-18] drug delivery systems,[12, 19] and smart materials.[6-7]

The rich functionality of amino acids is a double-edged sword. The nature and density of the functional groups makes it difficult to perform controlled reactions without resorting to protecting groups, which goes against Green Chemistry principle 8.[20] The challenges with amino acids are more severe when dealing with polymeric systems,[15, 17, 21] as it is often difficult to find common solvents for hydrophilic amino acids with hydrophobic synthetic polymers. Even if one resorts to protection/deprotection sequences, the efficiencies often drop as the molar mass of the polymer increases due, in part, to poor solubility.[12] The development of more sustainable methodologies to incorporate amino acids that bypass the need for protecting groups and the use of solvents would be highly desirable.

Natural or unnatural amino acids are typically incorporated in polymer networks into two different ways: in-chain amino acid-containing polymers prepared through ring-opening polymerization of α-amino acid N-carboxyanhydrides[11] or related peptidomimetic synthetic methods;[22-23] and, use of monomers with amino acid-containing side chains. The majority of literature reports involve polyacrylates with either pre-modification of the monomer starting material or post-modification of the polymer; in most cases protecting groups are used.[15, 17] Brisson et al. developed a protecting group free synthetic route to highly functional amino acid polymers via a robust Schiff base method that produces an amino acid-modified polymer which, due to the reversible nature of imine bonds, is dynamic.[24]

Click reactions typically adhere to the principles of green chemistry. Among click reactions, the Michael reaction has emerged as a powerful tool as, depending on nucleophile, it can be performed without catalysts, involves mild reaction conditions, high atom economy, and compatibility with many functional groups. The Michael addition is increasingly popular in materials chemistry as a mechanism to bridge amino acids or peptides to polymers.[25-28] For example, the thia-Michael reaction links proteins or peptides with polymers through the side chain of cysteine,[29-32] which conveys new properties to functional materials, including self-assembly,[33] cell-adhesion,[34] and other tailored bio-activities.[35-36] The aza-Michael addition analogously links other amine-containing molecules to amino acids first modified with acryloyl chloride.[19] However, due to their zwitterionic nature, a significant challenge that remains with the use of native amino acids in

the aza-Michael reaction is their poor solubility and poor reactivity towards acrylates if protecting groups are to be avoided.

Ionic liquids (ILs) are a unique class of liquids with very high ion density, typically possessing low volatility and high thermal stability.[37] They are used in fields of catalysis,[38] solvents for separation science[39] and cellulose dissolution,[40] among other applications. One example of ILs used in aza-Michael reactions demonstrated that the basic ionic liquid 3-butyl-1-methylimidazolium hydroxide can act as a recyclable green solvent for aza-Michael addition both as reaction media and catalyst.[41] Amino acid ILs have also gained attention due to their natural origin, biocompatibility, and high tunability. These ILs can be tailored by selecting different amino acids and appropriate counterions to allow the design of ILs with specific properties.[39, 42-43]

Amino acid ionic liquids derived from choline (ChAAILs), an essential nutrient, have gained considerable interest due to their excellent biodegradability, low toxicity, and versatile applications in catalysis, separations, material synthesis and CO_2 capture.[44-45] The cholinium ion is a convenient, natural, complimentary counter ion for amino acid ionic liquids. In this study, we report a strategy for amino acid incorporation using the aza-Michael reaction facilitated by ChAAILs. Several benefits should accrue from the employment of ChAAILs: the IL provides a suitable reaction environment that promotes the aza-Michael reaction by ionically protecting the carboxylic acid; it further increases the reactivity of the amino groups of amino acids; and acts as its own solvent for a solvent free synthesis.

Furthermore, this methodology offers a streamlined and efficient route to amino acid-functional polymer modification that eliminates the need for protecting groups.

3.3 Experimental

3.3.1 Materials

Hydroxyethyl acrylate (HEA), ethyl acrylate (EA), lysine (Lys), cysteine (Cys), serine (Ser), aspartic acid (Asp), phenylalanine (Phe), leucine (Leu), choline hydroxide (CholOH) 45% in water, glacial acetic acid, deuterated methanol (MeOD), deuterated chloroform ($CDCl_3$), deuterium oxide (D_2O), poly(ethylene glycol) diacrylate (**PEGACR**, M_n ~700 g mol^{-1}), glycerol 1,3-diglycerolate diacrylate (**OHGlyACR**) and all other solvents were purchased from Sigma Aldrich. Acrylate-terminated polydimethylsiloxane (PDMS) (Silmer ACR **Di10**, M_n ~1200 g mol^{-1}), 3-[2-(hydroxy-3-[(1-oxo-2-propenyl)oxy]propoxy)-propyl-terminated PDMS (Silmer ACR OH Di10, **HODi9**, M_n ~1200 g mol^{-1}, were kindly supplied by Siltech Corporation.

3.3.2 Methods

^1H NMR spectra were recorded on a Bruker NEO 600 MHz or NEO 500 MHz nuclear magnetic resonance spectrometer.

3.3.3 Synthesis of ChAAILs (Choline Amino Acid Ionic Liquids): General Procedure

Shown for lysine: Lys (4.0 g, 27.4 mmol) was dissolved in DI water (40 mL), and CholOH (0.9 equiv., 45wt% solution in water, 6.6 mL, 24.7 mmol) was added to the lysine solution and stirred for 72 h at 50 ℃, at which point NMR showed the

reaction was complete. The resulting solution was concentrated by rotary evaporation, then washed with a 1:9 methanol: acetonitrile mixture (15 mL x 3). Excess amino acid(s) were gravity filtered and the resulting solution was then concentrated by rotary evaporation to obtain the choline-lysine ionic liquid (ChLysIL). Aspartic acid (ChAspIL), leucine (ChLeuIL), serine (ChSerIL), phenylalanine (ChPheIL), and cysteine (ChCysIL) choline ionic liquids were prepared following the same procedures for reaction and purification (Table S7.3 and Figure S7.14-7.18).

3.3.4 ChAAIL Acrylates: Aqueous NMR Kinetic Studies

A kinetic study was conducted to compare the reactivity of the simple acrylates HEA and EA with choline ionic liquids made from phenylalanine, leucine, lysine, serine, and aspartic acid, respectively. The ionic liquids, for example ChLeuIL (0.17 mmol, 0.04 g), were weighed into a 1.5 mL centrifuge tube, and dissolved in D_2O (0.7 mL). HEA (0.17 mmol, 18.3 μL) or EA (0.17 mmol, 15.8 μL) were added in the centrifuge tube, respectively, mixed until homogenous and transferred to NMR tube just before NMR spectra were collected (0 min). The reactions were monitored by NMR at 1.5 min intervals for 15 min and then at time points of 30 min, 1 h, 2 h, 4 h, 8 h, 12 h and 24 h (Table S7.4, and Figure S7.19-7.28).

3.3.5 ChAAIL and Acrylate Solvent Free Reactions: General Procedure

Analogous kinetic studies were conducted in the absence of solvents. For example, ChLeuIL (0.20 g, 0.85 mmol) was weighed into a 10 mL vial equipped with a mini stir bar. HEA (0.10 g, 0.85 mmol, 1 equiv.) or EA (0.09 g, 0.85 mmol, 1 equiv.),

respectively, was directly added to the vial and the reaction was allowed to stir for 24 h and monitored at various time points, typically at 30 min, 1 h, 2 h, 4 h, 12 h, and 24 h. NMR was taken in MeOD for the product 'as is' without further purification. Some of the reaction mixtures of ChAAILs with EA were inhomogeneous, in which case the mixture was stirred by hand to produce a homogenous dispersion just before the NMR spectrum was taken (Table S7.4 and Figure S7.29-7.38).

3.3.6 Effect of Added Acids and Bases on aza-Michael Reactivity

3.3.6.1 Acid quench of neutral amino acid

ChPheIL (0.19 mmol, 0.05 g) was weighed into a 1.5 mL centrifuge tube and dissolved in D_2O (0.7 mL). HEA (0.19 mmol, 20.1 μL) or EA (0.19 mmol, 19.9 μL) were added in the centrifuge tube and mixed to homogeneity just before NMR spectra were collected. The reaction was monitored at times 30 min, 1 h and 2 h. AcOH (0.01 g, 0.19 mmol, 1 eq) was then added to the reaction mixture at the 2 h mark. A white precipitate formed. The precipitate was then centrifuged at 14000 rpm for 20 min, the supernatant was collected for NMR, then reactions in the supernatant was monitored again at 30 min, 1 h, 2 h, 4 h, 8 h and 12 h (Table S7.6 and Figure S7.43-7.44).

3.3.6.2 Base addition to acidic amino acids

ChAspIL did not react under the previous reaction conditions. To study the effect of basic conditions, ChAAIL (0.23 mmol, 0.05 g) was weighed into a 1.5 mL centrifuge tube and dissolved in D_2O (0.7 mL). HEA (0.23 mmol, 22.1 μL) was

added to the centrifuge tube and mixed until homogeneity just before NMR spectra were collected. The reaction was then left to react for 24 h; no reaction was observed. At the 24 h time point, ChOH (1 eq, 0.23 mmol, 62.7 μL, or trace, 0.0021 mmol, 0.63 μL) was then spiked into the reaction mixture and NMRs were immediately taken and monitored at 30 min, 1 h, 2 h, 4 h, 8 h, 12 h, and 24 h (Table S7.5 and Figure S7.39-7.42).

3.3.7 ChAAIL Reactivity with hydrophilic PEG: General procedure

Shown for ChLeuIL: ChLeuIL (0.66 mmol, 0.15 g), was weighed into a 10 mL vial, **PEGACR** (0.66 mmol, 209 μL) or **OHGlyACR** (0.66 mmol, 92 mL) were subsequently added into the vial. The mixture was then mixed by hand and a mini stir bar was added to the mixture that was then allowed to stir. The reaction was monitored by ^{1}H NMR at 1 h and 24 h (Table S7.7, Figure 3.4A and Figure S7.45-7.54).

3.3.8 ChAAIL Reactivity with Hydrophobic Silicones General Procedure

Shown for ChLeuIL: ChLeuIL (0.87 mmol, 0.2 g) was weighed into a FlackTek (max 10 g) cup. Silicones, **HODi9** (0.87 mmol, 508 μL) or **Di10** (0.87 mmol, 817 μL), were subsequently added into the FlackTek cup. The mixture was then hand mixed for 5 s followed by speed mixing at 3500 rpm for 1.5 min (Dual asymmetric centrifuge model DAC 150.1 FV7-K). A mini stir bar was then added to the mixture that was allowed to stir during the reaction, which was monitored by NMR at different time points of 30 min, 1 h, 2.5 h, 14 h and 24 h, respectively. In cases where the reaction mixture was inhomogeneous for the **Di10** trials, the mixture was

hand mixed first before NMR samples were taken (Table S7.7 and Figure S7.55-7.64).

3.4 Results and discussion

The reactivity of the nitrogen atom in native amino acids is limited by two factors. Firstly, under neutral conditions, many amino acids are only poorly soluble in aqueous media and have next to no solubility in organic solvents. Secondly, the zwitterionic nature of amino acids causes the amine to be protonated and therefore unable to act as an electron rich nucleophile; our observations show them not to be aza-Michael donors. It was proposed that conversion to an ionic liquid using the natural material choline would address the issues of solubility in aqueous and organic media such as alcohols, as well as enable the ammonium ion to be "deprotected' to act as a nucleophile. Such a change would increase the types and scales of reactions that could be performed with amino acids, eliminate the need for buffer or base catalyst, and also facilitate separation of the products from aqueous mixtures. The counterion of a series of different amino acids was changed to cholinium simply by exposing the relevant ammonium carboxylates to choline hydroxide to give the choline/amino acid ionic liquids ChAAIL (Figure 3.1A).

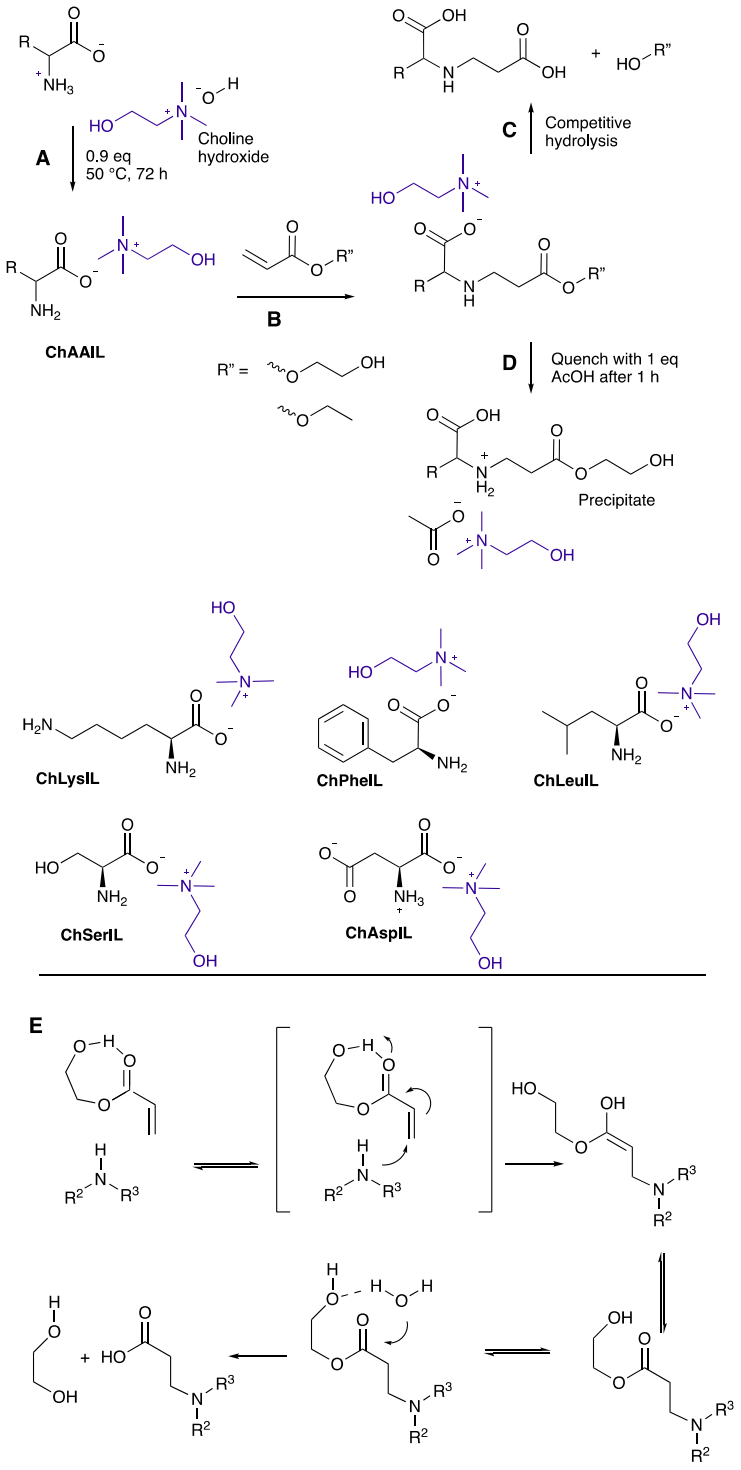

Figure 3.1 A) Formation of ChAAIL; B) aza-Michael reaction; C) undesired hydrolysis that occurs over time; and D) quenching with acid to stop hydrolysis. E) beta-Hydroxy-assisted aza-Michael and ester hydrolysis reactions.

3.4.1 ChAAIL Reactivity with Model Acrylates: Aqueous NMR Kinetic Studies

ChAAILs derived from leucine (ChLeuIL), phenylalanine (ChPheIL), serine (ChSerIL), aspartic acid (ChAspIL) and lysine (ChLysIL), respectively, were reacted with ethyl acrylate (EA) or hydroxyethyl acrylate (HEA), respectively, in D_2O. The reactions were monitored by NMR at 1.5 minutes intervals for 15 minutes and then at time points of 0.5, 1, 2, 4, 8, 12 and 24 hours at room temperature. The disappearance of the acrylate signal in the starting materials at 5.8 ppm to 6.4 ppm were used to monitor reaction progress (Figure S7.19-7.28). The linear regions of the plots were then used to calculate the initial rates of reaction in different media (Figure 3.2A, B). It was found that ChLysIL had the fastest reaction rate of the ChAAILs tested, with 100% conversion after 30 minutes; ChAspIL showed no reactivity in this study. ChLeuIL, ChPheIL and ChSerIL had comparable reactivities, and all reached ~70% conversion after 30 minutes (Figure 3.2C, Table S7.4).

A 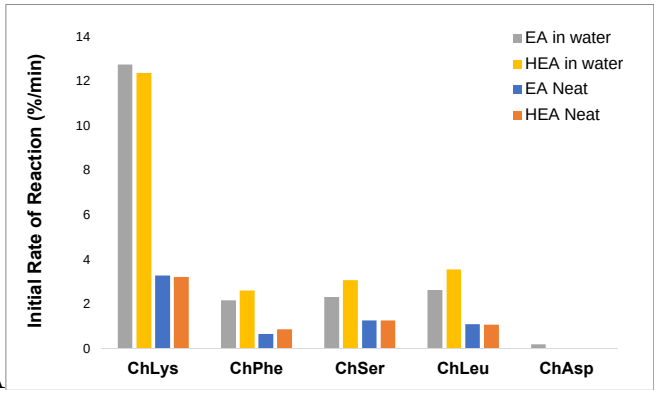

B

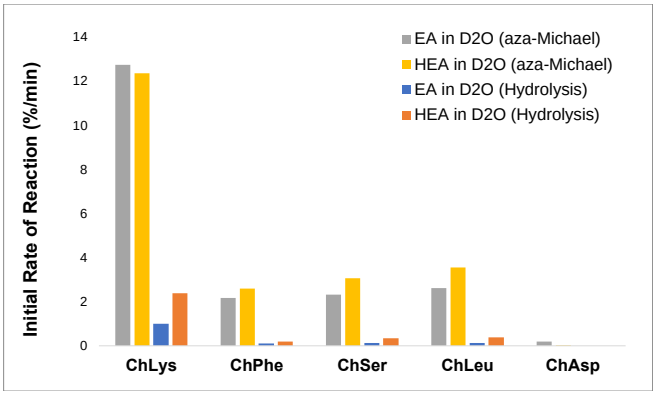

C

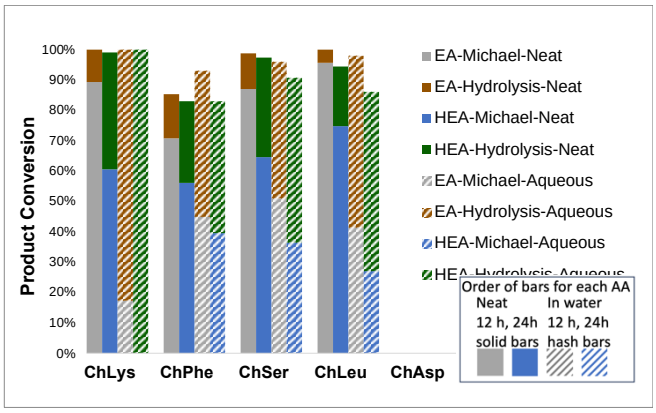

Figure 3.2. NMR kinetic study showing Initial rates of aza-Michael reactions between ChAAILs with EA or HEA. A) Initial aza-Michael product conversion rate comparison between reactions in water or solvent free. B) Initial product conversion rate comparison of aza-Michael reaction and hydrolysis. C) aza-Michael vs hydrolysis product conversion neat and in D2O at 12, 24 h.

The cholinium carboxylate in these amino acids allowed the amine to remain in its deprotonated form, and therefore to act as an aza-Michael donor. It is well known that aza-Michael reactions are accelerated under basic conditions.[27] ChLysIL exhibited the highest reactivity of the ChAAILs tested, which is attributed to the basic side chain that can act both as a base catalyst or a nucleophile. The less

hindered gamma, primary amine in lysine is expected to be the better amine nucleophile of the two present. By contrast, the lack of reactivity for aspartic acid is presumably due to the presence of a second carboxylic acid in the side chain. While one carboxylate has a cholinium counterion, the other carboxylic acid protonates the amine at neutral pH, leaving it with essentially no reactivity towards aza-Michael reactions (see below).

Although the aza-Michael reaction has been shown to be accelerated by proximal alcohol groups in non-polar solvents,[46] the reactivities of EA and HEA, were similar in water (for the five different ChAAILs, after 30 minutes an average conversion of 61% for EA and 63% conversion for HEA was observed). This result is consistent with hydrogen bonding through water masking any acceleration that might otherwise be seen with HEA when compared with EA.

3.4.2 ChAAIL Acrylate Solvent Free Reactions

Native amino acids are solids, which compromises their ability to undergo reactions under solvent free conditions; typically, water or buffer solutions are required. Ionic liquids are used as solvents for many catalyzed reactions,[38] including aza-Michael reactions.[41] To test the hypothesis that an amino acid complexed to choline will act as a self-solvating system, ChAAILs were mixed with an equivalent amount of acrylate, neat, and reactions were monitored by NMR over time (Figure S7.29-7.38). As seen in Figure 3.2A, the reactions occurred at slower rate than in aqueous solutions, which is unsurprising since it is well known that polar protic solvents catalyze the aza-Michael addition.[27] In the absence of

solvent, the general trends on reactivity were similar to those in aqueous conditions, with ChLysIL having the highest reactivity and no observed reactivity for ChAspIL. As expected, when run neat, HEA showed higher initial rate of reaction than the EA analogue, due to beta hydroxy group acceleration (Figure 3.1E).[46] However, the key benefit of utilizing choline as a counterion is the conversion of the amino acid to the liquid state that facilitate reactions without the need for any solvents.

3.4.3 Dealing with Competitive Hydrolysis

The desired aza-Michael reaction (Figure 3.1B) competes with ester hydrolysis of beta-alanine products, especially under basic conditions (Figure 3.1C, E). Partial hydrolysis of both HEA and EA derivatives were observed through a glycol signal detected at 3.6 ppm and ethanol signal at 3.6 ppm and 1.15 ppm, respectively. When the reaction was run in water (D_2O) rates of hydrolysis could be problematic (Figure 3.2B, C). Hydrolysis products already constituted ~50% of the product mixture after 12 hours for most of the ChAAIL, and up to 100% for ChLysIL if left unquenched (Figure 3.2B,C); ester hydrolysis was most rapid for ChLysIL due to the presence of the basic side chain. Hydrolysis is, of course, not desired in normal use but observing these products means that degradation will ultimately occur under relatively benign conditions at end of life.

These reactions were run on the bench without the use of a protective barrier, e.g., a nitrogen blanket. Fortunately, when run neat hydrolysis was much less problematic than in an aqueous solvent; adventitious water was introduced from

moisture in the air. The rates of hydrolysis are about one tenth of those of the aza-Michael reaction, such that one can arrest the process at high aza-Michael conversion without being compromised by hydrolysis (Figure 3.2C).

Although little difference in rates of reaction between EA or HEA educts were observed when reactions were run in water, differences were observed when reactions were run neat. Both the aza-Michael and hydrolysis reactions were accelerated with HEA: hydrolysis product conversion of 8% for EA, and 24% for HEA; in water 46% for EA, 51% for HEA (Figure 3.2C). The beta-hydroxy group acceleration of the aza-Michael may also be responsible for increased rate of ester hydrolysis (Figure 3.1E).

3.4.4 Optimizing Conversion

Fortunately, the aza-Michael reaction rate is about 10-fold faster than product hydrolysis (Figure 3.2), which allows one to control the desired forward reaction and minimize product hydrolysis by a kinetic quench (see next section). A further benefit of solvent free conditions is that hydrolysis was significantly retarded compared to the reaction under aqueous conditions (Figure 3.2C). For example, when left unquenched, 49% hydrolysis was observed after 12 hours in an aqueous environment, but only 16% after 24 hours under solvent free conditions. Thus, it is advantageous to run the aza-Michael reaction under solvent free conditions in terms of improving yield of the desired product and without having to deal with the solvent at reaction end (Figure 3.2C, Table S7.4).

3.4.5 The Special Case of Aspartic Acid: Just Add Base

As noted, ChAspIL had little or no reactivity towards acrylates in either aqueous or neat conditions, which was explained by the protonation of amines from the side chain carboxylic acid. It was hypothesized that base would fully deprotonate the amine or act as a base catalyst for the reaction. A study was designed to test this hypothesis by adding either 1 equivalent or trace (0.01 equiv.) quantities of ChOH to ChAspIL. When 1 equiv. ChOH was, the reaction had high conversion (81% for HEA and 94% for EA) by the time the first NMR was taken at 30 minutes but was accompanied by hydrolysis products (33% after 30 minutes, 92% after 24 hours for EA, Figure S7.39-7.42 and Table S7.5). The addition of catalytic amounts of ChOH showed that the reaction proceeded much slower and to lower conversions (45% for HEA and 24% for EA after 30 minutes). However, the reaction was much more selective and well controlled with lower levels of observed hydrolysis products (2% hydrolysis after 30 minutes and 15% after 24 hours for EA). These model studies demonstrate the requirement for free amines to participate in the aza-Michael reaction with acrylates and further indicated that forming cholinium carboxylates enabled the aza-Michael reaction. These results demonstrate that preferential incorporation of acidic, basic or neutral amino acids on acrylated substrates using the aza-Michael reaction is straightforward.

3.4.6 Reaction Quenching

To further reduce the incidence of product hydrolysis, especially when protic solvents are present, attempts were made to do an acid quench (Figure 3.1D).

ChPheIL was allowed to react with acrylates (EA or HEA) for 1 hour before the reaction was quenched by AcOH, leading to the immediate formation of a white precipitate. It was shown that the aza-Michael products that had already formed were subsequently removed as precipitates (Figure S7.43-7.44, Table S7.6), leaving phenylalanine starting material, choline acetate (ChAcOH), and EA in the reaction mixture. Neither further aza-Michael additions nor hydrolysis reactions were observed after the quench. This result showed that it was very easy for the product to be separated from educts by acidifying the reaction mixture and precipitating the protonated carboxylic acid at the appropriate time (most aza-Michael reactions were complete, hydrolysis was just starting). These behaviors – solubilization, reaction, isolation by precipitation – are advantageous when attempting the controlled synthesis of amino acid-containing polymers. The latter property is particularly beneficial in polymer synthesis, where separation is frequently difficult. To test this hypothesis, the ability to make hydrophilic and hydrophobic amino acid-modified polymers was examined.

3.4.7 ChAAIL Reactivity with Hydrophilic PEG polymers

After gaining an understanding of ChAAIL aza-Michael reactivity with small molecules, ChAAILs were tested in polymeric systems to investigate the feasibility of this method for post polymerization modification of polymers. Polyethylene glycol (PEG) is a generic hydrophilic polymer that has been used in biomedical applications including wound healing,[47] drug delivery[48] or even soft tissue mimics[49] and is available from monomer (1 EG unit) up to molar masses in the

millions (for PEO); acrylate-terminated PEG are commercially available in molar masses up to ~10,000 g mol^{-1}.

ChAAILs were reacted with telechelic, acrylated PEG (**PEGACR**, Figure 3.3A) or glycerol 1,3-diglycerolate diacrylate, which is an acrylated PEG-like structure with proximal OH (**OHGlyACR**). **PEGACR** or **OHGlyACR** reacted with ChAAILs neat in a small vial and were monitored at 1 hour and 24 hours. Amino acid-modified PEG formed from all amino acids, aside from ChAspIL (Figure S7.45-S7.49), following the general reactivity trends shown with small molecules (Figure 3.2, Table S7.7, ChLysIL 99% conversion after 24 hour). The reaction rates were faster for **OHGlyACR** than **PEGACR**, likely due to the beta hydroxy effect (Figure 3.1E).[46] The amino acid polyether products dissolved in water or methanol but not in DCM; there was no evidence of hydrolysis of the products during the reaction period of 24 hours. Product conversion depended on the specific ChAAIL, but conversion over 80% within 24 hours was observed in most cases (Figure 3.4A).

3.4.8 ChAAIL Reactivity with Hydrophobic Silicones

At the other end of the spectrum of polymers, with respect to water solubility, are silicones. Polydimethylsiloxane elastomers are widely used as adhesives, coatings and sealants and as polymeric biomaterials.[50] They are exceptionally water repellent, which makes them extremely difficult to react with hydrophilic molecules like amino acids. The few reported examples of amino acid-modified silicone synthesis required protecting groups, as in the Diels-Alder reaction with

phenylalanine-modified maleimides,[29] or radical catalysts for the thiol-ene reaction of cysteine with vinylsilicones;[6] an inefficient aza-Michael reaction of lysine with acrylates was also described.[6]

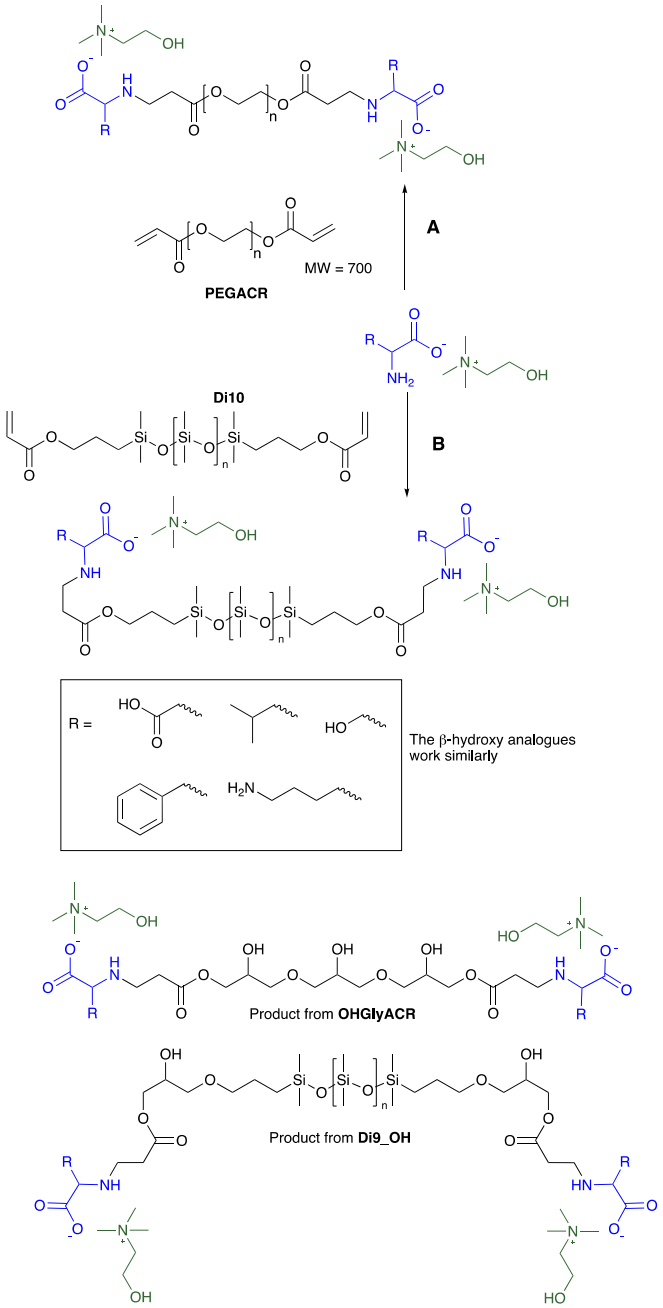

Figure 3.3. Formation of amino acid modified A) hydrophilic and B) hydrophobic polymers. Shown for simple acrylates; the β-hydroxy analogues also work (products shown on the bottom of the figure).

The self-catalyzing ChAAIL readily reacted with either silicone acrylates that possessed a beta hydroxy group (**Di9_OH**) or did not (**Di10**, Figure 3.3B). Here, silicone educts present a huge benefit over other polymers, as they are normally fluids and are therefore self-solvating; the reactions are easy to run neat. With beta hydroxy groups the rate was dramatically increased over simple acrylates, similar to previous reports (Figure 3.1E).[46] It was observed that at the 1 hour time point the **Di9_OH** reaction set had become very viscous liquids, and magnetic stirring stopped as a consequence of the build in viscosity in the case of ChLeuIL, ChLysIL, ChPheIL and ChSerIL; ChAspIL formed a cloudy mixture that did not undergo reaction. Conversions were over 80% in 24 hours, except for ChPheIL that was less effective and ChAspIL that never reacted (Figure 3.4B).

The process was slightly different for the **Di10** reactions, which initially appeared as inhomogeneous mixtures for ChPheIL, ChSerIL and ChAspIL. These mixtures slowly became homogeneous and led to conversions below 50% for ChPheIL and ChSerIL at 24 hours; the reactions here were just slow. By comparison, the ChLysIL and ChLeuIL processes rapidly formed homogeneous mixtures and after 24 hours had undergone almost complete reaction (Figure 3.4B, Table S7.7).

The small molecule reactions reveal the strategies needed to accelerate slow reactions: add base for ChAspIL, add solvents that must eventually be removed, or

be patient. The decisions will hang on the desire for incorporation of a specific amino acid and the ability to ensure neutralization and/or solvent removal at reaction end.

A

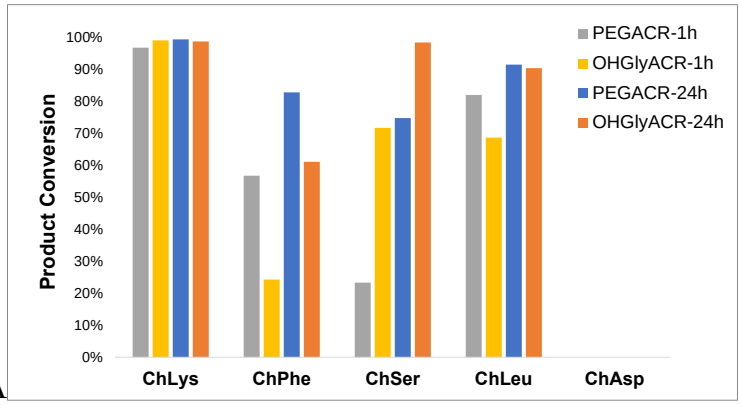

B

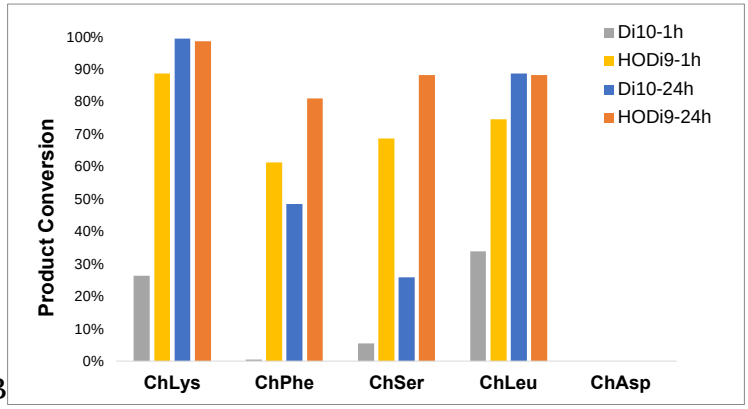

Figure 3.4. Conversion after 1 and 24 hours for formation of ChAAIL polymers from A) PEG or glycerol acrylates and, B) silicone acrylates.

The incorporation of choline amino acid ionic liquids in a silicone increased polymer hydrophilicity and enabled them to have much higher solubility in methanol. The silicone-AA products universally dissolve/disperse in methanol (they form a slightly cloudy solution in DCM due to residual unreacted ionic liquid left in the mixture). It was noted that ChLysIL formed a moldable elastomer that

was soluble in methanol; presumably here crosslinking is provided by ionic linkages.[51] The susceptibility of the ester linkage to hydrolysis was less noticeable in these silicone structures, except in the case of lysine-modified silicones, where traces of hydrolysis were observed after 24 hours. However, no hydrolytic degradation was observed for ChLeuIL, ChPheIL or ChSerIL. This provides further evidence that the hydrolysis rate is dependent on the constitution of the ester; ethyl groups in small molecules were very accessible to hydrolysis, whereas polymer esters effectively inhibited polar solvent access to the ester reaction site. In the case of silicone, the hydrophobicity further inhibited hydrolysis.

The present study expands our understanding of aza-Michael kinetics and product stability for reactions between ChAAILs and various acrylates. The aza-Michael reaction rate is highly dependent on the presence of an excellent nucleophile. Reactions involving basic amino acids, such as lysine, had faster reaction rates because of the free amine, while reactions with acidic amino acids showed no reactivity. The same trend was observed for ester hydrolysis rates after the Michael product was formed, that is, basic amino acids exhibited higher reaction rates but poorer selectivity (Figure 3.2C). The study also compared aqueous reactions with neat reactions and their impact on the reaction kinetics. Polar protic solvents, present in aqueous reactions, increased both the aza-Michael reaction rate and hydrolysis rate due to the abundance of water that promoted hydrolysis. On the other hand, neat reactions, although slower, demonstrated higher selectivity; the limited availability of nucleophiles reduced side reactions, as evidenced by the

relative Michael product and hydrolysis product conversion distribution (Table S7.4 and Figure 3.2C, Figure 3.4). Without solvent, it is fairly straightforward to target the desired product and either time the reaction quench at high conversion, or avoid hydrolysis by a simple acetic acid quench.

The acrylate partner contributed to the rates of both forward reactions and competitive hydrolysis. While no significant difference in aza-Michael reaction rates was observed between smaller acrylates and polymer acrylates, the hydrolysis of polymer esters proceeded at a much slower rate. This might be due to higher intrinsic viscosity or, in the case of silicones, lower water solubility. Acrylates that possess beta-hydroxy groups had higher reactivity for the forward reaction, in line with the expected beta-hydroxy effect (Figure 3.1E) and increased polarity, making them more compatible with ChAAILs. Furthermore, hydrophilic polymers exhibited greater reactivity compared to hydrophobic polymers due to their higher compatibility with ChAAILs. This is exemplified by the comparison of non-OH containing silicones, which exhibit lower reactivity compared to non-OH containing acrylic PEGs (Figure 3.4, Table S7.7).

The aza-Michael reaction is a powerful process for modifying small molecules or polymers. The product, when amino acids react with acrylates, is nominally a dipeptide: a selected amino acid tethered to beta-alanine. Many benefits accrue from performing the process with the aid of choline as a counterion for the amino acid carboxylate, among which the key benefit is solubility. The challenges of getting unprotected amino acids into solution, regardless of whether the medium is

polar or non-polar – even within silicones – is overcome; the process is universal. Conversions are excellent both with small molecules and polymers. The process is intrinsically green in the sense that natural materials (choline, the amino acids) are incorporated into the structure; the reactions do not generate any by-products, protection/deprotection sequences are not required, it has low energy demands with efficient reaction at room temperature and the one challenge it raises – competitive hydrolysis of the ester – is easily managed by forming an acetate buffer with acetic acid. The product zwitterions may be considered for materials applications[52] ranging from dielectric actuators,[53-54] drug delivery,[55-57] anti-biofouling,[58-59] sensors,[60] to flocculants.[61] The utilization of this process holds significant potential for expanding the scope of amino acid-based materials and facilitating their integration into diverse applications more sustainably.

3.5 Conclusions

ChAAILs are easily generated by simply mixing 2 types of natural materials: amino acids and choline hydroxide. The ChAAILs are effective nucleophiles for the aza-Michael addition without the need for solvent or protecting groups; conversions of 83-100% for small molecules based on EA and HEA were obtained after 24h. The undesired competing hydrolysis reaction was about ten times slower than the aza-Michael and its impact could be minimized by eliminating the use of solvent, and/or simply quenching with acetic acid once high conversion of the desired aza-Michael reaction was observed. The flexibility of the process was demonstrated by the ability to incorporate amino acids onto both hydrophilic and

hydrophobic polymers using the same process; issues of solubility were overcome. The features of this reaction: protecting group free, catalyst free, natural starting materials, mild conditions, no solvent, all fit the principles of Green Chemistry and provide viable strategies for incorporating amino acids into many materials.

3.6 Reference

(1) Bongioanni, A.; Bueno, M. S.; Mezzano, B. A.; Longhi, M. R.; Garnero, C. Amino acids and its pharmaceutical applications: A mini review. *Int. J. Pharma.* **2022**, *613*, 121375.
(2) Kissman, E. N.; Neugebauer, M. E.; Sumida, K. H.; Swenson, C. V.; Sambold, N. A.; Marchand, J. A.; Millar, D. C.; Chang, M. C. Y. Biocatalytic control of site-selectivity and chain length-selectivity in radical amino acid halogenases. *Proceedings of the National Academy of Sciences* **2023**, *120* (12), e2214512120.
(3) Bell, E. L.; Finnigan, W.; France, S. P.; Green, A. P.; Hayes, M. A.; Hepworth, L. J.; Lovelock, S. L.; Niikura, H.; Osuna, S.; Romero, E.; et al. Biocatalysis. *Nat Rev Methods Primers* **2021**, *1* (1), 1-21.
(4) Chen, M.; Liu, C.-T.; Tang, Y. Discovery and Biocatalytic Application of a PLP-Dependent Amino Acid γ-Substitution Enzyme That Catalyzes C–C Bond Formation. *Journal of the American Chemical Society* **2020**, *142* (23), 10506-10515.
(5) Agostini, F.; Völler, J.-S.; Koksch, B.; Acevedo-Rocha, C. G.; Kubyshkin, V.; Budisa, N. Biocatalysis with Unnatural Amino Acids: Enzymology Meets Xenobiology. *Angewandte Chemie International Edition* **2017**, *56* (33), 9680-9703.
(6) Camacho Ramirez, A.; Melendez-Zamudio, M.; Guerra Contreras, A.; Brook, M. A. Lysine-Based Silicone Surfactants. *Sustainable Chemistry* **2023**, *4* (2), 197-208.
(7) Infante, M. R.; Pérez, L.; Pinazo, A.; Clapés, P.; Morán, M. C.; Angelet, M.; García, M. T.; Vinardell, M. P. Amino acid-based surfactants. *Comptes Rendus Chimie* **2004**, *7* (6), 583-592.
(8) Leiske, M. N.; Kempe, K. A Guideline for the Synthesis of Amino-Acid-Functionalized Monomers and Their Polymerizations. *Macromol Rapid Commun* **2022**, *43* (2), e2100615.
(9) Nayak, K.; Ghosh, P.; Khan, M. E. H.; De, P. Side‐chain amino‐acid‐based polymers: self‐assembly and bioapplications. *Polym. Int.* **2021**, *71* (4), 411-425.
(10) Gupta, S. S.; Mishra, V.; Mukherjee, M. D.; Saini, P.; Ranjan, K. R. Amino acid derived biopolymers: Recent advances and biomedical applications. *International journal of biological macromolecules.* **2021**, *188*, 542-567.
(11) Rasines Mazo, A.; Allison-Logan, S.; Karimi, F.; Chan, N. J.; Qiu, W.; Duan, W.; O'Brien-Simpson, N. M.; Qiao, G. G. Ring opening polymerization of alpha-amino acids: advances in synthesis, architecture and applications of polypeptides and their hybrids. *Chem Soc Rev* **2020**, *49* (14), 4737-4834.

(12) Zhong, Y.; Zeberl, B. J.; Wang, X.; Luo, J. Combinatorial approaches in post-polymerization modification for rational development of therapeutic delivery systems. *Acta Biomater* **2018**, *73*, 21-37.
(13) Bauri, K.; Nandi, M.; De, P. Amino acid-derived stimuli-responsive polymers and their applications. *Polymer Chemistry* **2018**, *9* (11), 1257-1287.
(14) Mori, H.; Endo, T. Amino-acid-based block copolymers by RAFT polymerization. *Macromol Rapid Commun* **2012**, *33* (13), 1090-1107.
(15) Bao, Y.; He, J.; Li, Y. Synthesis of novel hyperbranched poly(ester-amide)s based on acidic and basic amino acids via "AD + CBB′" couple-monomer approach. *Polymer* **2012**, *53* (1), 145-152.
(16) Zaránd, M.; Szolomájer, J. Amino acids: chemistry, diversity and physical properties. In *Amino Acids, Peptides And Proteins*, Ryadnov, M., Hudecz, F. Eds.; Vol. 42; Royal Society of Chemistry, 2017; pp 1-84.
(17) Leiske, M. N.; Mazrad, Z. A. I.; Zelcak, A.; Wahi, K.; Davis, T. P.; McCarroll, J. A.; Holst, J.; Kempe, K. Zwitterionic Amino Acid-Derived Polyacrylates as Smart Materials Exhibiting Cellular Specificity and Therapeutic Activity. *Biomacromolecules* **2022**, *23* (6), 2374-2387.
(18) Gupta, S. S.; Mishra, V.; Mukherjee, M. D.; Saini, P.; Ranjan, K. R. Amino acid derived biopolymers: Recent advances and biomedical applications. *International Journal of Biological Macromolecules* **2021**, *188*, 542-567.
(19) Bertrand, E.; Gonçalves, C.; Billiet, L.; Gomez, J. P.; Pichon, C.; Cheradame, H.; Midoux, P.; Guégan, P. Histidinylated linear PEI: a new efficient non-toxic polymer for gene transfer. *Chem. Commun.* **2011**, *47* (46), 12547-12549.
(20) Anastas, P. T.; Warner, J. C. *Green chemistry: theory and practice*; Oxford University Press, 1998.
(21) Isidro-Llobet, A.; Álvarez, M.; Albericio, F. Amino Acid-Protecting Groups. *Chemical Reviews* **2009**, *109* (6), 2455-2504.
(22) Vagner, J.; Qu, H.; Hruby, V. J. Peptidomimetics, a synthetic tool of drug discovery. *Current Opinion in Chemical Biology* **2008**, *12* (3), 292-296.
(23) Wiley, R. A.; Rich, D. H. Peptidomimetics derived from natural products. *Medicinal Research Reviews* **1993**, *13* (3), 327-384.
(24) Brisson, E. R.; Xiao, Z.; Franks, G. V.; Connal, L. A. Versatile Synthesis of Amino Acid Functional Polymers without Protection Group Chemistry. *Biomacromolecules* **2017**, *18* (1), 272-280.
(25) Genest, A.; Portinha, D.; Pouget, E.; Lamnawar, K.; Ganachaud, F.; Fleury, E. Zwitterionic Silicone Materials Derived from Aza‐Michael Reaction of Amino‐Functional PDMS with Acrylic Acid. *Macromol. Rapid Commun.* **2021**, *42* (5), 2000372.
(26) Feng, L.; Zhou, L.; Feng, S. Preparation and characterization of silicone rubber cured via catalyst-free aza-Michael reaction. *RSC Advances* **2016**, *6* (113), 111648-111656.
(27) Genest, A.; Portinha, D.; Fleury, E.; Ganachaud, F. The aza-Michael reaction as an alternative strategy to generate advanced silicon-based (macro)molecules and materials. *Progress in Polymer Science* **2017**, *72*, 61-110.

(28) Mather, B. D.; Viswanathan, K.; Miller, K. M.; Long, T. E. Michael addition reactions in macromolecular design for emerging technologies. *Progress in Polymer Science* **2006**, *31* (5), 487-531.
(29) LaRonde, F. J.; Brook, M. A.; Hu, G. Amino acid and peptide chemistry on silicones. *Silicon Chemistry* **2002**, *1* (3), 215-222.
(30) Ferreira, P. M. T.; Maia, H. L. S.; Monteiro, L. S.; Sacramento, J. Michael addition of thiols, carbon nucleophiles and amines to dehydroamino acid and dehydropeptide derivatives. *J. Chem. Soc., Perkin Trans. 1* **2001**, (23), 3167-3173.
(31) Jebors, S.; Ciccione, J.; Al-Halifa, S.; Nottelet, B.; Enjalbal, C.; M'Kadmi, C.; Amblard, M.; Mehdi, A.; Martinez, J.; Subra, G. A new way to silicone-based peptide polymers. *Angewandte Chemie - International Edition* **2015**, *54* (12), 3778-3782.
(32) Chen, H.; Huang, R.; Li, Z.; Zhu, W.; Chen, J.; Zhan, Y.; Jiang, B. Selective lysine modification of native peptides via aza-Michael addition. *Org. Biomol. Chem.* **2017**, *15* (35), 7339-7345.
(33) Huo, Y.; Hu, J.; Yin, Y.; Liu, P.; Cai, K.; Ji, W. Self-Assembling Peptide-Based Functional Biomaterials. *Chembiochem* **2023**, *24* (2), e202200582.
(34) Jang, W.; Kim, D. Y.; Mun, S. J.; Choi, J. H.; Roh, Y. H.; Bong, K. W. Direct functionalization of cell‐adhesion promoters to hydrogel microparticles synthesized by stop‐flow lithography. *Journal of Polymer Science* **2022**, *60* (11), 1767-1777.
(35) Kumar, V. B.; Tiwari, O. S.; Finkelstein-Zuta, G.; Rencus-Lazar, S.; Gazit, E. Design of Functional RGD Peptide-Based Biomaterials for Tissue Engineering. *Pharmaceutics* **2023**, *15* (2).
(36) Hosoyama, K.; Lazurko, C.; Muñoz, M.; McTiernan, C. D.; Alarcon, E. I. Peptide-Based Functional Biomaterials for Soft-Tissue Repair. *Frontiers in Bioengineering and Biotechnology* **2019**, *7*.
(37) Koutsoukos, S.; Becker, J.; Dobre, A.; Fan, Z.; Othman, F.; Philippi, F.; Smith, G. J.; Welton, T. Synthesis of aprotic ionic liquids. *Nat Rev Methods Primers* **2022**, *2* (1).
(38) Steinrück, H.-P.; Wasserscheid, P. Ionic Liquids in Catalysis. *Catalysis Letters* **2014**, *145* (1), 380-397.
(39) Zafarani-Moattar, M. T.; Shekaari, H.; Jafari, P. Structural effects of choline amino acid ionic liquids on the extraction of bovine serum albumin by green and biocompatible aqueous biphasic systems composed of polypropylene glycol400 and choline amino acid ionic liquids. *Journal of Molecular Liquids* **2020**, *301*, 112397.
(40) Ha, K.; Ss, R.; Sp, G. Recent Advancements in Synthesis and Applications of Amino Acid Ionic Liquids (AAILs): A Mini Review. **2018**, *4* (3), 5.
(41) Xu, J.-M.; Wu, Q.; Zhang, Q.-Y.; Zhang, F.; Lin, X.-F. A Basic Ionic Liquid as Catalyst and Reaction Medium: A Rapid and Simple Procedure for Aza-Michael Addition Reactions. *Eur. J. Org. Chem.* **2007**, *2007* (11), 1798-1802.
(42) Wang, W.; Wang, J.; Qiao, C.; Liu, F.; Peng, Q. Amino Acid Ionic Liquids as a Potential Adjuvant for Fungicide Formulations: COSMO-RS Prediction and Dissolution Mechanism Elucidation. *ACS Sustainable Chem. Eng.* **2022**, *10* (10), 3295-3310.
(43) Miao, S.; Atkin, R.; Warr, G. G. Amphiphilic nanostructure in choline carboxylate and amino acid ionic liquids and solutions. *Phys. Chem. Chem. Phys.* **2020**, *22* (6), 3490-3498.

(44) Gontrani, L. Choline-amino acid ionic liquids: past and recent achievements about the structure and properties of these really "green" chemicals. *Biophys Rev* **2018**, *10* (3), 873-880.
(45) Zhang, S.; Ma, L.; Wen, P.; Ye, X.; Dong, R.; Sun, W.; Fan, M.; Yang, D.; Zhou, F.; Liu, W. The ecotoxicity and tribological properties of choline amino acid ionic liquid lubricants. *Tribology International* **2018**, *121*, 435-441.
(46) Lu, G.; Yepremyan, A.; Godfrey, S.; Mohr, C.; Herrlein, M.; Brook, M. A. Aza-Michael silicone cure is accelerated by β-hydroxyalkyl esters. *J. Polym. Sci.* **2021**, *59* (17), 1935-1941,
(47) Liu, S.; Jiang, T.; Guo, R.; Li, C.; Lu, C.; Yang, G.; Nie, J.; Wang, F.; Yang, X.; Chen, Z. Injectable and Degradable PEG Hydrogel with Antibacterial Performance for Promoting Wound Healing. *ACS Appl Bio Mater* **2021**, *4* (3), 2769-2780.
(48) Knop, K.; Hoogenboom, R.; Fischer, D.; Schubert, U. S. Poly(ethylene glycol) in drug delivery: pros and cons as well as potential alternatives. *Angew Chem Int Ed Engl* **2010**, *49* (36), 6288-6308.
(49) Kong, X. B.; Tang, Q. Y.; Chen, X. Y.; Tu, Y.; Sun, S. Z.; Sun, Z. L. Polyethylene glycol as a promising synthetic material for repair of spinal cord injury. *Neural Regen Res* **2017**, *12* (6), 1003-1008.
(50) Colas, A.; Curtis, J. Medical Applications of Silicones. In *Biomaterials Science (2nd Ed.)*, 2nd ed.; Ratner, B. D., Hoffman, A. S., Schoen, F. J., Lemons, J. E. Eds.; Elsevier, Inc., 2004; pp 697-707.
(51) Zheng, S.; Chen, Y.; Brook, M. A. Thermoplastic silicone elastomers based on Gemini ionic crosslinks. *Polymer Chemistry* **2020**, *11* (46), 7382-7392.
(52) Qu, K.; Yuan, Z.; Wang, Y.; Song, Z.; Gong, X.; Zhao, Y.; Mu, Q.; Zhan, Q.; Xu, W.; Wang, L. Structures, properties, and applications of zwitterionic polymers. *ChemPhysMater* **2022**, *1* (4), 294-309.
(53) Peltekoff, A. J.; Brixi, S.; Niskanen, J.; Lessard, B. H. Ionic Liquid Containing Block Copolymer Dielectrics: Designing for High-Frequency Capacitance, Low-Voltage Operation, and Fast Switching Speeds. *JACS Au* **2021**, *1* (7), 1044-1056.
(54) Kang, Z.; Yu, L.; Nie, Y.; Zhang, S.; Skov, A. L. L. High-permittivity silicone dielectric elastomers compatible with ionic liquid-grafted chloropropyl-silicone oil. In *Electroactive Polymer Actuators and Devices (EAPAD) XXIII*, 2021/03/22/, 2021; Madden, J. D., Anderson, I. A., Shea, H. R., Eds.; SPIE: Online Only, United States, p 37.
(55) Sun, H.; Chang, M. Y. Z.; Cheng, W. I.; Wang, Q.; Commisso, A.; Capeling, M.; Wu, Y.; Cheng, C. Biodegradable zwitterionic sulfobetaine polymer and its conjugate with paclitaxel for sustained drug delivery. *Acta Biomater* **2017**, *64*, 290-300.
(56) Jin, Q.; Chen, Y.; Wang, Y.; Ji, J. Zwitterionic drug nanocarriers: a biomimetic strategy for drug delivery. *Colloids Surf B Biointerfaces* **2014**, *124*, 80-86.
(57) Harijan, M.; Singh, M. Zwitterionic polymers in drug delivery: A review. *J Mol Recognit* **2022**, *35* (1), e2944.
(58) Woitschach, F.; Kloss, M.; Schlodder, K.; Rabes, A.; Morke, C.; Oschatz, S.; Senz, V.; Borck, A.; Grabow, N.; Reisinger, E. C.; et al. The Use of Zwitterionic Methylmethacrylat Coated Silicone Inhibits Bacterial Adhesion and Biofilm Formation of Staphylococcus aureus. *Front Bioeng Biotechnol* **2021**, *9*, 686192.

(59) Bengani-Lutz, P.; Converse, E.; Cebe, P.; Asatekin, A. Self-Assembling Zwitterionic Copolymers as Membrane Selective Layers with Excellent Fouling Resistance: Effect of Zwitterion Chemistry. *ACS Appl Mater Interfaces* **2017**, *9* (24), 20859-20872.
(60) Liu, C.; Li, F.; Li, G.; Li, P.; Hu, A.; Cui, Z.; Cong, Z.; Niu, J. Zwitterionic Hydrogel Electrolyte with Tunable Mechanical and Electrochemical Properties for a Wearable Motion and Thermal Sensor. *ACS Appl Mater Interfaces* **2022**, *14* (7), 9608-9617.
(61) Arun, Y.; Daifa, M.; Domb, A. J. Polyhydroxamic acid as an efficient metal chelator and flocculant for wastewater treatment. *Polymers for Advanced Technologies* **2020**, *32* (2), 842-852.

Chapter 4. Cholinium Amino Acid Ionic Liquid-Modified Silicones for Dielectric Elastomer Actuation[2]

4.1 Abstract

The development of suitable materials for soft-robotic and artificial muscle applications has driven intense research efforts. Dielectric elastomers actuators (DEAs) offer promising potential in transforming electrical signals into mechanical movement. Silicone stands out as a key material for these devices due to high response rate, low viscous loss, and durability. However, its relatively lower dielectric permeability poses challenges in artificial muscle applications. To address this, various studies have explored the incorporation of polar groups into silicone networks, including ionic liquids, to improve dielectric permeability. This study investigates the utilization of cholinium amino acid ionic liquids (ChAAILs) as crosslinkers for silicone dielectric elastomers that can convey polar/ionic interactions using natural materials. Different amino acid-based ionic liquids provided different enhanced levels of dielectric permittivity. Partially degraded ChAAIL-modified silicones exhibit significantly higher dielectric permittivity, suggesting opportunities for controlled actuation by managing the degradation rate.

4.2 Introduction

Elastomeric Dielectric Actuators (DEA) are able to transform electrical signals to mechanical movement. These materials are undergoing intense research investigation for their potential utility in soft-robotic and for artificial muscle. DEAs consist of two

[2] This chapter will require further experimentation before it can be submitted for publication. A manuscript structure was chosen to facilitate its ultimate submission to a journal.

components: a thin soft semiconductive elastomer; and two compliant electrodes that are assembled so that the elastomer is sandwiched between the electrodes. When voltage is applied to the system, the charge that builds up on the electrodes will deform the elastomer to transfer the applied electrical energy to mechanical energy; this movement is called actuation. There are three parameters that dictates the performance of DEAs: the relative permittivity (ε_r); which determines the ability for the semiconductive material to respond to electrical energy; Young's modulus; and dielectric breakdown strength. The actuation can be described by eqn (1).[1,2]

$$s = \frac{\varepsilon_0 * \varepsilon_r}{Y}\left(\frac{V}{d}\right)^2 \qquad (1)$$

Elastomers that meet the conditions of low Young's modulus, high relative permittivity and dielectric breakdown strengths are ideal candidates for soft-robotic applications. The most popular materials for DEA are polyacrylates and silicones. The latter polymers are superior to their competitors due to high response rate, low viscous loss, and high durability over large number of actuation cycles. However, silicones suffer from comparatively lower dielectric permeability, which requires high voltages to achieve actuation.

The need for high voltage can be problematic per se, and particularly in applications such as artificial muscle, where human biology is involved.[3] Numerous research studies on improving dielectric permeability of silicone DEA have been reported by Skov and coworkers,[3–10] most of which involve introducing polar groups in the form of liquid fillers, solid fillers, and/or chemically modifying the network. In all cases, it was demonstrated

that the incorporation of polar groups like ionic liquids, glycerol, TiO_2 and dipole rich co-polymers into the elastomer network led to increases in dielectric permeability.[3–10]

Solid fillers can significantly improve the dielectric permittivity of dielectric elastomers, however, due to inhomogeneity and mechanical reinforcement,[8] the dielectric breakdown strength typically decreases, and Young's modulus increases, referring to equation (1); one would instead prefer lower resistance to motion.

Ionic liquids (ILs) are highly polar salts that are in liquid form at room temperature. ILs containing imidazolium ions are the most common ionic liquids being studied.[11] They may be incorporated as virgin liquids[2] or covalently grafted onto silicone oil as additives to silicone DEAs.[12] The resulting materials were shown to have increased dielectric permittivity as a benefit,[6,13] and encouragingly, Young's moduli were shown to decrease when this IL was incorporated into the silicone network. Although this approach solves the hardening problem, the high polarity difference between the silicone and ionic liquid remains an issue, as phase separated domains of phase can lead to a decrease in dielectric breakdown strength and low elongation at break. To address this, in the most recent study by Kang et al., difunctional imidazole was used as a crosslinker for silicone dielectric elastomers and shown to lead to a significant improvement in compatibility while also leading to improvements in dielectric properties.[14] However, multistep synthesis was required for this approach.

We previously reported the uses of the aza-Michael reactivity of cholinum amino acid ionic liquid (ChAAIL) to create silicone elastomers by reacting with silicone acrylates; acrylated silicones that possess beta-hydroxy groups were particularly reactive. To further

investigate the utility of the resulting ChAAIL-modified silicone polymers the present study examines the different formulations of ChAAIL-modified silicone oils and elastomers as potential constituents in DEAs.

4.3 Experimental

4.3.1 Materials

Lysine (Lys), cysteine (Cys), aspartic acid (Asp), leucine (Leu), choline hydroxide (CholOH, 45%wt water solution), deuterated chloroform, deuterium oxide, methanol and acetonitrile and all other solvents were purchased from Sigma Aldrich. 3-[2-(Hydroxy-3-[(1-oxo-2-propenyl)oxy]propoxy)propyl group-terminated PDMS (Silmer ACR OH Di10, **Di9_OH**, M_n ~1200 g mol^{-1}, Silmer ACR OH **Di25_OH,** M_n ~2600 g mol^{-1}, Silmer ACR OH **Di50_OH,** M_n ~4000 g mol^{-1}, Silmer ACR OH **Di400_OH,** M_n ~25000 g mol^{-1}), 3-[2-(hydroxy-3-[(1-oxo-2-propenyl)oxy]propoxy)propyl dimethyl copolymer PDMS (Silmer ACR OH D25, M_n ~8000 g mol^{-1}, **PACR4**) were kindly supplied by Siltech Corporation. Aminopropylmethyl-terminated polydimethylsiloxane (DMS-A21, 5000 g mol^{-1}, **TA67**) and 6-7% aminopropylmethylsiloxane, dimethylsiloxane copolymer (AMS-162, 4500 g mol^{-1}, **PA6**) were purchased from Gelest.

^{1}H NMR spectra were recorded on Magritec spinsolve 80 ultra multiX benchtop NMR,

4.3.2 Methods

4.3.2.1 Young's modulus

The tensile stress-strain of the elastomers was measured using a material tester (Instron 3340 materials testing system, INSTRON, US). The sample of 3.18 mm width, and

specific length was measured before measurement. The sample was placed between two clamps. The test specimen was elongated uniaxially at 500 mm min^{-1} with respect to length and forced throughout the test to a level of accuracy within ±2% until sample failure at the middle part. Each composition was subjected to 5 tensile measurements which were then averaged. The Young's moduli were calculated by taking the tangent of the stress–strain curve at 2%-10% strain.

4.3.2.2 Dielectric permittivity test

Dielectric relaxation spectroscopy (DRS) was performed on a Novocontrol Alpha-A high-performance frequency analyzer (Novocontrol Technologies GmbH & Co, Germany) operating in the frequency range 10^{-1}–10^{6} Hz at room temperature and low electrical field (~1 V mm^{-1}). The diameter of the tested approximately 1 mm thick samples was 20 mm.

4.3.2.3 Electrical breakdown strength determination

Electrical breakdown tests were performed on an in-house-built device based on international standards (IEC 60243-1 (1998) and IEC 60243-2 (2001)), while film thicknesses were measured through the microscopy of cross-sectional cuts, and the distance between the spherical electrodes was set accordingly with a micrometer stage and gauge. An indent of less than 5% of sample thickness was added, to ensure that the spheres were in contact with the sample. A polymer film of approximately 20mm by 80mm was sandwiched between two plastic moulds with 12 6mm diameter holes and slid between the two spherical electrodes through each hole for measurements. The breakdown was measured at the point of contact by applying a stepwise increasing voltage (50-100 V $step^{-1}$) at a rate of 0.5-1 steps s^{-1}. Each sample was subjected to 10-

12 breakdown measurements, and an average of these values was given as the breakdown strength of the sample.

4.3.2.4 Film preparation

The mixtures were mixed on a FlackTek Inc. DAC 150.1 FVZ-K SpeedMixer™. The uniform mixtures thus made were coated on a polycarbonate substrate using a film applicator (3540 bird, Elcometer, Germany) with adjustable blade ranging from 100 um to 500 um.

4.3.3 Amino acid supramolecular crosslinked silicones: General Procedure

Shown for **Di9_OH: Di9_OH** (2.00 g, 3.22 mmol) was added to lysine (0.157 g, 1.07 mmol) in a 20 mL vial equipped with stir bar. A catalytic amount of water (0.019 g, 1.07 mmol) was added, and the reaction was stirred for 14 h to yield an opaque yellow elastomer behaving solid (**Lys_Di9OH**). **Di25_OH** (2 g, 1.54 mmol), lysine (0.075 g, 0.51 mmol) and water (0.019g, 1.07 mmol) were mixed and stirred for 24 h; **Di50_OH** (2 g, 0.99 mmol), lysine (0.048 g, 0.33 mmol) and water (0.019 g, 1.07 mmol) were stirred for 24 h, in both cases yielded a light yellow, caramel like material; after 72 h the product had an elastomeric feel where elasticity is felt when compressed (**Lys_Di25OH** and **Lys_Di50OH**).

Di400_OH (2 g, 0.16 mmol); lysine (0.023 g, 0.16 mmol); water (0.019 g, 1.07 mmol); after 72 h the reaction mixture was still liquid. More lysine was added to try to push the reaction, but no elastomer was formed even after three more equal portions of lysine was added. (**Lys_Di400OH**)

4.3.4 Thermoplastic behavior

Lysine-crosslinked silicones were tested for thermoplastic behavior. Pieces of **Lys_Di9OH**, **Lys_Di25OH**, and **Lys_Di50OH**, respectively (~0.5 g) were broken into roughly half and placed in a glass Petri dish in contact. The samples were heated at 80 ℃ for one hour. The resulted broken pieces were then placed back together and let sit to cool to room temperature, the resulted product was then tested by hand pulling on the products to determine if the broken pieces were healed.

4.3.5 ChAAIL Synthesis

Lysine (2.0 g, 13.7 mmol) was dissolved in 40 mL of DI water, and 0.9 equivalent of **CholOH** (45% wt solution in water, 3.3 mL, 2.1 mmol) was added in the lysine solution and stirred for 72 h at 50 ℃. The resulting solution then concentrated by rotary evaporation, then washed with 1:9 methanol: acetonitrile; excess amino acids were gravity filtered and the resulting solution was the concentrated by rotary evaporation to obtain the ionic liquid. Aspartic acid (ChAspIL), leucine (ChLeuIL), and cysteine (ChCysIL) ionic liquid were prepared at the same scale (2.0 g) following same procedure for reaction and purification.

4.3.6 ChLysIL crosslinked silicone for dielectric property measurements

4.3.6.1 Direct crosslinking method

Two general methods were used to prepare ChLysIL-crosslinked silicones to be evaluated for their dielectric and physical property measurements. The direct crosslinking of silicone using ChLysIL (**PACR4_XXLys**, XX indicating % mole modification) was done by adding two different amounts of ChLysIL (50 mol% and 100 mol%, the percentage

represent lysine eq to acrylate groups eq, and not based on amine), respectively, depending on the target modification percentage (for 50% modification 0.12 g, 0.5 mmol) in a max 10 g FlackTek cup and followed by addition of **PACR4** (2.0 g, 1.0 mmol) the mixture was hand mixed for 10 s and speed mixed for 45 s for the 100% ChLysIL modification and 1 min 45 s for 50% ChLysIL modification. The resulting mixtures were, respectively, immediately poured into disk molds (approximately 1 mm height, 20 mm diameter) or onto a polycarbonate surface for film preparation. Films of 100 μm and 200 μm were cast onto a polycarbonate film using an automated film caster, 100 μm films were used for dielectric breakdown measurements and 500 μm films were used for tensile measurements. The samples resulted from the disk mold (1 mm height, 20 mm diameter) was used for dielectric permittivity testing.

4.3.6.2 Three-component crosslinking method

It was found that the curing rate was too rapid to obtain bubble free samples. Therefore, an alternative method with different percentages of linear amino silicone **TA67** was used in order to slow down the crosslinking process. (**TA67_PACR4_XXLys**, XX indicating % mole modification) Different amounts of ChAAIL (12.5%, 25%, 50%, 75mol%, the percentage represent equivalent of lysine to acrylate groups, and not based on amine) was added into a max 10 g FlackTek cup (for 50% loading formulation, 0.12 g, 0.5 mmol), different equivalent amounts of **TA67** (87.5%, 75%, 50%, 25mol%, the percentage represents the equivalents of amine to acrylate groups) was then added to the same cup (for 50% loading formulation, 1.3 g, 0.5 mmol), hand mixed for 10 s and speed mixed for 30 s. **PACR4** (2.0 g, 1.0 mmol) was then added to the resulting **TA67**-ChLysIL

emulsion mixture. The mixtures were then hand mixed for 10 s and speed mixed for 5 s, and then immediately poured into a disk-shaped mold (1 mm height, 20 mm diameter) or onto a polycarbonate film.

4.3.6.3 ChAAIL grafting method

Since the R groups of ChCysIL, ChLeuIL and ChAspIL do not have the ability react like ChLysIL, another formulation was developed where half of the available functional groups on a pendant acrylate silicone were first modified, and the resulting polymers was subsequently crosslinked with a pendant amino silicone (**PA6_PACR4_50AA**, AA indicating the type of ChAAILs used). ChCysIL, ChLeuIL, and ChAspIL (0.5 eq., for ChLeuIL, 0.09 g, 0.4 mmol) were first weighed into a max 10 g FlackTek cup and then **PACR4** (1.5 g, 0.75 mmol) was added. The reaction was stirred overnight, and the resulting homogeneous oil had a honey-like consistency. For ChAspIL, due to poor reactivity caused by side chain ChAspIL, catalytic amount (0.1 mol eq) of ChOH was added to facilitate the reaction. Pendant amino silicone **PA6** (0.4 g, 0.4 mmol) was then added to the reaction mixtures of ChCysIL, ChLeuIL and ChAspIL, respectively. The mixtures were hand mixed for 10 s, then speed mixed for 2 min. The resulting mixture were then immediately poured into a disk mold (1 mm height, 20 mm diameter) or onto a polycarbonate film to case films. Similar formulations were also prepared for ChLysIL. However, since it would crosslink upon exposure to the pendant acrylic silicone **PACR4** the order of addition was modified. ChLysIL (0.09 g, 0.4 mmol) was first mixed with **PA6** (0.4 g, 0.4 mmol), hand mixed for 10 s, and speed mixed for 30 s. The pendant acrylic silicone **PACR4** was then added, and hand mixed for 10 s then speed mixed for 2

s. Films (500 μm thick) of all samples were cast on a polycarbonate surface using an automated film caster using the low-speed setting; the films were used for tensile measurements. The samples prepared in a disk mold (1.0 mm height, 20 mm diameter) were used for dielectric permittivity testing.

4.3.7 Hydrolytic stability of ChLysIL silicone elastomers

Samples of ChLysIL crosslinked silicones using the three-component method (**TA67_PACR4_12.5Lys**, **TA67_PACR4_50Lys**, and **TA67_PACR4_75Lys**) were left in air over one month, and additional dielectric permittivity measurements were performed on samples showed softening. Further hydrolytic stability tests were performed by placing of ChLysIL (~ 0.5 g) in a 250 mL round-bottomed flask with DI water (100 mL of) equipped with a stir bar. The reaction mixture was reflexed overnight.

4.4. Results and discussion

4.4.1 Lysine-modified silicone synthesis gives thermoplastic elastomers

The reaction between lysine and silicone acrylates generated soft elastomers with hardness that depended on the starting chain length of the acrylic silicone with a lysine/ acrylate ratio of 1:2 (**Lys_Di9, 25, 50, and 400OH,** Figure 4.1). The observed crosslinking can be explained by an increase in viscosity due to chain extension, and a combination of hydrogen bonding interactions and ionic interactions between the carboxylic acid and the amine (carboxylate and ammonium) groups on lysine, which can bridge adjacent chains.[15] These weak dynamic interactions give the materials thermoplastic properties; once heated at 80 ℃ for one hour, the materials became moldable (Figure 4.2). Chain extended polymers derived from telechelic **Di9OH**,

Lys_Di9OH, with its shorter chain length and higher ionic density, was more rigid than either **Lys_Di25OH** or **Lys_Di50OH**. After heating at 80 ℃ for one hour, the broken **Lys_Di9OH** elastomer had not completely healed, but the other two completely healed, and the healing site showed no weakening, as the elastomer was able to be stretched by hand to ~300% for **Lys_Di25OH** and **Lys_Di50OH** and the elastomer did not break at the previously broken site. (Figure 4.2) **Lys_Di400OH** was never crosslinked due to low lysine content, nevertheless the sample had increased viscosity. Even though covalent crosslinking is not present, the hydrogen bonding and ionic interactions between amino groups and carboxylic acid groups of lysin create a supramolecular crosslinked material with thermoplastic properties.

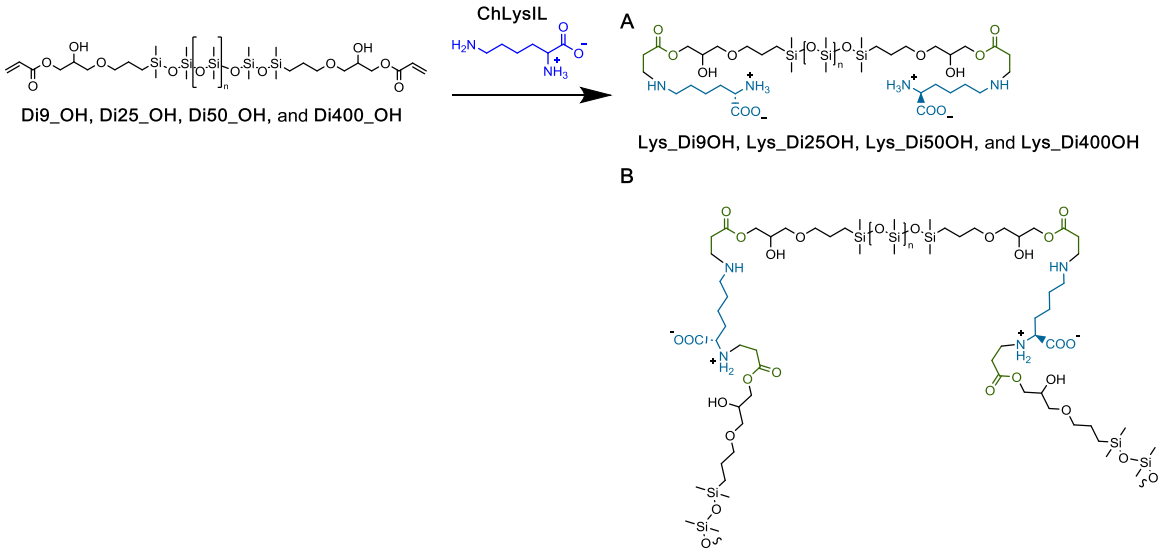

Figure 4.1. Synthesis of **Lys_Di9OH**, **Lys_Di25OH**, **Lys_Di50OH**, and **Lys_Di400OH**, as proposed structure A) telechelic modified for **Lys_Di400OH** or B) chain extended for **Lys_Di9OH**, **Lys_Di25OH** and **Lys_Di50OH.**

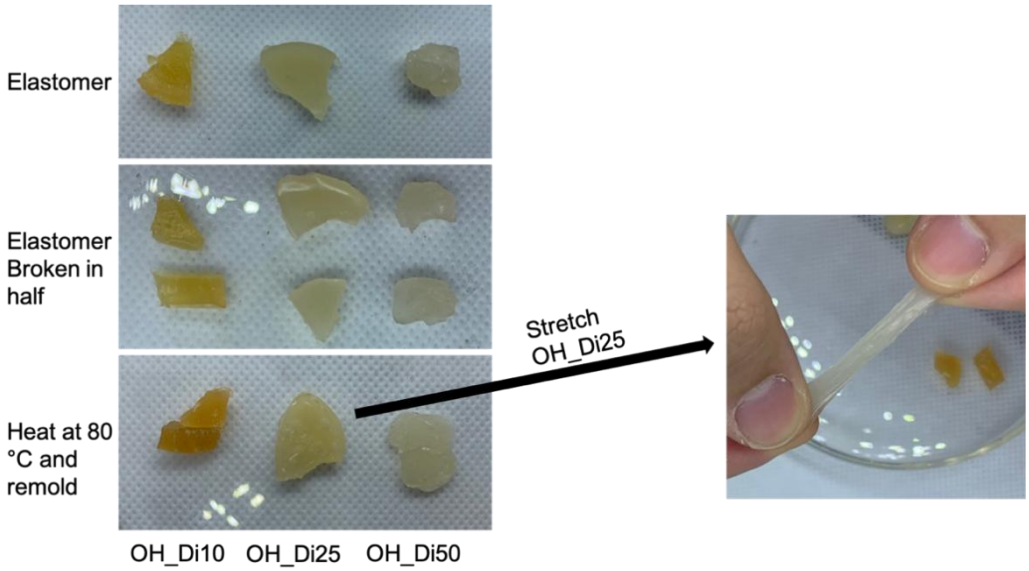

Figure 4.2. Qualitative thermoplastic behaviour of lysine modified acrylic silicones. ~ 300% elongation by estimate.

4.4.2 Covalently crosslinked lysine-modified (ChLysIL) silicones

4.4.2.1 Direct crosslinking method

The amino acid can be used for the covalent crosslinking when pendent silicone acrylate (**PACR4**) is used (Figure 4.3A). The elastomer can be readily prepared by simply mixing ChLysIL and **PACR4**. For example, at 50% loading (1:2 ratio lysine: acrylate), silicone acrylates yielded clear, bubble-free elastomers and films under mild conditions (**PACR4_50Lys**, Figure 4.4A). Note that efficient mixing is required and, if care is not taken, bubbles can be entrapped during crosslinking. The curing rate of the reaction with starting materials having high acrylate concentrations can be very fast (<1 min). In these cases, inefficient mixing is manifested through cloudy products that are assumed to arise from inefficient reactions between the ChAAIL and the silicone leading to 2 phases in the elastomeric product: silicone-rich and ChAAIL-rich. A slightly cloudy sample

(**PACR4_100Lys,** Figure 4.4B) was formed at 100% loading (1:1 Lysine to acrylate groups), this cloudiness attributed to that each lysine can react twice and leaving some amount of ChlysIL in its free form and causing the cloudiness.

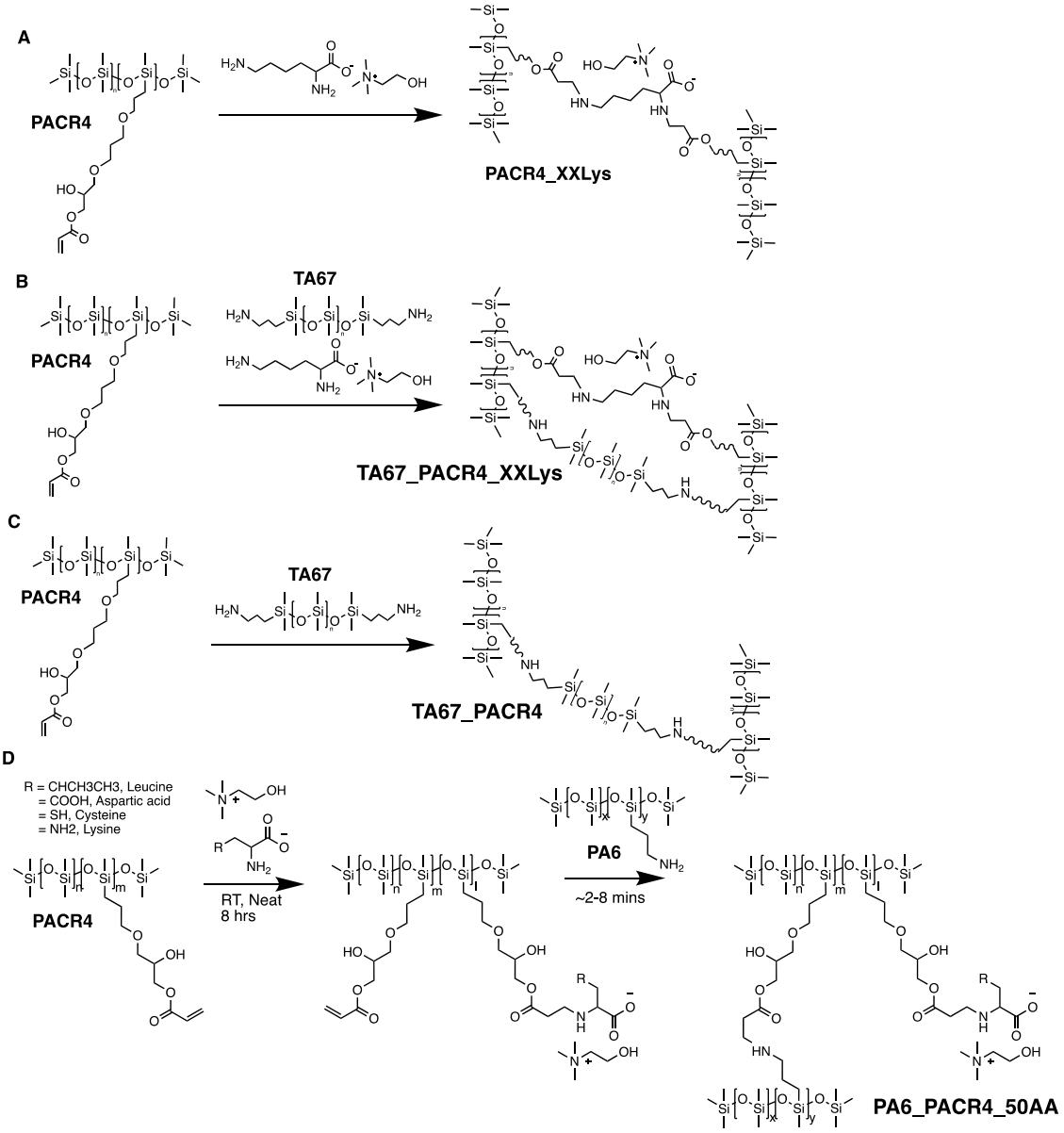

Figure 4.3. Silicone dielectric elastomer synthesis through A) Direct synthesis method with pendant acrylic silicone with ChAAIL. B) Three component synthesis method with

pendant acrylic silicone with telechelic amino silicone and ChAAIL. C) Non-ChAAIL containing control.

A 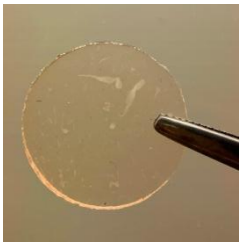 B 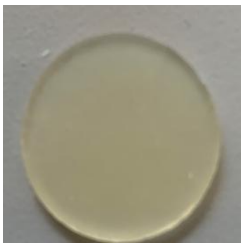

C

Figure 4.4. A) **PACR4_50Lys**, 50% ChLysIL crosslinked silicone by direct crosslinking method B) **PACR4_100Lys**, 100% ChLysIL crosslinked silicone by direct crosslinking method C) From left to right, **TA67_PACR4_12.5Lys**, **TA67_PACR4_25Lys**, **TA67_PACR4_50Lys**, **TA67_PACR4_75Lys**. 12.5%, 25%, 50%, and 75% ChLysIL crosslinked silicone by three component crosslinking method.

4.4.2.2 Three-component crosslinking method

An alternative strategy to slow the cure rate and facilitate bubble-free elastomer preparation involved use of telechelic amino silicones as a co-crosslinker that, at the same time, diluted the amine concentration (Figure 4.3B). This also allowed all the excess acrylates to react with the aminosilicones when lower quantities of ChLysIL were present. These reactions resulted in nice elastomers (**TA67_PACR4_12.5, 25, 50, and 75Lys,** Figure 4.4C) with increasing in cloudiness as the loading was higher. Non-ChAAIL containing elastomer controls are formed through this formulation when ChLysIL is not added (Figure 4.3C)

4.4.2.3 ChAAIL grafting method

When the amino acids ChCysIL, ChLeuIL and ChAspIL participated in the reactions with silicone acrylates, alternative crosslinking strategies were needed because the R group does not possess a second nucleophile as lysine does. (**PA6_PACR4_50Leu, Asp** and **Cys,** Figure 4.3D) The ChAAILs were first reacted with **PACR4**, since each chain average of four acrylic units, half of the acrylate (50% modification, 1:2 eq amine: ACR) was first performed to give viscous liquids (similar to liquid honey). The resulting oil was then mixed with a pendant aminosilicone **PA6** to give the elastomers shown in Figure 4.5. Among the amino acids tested, leucine, the most hydrophobic amino acid had the best compatibility with the hydrophobic silicones; the product was a clear elastomer. ChLysIL followed a slightly different protocol, since it crosslink by itself with PACR4, for consistency in formulation, ChAAIL was added together with **PA6** and **PACR4**, in similar fashion as three-component method, and yielded nice yellow elastomers (Figure 4.5)

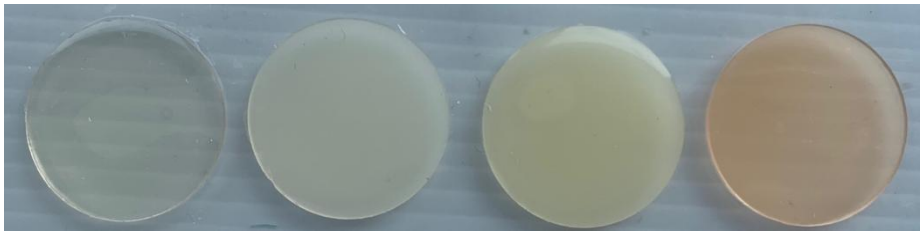

Figure 4.5. The resulted ChAAIL Elastomer from the grafting method, from left to right, **PA6_PACR4_50Leu**, **PA6_PACR4_50Asp**, **PA6_PACR4_50Lys** and **PA6_PACR4_50Cys** silicone elastomer.

4.4.3 Young's modulus data

The ChLysIL crosslinked silicone did slightly increase in Young's modulus compared with **TA67** crosslinked control (Figure 4.3C, Figure 4.6), this is an expected result since that the length of crosslinker ChLysIL is significantly shorter and less flexible than **TA67**. Otherwise, there was no direct trend different types of ChAAILs that crosslinked pendent aminosilicone and Young's modulus. This result is not ideal – we hoped for a reduction in modulus – but the difference is not significant enough to pose an issue for the use in potential actuator.

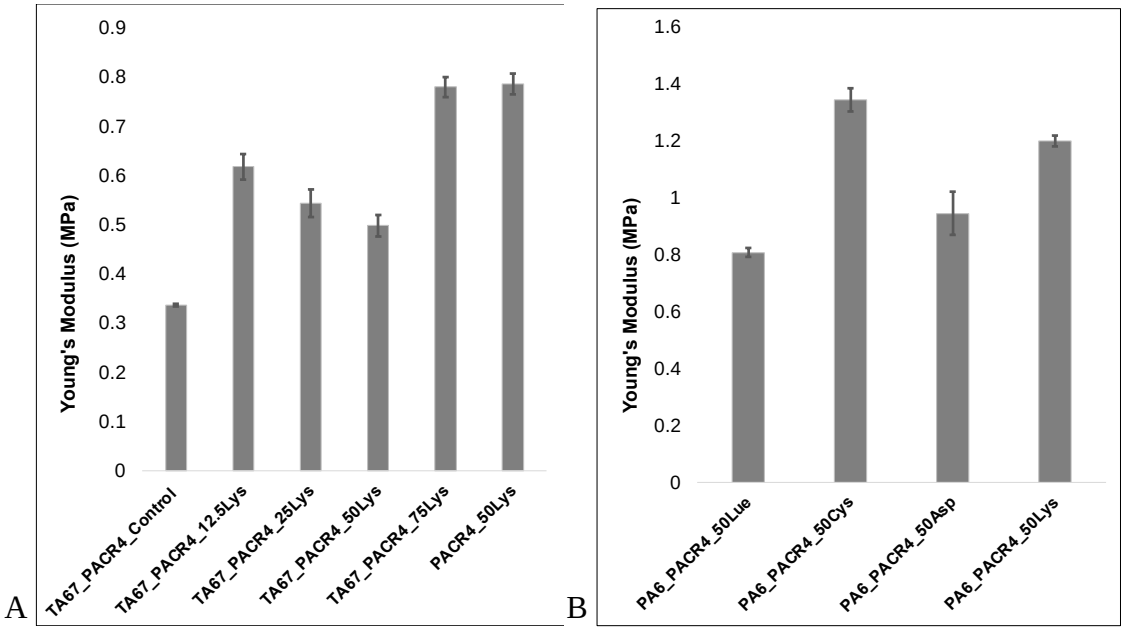

Figure 4.6. Young's Modulus data for A) ChLysIL crosslinked silicone elastomer with different loading. B) Different types of ChAAIL modified silicone at 50% loading.

4.4.4 Dielectric permittivity

It was hypothesized that the dielectric permittivities of silicones modified with amino acid ionic liquids and mobile choline counterions could be competitive with unmodified silicone elastomers. Initially, the permittivities of different types of ChAAILs were surveyed (Figure 4.7A). As can be seen, there are large differences at low frequency, but much smaller differences as frequencies increased. The lysine derivative, ChLysIL, was an outlier at higher frequencies and, therefore, this compound was examined in more detail at a variety of loadings in the silicone (Figure 4.7B). A separate graph showing more direct comparison of dielectric permittivity against molar % of ChLysIL may be found in Figure 4.7B.

A 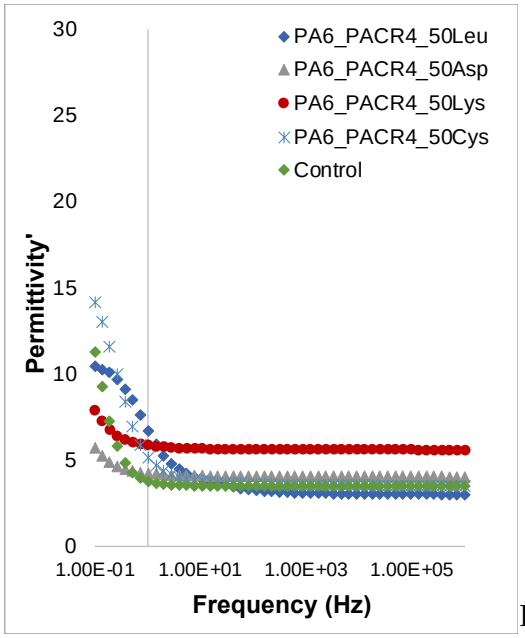

B 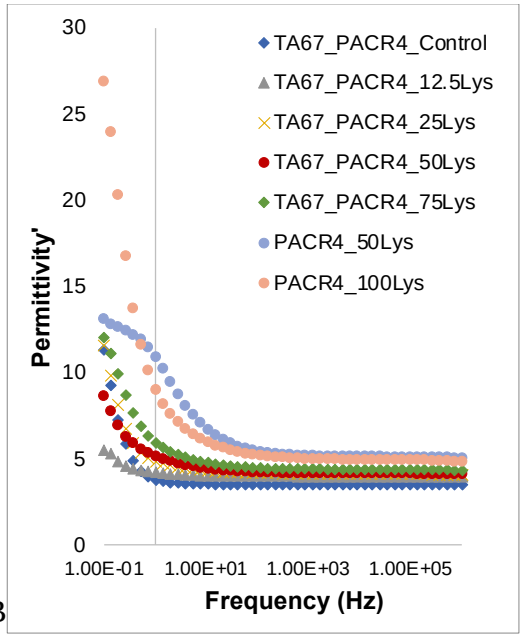

Figure 4.7. Dielectric permittivity comparison between A) Silicone dielectric elastomer with different types of ChAAILs incorporated. B) Silicone dielectric elastomer at different ChLysIL loadings.

A 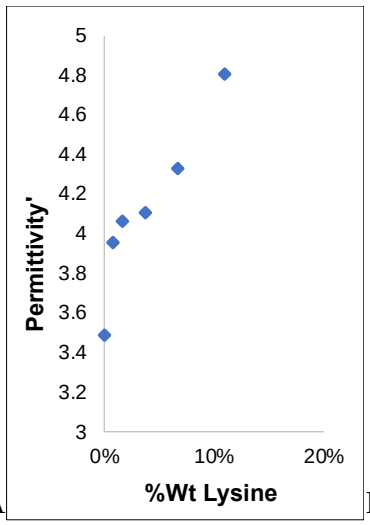

B 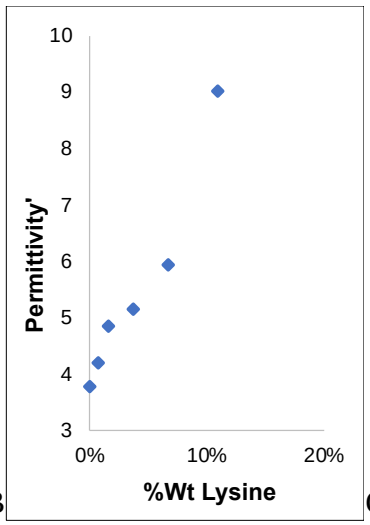

C 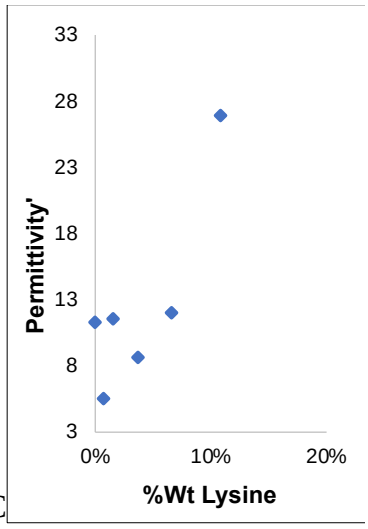

Figure 4.8. Dependency of dielectric permittivity on ChLysIL content (Wt %) at different frequencies A) 10^6 Hz, B) 1 Hz, and C) 0.1 Hz. Note the y axis is in different scales.

Figure 4.7B and Figure 4.8 show that the dielectric permittivity increases with an increase in ChLysIL content. At a high oscillating frequency, the overall polarity of the elastomer is manifested, and mobile polar groups (possible free ionic liquids) have no time to reorient themselves to increase the overall dipole moment. At 1 Hz, depending on the size and mobility of the polar molecules, the time frame is long enough for some molecules to reorient themself to show an overall increase in dipole moments and in turn increase the overall dielectric permittivity of the material. At 0.1 Hz, most polar molecules in the matrix will have time to undergo reorientation to exert an effect on the overall dielectric permittivity. However, the lack of a trend (Figure 4.8C) is likely due to the surface charging effects that exist to some degree for most of the elastomer samples with slight surface defects, especially at low ionic loadings where the increase in dielectric permittivity is not significant enough compare to the common surface charging effect. On both graphs one can see that at 1 Hz most curves have started to have an increase in dielectric permittivity. This may indicate that the ChAAILs tethered onto the silicone chains started to gain enough mobility and contribute more significantly to the overall dielectric permittivity, and at 0.1 Hz the slight cloudy samples that had possible unreacted ChAAILs, especially at very high ChAAIL loading of 100%, which may contain higher amount of unreacted ChAAIL, the dielectric permittivity dramatically increased at <1 Hz range. However, for 50% ChLysIL loading where a homogeneous sample was able to be obtained, at < 1 Hz region it plateaued. This indicate that when elastomer appears homogenous, all ChLysIL could efficiently incorporated into the elastomer system, and no free ChLysIL dipole migration was observed. In Figure 4.7B, similar effect was

observed, where the most homogeneous elastomer made out of ChLeuIL had the similar plateau at < 1 Hz region, despite having the lowest dielectric permittivity at high frequency, and this was attributed to the lack of polar R group out of the other three amino acids. Interestingly ChAspIL which contained a negatively charged R group had the lowest dielectric permittivity which was comparable to the control where no ionic liquid was incorporated. This is hypothesized to be due to the extra negative charge; it significantly limited the mobility of the Cholinium ion's mobility, which lowered dipole moments, therefore no significant increase in dielectric permittivity was observe. The high base ChLysIL dielectric permittivity is attributed to the difference in preparation, where the three other ChAAILs were first tethered onto **PACR4** and ChLysIL was mixed directly with **PA6** and **PACR4**, which may have rendered more free amine groups of lysine due to the competitive reactions of amino silicone to acrylic silicones. Overall, the results showed a clear trend that with higher ChLysIL content, an increasing in dielectric permittivity was observed, and when higher compatible ChAAIL or on-ratio ChLysIL was used, homogenous elastomers showed plateau effect at low current oscillation frequency, this is ideal since it provide a more controlled system and can provide stability during actual applications. With the insight of ChAspIL trial and the increase in dielectric permittivity when higher amine side chains are exposed, it is hypothesized that the mobility of choline cat ions or total positive charge (free amines) have higher effect on the overall material dielectric permittivity.

4.4.5 Dielectric breakdown strength

Normally, dielectric breakdown strength is expected to decrease with an increase in the concentration of polar groups within the dielectric material.[3,16] As seen in Table 4.1, however, the dielectric breakdown across different loadings of ChLysIL were not dramatically different. The slight decrease at higher loadings is attributed to a thinner sample, which will have more microdefects and therefore a lower breakdown voltage, rather than to intrinsic differences in ion content.

Table 4.1 Dielectric breakdown data for different ChLysIL loadings.

Chapter 1	Breakdown voltage (V/m)	Average thickness (mm)	Standard error (V/m) (n=10)
TA67_PACR4_12.5Lys	47.0	0.096	1.6
TA67_PACR4_25Lys	49.0	0.084	1.4
TA67_PACR4_50Lys	46.7	0.094	1.6
TA67_PACR4_75Lys	53.9	0.067	1.0

4.4.6 Hydrolytic stability affecting dielectric permittivity; A cautionary tale

Some of the samples changed their character after sitting in air for one month. ChLysIL elastomers made with two component method began to flow, while those that were additionally crosslinked with linear amino silicones became softer elastomers, or even gel like, depending on the ChLysIL loading. It was hypothesized that the ester bond shown in Figure 4.9 had hydrolyzed in air over weeks (as was the case overnight at reflux in water (Figure 4.10A).

A comparison was made between the dielectric permittivity of freshly made samples and those that had aged for 1 month. It was noted that at low ChLysIL content (12.5%), no significant difference was observed, but at high ChLysIL content (75%), the aged sample had higher dielectric permittivity at high frequency and an early rise when measured at ~ 1Hz (Figure 4.11C). This data suggests that, as the ChLysIL crosslinked silicone system breaks down, the resulting short chain silicone-containing ionic liquid motif, newly formed glycol pendant silicone and the extra carboxylic acid formed due to hydrolysis on the ChLysIL degradation product all contribute to a higher overall dipole moment and therefore higher dielectric permittivity within the material. The significant increase in dielectric permittivity points to new investigations that would examine the ability to balance permanent crosslinks with fragile crosslinks that, upon hydrolysis, enhance permittivity. This should allow the newly formed elastomer to have stronger response to the given voltage applied. Examining if one use controlled degradation to enhance dielectric permittivity while maintaining sufficient structural integrity in silicon DEAs will form the basis of further studies.

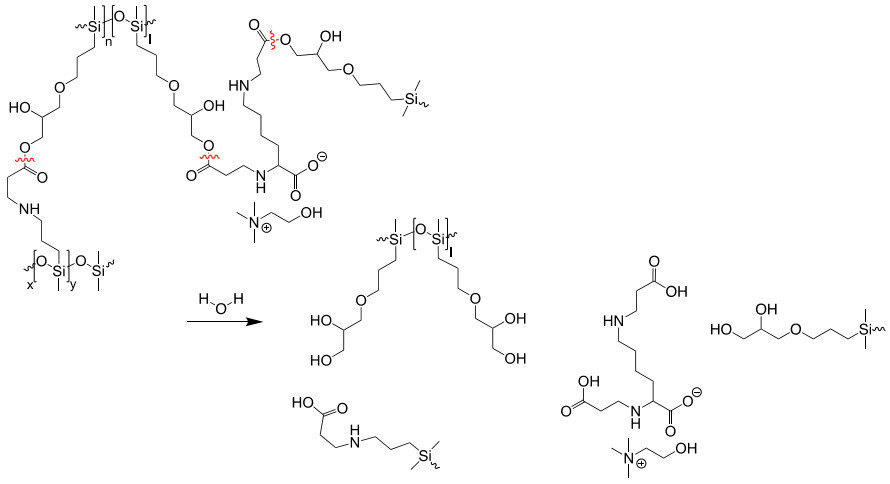

Figure 4.9 Proposed hydrolytic degradation scheme for the ChLysIL crosslinked system.

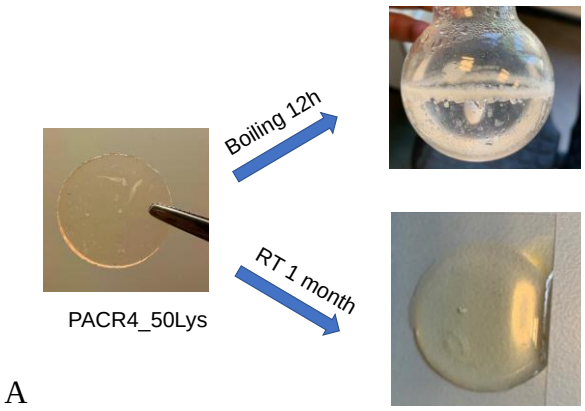

A

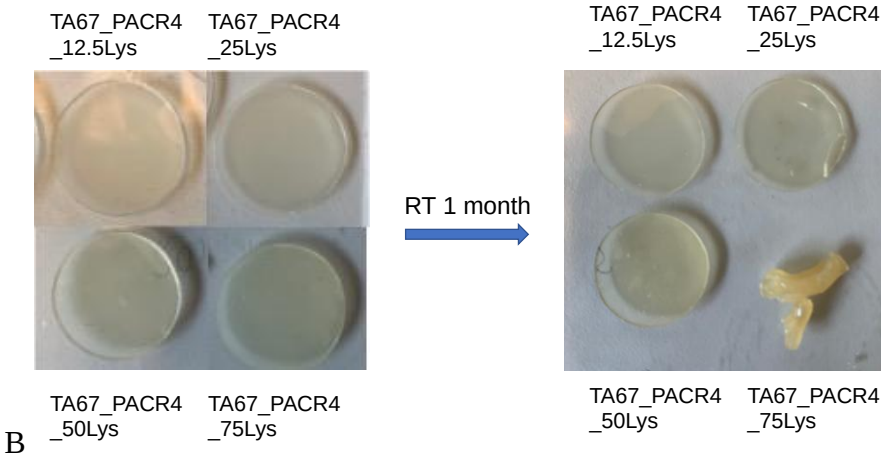

B

Figure 4.10. Pictures of A) Hydrolytic stability of ChLysIL crosslinked through direct method, after reflux in water for 8 hours and room temperature for one month. B) Hydrolytic stability of ChLysIL crosslinked through three component method in room temperature for one month.

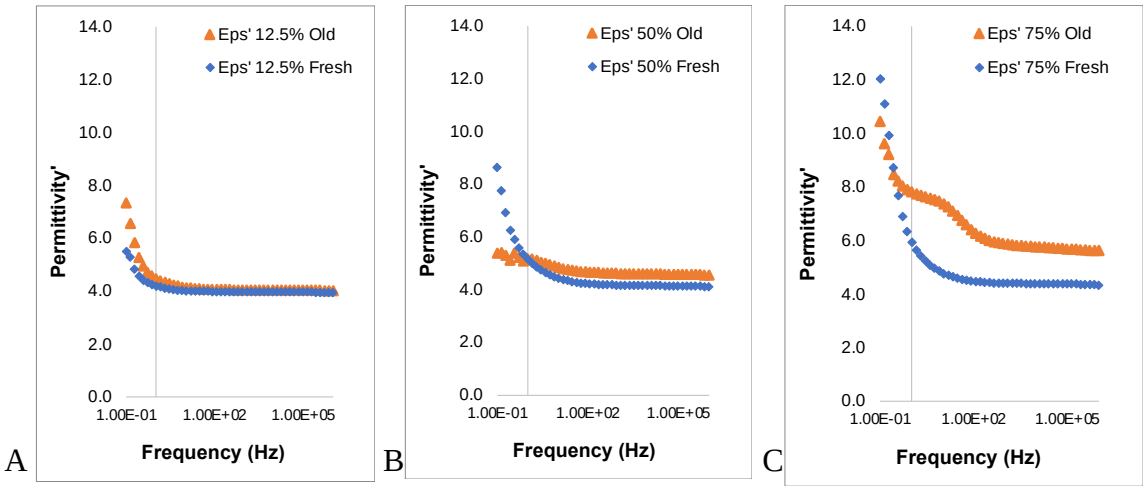

Figure 4.11. A comparison of dielectric permittivity of freshly made and one month old ChLysIL silicones. A) **TA67_PACR4_12.5Lys**, B) **TA67_PACR4_50Lys** and C) **TA67_PACR4_75Lys**.

The dielectric permittivity of the lysine-based ionic liquids shows them to be comparable with other systems in recent literature results. Li et al. demonstrated that utilizing an ionic network of aminosilicone with carboxylic acid silicones led to significantly higher dielectric permittivity.[9] In their pure ionic networks, the dielectric permittivity reached 4500 at 0.1 Hz, which is significantly higher than the highest dielectric permittivity this work achieved at 26.9, but remained comparable at 1 MHz.[14] In their interpenetrating network samples, where the ionic network is combined with commercial silicone and silica filler, which is more similar structure with the three component crosslinked

elastomers, some formulations exhibited comparable results to this study. Specifically, their permittivity values ranged from 6.7 to 13.3, in contrast to the range of 5.5 to 26.9 achieved in this work. The variations in permittivity values depended on the loading or commercial silicone formulation used in the interpenetrating network.

However, the materials described here, based on the natural amino acid, benefit from the ability to undergo degradation to natural materials in the environment. Currently, that degradation is occurring too quickly, but also shows that the degradation products can also lead to enhancement of dielectric response. We plan to further explore these trends to further increase the practicality of these materials in use, including better stability to hydrolysis, and to further enhance their sustainability at end of life.

4.5 Conclusion

The present work investigated the application of cholinium ionic liquid forms of the natural amino acid lysine as a crosslinkers and ionic motifs for a straightforward, solvent-free, and catalyst-free synthesis of silicone dielectric elastomers. Initial data indicates that silicone crosslinked with native lysine demonstrates promising potential as a thermoplastic material, suggesting possible self-healing capabilities for dielectric applications. A more comprehensive study of the dielectric properties of ChAAIL-modified silicone showed that increased loading of ChLysIL led to a significant increase in dielectric permittivity without compromising the dielectric breakdown strength. A comparison among different types of ChAAILs suggested that the increased dielectric permittivity may be attributed to the mobility of cholinium ions or the overall positive charge in the system. An unexpected discovery emerged when partially degraded

ChLysIL crosslinked silicone exhibited significantly higher dielectric permittivity compared to freshly synthesized samples. The work not only presents a simplified and sustainable synthetic pathway for ionic liquid-containing silicone actuators but also offers a prospective avenue for controlled actuation by regulating the degree and rate of degradation in silicone actuators.

4.6 References

(1) Gale, C. B.; Brook, M. A.; Skov, A. L. Compatibilization of Porphyrins for Use as High Permittivity Fillers in Low Voltage Actuating Silicone Dielectric Elastomers. RSC Adv. **2020**, 10 (31), 18477–18486.

(2) Michel, S.; Zhang, X. Q.; Wissler, M.; Löwe, C.; Kovacs, G. A Comparison between Silicone and Acrylic Elastomers as Dielectric Materials in Electroactive Polymer Actuators. Polym. Int. **2009**, 59 (3), 391–399.

(3) Madsen, F. B.; Daugaard, A. E.; Hvilsted, S.; Skov, A. L. The Current State of Silicone-Based Dielectric Elastomer Transducers. Macromol. Rapid Commun. **2016**, 37 (5), 378–413.

(4) Chiaula, V.; Mazurek, P.; Eiler, J.; Nielsen, A. C.; Skov, A. L. Glycerol-Silicone Adhesives with Excellent Fluid Handling and Mechanical Properties for Advanced Wound Care Applications. Int. J. Adhes. Adhes. **2020**, 102, 102667.

(5) Hassouneh, S. S.; Yu, L.; Skov, A. L.; Daugaard, A. E. Soft and Flexible Conductive PDMS/MWCNT Composites. J. Appl. Polym. Sci. **2017**, 134 (18).

(6) Liu, X.; Yu, L.; Nie, Y.; Skov, A. L. Silicone Elastomers with High-Permittivity Ionic Liquids Loading. Adv. Eng. Mater. **2019**, 21 (10), 1900481.

(7) Skov, A. L.; Yu, L. Optimization Techniques for Improving the Performance of Silicone-Based Dielectric Elastomers. Adv. Eng. Mater. **2018**, 20 (5), 1700762.

(8) Yu, L.; Skov, A. L. Silicone Rubbers for Dielectric Elastomers with Improved Dielectric and Mechanical Properties as a Result of Substituting Silica with Titanium Dioxide. Int. J. Smart Nano Mater. **2015**, 6 (4), 268–289.

(9) Yu, L.; Madsen, F. B.; Hvilsted, S.; Skov, A. L. Dielectric Elastomers, with Very High Dielectric Permittivity, Based on Silicone and Ionic Interpenetrating Networks. RSC Adv **2015**, 5 (61), 49739–49747.

(10) Su, J.; Yu, L.; Skov, A. L. Remarkable Improvement of the Electro-Mechanical Properties of Polydimethylsiloxane Elastomers through the Combined Usage of Glycerol and Pyridinium-Based Ionic Liquids. Polym.-Plast. Technol. Mater. **2020**, 59 (3), 271–281.

(11) Correia, D. M.; Fernandes, L. C.; Martins, P. M.; García-Astrain, C.; Costa, C. M.; Reguera, J.; Lanceros-Méndez, S. Ionic Liquid–Polymer Composites: A New Platform for Multifunctional Applications. Adv. Funct. Mater. **2020**, 30 (24), 1909736.

(12) Kang, Z.; Yu, L.; Nie, Y.; Zhang, S.; Skov, A. L. L. High-Permittivity Silicone Dielectric Elastomers Compatible with Ionic Liquid-Grafted Chloropropyl-Silicone Oil. In Electroactive Polymer Actuators and Devices (EAPAD) XXIII; Madden, J. D., Anderson, I. A., Shea, H. R., Eds.; SPIE: Online Only, United States, 2021; p 37.
(13) Liu, X.; Yu, L.; Zhu, Z.; Nie, Y.; Skov, A. L. Silicone-Ionic Liquid Elastomer Composite with Keratin as Reinforcing Agent Utilized as Pressure Sensor. Macromol. Rapid Commun. **2021**, 42 (5), 2000602.
(14) Kang, Z.; Yu, L.; Skov, A. L. A Novel PDMS Dielectric Elastomer Actuator with Bis-Ionic Liquid as Crosslinker. In Electroactive Polymer Actuators and Devices (EAPAD) XXIV; SPIE, 2022; Vol. 12042, pp 335–341.
(15) Tamim, K.; Gale, C. B.; Silverthorne, K. E. C.; Lu, G.; Iao, C. H.; Brook, M. A. Antioxidant Silicone Elastomers without Covalent Cross-Links. ACS Sustain. Chem. Eng. **2023**.
(16) Madsen, F. B.; Yu, L.; Daugaard, A. E.; Hvilsted, S.; Skov, A. L. Silicone Elastomers with High Dielectric Permittivity and High Dielectric Breakdown Strength Based on Dipolar Copolymers. Polymer **2014**, 55 (24), 6212–6219.

Chapter 5. Antioxidant Silicone Curing via an accelerated aza-Michael addition

5.1 Abstract

Vitamin C is widely used as an antioxidant in biological systems. The very high density of functional groups makes it challenging to selectively tether this molecule to other moieties. We report that, following protection of the enediol as benzyl ethers, introduction of an acrylate ester at C1 is straightforward. Ascorbic acid-modified silicones were synthesized via azaMichael reactions of aminoalkylsilicones with the ascorbic acrylate. Viscous oils formed when the amine/acrylate ratios were <1. However, at higher amine/acrylate ratios with pendent silicones a double reaction occurred to give robust elastomers whose modulus is readily tuned simply by controlling the ascorbic acid amine ratio that leads to crosslinks. Reduction with H_2/Pd removed the benzyl ethers, cleaved the crosslinks, and liberated the antioxidant small molecule. These pro-antioxidant elastomers show the power of exploiting natural materials a co-constituents of silicone polymers.

5.2 Introduction

Antioxidants are needed by both biological and synthetic materials for protection against the detrimental effects of oxidative radical species [1–7]. Their presence has been demonstrated to preserve mechanical and other properties of polymers, especially in high oxidative stress environments, including high temperatures or biological environments. Frequently, antioxidants are simply added into a material and their efficacy and longevity depend both on their specific chemistry – their response to oxidative stress [4,7] – and

whether they leach from the material to adjacent media [7,8]. Covalently attaching antioxidants to polymer matrices avoids the latter problem [9–15]. Some simple examples of grafted antioxidants include gallic acid or catechin grafted to gelatin [11], and use of grafted phenolic antioxidants on fuel cells [12] or polyisobutylene [10].

Silicone polymers well known for their biocompatibility, electrical resistance, thermostability, and high oxidative resistance [16]; they are redox insensitive. However, in many of their applications there would be benefit if they could convey antioxidant activity to adjacent materials. For example, biomaterials applications ranging from topical contact lenses / cosmetics products to implanted biomaterials such as breast implants and catheters would benefit from the presence of antioxidants [17]. However, release of any bioactive from the silicone polymer could be disadvantageous [18].

Leivo et al. demonstrated the use of ascorbic acid as a linker between amine-modified silicone elastomer surfaces and collagen for cell culture [19]. The enediol was involved in forming one imine with amines from each entity and, eventually, undergoing oxidative cleavage and ceasing to function as an antioxidant. In essence, ascorbic acid was analogous to, but less toxic than, glutaraldehyde because both can react twice with amine to form imines.

Our objective was to graft ascorbic acid to silicones while maintaining antioxidant activity. Ascorbic acid/vitamin C was chosen as the candidate antioxidant modification to graft to silicones because of its robust antioxidant and antiviral properties [1,5,20,21], which may be due to its redox properties [22]. It is found in a wide variety of fresh vegetables and fruits, and at the highest concentrations in citrus fruits and green leafy vegetables [23]. Due

to the hydrophilic nature of ascorbic acid, it is challenging to incorporate it into very low energy, hydrophobic silicone matrices. We report the formation of more hydrophobic, protected ascorbic acid-modified silicones that can be crosslinked and, when desired, uncrosslinked and deprotected with concomitant release of the antioxidant.

5.3 Experimental

5.3.1 Materials

Potassium carbonate, sodium sulfate benzyl bromide, acryloyl chloride, triethylamine, ascorbic acid (vitamin C), deuterated methanol (MeOD-d_4), deuterated chloroform ($CDCl_3$), Pd/C (palladium, 5%wt. % (dry basis) on activated carbon), EtOAc, hexanes, DMF and all other solvents were purchased from Sigma Aldrich. H_2 (ultra high purity 5.0) was taken from a Praxair gas cylinder. Telechelic aminopropylsilicone **T334** (DMS-A31, 0.11–0.12% mol aminopropylmethylsiloxane, molar mass ~25000 g mol^{-1}); a lower molar mass **P21** (AMS-152, 4-5% mol aminopropylmethylsiloxane, molar mass ~8000 g mol^{-1}) pendent silicone and an analogous higher mass material **P22** (AMS-1203, 20–25% mol aminopropylmethylsiloxane, molar mass ~20000 g mol^{-1}) were purchased from Gelest.

5.3.2 Methods

^{1}H NMR were recorded on Bruker NEO 600 MHz or NEO 500 MHz nuclear magnetic resonance spectrometer. A Shore OO durometer (Rex Gauge Company, Inc. U.S.) was used to characterize the hardness of the elastomer. A centrifuge was used for sedimentation of of charcoal during purification of the hydrogenated product.

5.3.3 Synthesis of benzyl-protected ascorbic acid and modification with acrylate.

Ascorbic acid (6 g, 34 mmol) was dissolved in DMF (20 mL). K_2CO_3 (11.8 g, 85 mmol) was added, and the mixture was stirred for 1 h at 50 ℃. A solution of benzyl bromide (12 g, 70 mmol) in DMF (15 mL) was added dropwise to the ascorbic acid mixture and stirred for 5 h at room temperature. The reaction solution was filtered through a pad of Celite and washed with ethyl acetate. The combined organic phases were extracted with H_2O (100 ml x 3). The organic layer was collected, dried over Na_2SO_4, and filtered. Following concentration by rotary evaporation, the crude product was purified by flash column chromatography (hexanes: EtOAc 1:3 to 1:1) to afford benzylated ascorbic acid (4.3 g, 36%) as light yellow oil. ^{1}H NMR ($CDCl_3$, 600 MHz): 7.41-7.16 (m, 10H), 5.46-5.05 m, 4H), 4.68 (d, J = 2.0 Hz, 1H), 4.10-4.01 (m, 1H), 3.86–3.66 (m, 2H), 3.52 (br, 1H), 3.35 (br, 1H).

To a stirred solution of the benzylated product (4.008 g, 11.3 mmol) in anhydrous CH_2Cl_2 (50 mL) was added and stirred over ice for 10 minutes. Et_3N (1.57 mL, 11.3 mmol) was added to the reaction mixture and let stir for 5 minutes. acryloyl chloride (0.91 mL, 11.3 mmol) was first dissolved in 1o mL of anhydrous CH_2Cl_2 and added into the reaction mixture dropwise over 1 hour. The reaction was stirred for 5h at 0 ℃ and filtered over Celite. The organic layer washed with brine (3 x 40 mL), dried over (Na_2SO_4), and filtered. Following concentration, the crude product was purified by flash column chromatography (hexanes: EtOAc 2 : 1) to afford compound (858 mg, 18.6%) as a white solid (for NMR, see SI).^{1}H NMR ($CDCl_3$, 600 MHz): 7.52-7.29 (m, 10H), 6.57 (dd, J = 17.2, 1.5 Hz, 1H), 6.25 (dd, J = 17.2, 10.3 Hz, 1H), 5.99 (dd, J = 10.3, 1.5 Hz,

1H), 5.38-5.18 (m, 4H), 4.83 (d, J = 1.9 Hz, 1H), 4.49 (qd, J = 11.5, 6.2 Hz, 2H), 4.33-4.17 (m, 1H), 3.06 (br, 1H).

5.3.4 Reactions with benzylated acryl ascorbic acid by butyl amine (Bn2AA)

Benzylated acryl ascorbic acid **1** (0.026 g, 0.06 mmol) and excess butylamine (0.3 g, 4 mmol) were mixed neat and stirred overnight. The product mixture was concentrated over vacuum and dried under nitrogen for 2 h before NMR was taken.

5.3.5 Benzylated, acryl ascorbic acid -modified silicones

Telechelic silicone

Benzylated acryl ascorbic acid **1** (0.05 g, 0.12 mmol) and **T334** (1.16 g, 0.12 mmol amine) were dissolved in IPA (5 mL) and stirred overnight. The reaction solution was concentrated, and a yellow oil was obtained.

Pendant silicones

Benzylated acryl ascorbic acid **1** (0.4g, 0.96 mmol) was first dissolved in IPA (20 mL) to generate a 0.02 mg/mL stock solution. The stock solution (2.5 mL) and different quantities of **P22** (2% **P22-2**, 5% **P22-5**, 10% **P22-10**, 15% **P22-15**, 20% **P22-20**, 50% **P22-50**, 75% **P22-75**, and 100% **P22-100)** and **P21** (25% **P21-25**) (Table S7.8), in quantities based on 1:1 amine: acrylate) were added and stirred in additional IPA (5 mL total volume) overnight; the product solution was concentrated by evaporating the solvent in oven overnight at 50 ℃. NMR was taken for resulting yellow oil.

5.3.6 Debenzylation (hydrogenation) of benzylated ascorbic acid silicones

Hydrogenation was performed by first dissolving benzylated ascorbic acid silicone **P22-20** (0.049 g, 0.12 mmol) in IPA (50 mL) in a 100 mL round-bottomed flask equipped

with stir bar. Based on the benzyl group 15% mole Pd (0.039 g 10% Pd/C, 0.037 mmol) was then added to the solution. The round-bottomed flask was then connected to a dual manifold, after 10 x de-gas/ nitrogen purges, the manifold was then connected to an H_2 balloon, the system was then 5 x de-gas/ hydrogen purged before switching to hydrogen overnight. After the reaction was done, the solution was then centrifuged at 14000 rpm for 30 min to give a slightly grey solution that was vacuum filtered through a Celite plug following by concentration using rotary evaporation, the resulting clear oil was then washed with $CDCl_3$ and centrifuged at 14000 rpm for 5 min. Two phases resulted: a $CDCl_3$ phase (from which NMR was measured) supernatant and a cloudy oil. MeOD-d_4 was added to the oily residue with shaking. After centrifugation at 14000 rpm for 5 min, the solution phase was collected and NMR was recorded, the remaining solid (ascorbic acid) was then dissolved in D_2O and an NMR was recorded.

For most compounds, however, including **P22-10**, and **P21-25**, reduction was accompanied by a change in color: **P22-2** went from a pale-yellow oil to a brown oil; **P22-10** and **P21-25** yielded black elastomers.

5.3.7 Kinetic study of benzyl acryl ascorbic acid and pendant silicone

A kinetic study was done using NMR. Benzylated acryl ascorbic acid (0.05 g, 0.12 mmol) was first dissolved in deuterated chloroform or MeOD-d_4 (0.35 mL); **P22** (0.049g, 0.12 mmol) was dissolved separately in deuterated chloroform or MeOD-d_4 (0.35 mL). The two components were combined right before the first NMR spectrum was collected at time 0 min, and then at 0.5 h, 1 h, 2 h, 4 h, 8 h, 12 h, and 24 h to monitor the reaction process (Figure S7.73, S7.74).

5.3.8 DPPH Assay for elastomer samples

For quantitative analyses, the debenzylated products of **P21-25** (84.6 mM, based on concentration of ascorbic acid in 50 mg of **P21**) was swelled in IPA (1 mL) in a 1.5 mL centrifuge tube in quantities (Table S7.9); the sample was allowed to swell for 2 h. The DPPH solution (0.5 mL of 0.2 mM) was then added to the sample and the mixture sat in the dark for 30 min to react. The resulting solution was then filtered, 200 μL aliquot of the resulting solution was added to a 96 well plate in triplicate. Scans were taken for each well at 520 nm from the plate reader and the results were recorded (Table S7.10). **P21-25** and **P22-2** samples, after hydrogenation, were similarly treated. **P22-10** and **P21-25** elastomers showed moderate antioxidant activity where **P22-2** showed no significant antioxidant activity.

5.3.9 DPPH Assay of ascorbic acid and benzylated ascorbic acid control

DPPH assays were done for ascorbic acid (AA) and benzylated ascorbic acid as controls to the ascorbic acid modified elastomer samples. Stock solutions were prepared by dissolving ascorbic acid (74.5 mg) in DI water (5 mL) or benzylated ascorbic acid (150.7 mg) in IPA (5 mL), respectively. The stock solution was then diluted 2-fold, 4-fold, 10-fold or 20-fold. Each concentration (0.5 mL) of the control solution was added to a 1.5 mL centrifuge tube, subsequently (0.5 mL of 0.2 mM DPPH solution) was added to the tube, mixed, and allowed to rest in the dark for 30 min. An aliquot (200 μL) of the resulting solution was added to a 96 well plate in triplicate. Scans were taken for each well at 520 nm from the plate reader and the results were recorded. (Table S7.10).

5.4 Results

5.4.1 Synthesis of benzyl-protected ascorbic acid and modification with acrylate.

Survey experiments demonstrated that ascorbic acid (AA) was both too polar and too reactive, in particular to oxidation, for many of the desired synthetic processes to succeed. Therefore, the enols in AA were protected as benzyl ethers using a simple Williamson approach (Figure 5.1A). Acrylic ester formation using acryloyl chloride preferentially occurred at the primary alcohol to give **1** (Figure 5.1B); no secondary alcohol modification was observed, as shown by NMR (Figure S7.68).

5.4.2 Benzylated, acryl ascorbic acid-modified silicones and cleavage of acylated, benzylated ascorbic acid by butyl amine

Under oxidizing conditions ascorbic acid can be induced to react twice with amines to (putatively) form a 1,2-dimine from dienol[19]. Model studies were undertaken with the protected derivative **1** to understand how the functional differences with the protected compound would manifest when aminosilicones were present. ^{1}H NMR showed that two equivalents of butylamine also reacted with benzylated acryl ascorbic acid **1**: the first performed an aza-Michael addition with the acrylate; and the second led to amidation and cleavage of the azaMichael acrylate (Figure 5.1C,D, Figure S1.69). Other motifs are also likely involved, including ring-opening cleavage or secondary Michael additions (**2**, **3**). It was, therefore, anticipated that linear silicone oils, modified with ascorbic acid, would arise from azaMichael reactions between **1** and aminoalkylsilicones provided that the stoichiometry of [H_2N]/[acrylate] was kept below 1:1.

The aza-Michael process was both trivial and facile, requiring only stirring in IPA (isopropanol). A library of ascorbic acid-modified silicones could then be prepared from this key functional molecule **1** by the aza-Michael reaction with either pendent (Figure 5.1E) or telechelic (Figure 5.1F) aminoalkylsilicones containing different amine densities. The telechelic sample **T334** (nomenclature: **Tn**, where n is the number of Me_2SiO units in the chain, **T334**, n = 334, Figure 5.1) was modified completely at both termini with **1**. With the pendent silicones both partial **P22-x** (nomenclature: **Pt-x** where t is the % of aminopropyl monomers m in the chain (m/(m+n)*100, normally t = 22, and x = 2, 5, 10, 15, 20, 50, 75, 100, Figure 5.1) and complete modification **P22-100** with **1** was performed. The telechelic products and pendent products made with lower equivalents of AA (**P22-2 → P22-15**), or 100% **P22-100** were yellow oils that were stable for extended periods of time; so far, over one year. A lower molecular weight analogue **P21-25** was also prepared as a yellow oil. The rates of reaction were shown to be faster in more polar methanol (2 hours) than in chloroform (12 hours, Figure S1.73, S1.74).

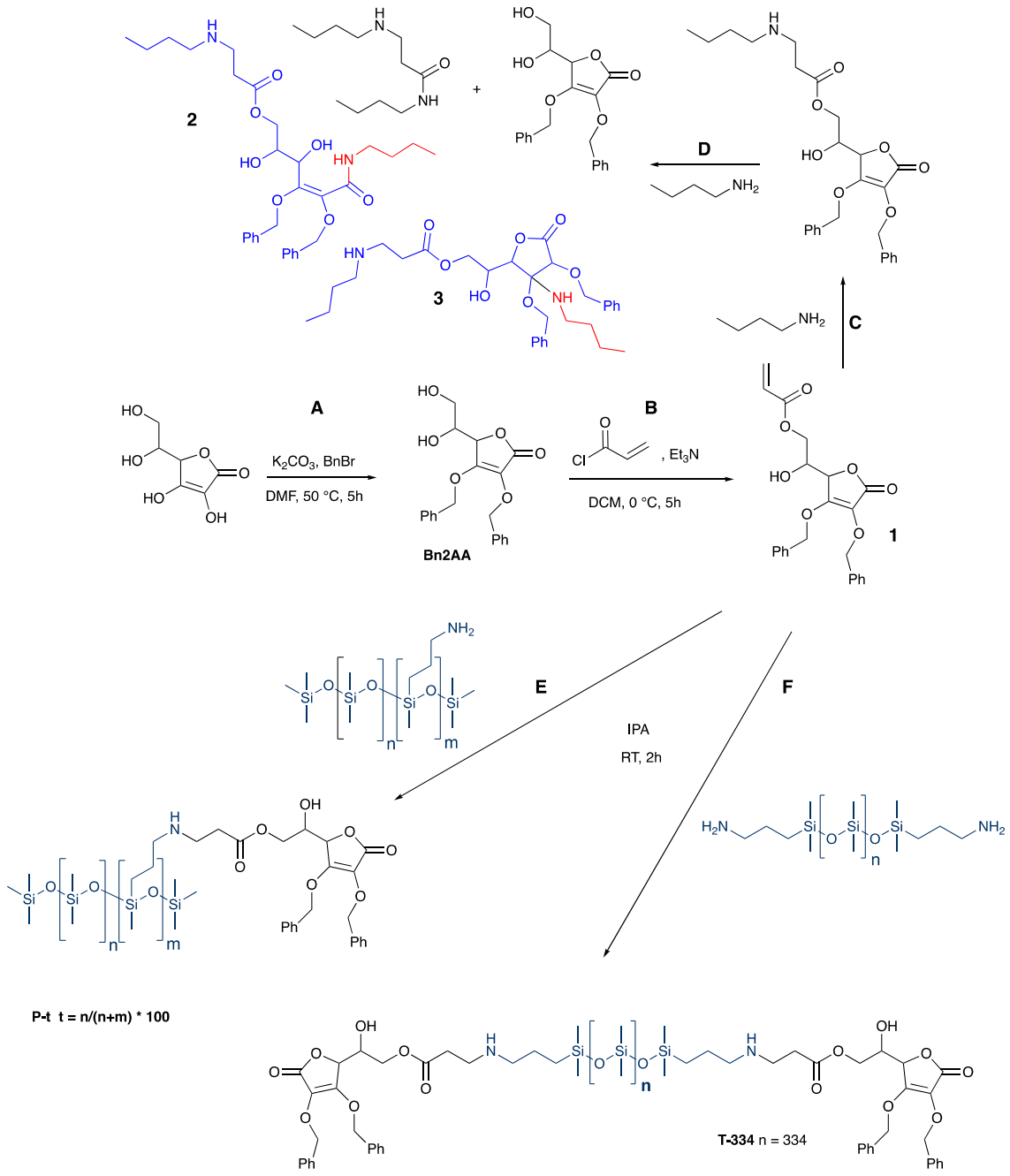

Figure 5.1. Synthesis of A, B: benzyl protected, acrylated ascorbic acid and conversion to C: mono or D: dibutyl amine derivatives, or conversion to E: pendent, or F: telechelic ascorbic acid-modified silicone polymers.

If the higher molar mass pendent polymers based on **P22** were modified with higher quantities of **1** they ceased to be oils and were instead isolated as elastomers (**P22-20 → P22-75**). There was a direct correlation between the quantity of AA 'crosslinker' **1** added and the Shore hardness of the resulting elastomer (Figure 5.3A), consistent with the formation of typical silicone elastomers [24,25]. The model study with butylamine suggests the origin of the observed crosslinking. When the stoichiometric excess of amines to acylates exceeds 1:1 the initial azaMichael (similar to Figure 5.1C) is accompanied by secondary rection (similar to Figure 5.1D) compound **1** bridges polymer chains leading to crosslinks analogous to **2**, **3**. One is obliged to explain, however, why there is an onset of elastomer formation only at 20% **1**. The silicone polymer has about 1 aminopropyl-containing monomer for each 5 D units (Me_2SiO). At low concentrations of **1**, the secondary reaction process will lead to both chain extension and intramolecular processes giving cycles (Figure 5.2B,C). In addition, not all the added **1** will undergo both processes. Thus, at lower concentrations of **1** the aza-Michael reaction will lead to higher molecular weight silicone oils of viscosities that increase with the available fraction of **1**. At higher concentrations sufficient crosslink arises that elastomers form, with crosslink density and durometer increasing in line with the relative quantity of **1** added.

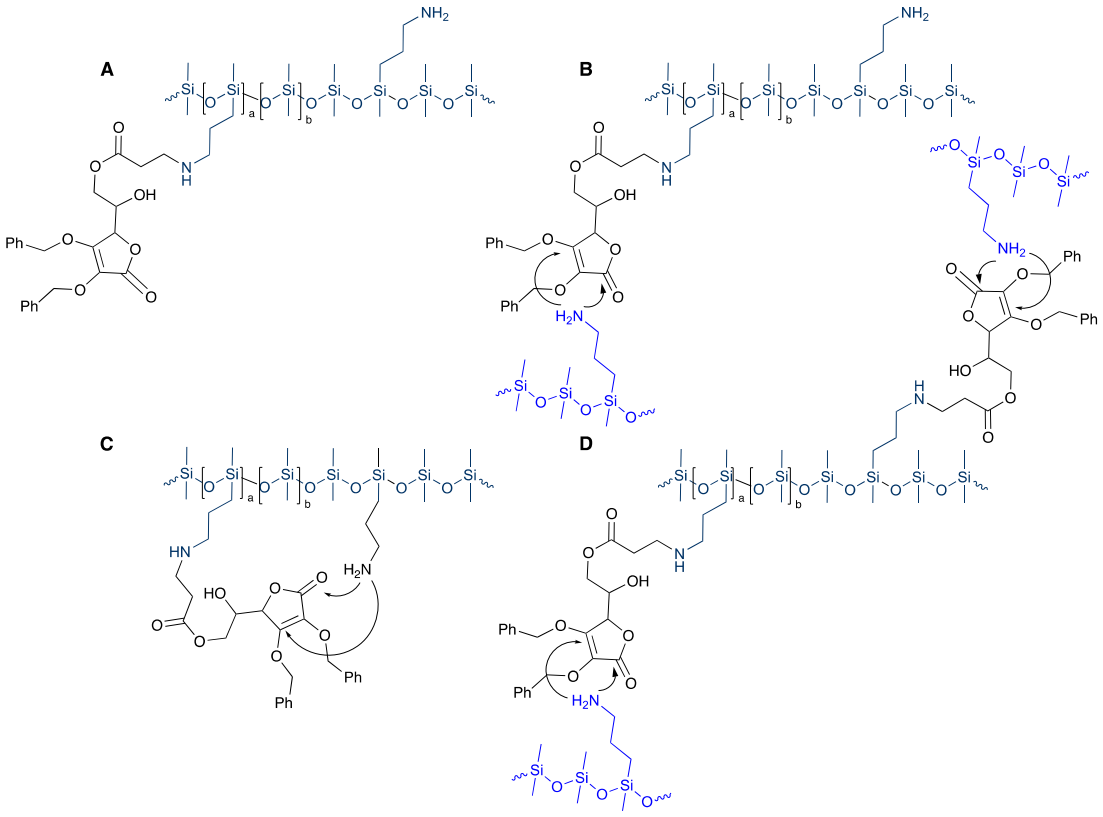

Figure 5.2. **1** as A: monofunctional modifier; B: chain extender; C: loop reagent; or, at higher concentrations, D: crosslinker.

5.4.3 Antioxidant activity

The antioxidant activity of vitamin C is associated with the relative ease with which the ene-diol can undergo oxidation [26]. The ene-diols in products **T334**, **P21-25** and **P22-x** were protected and, therefore, were not expected to have antioxidant activity. DPPH (2,2-diphenyl-1-picrylhydrazyl), a stable radical species, is a particularly convenient reagent for colorimetrically observing qualitatively, or determining quantitatively, antioxidant activity [27]. Neither **T334** nor any of the **P22-x** products exhibited significant antioxidant activity, as shown qualitatively when tested with 0.2 mM DPPH; over a period of 2 hours the solution only very slowly turned yellow for oil samples, and 6-12 hours for

elastomeric samples, whereas ascorbic acid control solutions exhibited high antioxidant activity, immediately turning yellow. In quantitative DPPH assays the benzylated ascorbic acid control also showed nearly no antioxidant activity (Figure 5.3AB). It was inferred that, in order to reveal antioxidant activity, deprotection of the benzyl ethers to regenerate the ene-diol would first be necessary.

Benzyl ethers are conveniently cleaved by hydrogenation of Pd/C to yield the free alcohol and toluene. In our hands the reduction process with both oils and elastomers led to the release of ascorbic acid (Figure 5.4) or its derivatives from the silicone. The reaction could be capricious; in one case, free ascorbic acid was isolated in an aqueous extract. More commonly, upon reduction of oils such as **P22-2**, **P22-10, P22-100** or **P21-25** in IPA, the products took on a darker color and, in the case, of **P22-10** and **P21-25,** yielded black elastomers. That is, deprotection led to further crosslinking/chain extension. However, it also led to liberation of antioxidant activity, as shown by DPPH assays (Table S7.9, S7.10, Figure S7.75). This suggests free enediols present in the product either as liberated ascorbic acid, or as tethered, crosslinking AA moieties.

A 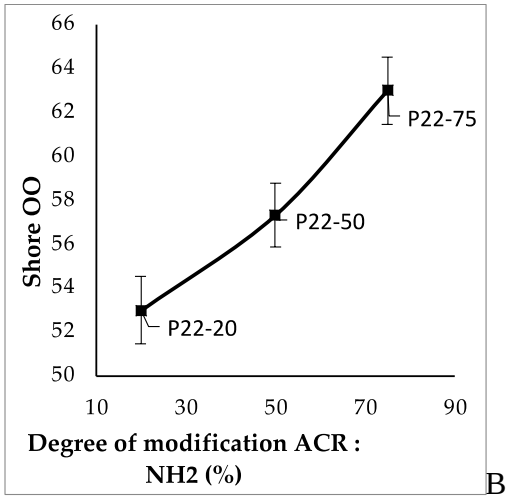

B 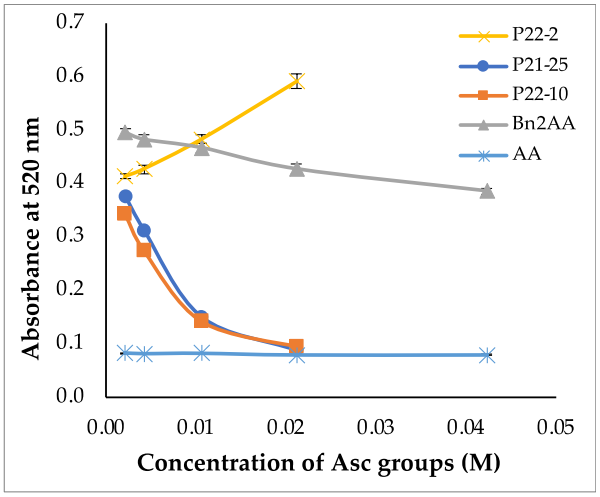

Figure 5.3. A: DPPH assay results shown antioxidant activity of ascorbic acid and benzylated ascorbic acid control comparing with different debenzylated ascorbic acids. B: Shore hardness data of benzylated ascorbic acid crosslinked aminoalkylsilicones for samples **P22-20**, **P22-50** and **P22-75**.

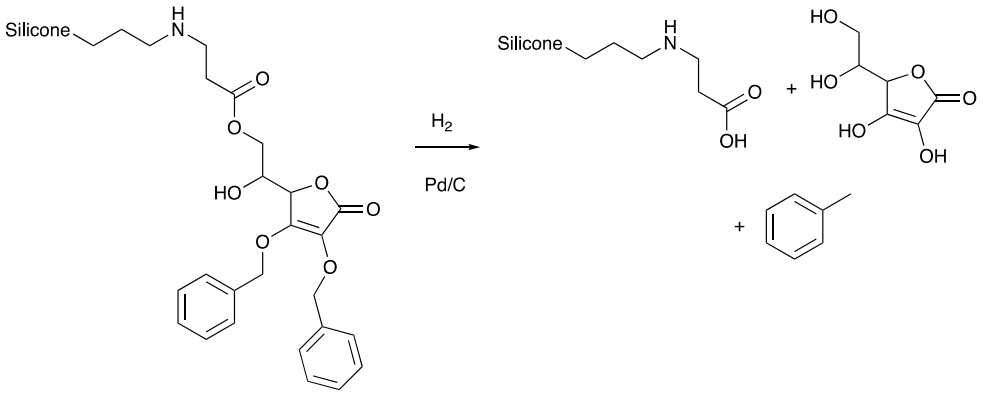

Figure 5.4. Reductive cleavage of benzyl ethers and the linking ester.

5.5 Discussion

For the reasons articulated above, there remains much interest in use of/release of vitamin C because of its powerful biological activities, including as an antioxidant. We do not consider materials in which vitamin C that is simply mixed into a matrix and focus on materials in which the ascorbic acid is chemically grafted. There are surprisingly few examples of Vitamin C being used in a prodrug format. These include reports of formation of esters of the ene-diol or at the C1 position to give materials that exhibit biological activity of various types after exposure to a biological environment. Proof of release of the ascorbic acid via ester hydrolysis is typically inferred. A vitamin C-ibuprofen ester was shown, for example, to cross the blood brain barrier where a response

to the ibuprofen was shown [28]; in this case, vitamin C was the carrier. Other examples describe the use of glycosides [29], or a combination of glycosides + aliphatic esters to link to vitamin C. In these cases, biological release of vitamin C was reported after exposure the spleen homogenates [30] or esterase [31]; in neither case was proof of release of free vitamin C shown. In these examples the ester linkages operate, in part, to stabilize the vitamin C from degradation.

Although vitamin C has been shown to be involved in various forms of crosslinking of polymers, particularly biological polymers, its role is generally to mediate the chemistry of the polymers themselves, including the crosslinking of proteins, for example, by inducing the Maillard reaction [32]. An important exception is the work of Leivo et al. who showed that the direct reaction of amine-modified silicone elastomer surfaces and with collagen permitted ascorbic acid to link the two materials together via imines; the ascorbic acid moiety was then subject to autoxidative decomposition [19].

In the reactions described here, it is clear that – even when protected as benzyl ethers, **1** can undergo at least 2 sequential reactions under mild conditions (Figure 5.1C,D, Figure 5.2) leading first to chain extension and then crosslinking to give robust silicone elastomers that do not have antioxidant activity – the enediol is protected. This form of vitamin C is thus a convenient, natural crosslinking agent.

Upon liberation of the enediol by reductive deprotection of the benzyl ethers further crosslinking ensued. The accompanying darkening in color is consistent with a Maillard reaction. Elaborating the subtleties of these processes is a current occupation. Regardless,

the products are also efficient antioxidants whether free ascorbic acid is liberated, or the crosslinker retains the enediol.

Simple silicone fluids undergo rather efficient environmental depolymerization [33,34]. While speculation only, it is expected that silicone fluids modified by **1**, and elastomers formed following reductive deprotection, will be subject to ester hydrolysis to regenerate silicon oils (Figure 5.4) that will also undergo facile depolymerization. The new crosslinks formed by ascorbic acid self-reaction should be analogous to the normal outcomes of ascorbic acid self-condensation and should also be readily degraded. The conditions for reductive cleavage of benzyl ethers are mild but require the transition metal catalyst for efficient cleavage. This is an aspect that is clearly disadvantageous. However, it may be possible to elicit reductive cleavage without the need for platinum; it is noted that some benzyl ethers are susceptible to both oxidative and reductive cleavage under biological conditions [35].

The Green chemistry rules call for materials that make better use of natural feedstocks [36]. In the present case, while **1** does dilute the synthetic silicone, it is to a small extent only. However, the use of vitamin C delivers function during crosslinking and new function during cleavage to give both useful, natural antioxidant activities and, as we hope to demonstrate, more facile decomposition of the silicone component at end of life.

5.6 Conclusion

Benzyl-protected ascorbic acid modified silicones were successfully synthesized using an azaMichael addition; the ascorbic acid ranged from 2% to 100% on both telechelic and aminoalkylsilicones. The ascorbic acid acts as a crosslinker for pendent silicones to give

robust silicone elastomers without significant antioxidant behavior. Reductive debenzylation was expected to liberate antioxidant activity but, surprisingly, also lead to cleavage of the crosslink to give silicone oils and vitamin C. Thus, aspects of this work: natural materials, function, programmed degradation fall within the rules of Green Chemistry.

5.7 Reference

(1) Mangir, N.; Bullock, A. J.; Roman, S.; Osman, N.; Chapple, C.; MacNeil, S. Production of Ascorbic Acid Releasing Biomaterials for Pelvic Floor Repair. *Acta Biomater.* **2016**, *29*, 188–197.

(2) Nagarajan, S.; Nagarajan, R.; Kumar, J.; Salemme, A.; Togna, A. R.; Saso, L.; Bruno, F. Antioxidant Activity of Synthetic Polymers of Phenolic Compounds. *Polymers* **2020**, *12* (8), 1–27.

(3) Norsuzila Ya'acob1, Mardina Abdullah1, 2 and Mahamod Ismail1, 2; Medina, M.; Talarico, T. L.; Casas, I. A.; Chung, T. C.; Dobrogosz, W. J.; Axelsson, L.; Lindgren, S. E.; Dobrogosz, W. J.; Kerkeni, L.; Ruano, P.; Delgado, L. L.; Picco, S.; Villegas, L.; Tonelli, F.; Merlo, M.; Rigau, J.; Diaz, D.; Masuelli, M. We Are IntechOpen , the World ' s Leading Publisher of Open Access Books Built by Scientists , for Scientists TOP 1 %. *Intech* **1989**, *32*, 137–144.

(4) Pospíšil, J. Mechanistic Action of Phenolic Antioxidants in Polymers-A Review. *Polym. Degrad. Stab.* **1988**, *20* (3–4), 181–202.

(5) Estevinho, B. N.; Carlan, I.; Blaga, A.; Rocha, F. Soluble Vitamins (Vitamin B12 and Vitamin C) Microencapsulated with Different Biopolymers by a Spray Drying Process. *Powder Technol.* **2016**, *289*, 71–78.

(6) Paradiso, P.; Serro, A. P.; Saramago, B.; Colaço, R.; Chauhan, A. Controlled Release of Antibiotics from Vitamin E-Loaded Silicone-Hydrogel Contact Lenses. *J. Pharm. Sci.* **2016**, *105* (3), 1164–1172.

(7) AL-MALAIKA, S. *Reactive Modifiers for Polymers*, 1 ed.; 1997.

(8) Billingham, N.C. and Calvert, P. D. Developments in Polymer Degradation; 1980; p 136.

(9) Huang, S.; Kong, X.; Xiong, Y.; Zhang, X.; Chen, H.; Jiang, W.; Niu, Y.; Xu, W.; Ren, C. An Overview of Dynamic Covalent Bonds in Polymer Material and Their Applications. *Eur. Polym. J.* **2020**, *141* (September), 110094.

(10) Parada, C. M.; Parker, G. L.; Storey, R. F. Polyisobutylene Containing Covalently Bound Antioxidant Moieties. *J. Polym. Sci. Part Polym. Chem.* **2019**, *57* (17), 1836–1846.

(11) Spizzirri, U. G.; Iemma, F.; Puoci, F.; Cirillo, G.; Curcio, M.; Parisi, O. I.; Picci, N. Synthesis of Antioxidant Polymers by Grafting of Gallic Acid and Catechin on Gelatin. *Biomacromolecules* **2009**, *10* (7), 1923–1930.

(12) Buchmüller, Y.; Wokaun, A.; Gubler, L. Polymer-Bound Antioxidants in Grafted Membranes for Fuel Cells. *J. Mater. Chem. A* **2014**, *2* (16), 5870–5882.
(13) Buchmüller, Y.; Zhang, Z.; Wokaun, A.; Gubler, L. Antioxidants in Non-Perfluorinated Fuel Cell Membranes: Prospects and Limitations. *RSC Adv.* **2014**, *4* (94), 51911–51915.
(14) Zhang, W.; Li, J. X.; Tang, R. C.; Zhai, A. D. Hydrophilic and Antibacterial Surface Functionalization of Polyamide Fabric by Coating with Polylysine Biomolecule. *Prog. Org. Coat.* **2020**, *142* (August 2019), 105571.
(15) Wang, H.; Zhu, D.; Paul, A.; Cai, L.; Enejder, A.; Yang, F.; Heilshorn, S. C. Covalently Adaptable Elastin-Like Protein–Hyaluronic Acid (ELP–HA) Hybrid Hydrogels with Secondary Thermoresponsive Crosslinking for Injectable Stem Cell Delivery. *Adv. Funct. Mater.* **2017**, *27* (28), 1–11.
(16) Brook, M. A. *Silicon in Organic, Organometallic, and Polymer Chemistry*; Wiley, 1999.
(17) Kaliyathan, A. V.; Mathew, A.; Rane, A. V.; Kanny, K.; Thomas, S. *Natural Rubber and Silicone Rubber-Based Biomaterials*; Elsevier Ltd., 2018.
(18) Ibrahim, M.; Bond, J.; Medina, M. A.; Chen, L.; Quiles, C.; Kokosis, G.; Bashirov, L.; Klitzman, B.; Levinson, H. Characterization of the Foreign Body Response to Common Surgical Biomaterials in a Murine Model. *Eur. J. Plast. Surg.* **2017**, *40* (5), 383–392.
(19) Leivo, J.; Virjula, S.; Vanhatupa, S.; Kartasalo, K.; Kreutzer, J.; Miettinen, S.; Kallio, P. A Durable and Biocompatible Ascorbic Acid-Based Covalent Coating Method of Polydimethylsiloxane for Dynamic Cell Culture. *J. R. Soc. Interface* **2017**, *14* (132).
(20) Marik, P. E.; Khangoora, V.; Rivera, R.; Hooper, M. H.; Catravas, J. Hydrocortisone, Vitamin C, and Thiamine for the Treatment of Severe Sepsis and Septic Shock: A Retrospective Before-After Study. *Chest* **2017**, *151* (6), 1229–1238.
(21) Suraeva, O.; Champanhac, C.; Mailänder, V.; Wurm, F. R.; Weiss, H.; Berger, R.; Mezger, M.; Landfester, K.; Lieberwirth, I. Vitamin C Loaded Polyethylene: Synthesis and Properties of Precise Polyethylene with Vitamin C Defects via Acyclic Diene Metathesis Polycondensation. *Macromolecules* **2020**.
(22) Sivakanthan, S.; Rajendran, S.; Gamage, A.; Madhujith, T.; Mani, S. Antioxidant and Antimicrobial Applications of Biopolymers: A Review. *Food Res. Int.* **2020**, *136*, 109327.
(23) Norsuzila Ya'acob1, Mardina Abdullah1, 2 and Mahamod Ismail1, 2; Medina, M.; Talarico, T. L.; Casas, I. A.; Chung, T. C.; Dobrogosz, W. J.; Axelsson, L.; Lindgren, S. E.; Dobrogosz, W. J.; Kerkeni, L.; Ruano, P.; Delgado, L. L.; Picco, S.; Villegas, L.; Tonelli, F.; Merlo, M.; Rigau, J.; Diaz, D.; Masuelli, M. We Are IntechOpen , the World ' s Leading Publisher of Open Access Books Built by Scientists , for Scientists TOP 1 %. *Intech* **1989**, *32*, 137–144.
(24) Meththananda, I. M.; Parker, S.; Patel, M. P.; Braden, M. The Relationship between Shore Hardness of Elastomeric Dental Materials and Young's Modulus. *Dent. Mater.* **2009**, *25* (8), 956–959.

(25) Bui, R.; Brook, M. A. Catalyst Free Silicone Sealants That Cure Underwater. *Adv. Funct. Mater.* **2020**, *30* (23), 2000737.
(26) L ü, J.-M.; Lin, P. H.; Yao, Q.; Chen, C. Chemical and Molecular Mechanisms of Antioxidants: Experimental Approaches and Model Systems. *J. Cell. Mol. Med.* **2010**, *14* (4), 840–860.
(27) Ogliani, E.; Skov, A. L.; Brook, M. A. Purple to Yellow Silicone Elastomers: Design of a Versatile Sensor for Screening Antioxidant Activity. *Adv. Mater. Technol.* **2019**, *4* (11), 1–7.
(28) Wu, X.-Y.; Li, X.-C.; Mi, J.; You, J.; Hai, L. Design, Synthesis and Preliminary Biological Evaluation of Brain Targeting l-Ascorbic Acid Prodrugs of Ibuprofen. *Chin. Chem. Lett.* **2013**, *24* (2), 117–119.
(29) Jacques, C.; Genies, C.; Bacqueville, D.; Borotra, N.; Noizet, M.; Tourette, A.; Bessou-Touya, S.; Duplan, H. 776 Optimized Vitamin C Prodrug for Controlled Release and Antioxidant Activity. *J. Invest. Dermatol.* **2020**, *140* (7), S103.
(30) Tai, A.; Goto, S.; Ishiguro, Y.; Suzuki, K.; Nitoda, T.; Yamamoto, I. Permeation and Metabolism of a Series of Novel Lipophilic Ascorbic Acid Derivatives, 6-O-Acyl-2-O-α-d-Glucopyranosyl-l-Ascorbic Acids with a Branched-Acyl Chain, in a Human Living Skin Equivalent Model. *Bioorg. Med. Chem. Lett.* **2004**, *14* (3), 623–627.
(31) Shibayama, H.; Hisama, M.; Matsuda, S.; Ohtsuki, M. Permeation and Metabolism of a Novel Ascorbic Acid Derivative, Disodium Isostearyl 2-O-L-Ascorbyl Phosphate, in Human Living Skin Equivalent Models. *Skin Pharmacol. Physiol.* **2008**, *21* (4), 235–243.
(32) Mohammadi Nafchi, A.; Tabatabaei, R. H.; Pashania, B.; Rajabi, H. Z.; Karim, A. A. Effects of Ascorbic Acid and Sugars on Solubility, Thermal, and Mechanical Properties of Egg White Protein Gels. *Int. J. Biol. Macromol.* **2013**, *62*, 397–404.
(33) Lehmann, R. G.; Varaprath, S.; Annelin, R. B.; Arndt, J. L. Degradation of Silicone Polymer in a Variety of Soils. *Environ. Toxicol. Chem.* **1995**, *14* (8), 1299–1305.
(34) Lehmann, R. g.; Varaprath, S.; Frye, C. l. Degradation of Silicone Polymers in Soil. *Environ. Toxicol. Chem.* **1994**, *13* (7), 1061–1064.
(35) Kinne, M.; Poraj-Kobielska, M.; Ralph, S. A.; Ullrich, R.; Hofrichter, M.; Hammel, K. E. Oxidative Cleavage of Diverse Ethers by an Extracellular Fungal Peroxygenase. *J. Biol. Chem.* **2009**, *284* (43), 29343–29349.
(36) Anastas, P.; Warner, J. *Green Chemistry: Theory and Practice*, Revised ed. edition.; Oxford University Press: Oxford, 2000.

Chapter 6. General Conclusion

Silicone polymers are indispensable materials in numerous applications. However, the high energy-cost required for their synthesis from silicon compromises their sustainability. Creating bio-based silicones is a promising strategy for both diluting energy density and implementing additional functionality. The main objective of this thesis was to develop sustainable synthetic strategies to incorporate bio-based molecules into silicone systems and explore the potential functionalities of the resulting bio-based silicone materials. To do so, it was important to first develop an understanding of the mechanistic details of the reactions, and then exploit the methodologies; there are the two main foci.

Chapter 2 laid the foundation for the entire thesis by developing strategies to increase the rates of aza-Michael reaction kinetics through the utilization of beta-hydroxy acrylates; these compounds reacted 10 – 100 times faster than simple acrylates. A series of model studies provided mechanistic and kinetic understanding of this method, where the geometric proximity of the hydroxy on the acrylic ester was determined to be essential for rate enhancement. It was hypothesized that a 7-membered ring transition state provided self-activation of beta-hydroxy acrylic esters, leading to faster aza-Michael reactions, as shown in FIGURE 2.1. When the process was used for crosslinking acrylates with aminosilicones, acrylic silicones functionalized with beta-hydroxy groups had even higher degrees of rate enhancement compared with simple acrylic silicones; a 900x rate enhancement was observed under solvent-free conditions.

Chapter 3 then utilized this efficient aza-Michael reaction described in Chapter 2 for the incorporation of amino acids into silicone. The challenges of getting zwitterionic amino

acids to participate in aza-Michael reactions were overcome by utilizing ChAAILs. It was shown that the ChAAILs are effective nucleophiles for the aza-Michael addition without the need for solvents or protecting groups once converted to a cholinium ionic liquid. This process is intrinsically green in the sense that two natural molecules, choline and amino acids, are incorporated into silicone under solvent-free, catalyst-free, and mild reaction conditions. Competitive hydrolysis of the ester was observed in the process but is easily managed by forming an acetate buffer with acetic acid. The flexibility of the process was demonstrated by the ability to incorporate amino acids onto both hydrophilic and hydrophobic polymers using the same process; issues of solubility were overcome. Conversions are excellent both with small molecules and polymers shown in Figure 2C and Figure 4. The utilization of this process holds significant potential for expanding the scope of amino acid-based materials and facilitating their integration into diverse applications more sustainably.

In Chapter 4, the ChAAIL-functional silicones synthesized in Chapter 3 were then investigated for their application as dielectric elastomers. Initial data indicates that silicones crosslinked with native lysine demonstrates potential as a thermoplastic material, suggesting possible self-healing capabilities for dielectric applications. A more comprehensive study of the dielectric properties of ChAAIL-modified silicone showed that increased loading of ChLysIL led to a significant increase in dielectric permittivity without compromising the dielectric breakdown strength. A comparison among different types of ChAAILs suggested that the increased dielectric permittivity may be attributed to the mobility of cholinium ions or the overall positive charge in the system. (Figure 4.7)

An unexpected discovery emerged when partially degraded ChLysIL crosslinked silicone exhibited significantly higher dielectric permittivity compared to freshly synthesized samples. The work not only presents a simplified and sustainable synthetic pathway for ionic liquid-containing silicone actuators but also offers a prospective avenue for controlled actuation by regulating the degree and rate of degradation in silicone actuators. In Chapter 5, another type of bio-based molecule, vitamin C, is incorporated into silicones with a focus on the antioxidant activity it provides to the material. Benzyl-protected ascorbic acid-modified silicones are successfully synthesized using the fast aza-Michael addition described in Chapter 2; the ascorbic acid loading ranged from 2% to 100% on aminoalkylsilicones. The ascorbic acid acts as a crosslinker for pendent silicones at lower loading to give robust silicone elastomers without significant antioxidant behavior. However, when exposed to a reductive environment, vitamin C is liberated to liberate antioxidant activity. Thus, this chapter had described a programmed degradation and antioxidant activity activation that can be utilized in fields like antimicrobial coating and antioxidant cosmetic formulations.

Overall, this thesis utilized an innovative, efficient, and sustainable aza-Michael reaction to expand the bio-based silicone material library. By gaining a detailed kinetic and mechanistic understanding of aza-Michael additions in the synthesis of bio-based silicones, it opens new avenues for creating materials that not only address environmental concerns but also possess tailored functional properties. The findings presented highlighted the potential of bio-based silicone materials as key contenders in sustainable materials science, with the prospect of high-performance, environmentally friendly

solutions for diverse industrial applications. As the global drive for sustainability intensifies, this research serves as a steppingstone towards more sustainable and functional materials in the future.

Chapter 7. Appendix

7.1 Appendix I: Supporting Information for Chapter 2

7.1.1 Products and rates of reaction: small molecules

Table S7.1 Influence of the presence and position of hydroxyl groups on the rate of aza-Michael reaction in protic and aprotic solvents. (NMR Conversion yield of aza-Michael reactions)

Entry	Michael Acceptor	Michael Donor	Compound Number (Figure 2)	Solvent	Conversion yield (%[a])	Initial rate of reaction (mol% / min)
1	BAcr	BA	**1**	$CDCl_3$	1	0.01
2	BAcr	BA	**1**	MeOD	75	3.02
3	BAcr	BA	**1**	$CDCl_3$+1eq MeOD	10	0.17
4	BAcr	EA	**2**	$CDCl_3$	22	0.44
5	BAcr	EA	**2**	MeOD	75	2.46
6	BAcr	EA	**2**	$CDCl_3$+1eq MeOD	26	0.45
7	HEA	BA	**3**	$CDCl_3$	57	1.42
8	HEA	BA	**3**	MeOD	88	3.70
9	HEA	BA	**3**	$CDCl_3$+1eq MeOD	61	1.40
10	HEA	EA	**4**	$CDCl_3$	71	2.07
11	HEA	EA	**4**	MeOD	86	3.67
12	HEA	EA	**4**	$CDCl_3$+1eq MeOD	65	1.52
13	HBAcr	BA	**5**	$CDCl_3$	22	0.37
14	HBAcr	EA	**6**	$CDCl_3$	44	0.88
15	HBAcr	AP	**7**	$CDCl_3$	50	0.67
16	BAcr	AP	**8**	CDCl3	19	0.33
17	HEA	AP	**9**	CDCl3	75	1.93
18	Di11	BA	**10**	$CDCl_3$	0	0.003
19	Di11	EA	**11**	$CDCl_3$	16	0.20
20	Di9_OH	BA	**12**	$CDCl_3$	34	0.69
21	Di9_OH	EA	**13**	$CDCl_3$	40	0.90

[a] Degree of conversion at 1 h. These data are normalized against an internal signal that didn't change during the reaction. For example, in BA the Me group (entries 1-3) at the end of the butyl chain was used as an internal standard against which loss of H_2C=CH signals were measured.

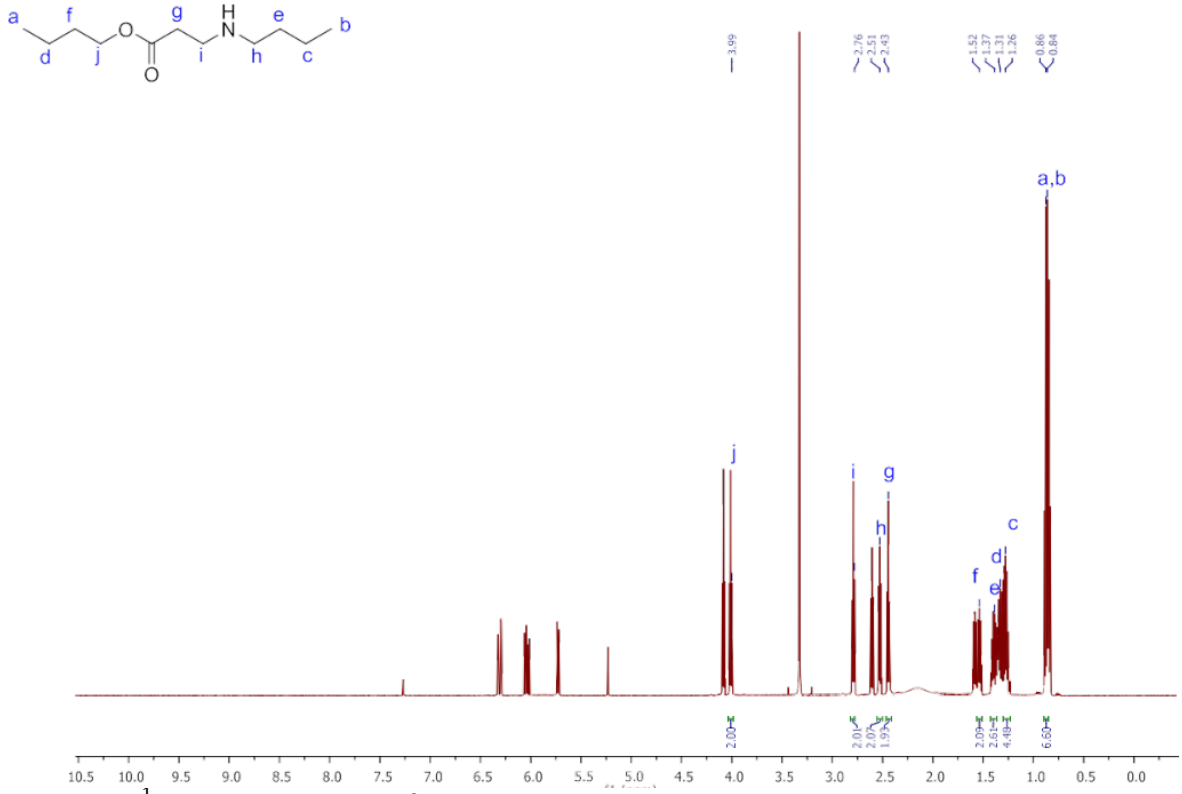

Figure S7.1. ^{1}H NMR spectrum of BAcr/BA : molecule **1** (1 : 1) conversion in $CDCl_3$ with 1 eq. of MeOD after 12 h. ^{1}H-NMR (600 MHz, chloroform-d, ppm) = 4.00 (t, J = 6.7 Hz, 2H), 2.78 (t, J = 6.5 Hz, 2H), 2.51 (t, J = 7.3 Hz, 2H), 2.43 (t, J = 6.5Hz, 2H), 1.55 – 1.49 (m, 2H), 1.41 – 1.21 (m, 6H), 0.86 (t, J = 7.6 Hz, 3H), 0.83 (t, J = 6.5 Hz, 3H).

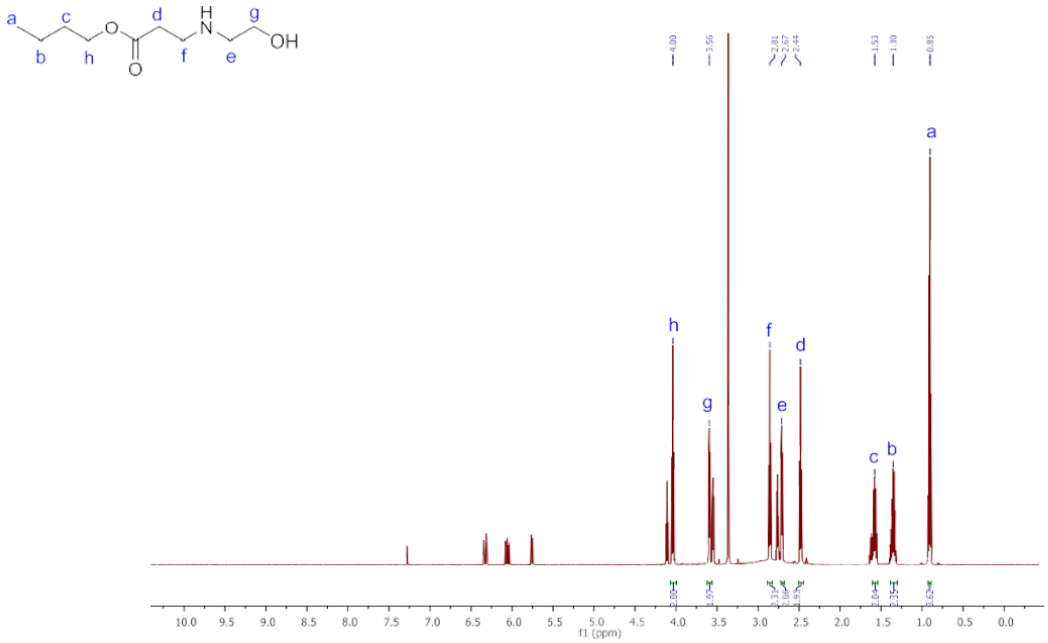

Figure S7.2. ^{1}H NMR spectrum of BAcr/EA : molecule **2** (1 : 4) conversion in $CDCl_3$ with 1 eq. of MeOD after 12 h. ^{1}H-NMR (600 MHz, chloroform-d, ppm) = 4.00 (t, J = 6.7 Hz, 2H), 3.56 (t, J = 5.2 Hz, 2H), 2.81 (t, J = 6.5 Hz, 2H), 2.67 (t, J = 5.2 Hz, 2H), 2.44 (t, J = 6.5 Hz, 2H), 1.55 – 1.40 (m, 2H), 1.36 – 1.26 (m, 2H), 0.85 (t, J = 7.3 Hz, 3H

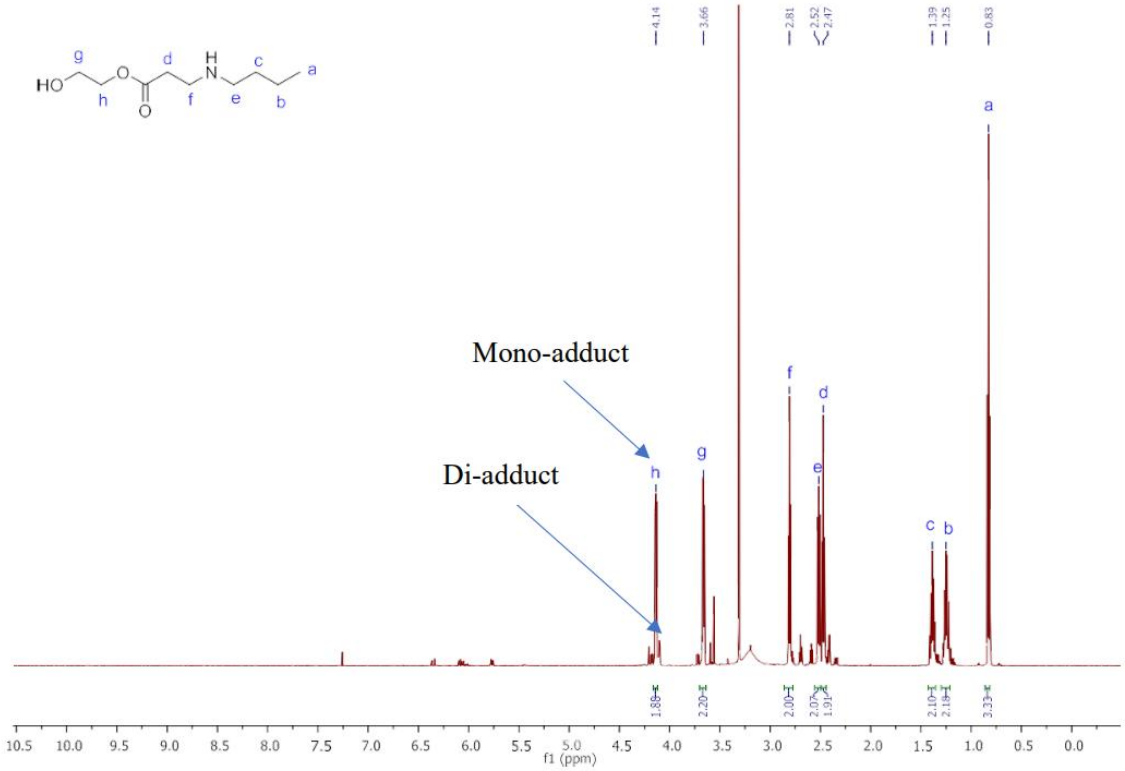

Figure S7.3. ^{1}H NMR spectrum of HEA/BA : molecule **3** (1 : 19) conversion in $CDCl_3$ with 1 eq. of MeOD after 12 h. ^{1}H-NMR (600 MHz, chloroform-d, ppm) = 4.15 - 4.13 (m, 2H), 3.67 – 3.65 (m, 2H), 2.81 (t, J = 6.4 Hz, 2H), 2.51 (t, J = 7.5 Hz, 2H), 2.47 (t, J = 6.4 Hz, 2H), 1.42 – 1.36 (m, 2H), 1.29 – 1.21 (m, 2H), 0.85 (t, J = 7.4 Hz, 3H).

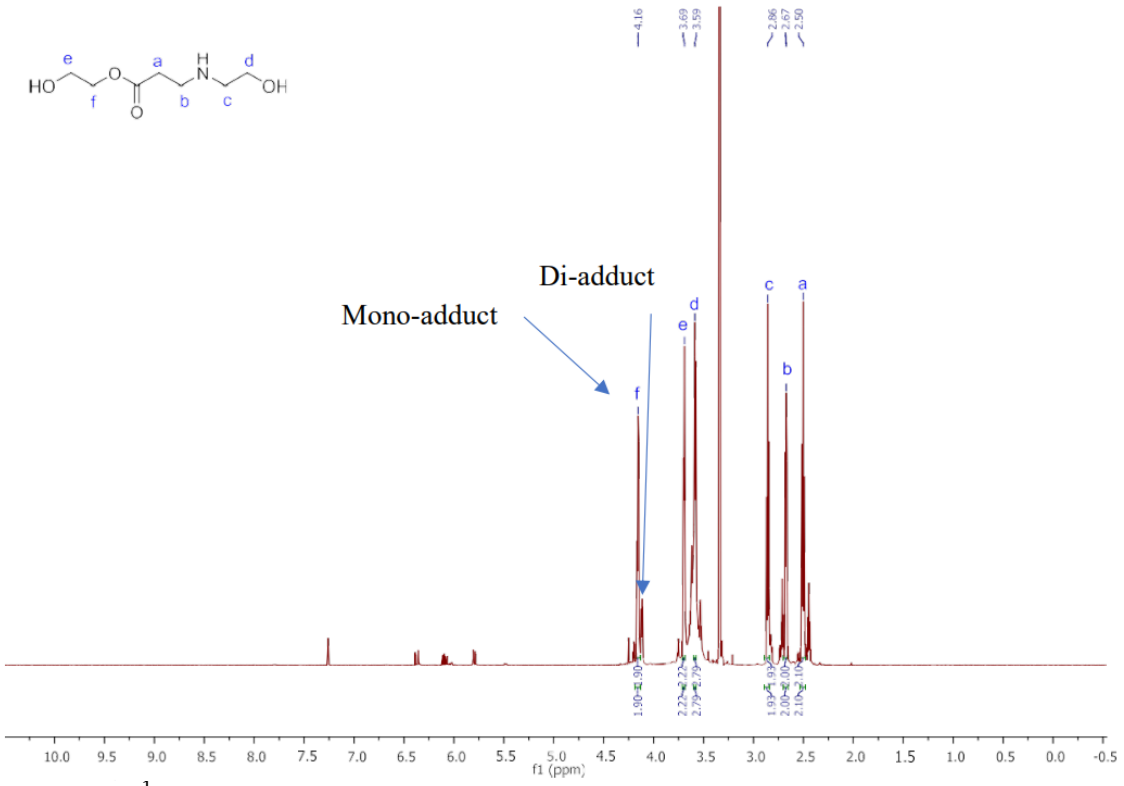

Figure S7.4. ^{1}H NMR spectrum of HEA/EA : molecule **4** (1 : 15) conversion in $CDCl_3$ with 1 eq. of MeOD after 12 h. ^{1}H-NMR (600 MHz, chloroform-d, ppm) = 4.17 – 4.14 (m, 2H), 3.71 - 3.67 (m, 2H), 3.61 – 3.55 (m, 2H), 2.85 (t, J = 6.3 Hz, 2H), 2.67 (t, J = 5.0 Hz, 2H), 2.50 (t, J = 6.2 Hz, 2H)

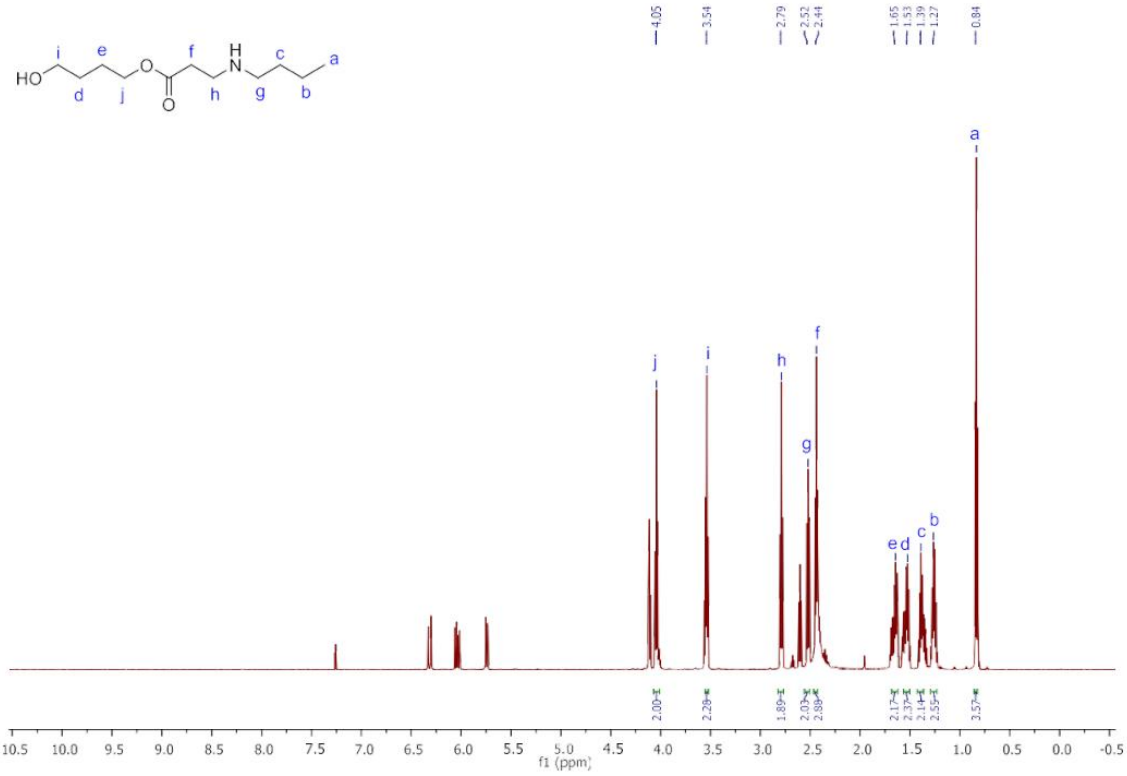

Figure S7.5. ^{1}H NMR spectrum of HBAcr/BA : molecule **5** (1 : 2.3) conversion in $CDCl_3$ after 12 h. ^{1}H-NMR (600 MHz, chloroform-d, ppm) = 4.05 (t, J = 6.6 Hz, 2H), 3.53 (t, J = 6.4 Hz, 2H), 2.79 (t, J = 6.5 Hz, 2H), 2.53 (t, J = 7.3 Hz, 2H), 2.44 (t, J = 6.5 Hz, 2H), 1.67 – 1.50 (m, 4H), 1.42 – 1.22 (m, 4H), 0.85 (t, J = 7.4 Hz, 3H).

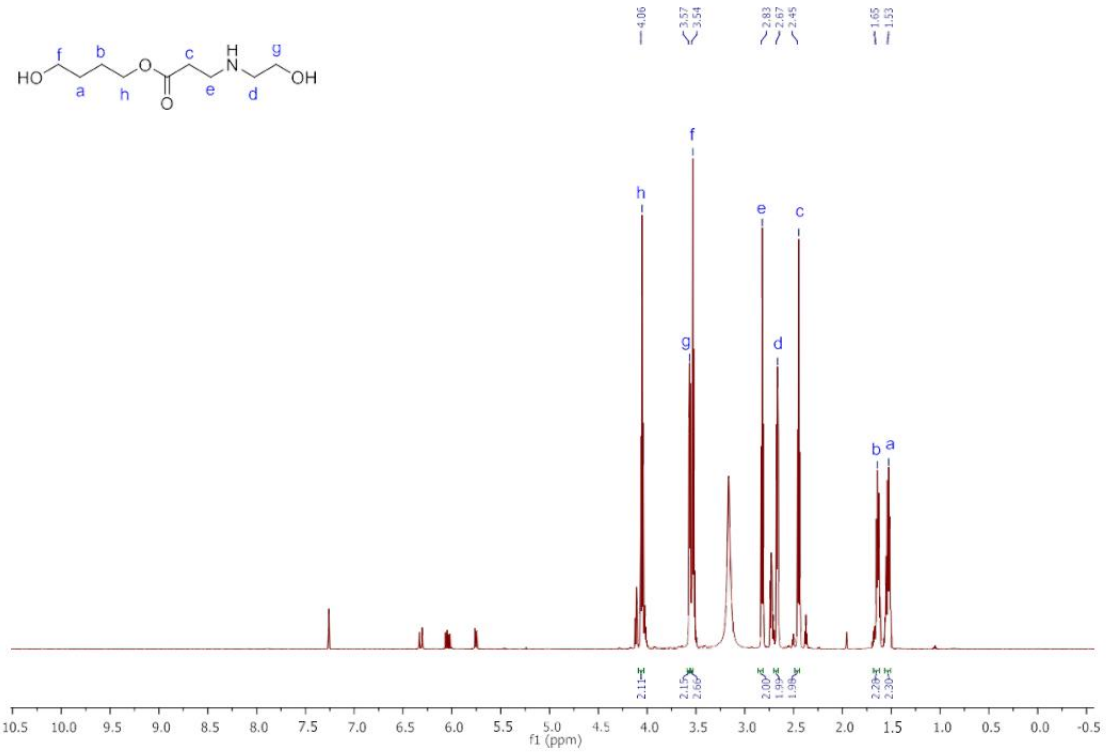

Figure S7.6. 1H NMR spectrum of HBAcr/EA : molecule 6 (1 : 10) conversion in CDCl3 after 12 h. ^{1}H-NMR (600 MHz, chloroform-d, ppm) = 4.06 (t, J =6.5 Hz, 2H), 3.59 - 3.56 (m, 2H), 3.55 (t, J = 6.5 Hz, 2H), 2.83 (t, J = 6.4 Hz, 2H), 2.67 (t, J = 5.2 Hz, 2H), 2.45 (t, J = 6.4 Hz, 2H), 1.68 – 1.61 (m, 2H), 1.57 – 1.50 (m, 2H

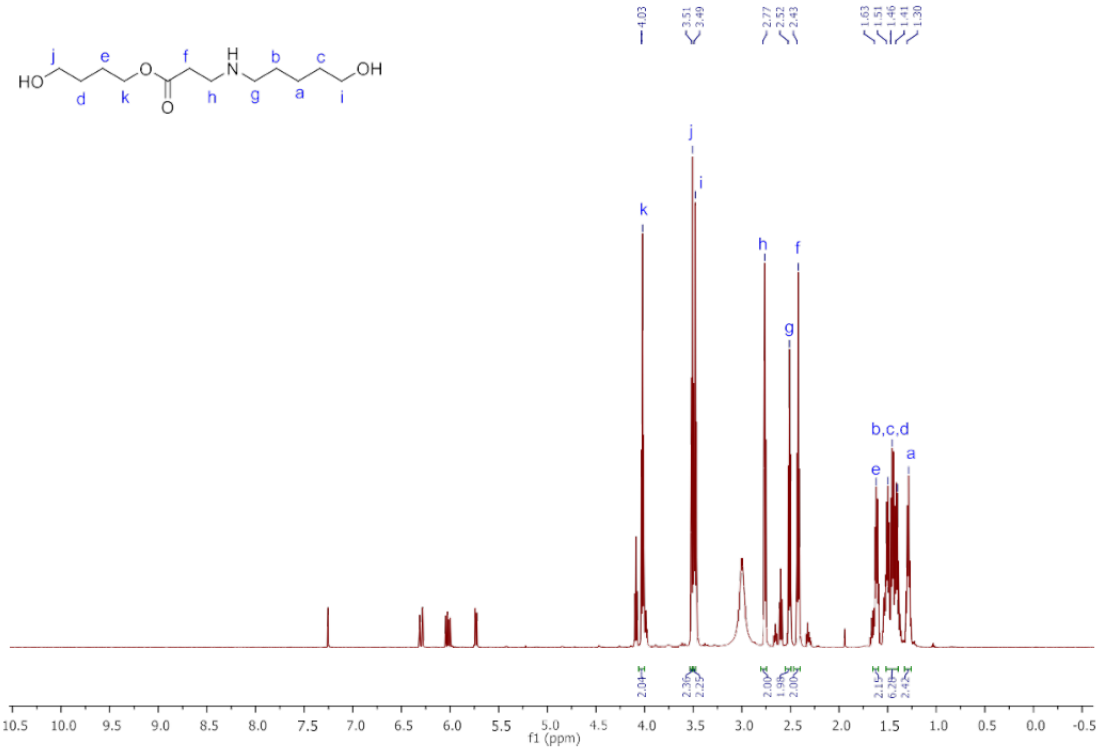

Figure S7.7. ^{1}H NMR spectrum of HBAcr/AP : molecule **7** (1 : 4.7) conversion in $CDCl_3$ after 12 h. ^{1}H-NMR (600 MHz, chloroform-d, ppm) = 4.03 (t, J =6.6 Hz, 2H), 3.52 (t, J = 6.3 Hz, 2H), 3.48 (t, J = 6.5 Hz, 2H), 2.77 (t, J = 6.5 Hz, 2H), 2.52 (t, J = 7.1 Hz, 2H), 2.43 (t, J = 6.4 Hz, 2H), 1.66 – 1.25 (m, 10H)

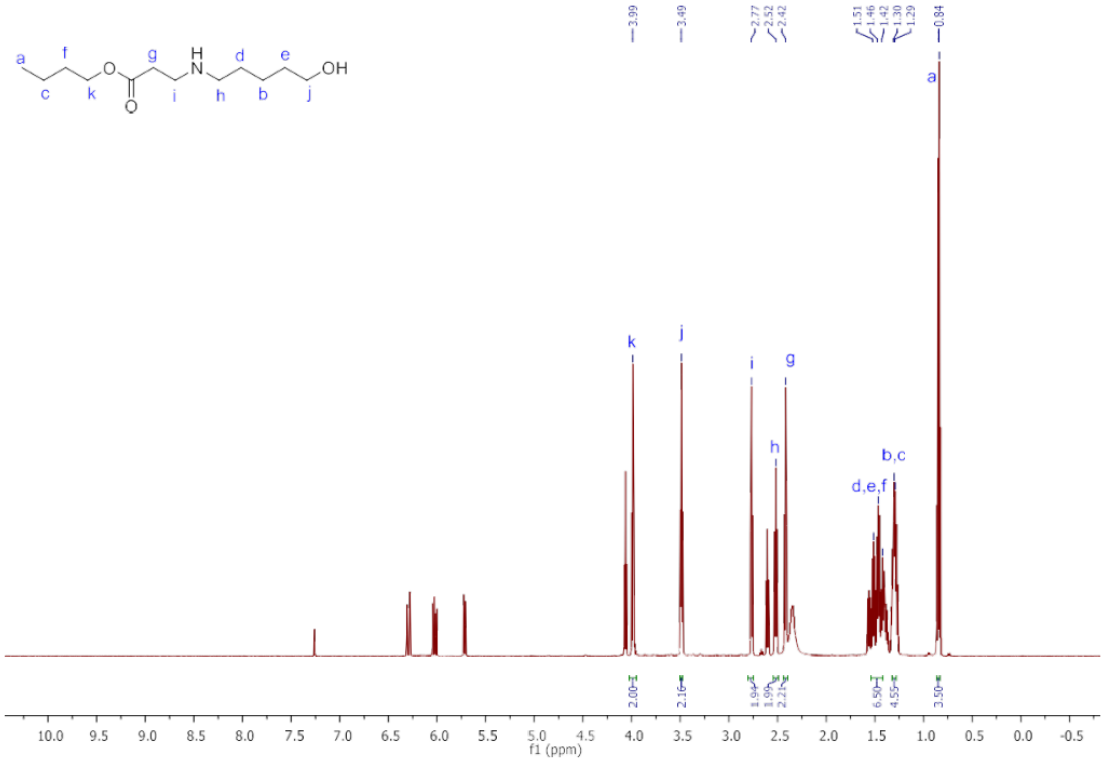

Figure S7.8. ^{1}H NMR spectrum of BAcr/AP : molecule **8** (1 : 1.9) conversion in $CDCl_3$ after 12 h. ^{1}H-NMR (600 MHz, chloroform-d, ppm) = 3.99 (t, J = 6.7 Hz, 2H), 3.49 (t, J = 7.2 Hz, 2H), 2.77 (t, J = 6.5 Hz, 2H), 2.52 (t, J = 7.2 Hz, 2H), 2.42 (t, J = 6.5 Hz, 2H), 1.58 – 1.24 (m, 10H), 0.86 (t, J = 7.6 Hz, 3H).

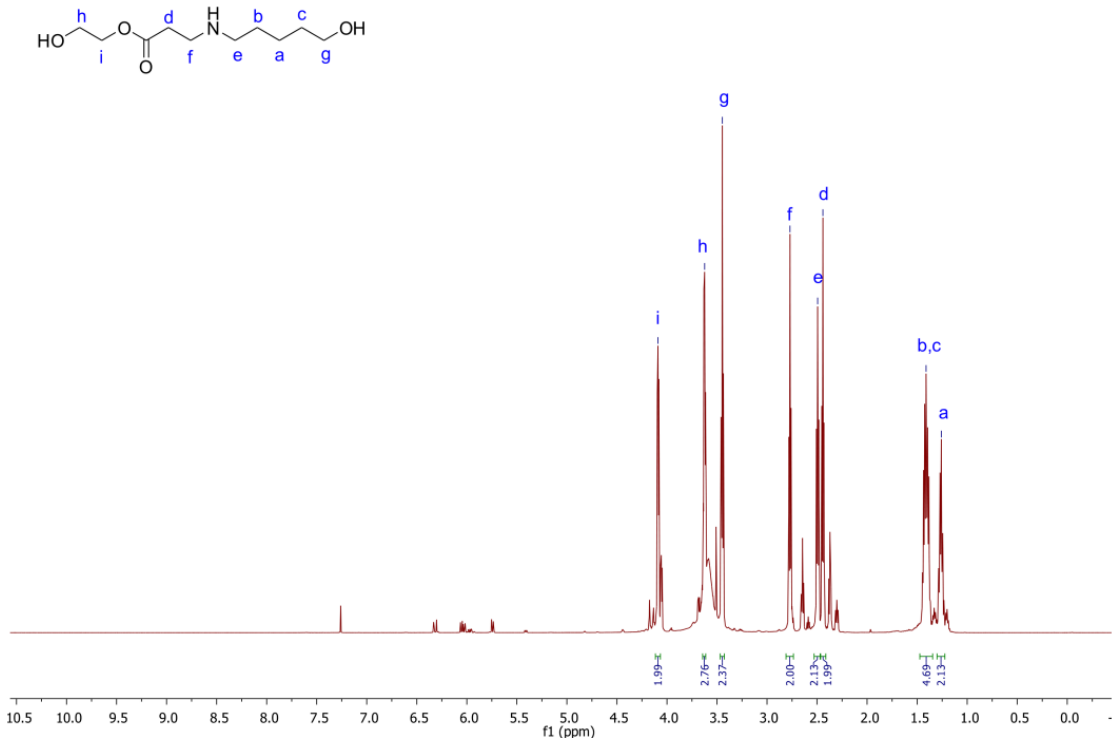

Figure S7.9. ^{1}H NMR spectrum of HEA/AP : molecule **9** (1 : 17) conversion in $CDCl_3$ after 8 h. ^{1}H-NMR (600 MHz, chloroform-d, ppm) = 4.10 – 4.06 (m, 2H), 3.63 – 3.60 (m, 2H), 3.45 – 3.42 (m, 2H), 2.75 (t, J = 6.5 Hz, 2H), 2.48 (t, J = 7.2 Hz, 2H), 2.43 (t, J = 6.3 Hz, 2H), 1.45 – 1.21 (m, 6H).

7.1.2 Products and rates of reaction: Silicones and small molecules

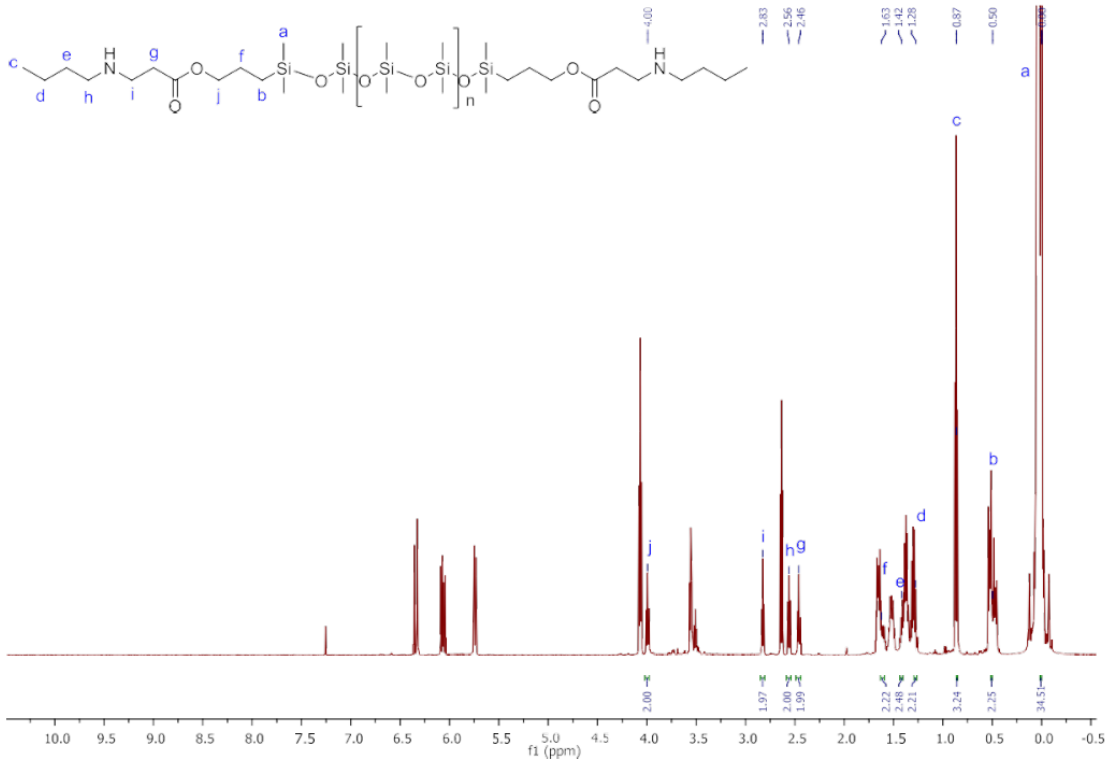

Figure S7.10. ^{1}H NMR spectrum of Di11/BA : polymer **10** (3.6 : 1) conersion in $CDCl_3$ after 24 h. ^{1}H-NMR (600 MHz, chloroform-d, ppm) = 4.00 (t, J =7.0 Hz, 4H), 3.58 (t, J = 5.3 Hz, 4H), 2.83 (t, J = 7.2 Hz, 4H), 2.57 (t, J = 7.2 Hz, 4H), 2.46 (t, J = 6.5 Hz, 4H), 1.66 – 1.38 (m, 8H), 0.87 (t, J = 7.2 Hz, 6H), 0.55 – 0.45 (m, 4H), 0.16 – -0.10 (m, 60H).

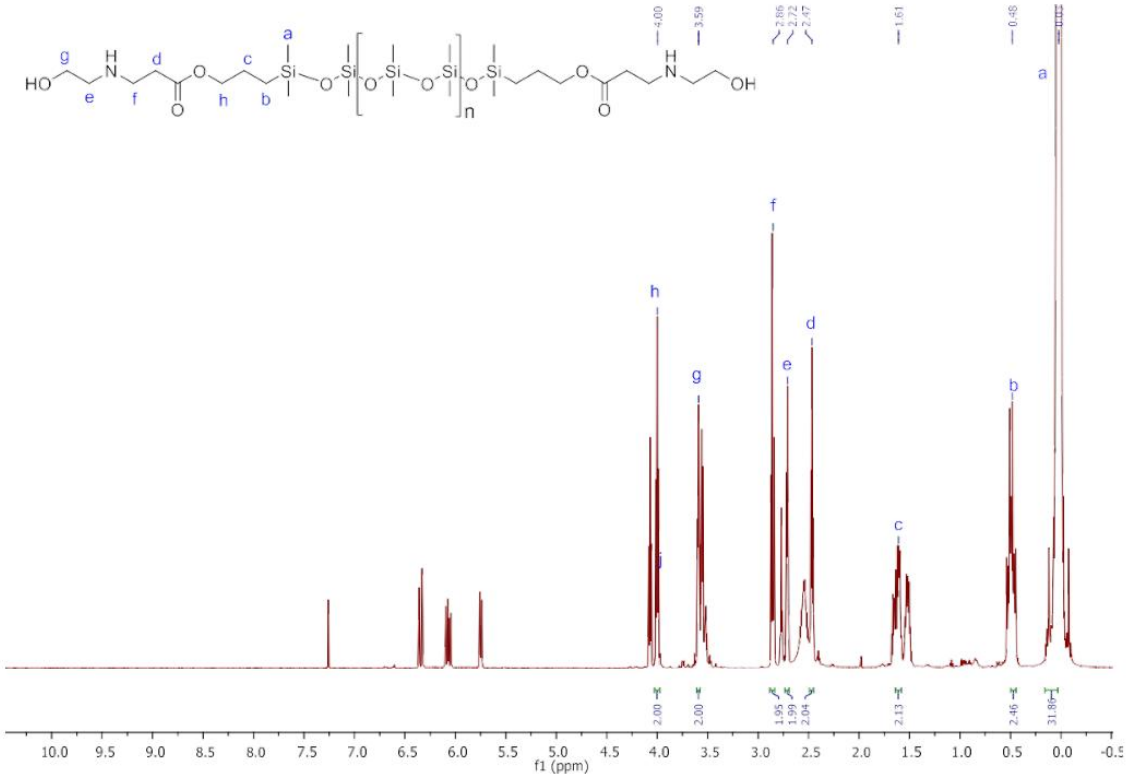

Figure S7.11. ^{1}H NMR spectrum of Di11/EA : polymer **11** (1 : 1.8) conversion in $CDCl_3$ after 24 h. ^{1}H-NMR (600 MHz, chloroform-d, ppm) = 4.00 (t, J =7.0 Hz, 4H), 3.59 (t, J = 5.3 Hz, 4H), 2.86 (t, J = 6.5 Hz, 4H), 2.72 (t, J = 5.3 Hz, 4H), 2.47 (t, J = 6.4 Hz, 4H), 1.66 – 1.58 (m, 4H), 0.55 – 0.45 (m, 4H), 0.16 – -0.10 (m, 60H).

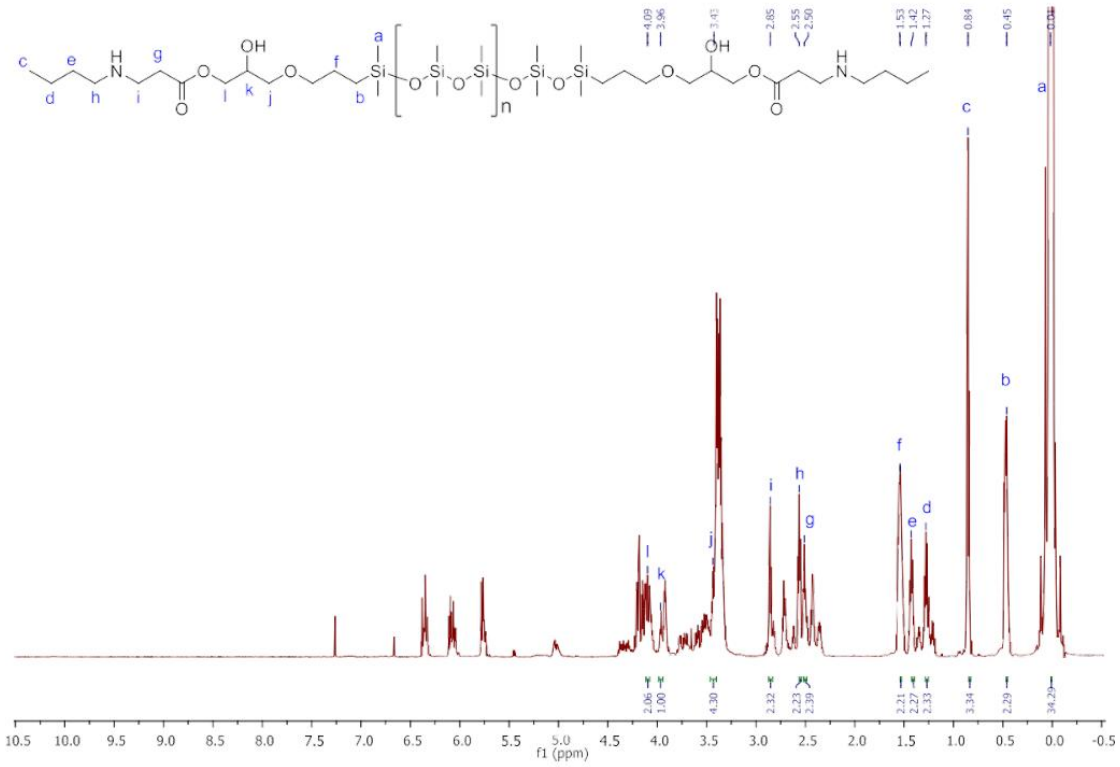

Figure S7.12. ^{1}H NMR spectrum of Di9_OH/BA : polymer **12** (1.5 : 1) conversion in $CDCl_3$ after 24 h. ^{1}H-NMR (600 MHz, chloroform-d, ppm) = 4.22 – 4.05 (m, 4H), 3.95 – 3.91 (m, 2H), 3.43 – 3.29 (m, 8H), 2.87 – 2.83 (m, 4H), 2.58 – 2.53 (m, 4H), 2.52 – 2.48 (m, 4H), 1.58 – 1.48 (m, 4H), 1.45 – 1.38 (m, 4H), 1.30 – 1.24 (m, 4H), 0.84 (t, J = 7.8 Hz, 6H), 0.49 – 0.41 (m, 4H), 0.12 – -0.12 (m, 60H)

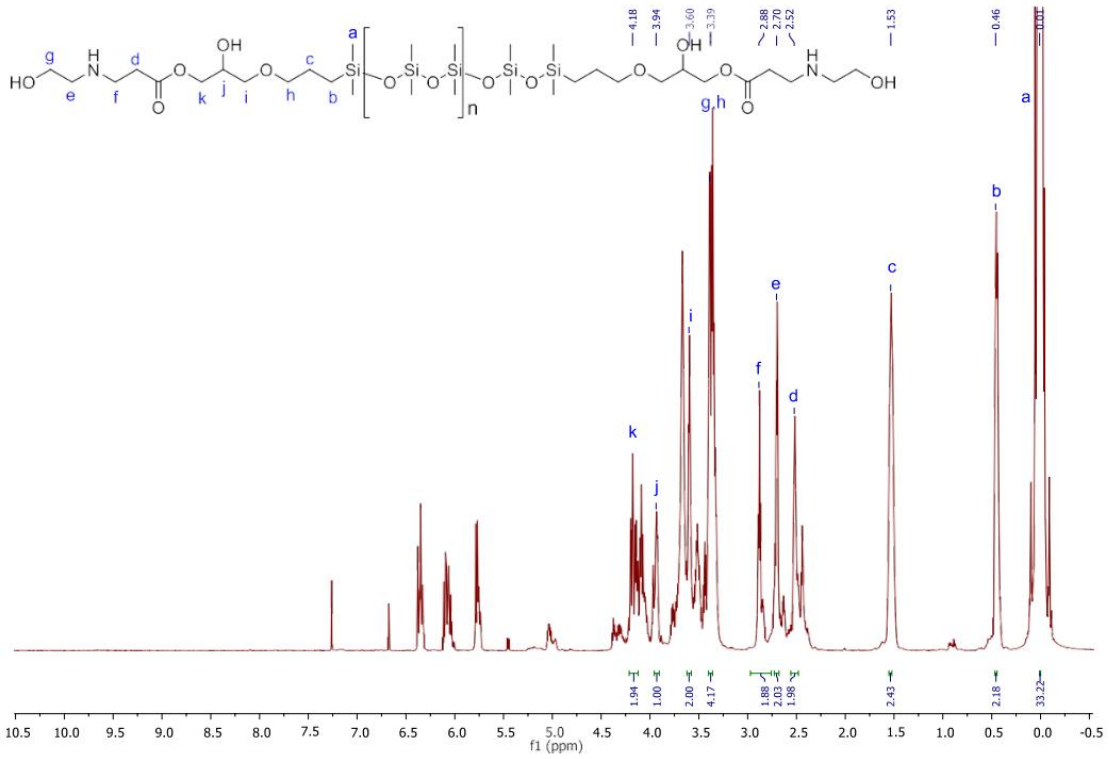

Figure S7.13. ^{1}H NMR spectrum of Di10_OH/EA : polymer **13** (1 : 1.5) conversion in $CDCl_3$ after 24 h. ^{1}H-NMR (600 MHz, chloroform-d, ppm) = 4.22 – 4.05 (m, 4H), 3.96 – 3.91 (m, 2H), 3.62 – 3.58 (m, 4H), 3.42 – 3.31 (m, 8H), 2.91 – 2.86 (m, 4H), 2.72 – 2.68 (m, 4H), 2.55 – 2.49 (m, 4H), 1.58 – 1.48 (m, 4H), 0.49 – 0.41 (m, 4H), 0.12 – -0.12 (m, 60H)

7.1.3 Elastomer synthesis

Table S7.2 Production of silicone elastomers

Amino Silicone	Weigh t (g)	Acrylate Silicone	Weight (g)	Gelation Time (min)	Hardness at 30 min (Shore OO)	Harness at Full Cure (Shore OO)	% of Cure
AMS-152	2	Di10	0.58	>12 hours	No Cure	82	
AMS-152	1.5	Di25	0.91	>12 hours	No Cure	57	
AMS-1203	1	Di10	1.54	20	54	82	66%
AMS-1203	0.63	Di25	2	35	25	78	
AMS-152	2	Di10 OH	0.58	20	49	83	59%

AMS-152	1.5	Di25 OH	0.91	35	29	61	48%
AMS-1203	1	Di10 OH	1.54	<2	90	92	98%
AMS-1203	0.63	Di25 OH	2	<2	82	93	88%

7.2 Appendix II: Supporting Information for Chapter 3

7.2.1 Synthesis of ChAAILs (Choline Amino Acid Ionic Liquids)

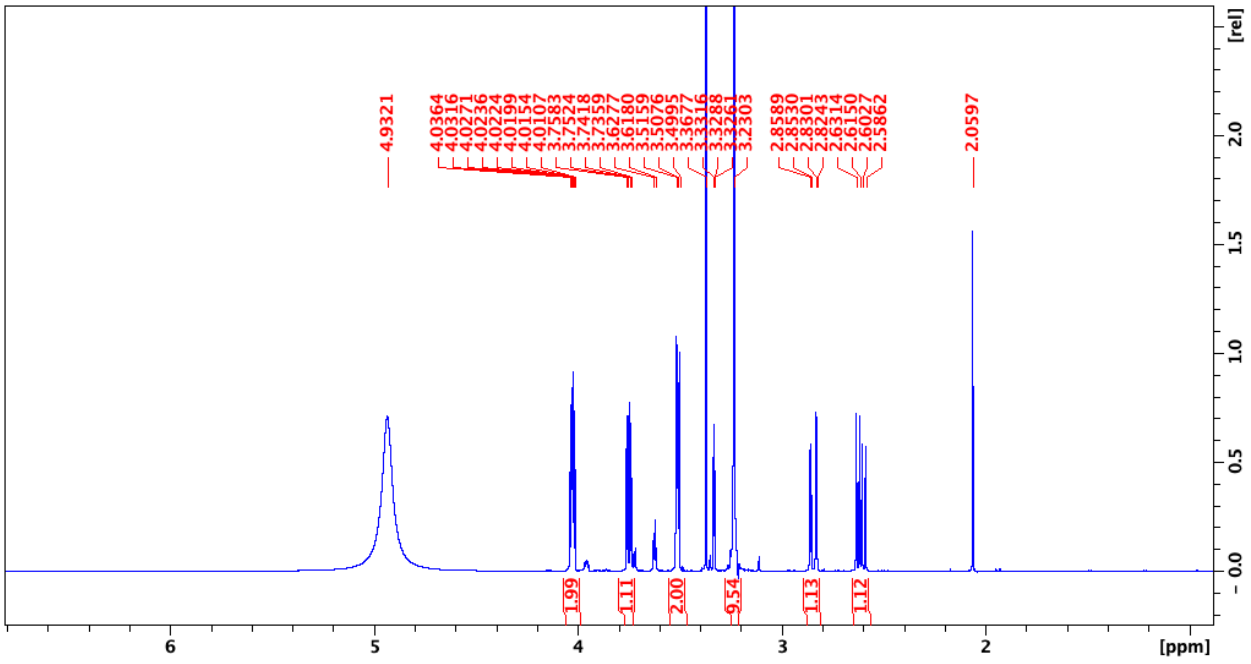

Figure S7.14. ^{1}H NMR of ChAspIL.

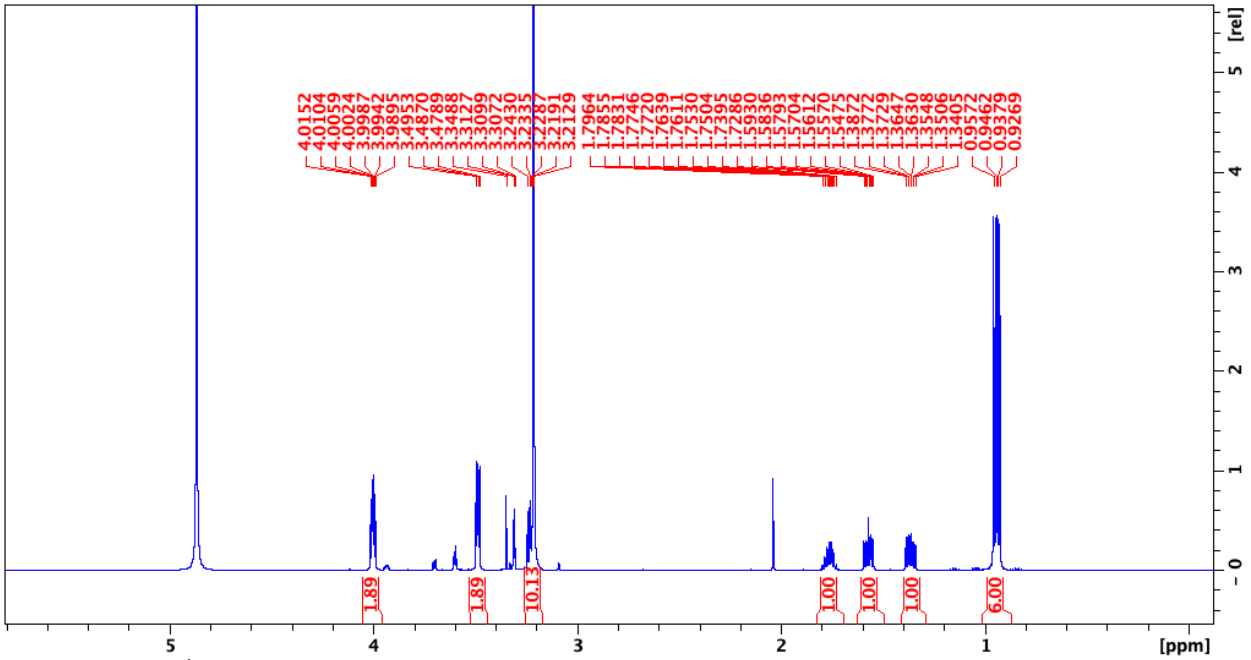

Figure S7.15. ^{1}H NMR of ChLeuIL.

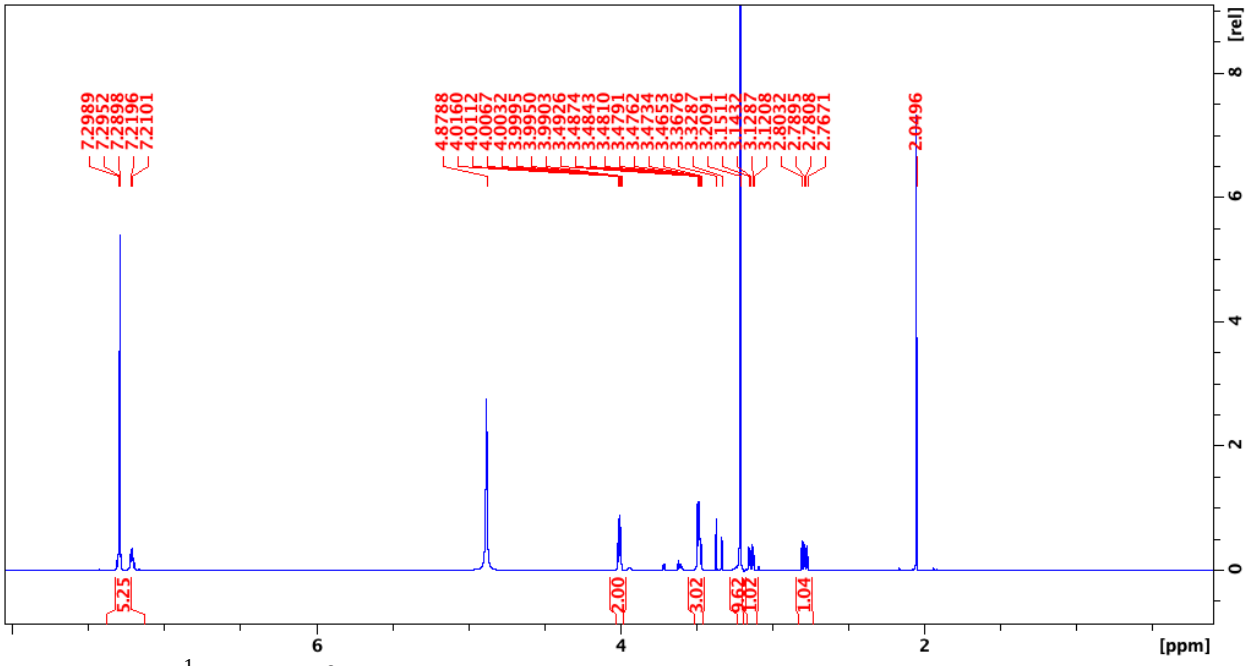

Figure S7.16. ^{1}H NMR of ChPheIL.

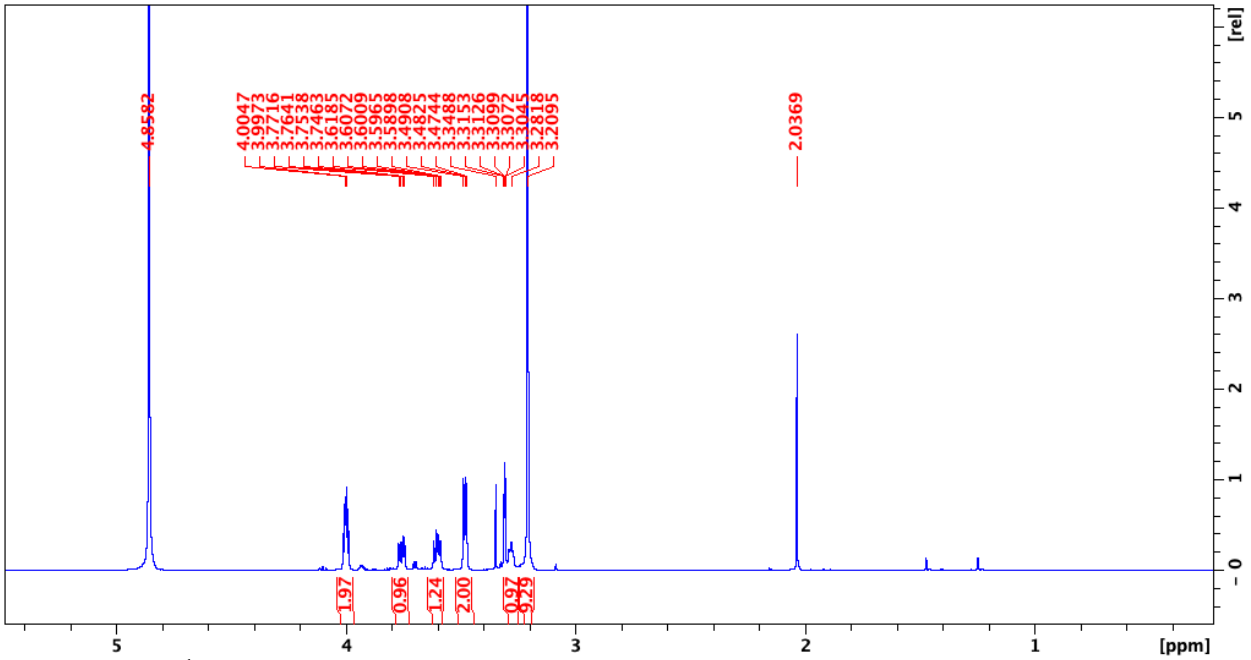

Figure S7.17. ^{1}H NMR of ChSerIL.

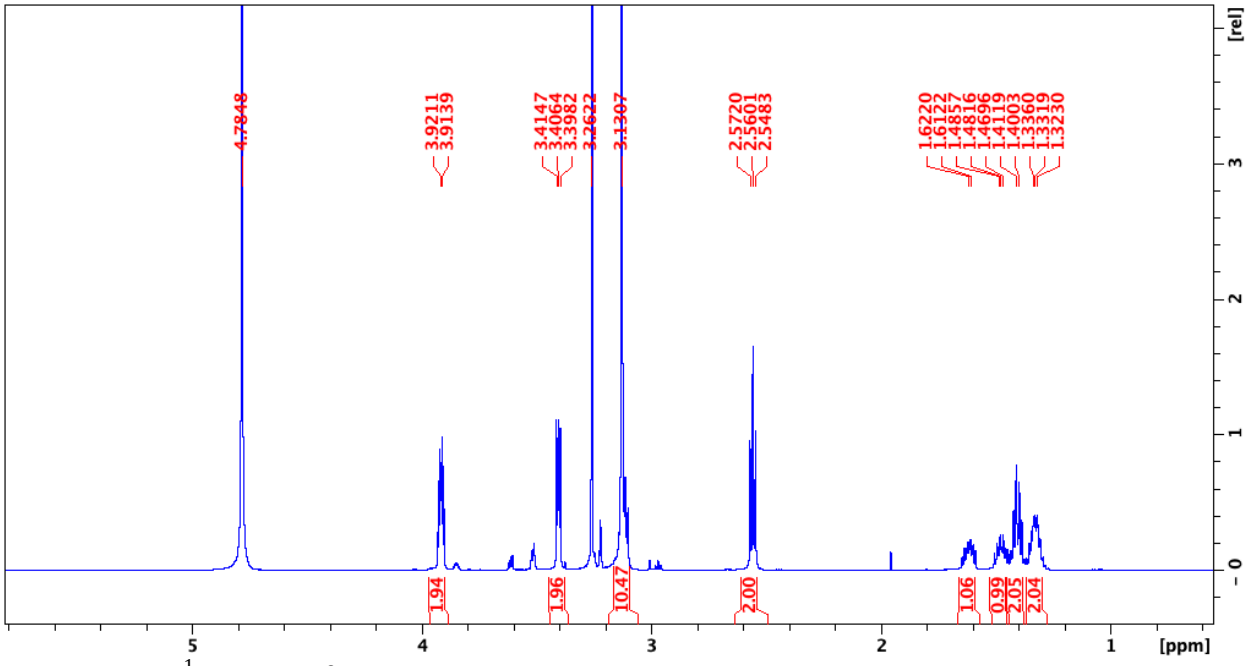

Figure S7.18. ^{1}H NMR of ChLysIL.

Table S7.3. Ionic liquid synthesis conditions

Amino acid	Mole AA (mmol)	Choline OH (mmol)	Temperature (℃)	Water (mL)	Reaction time (h)
Asp	15.1	13.6	50	40	72
Lys	13.7	12.4	50	40	72
Ser	19.1	17.2	50	40	72
Phe	12.1	10.9	50	40	72
Leu	15.3	13.8	50	40	72

7.2.2 ChAAIL and Acrylates Aqueous NMR Kinetic Studies

Table S7.4. Reaction summary of ChAAILs with simple acylates.

ChAAILs	Acrylate	Solvent	Reaction Time (min)	Total conversion*	Michael product*	Degradation product*
ChLysIL	EA	Water	30	100%	68%	32%
ChLysIL	HEA	Water	30	100%	40%	60%
ChLysIL	EA	Water	720	100%	17%	83%
ChLysIL	HEA	Water	720	100%	0%	100%
ChLysIL	EA	Neat	30	97%	86%	10%
ChLysIL	HEA	Neat	30	99%	59%	40%
ChLysIL	EA	Neat	1440	100%	89%	11%
ChLysIL	HEA	Neat	1440	99%	61%	39%
ChSerIL	EA	Water	30	70%	64%	6%
ChSerIL	HEA	Water	30	72%	57%	14%
ChSerIL	EA	Water	720	96%	51%	45%
ChSerIL	HEA	Water	720	91%	36%	54%
ChSerIL	EA	Neat	30	34%	31%	3%
ChSerIL	HEA	Neat	30	75%	56%	20%
ChSerIL	EA	Neat	1440	99%	87%	12%
ChSerIL	HEA	Neat	1440	97%	65%	33%
ChPheIL	EA	Water	30	64%	59%	4%
ChPheIL	HEA	Water	30	67%	58%	9%
ChPheIL	EA	Water	720	93%	45%	48%
ChPheIL	HEA	Water	720	83%	40%	44%
ChPheIL	EA	Neat	30	31%	23%	8%
ChPheIL	HEA	Neat	30	60%	55%	5%

ChPheIL	EA	Neat	1440	85%	71%	15%
ChPheIL	HEA	Neat	1440	83%	56%	27%
ChLeuIL	EA	Water	30	69%	64%	5%
ChLeuIL	HEA	Water	30	75%	62%	13%
ChLeuIL	EA	Water	720	98%	41%	57%
ChLeuIL	HEA	Water	720	86%	27%	59%
ChLeuIL	EA	Neat	30	48%	45%	3%
ChLeuIL	HEA	Neat	30	61%	51%	10%
ChLeuIL	EA	Neat	1440	100%	96%	4%
ChLeuIL	HEA	Neat	1440	94%	75%	20%
ChAspIL	EA	Water	30	0%	0%	0%
ChAspIL	HEA	Water	30	0%	0%	0%
ChAspIL	EA	Water	720	0%	0%	0%
ChAspIL	HEA	Water	720	0%	0%	0%
ChAspIL	EA	Neat	30	0%	0%	0%
ChAspIL	HEA	Neat	30	0%	0%	0%
ChAspIL	EA	Neat	1440	0%	0%	0%
ChAspIL	HEA	Neat	1440	0%	0%	0%

*Total conversion is defined by the % of acrylate reacted, Michael or degradation product conversion is determined by the ratio of the relative products of Michael product and degradation product by NMR out of the total conversion.

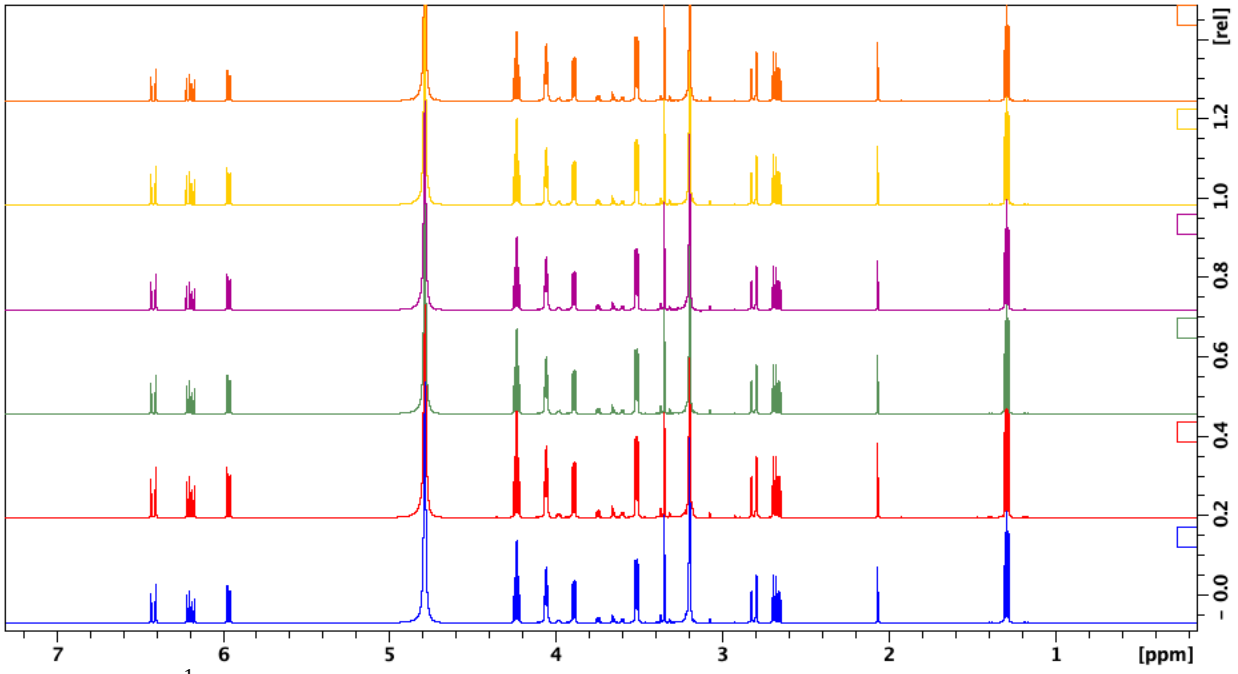

Figure S7.19. ^{1}H NMR stacked plots of reaction monitoring of ChAspIL and EA in D_2O, at 30min, 1h, 2h, 4h, 12h, 24h from bottom to top.

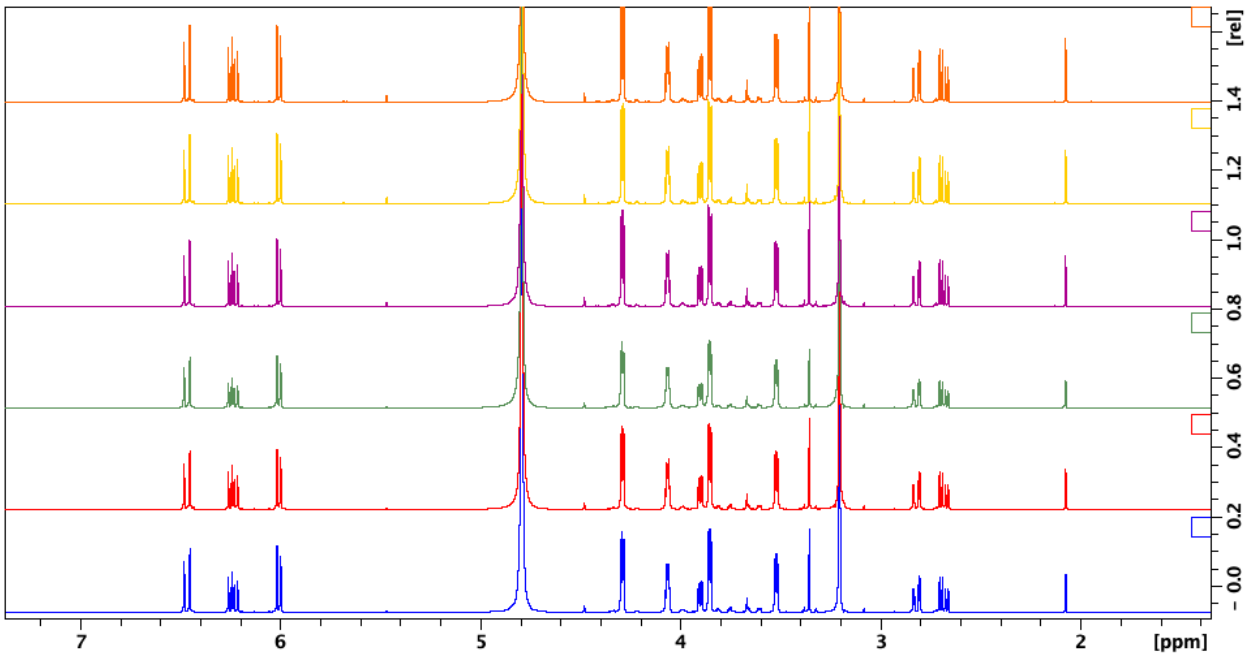

Figure S7.20. ^{1}H NMR stacked plots for reaction monitoring of ChAspIL and HEA in D_2O, at 30min, 1h, 2h, 4h, 12h, 24h from bottom to top.

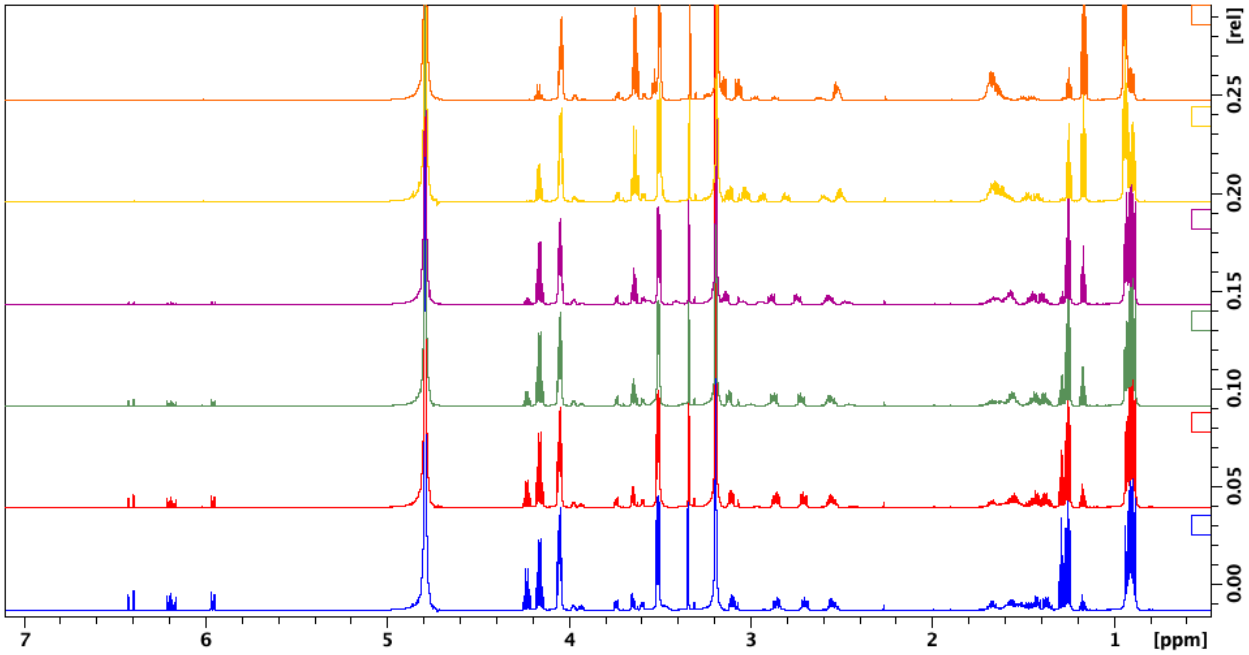

Figure S7.21. ^{1}H NMR stacked plots for reaction monitoring of ChLeuIL and EA in D_2O, at 30min, 1h, 2h, 4h, 12h, 24h from bottom to top.

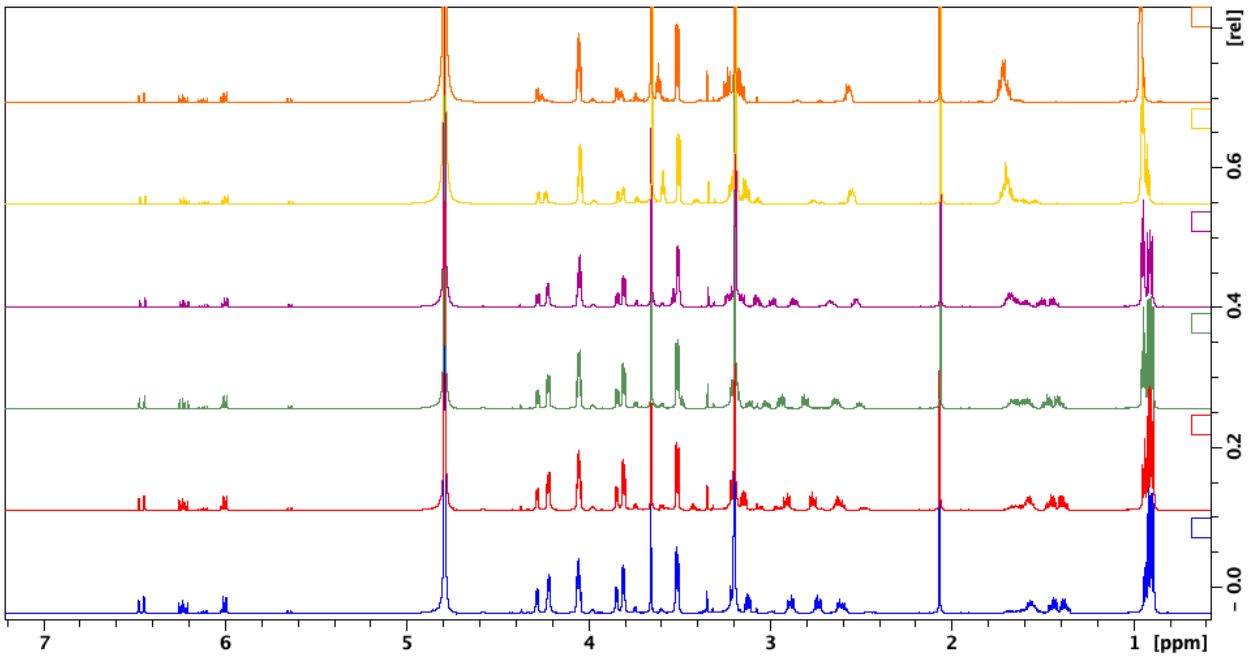

Figure S7.22. ^{1}H NMR stacked plots for reaction monitoring of ChLeuIL and HEA in D_2O, at 30min, 1h, 2h, 4h, 12h, 24h from bottom to top.

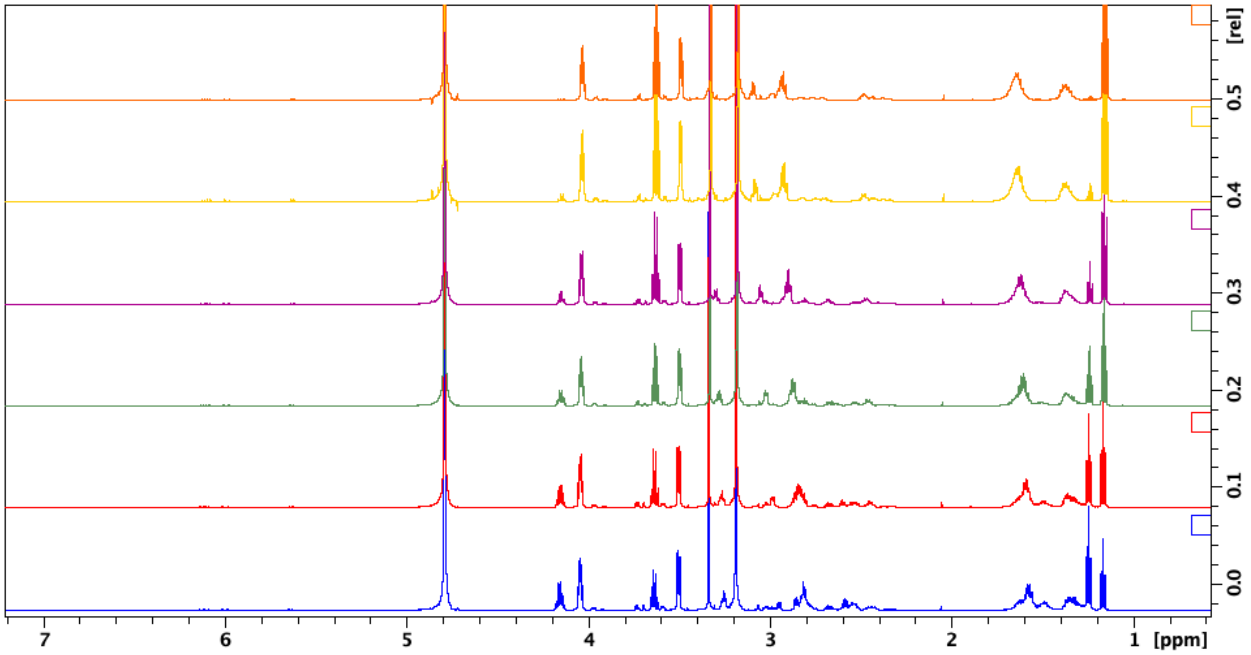

Figure S7.23. ^{1}H NMR stacked plots for reaction monitoring of ChLysIL and EA in D_2O, at 30min, 1h, 2h, 4h, 12h, 24h from bottom to top.

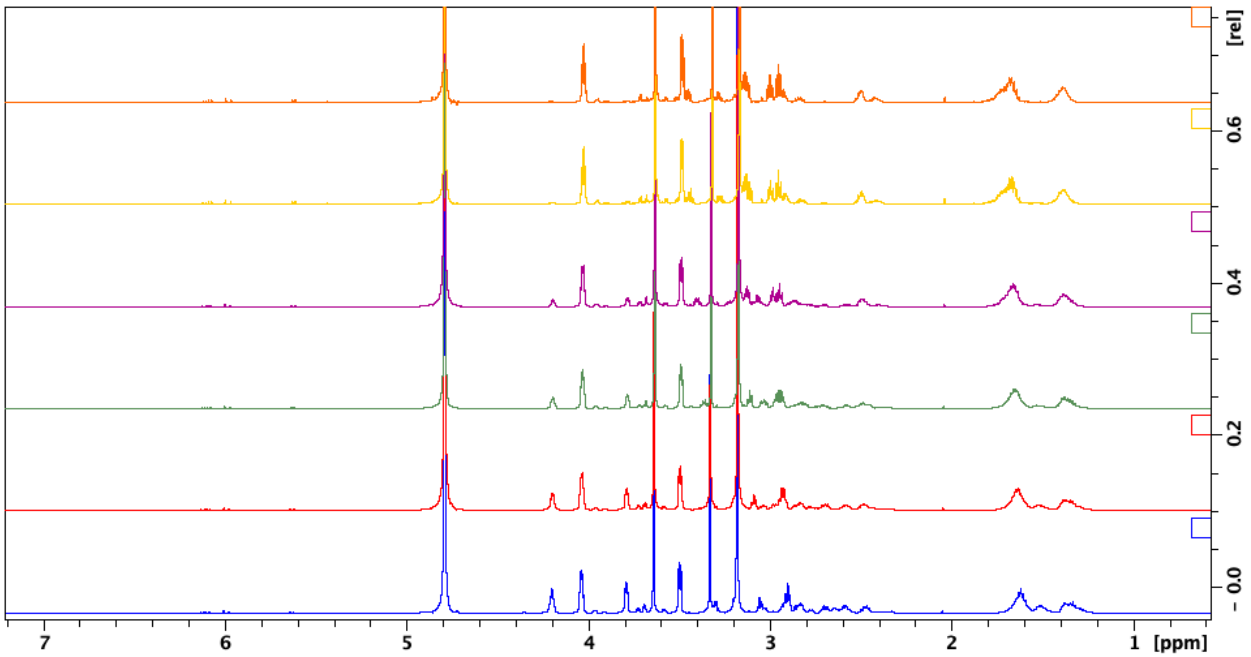

Figure S7.24. ^{1}H NMR stacked plots for reaction monitoring of ChLysIL and HEA in D_2O, at 30min, 1h, 2h, 4h, 12h, 24h from bottom to top.

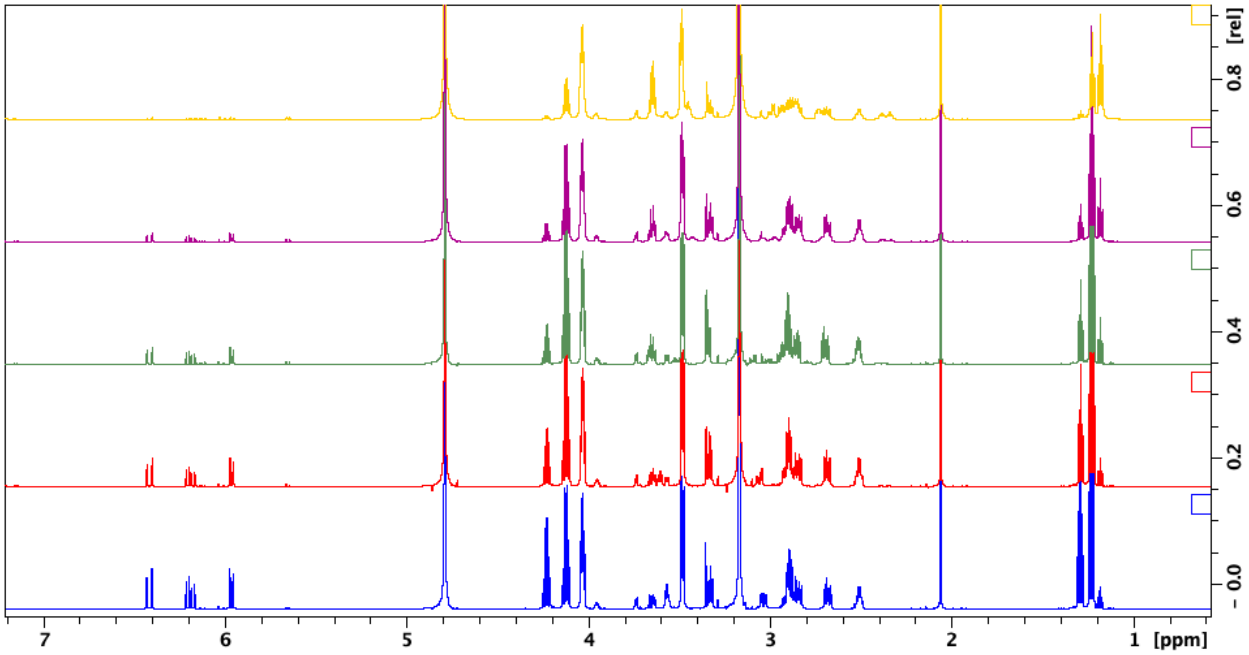

Figure S7.25. ^{1}H NMR stacked plots for reaction monitoring of ChPheIL and EA in D_2O, at 30min, 1h, 2h, 4h, 12h from bottom to top.

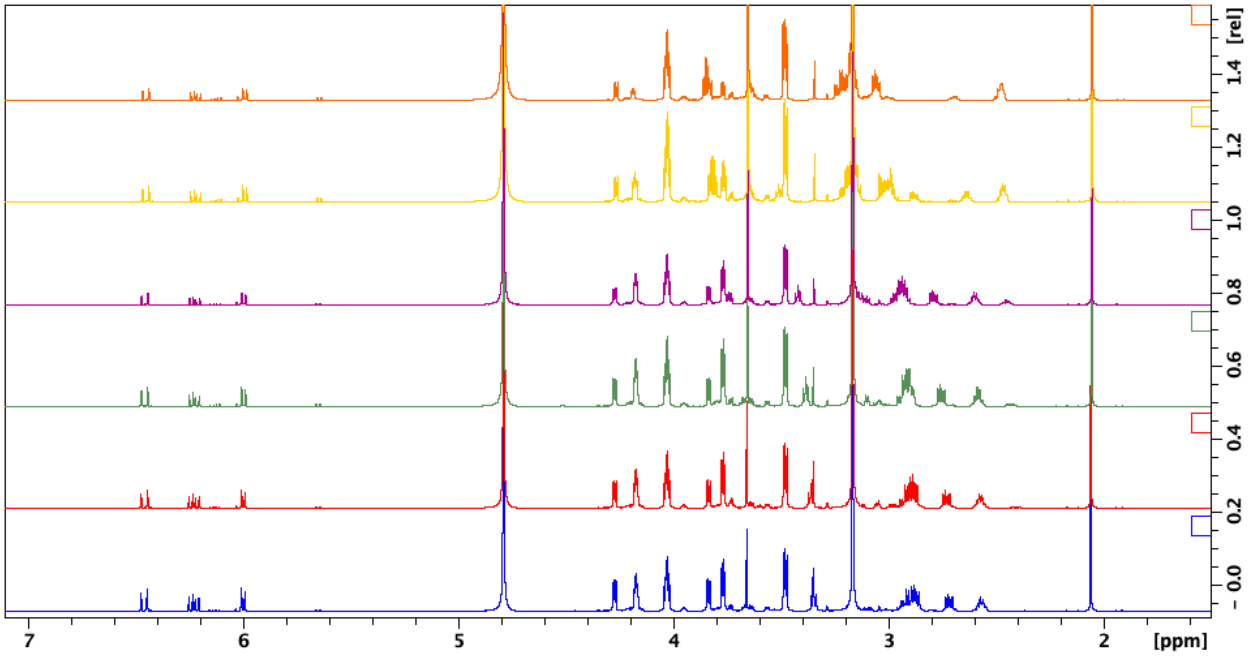

Figure S7.26. ^{1}H NMR stacked plots for reaction monitoring of ChPheIL and HEA in D_2O, at 30min, 1h, 2h, 4h, 12h, 24h from bottom to top.

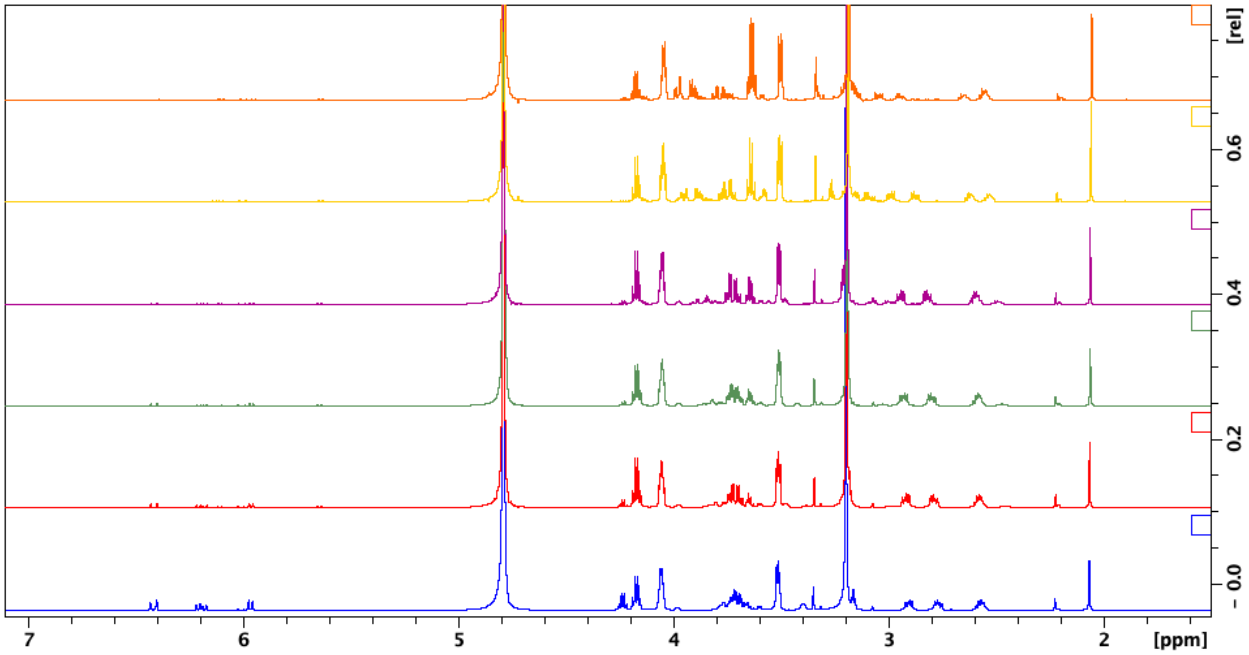

Figure S7.27. ^{1}H NMR stacked plots for reaction monitoring of ChSerIL and EA in D_2O, at 30min, 1h, 2h, 4h, 12h, 24h from bottom to top.

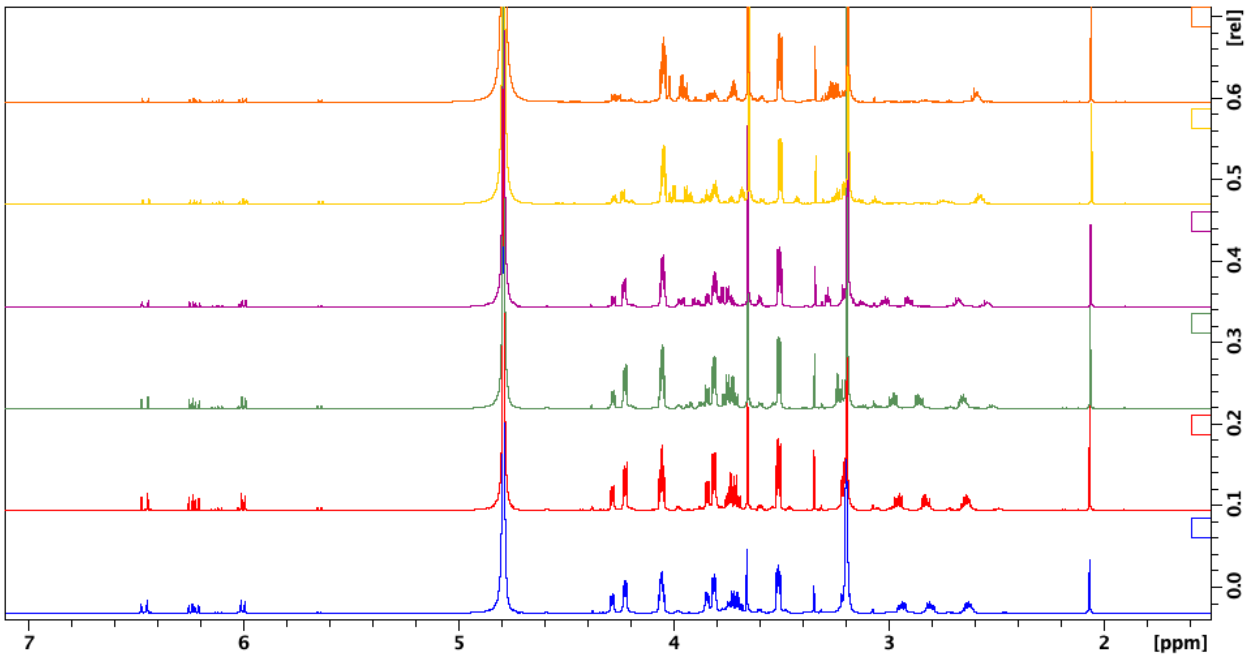

Figure S7.28. ^{1}H NMR stacked plots for reaction monitoring of ChSerIL and HEA in D_2O, at 30min, 1h, 2h, 4h, 12h, 24h from bottom to top.

7.2.3 ChAAIL and Acrylate Solvent Free Reactions

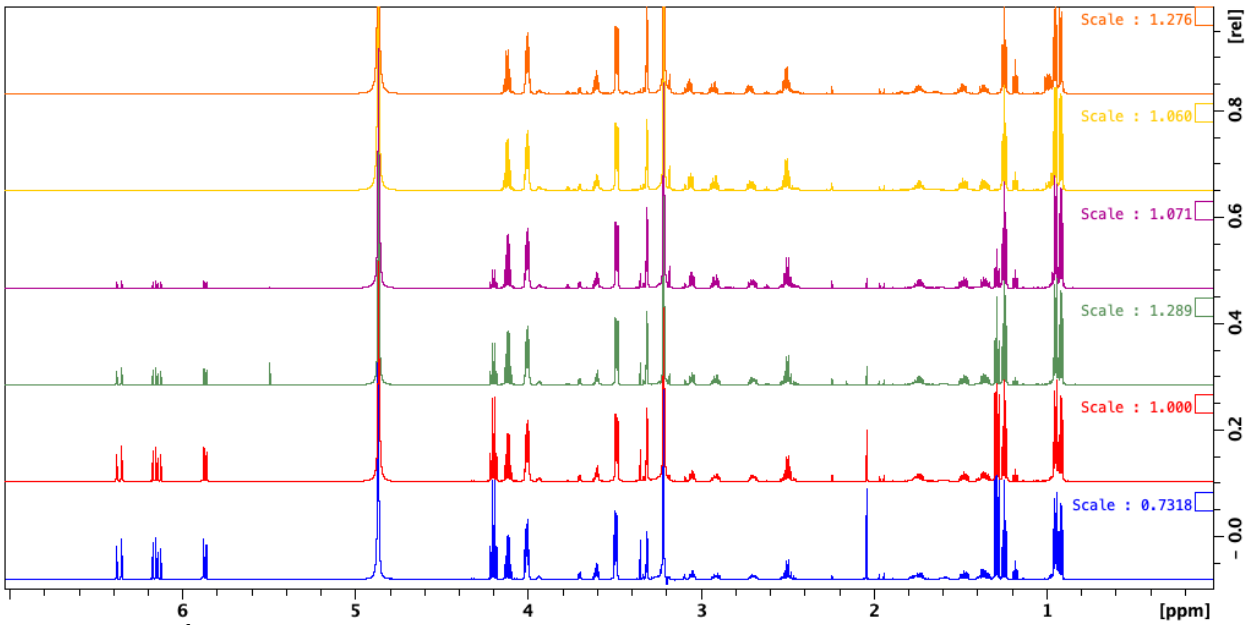

Figure S7.29. ^{1}H NMR stacked plots for reaction monitoring of ChAspIL and EA neat, at 30min, 1h, 2h, 4h, 12h, 24h from bottom to top. The spectral window is scaled to the height of choline peak at ~3.5 ppm for better relative comparison between different time points.

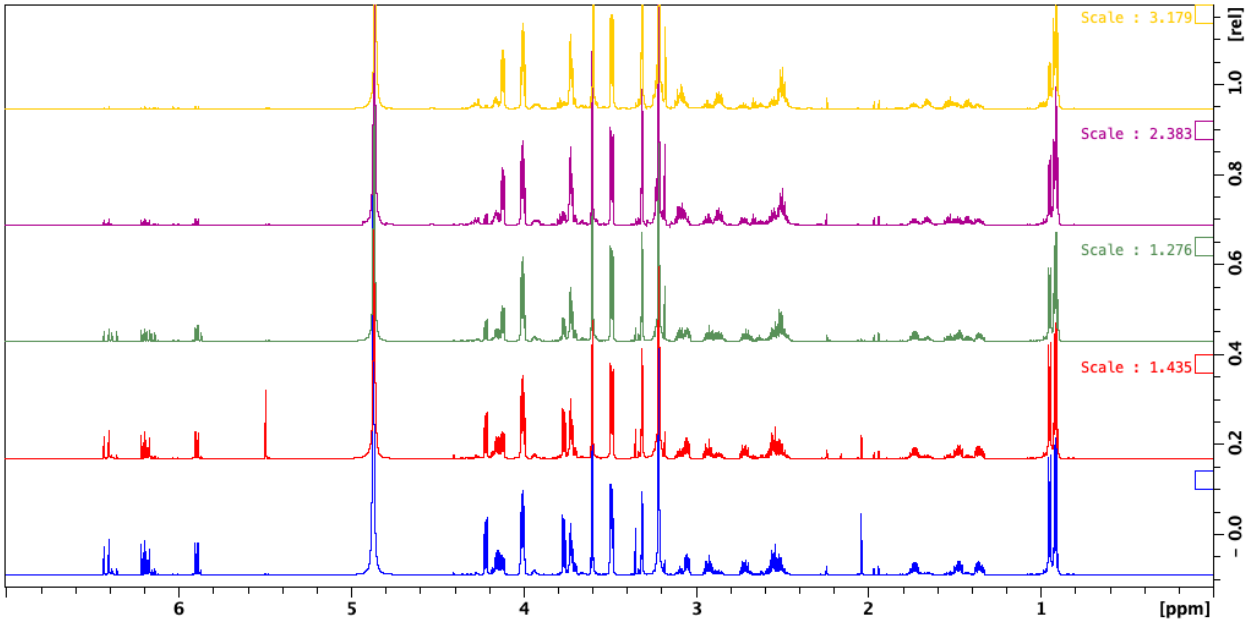

Figure S7.30. ^{1}H NMR stacked plots for reaction monitoring of ChAspIL and HEA neat, at 1h, 2h, 4h, 12h, 24h from bottom to top. The spectral window is scaled to the height of choline peak at ~3.5 ppm for better relative comparison between different time points.

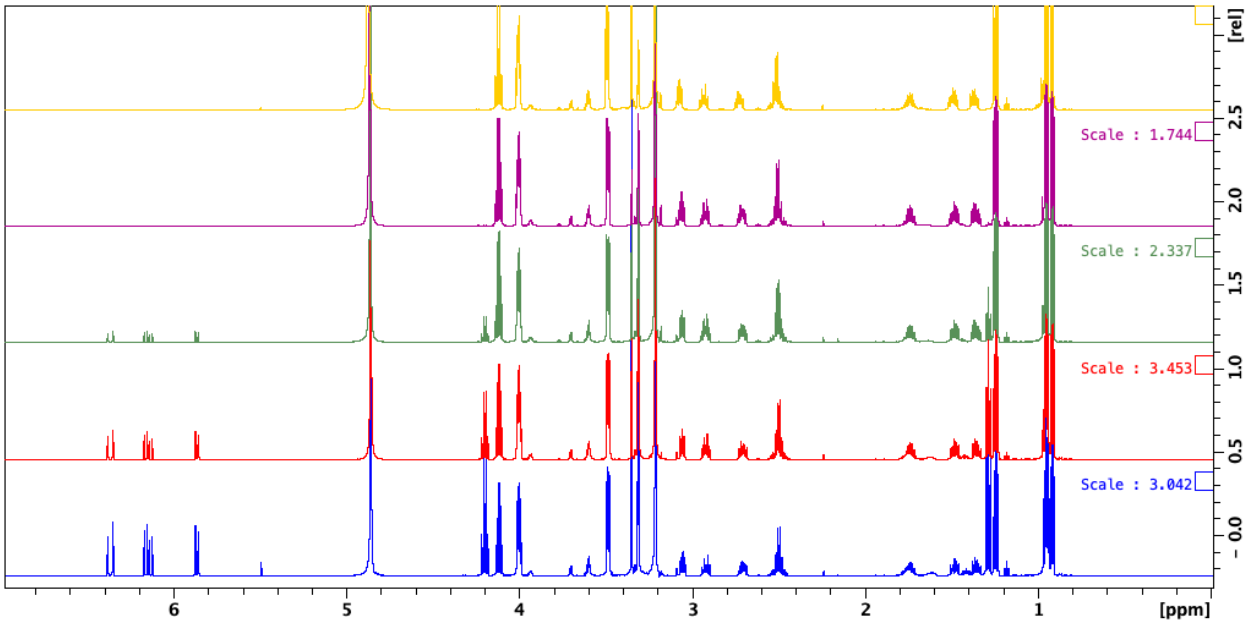

Figure S7.31. ^{1}H NMR stacked plots for reaction monitoring of ChLeuIL and EA neat, at 30min, 1h, 2h, 4h, 24h from bottom to top. The spectral window is scaled to the height of choline peak at ~3.5 ppm for better relative comparison between different time points.

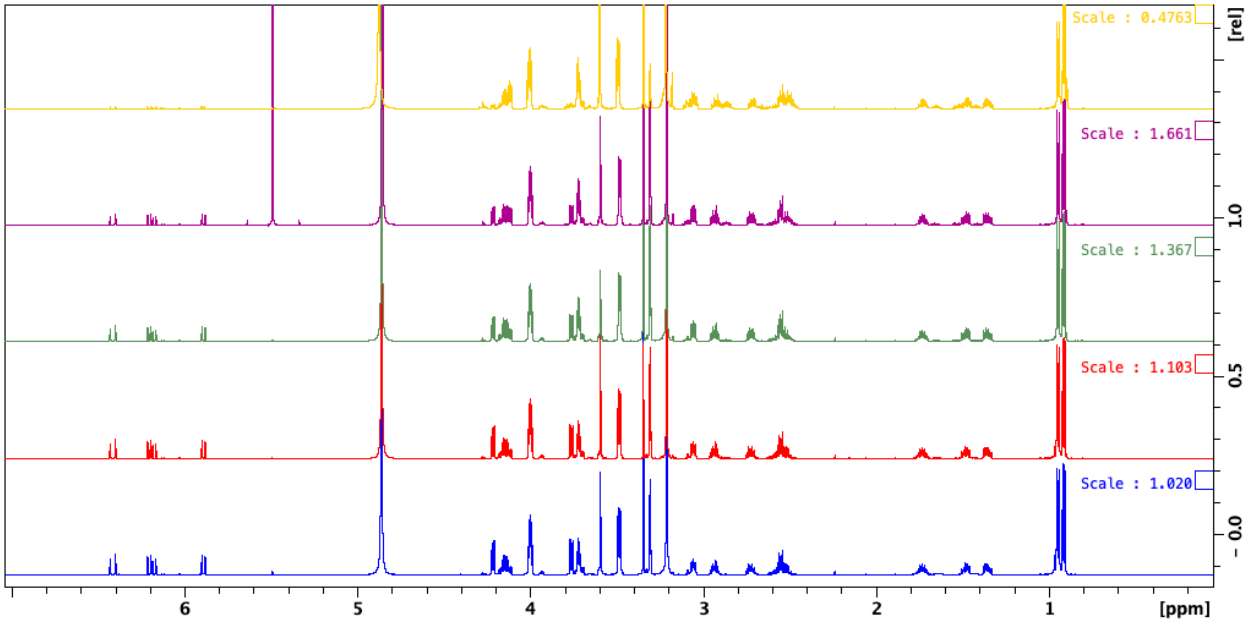

Figure S7.32 ^{1}H NMR stacked plots for reaction monitoring of ChLeuIL and HEA neat, at 30min, 1h, 2h, 4h, 24h from bottom to top. The spectral window is scaled to the height of choline peak at ~3.5 ppm for better relative comparison between different time points.

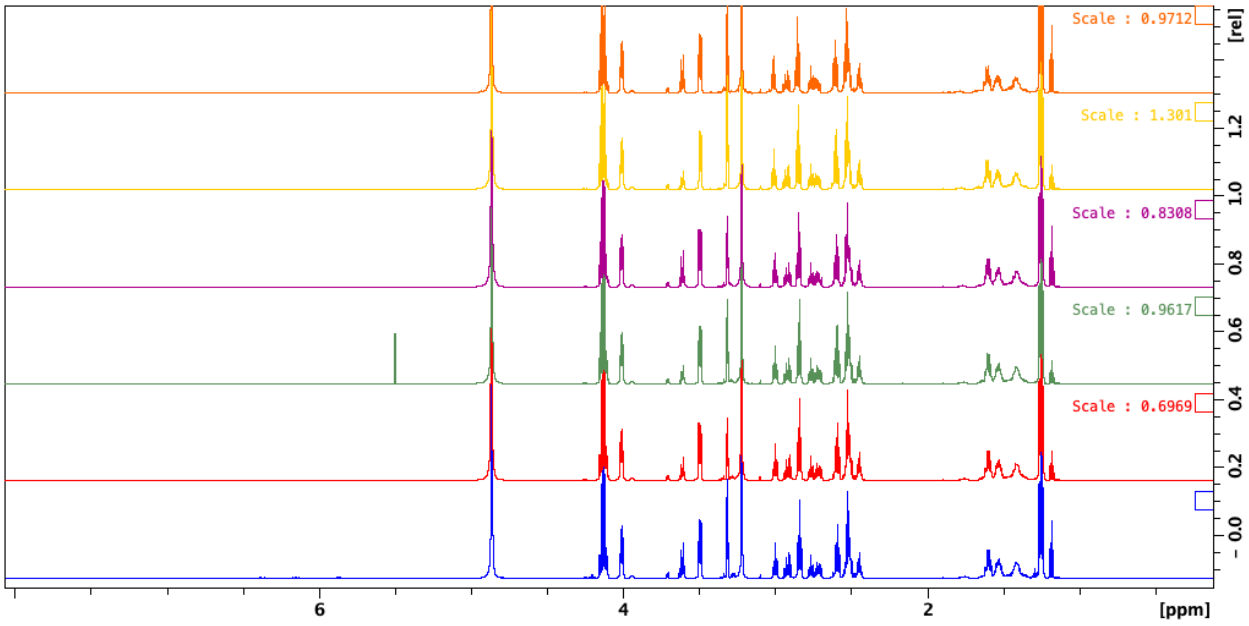

Figure S7.33. ^{1}H NMR stacked plots for reaction monitoring of ChLysIL and EA neat, at 30min, 1h, 2h, 4h, 12h, 24h from bottom to top. The spectral window is scaled to the height of choline peak at ~3.5 ppm for better relative comparison between different time points.

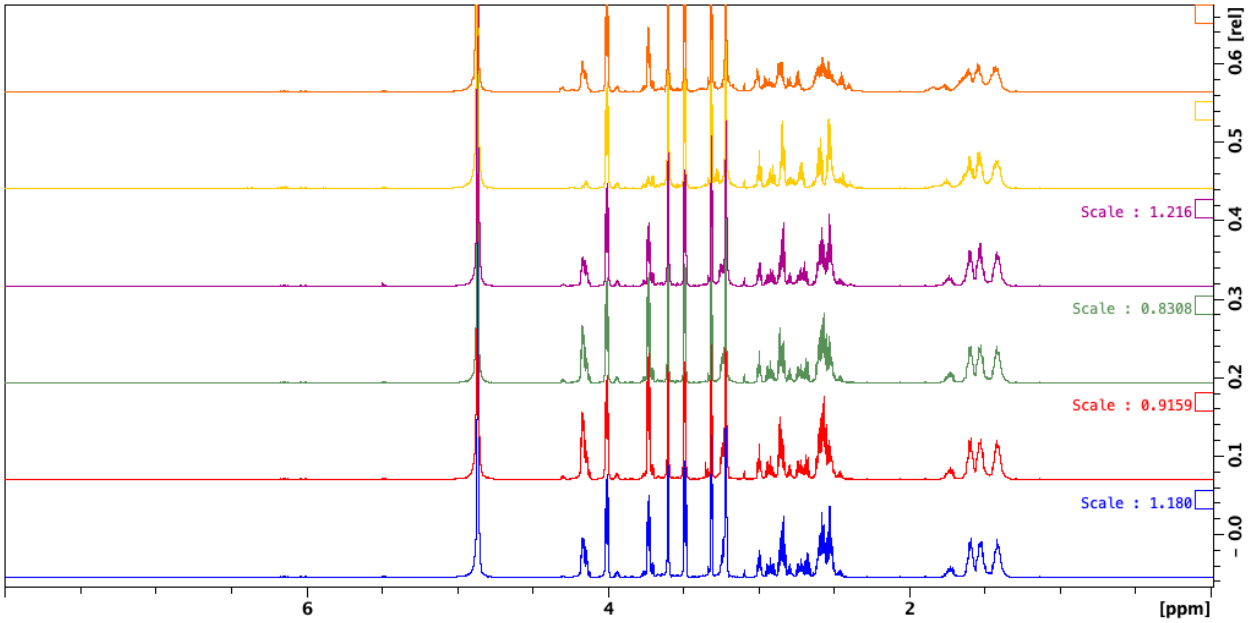

Figure S7.34. ^{1}H NMR stacked plots for reaction monitoring of ChLysIL and HEA neat, at 30min, 1h, 2h, 4h, 12h, 24h from bottom to top. The spectral window is scaled to the height of choline peak at ~3.5 ppm for better relative comparison between different time points.

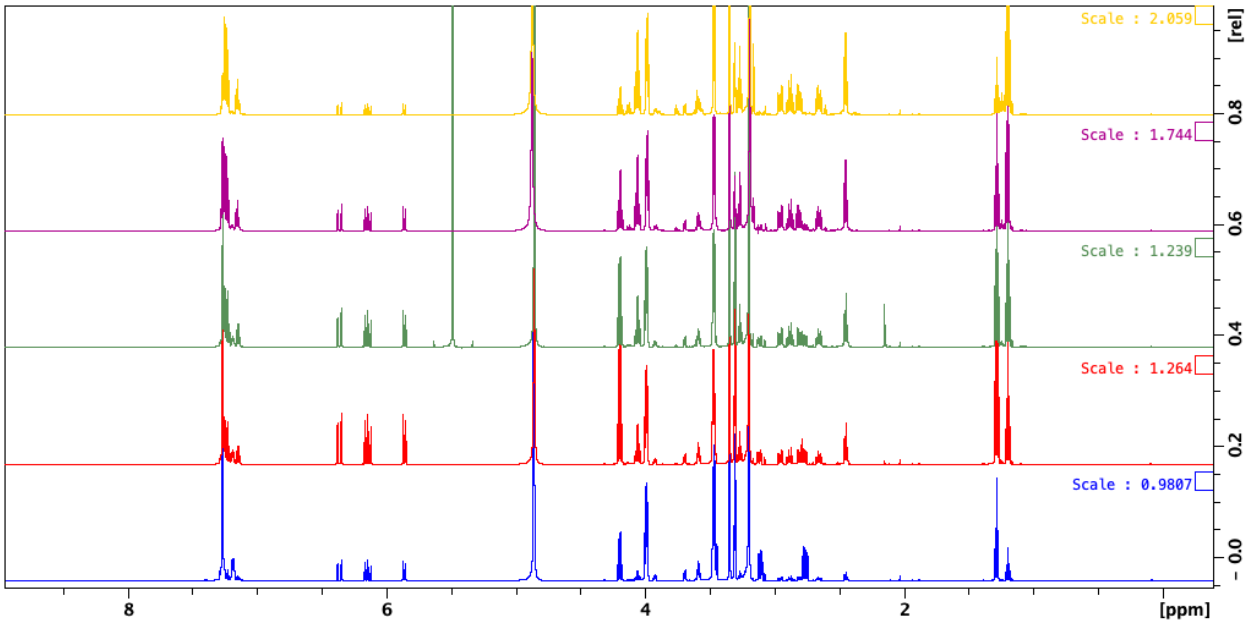

Figure S7.35. ^{1}H NMR stacked plots for reaction monitoring of ChPheIL and EA neat, at 30min, 1h, 2h, 6h, 24h from bottom to top. The spectral window is scaled to the height of choline peak at ~3.5 ppm for better relative comparison between different time points. It is noted that the mixture was inhomogeneous and liquid sample was not able to be

collected uniformly at different time points.

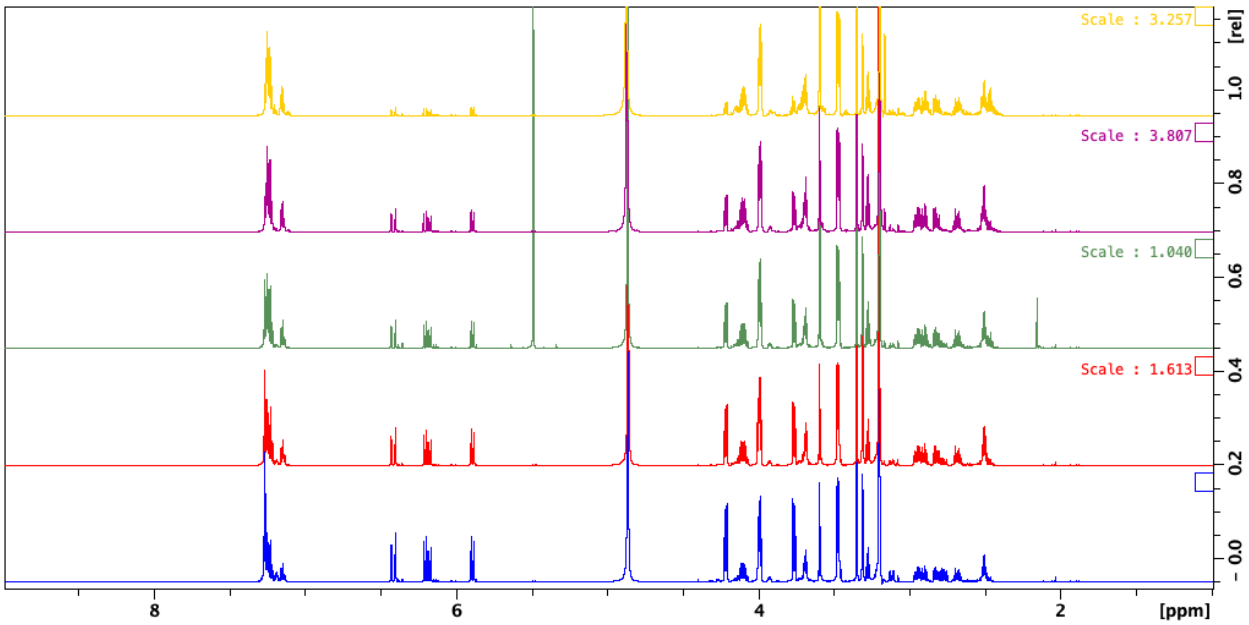

Figure S7.36. ^{1}H NMR stacked plots for reaction monitoring of ChPheIL and HEA neat, at 30min, 1h, 2h, 6h, 24h from bottom to top. The spectral window is scaled to the height of choline peak at ~3.5 ppm for better relative comparison between different time points.

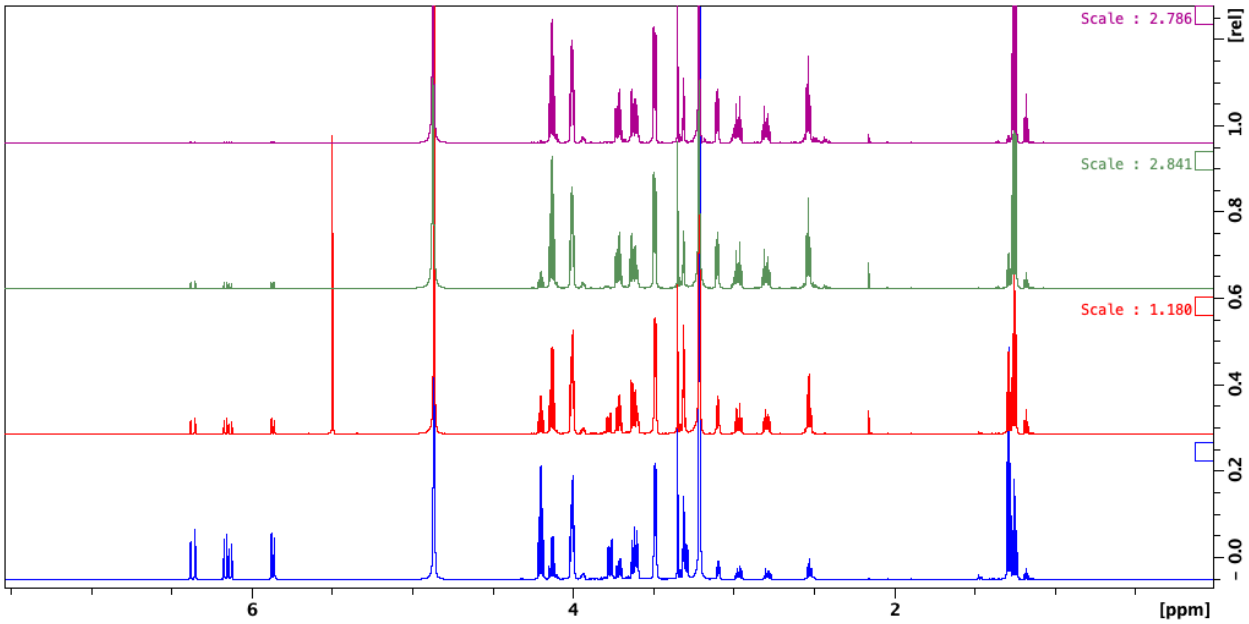

Figure S7.37. ^{1}H NMR stacked plots for reaction monitoring of ChSerIL and EA neat, at 30min, 1h, 7h, 24h from bottom to top. The spectral window is scaled to the height of choline peak at ~3.5 ppm for better relative comparison between different time points.

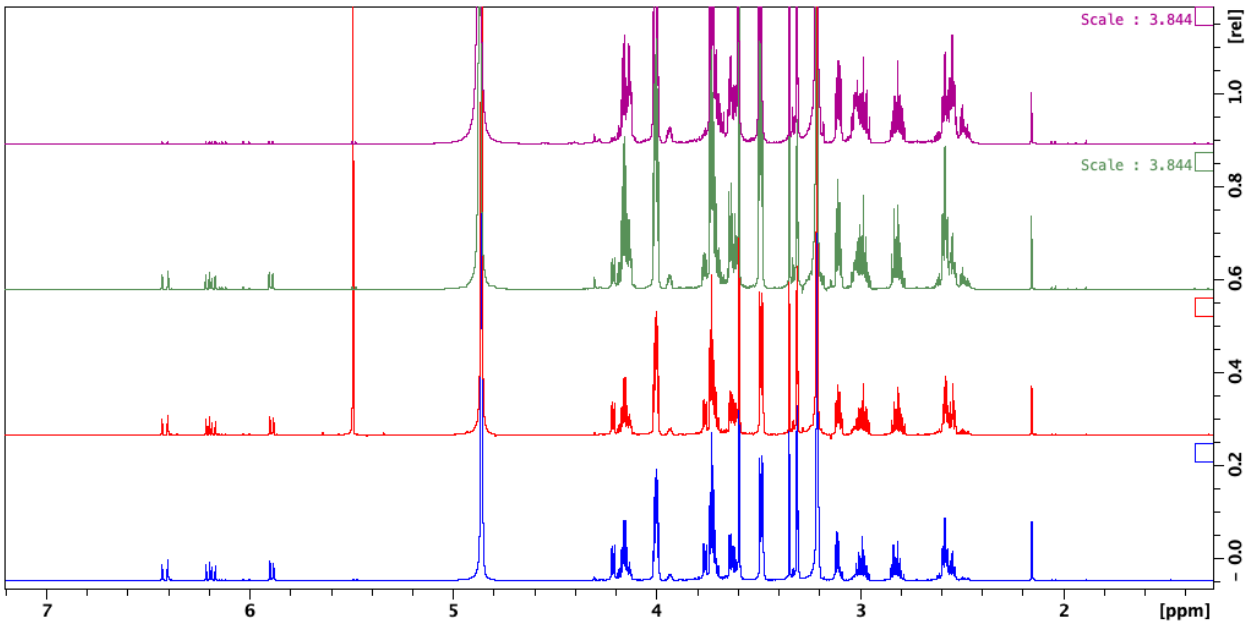

Figure S7.38. ^{1}H NMR stacked plots for reaction monitoring of ChSerIL and HEA neat, at 30min, 1h, 7h, 24h from bottom to top. The spectral window is scaled to the height of choline peak at ~3.5 ppm for better relative comparison between different time points.

7.2.4 Reaction Quenching and Effect of Base on aza-Michael Reactivity

Table S7.5 Effect of base on aza-Michael reaction

ChAAILs	Acrylate	ChOH mole eq	24 h Conversion before ChOH	reaction time after ChOH	Conversion after ChOH
ChAspIL	EA	1	0%	30 min	94%
ChAspIL	EA	1	0%	24 h	100%
ChAspIL	EA	0.01	0%	30 min	24%
ChAspIL	EA	0.01	0%	24 h	81%
ChAspIL	HEA	1	0%	30 min	81%
ChAspIL	HEA	1	0%	24 h	100%
ChAspIL	HEA	0.01	0%	30 min	45%
ChAspIL	HEA	0.01	0%	24 h	69%

Table S7.6 Effect of Acid quenching on aza-Michael reaction

ChAAILs	Acrylate	AcOH mole eq	2 h Conversion before ChOH	reaction time after AcOH (h)	Conversion after AcOH
ChPheIL	EA	1	71%	24	0%
ChPheIL	HEA	1	50%	24	0%

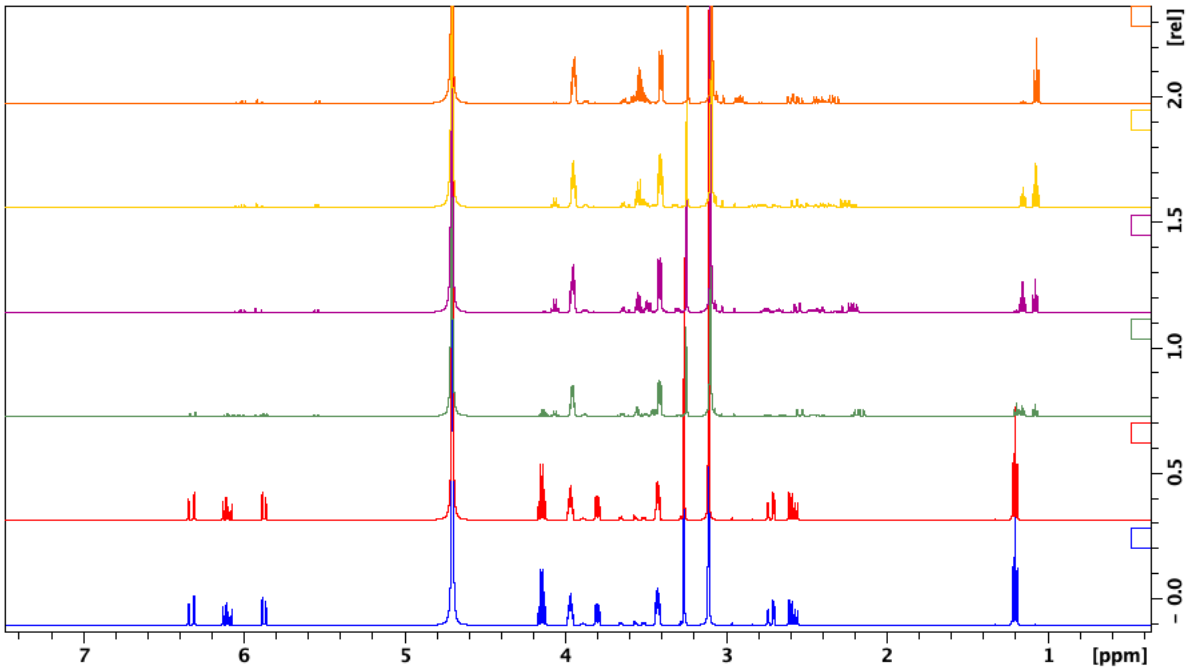

Figure S7.39. ^{1}H NMR stacked plots for reaction monitoring of ChAspIL with EA, before and after 1 eq ChOH added after 24 hours. From bottom to top first two spectra represent 5 mins and 24 h after reaction before ChOH is added. 1eq ChOH added at 24 hours timepoint, then the top four spectra representing reaction monitored at 30 min, 1h, 4h, and 24h after the addition of ChOH.

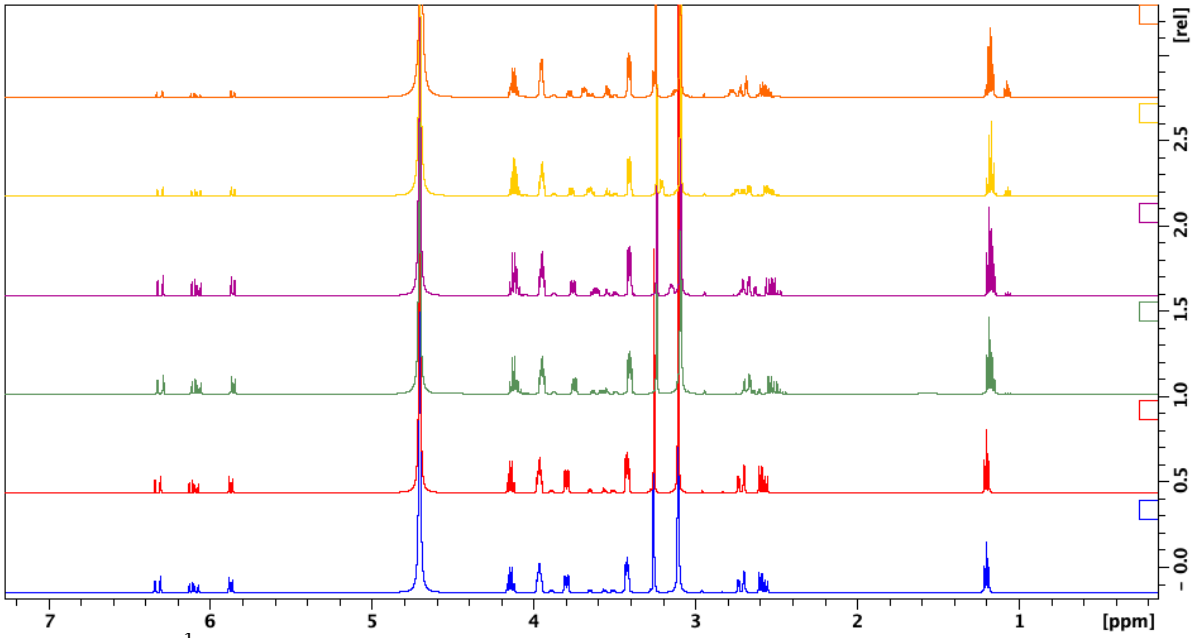

Figure S7.40. ^{1}H NMR stacked plots for reaction monitoring of ChAspIL with EA, before and after 0.01 eq ChOH added after 24 hours. From bottom to top first two spectra represent 5 mins and 24 h after reaction before ChOH is added. 1eq ChOH added at 24 hours timepoint, then the top four spectra representing reaction monitored at 30 min, 1h, 4h, and 24h after the addition of ChOH.

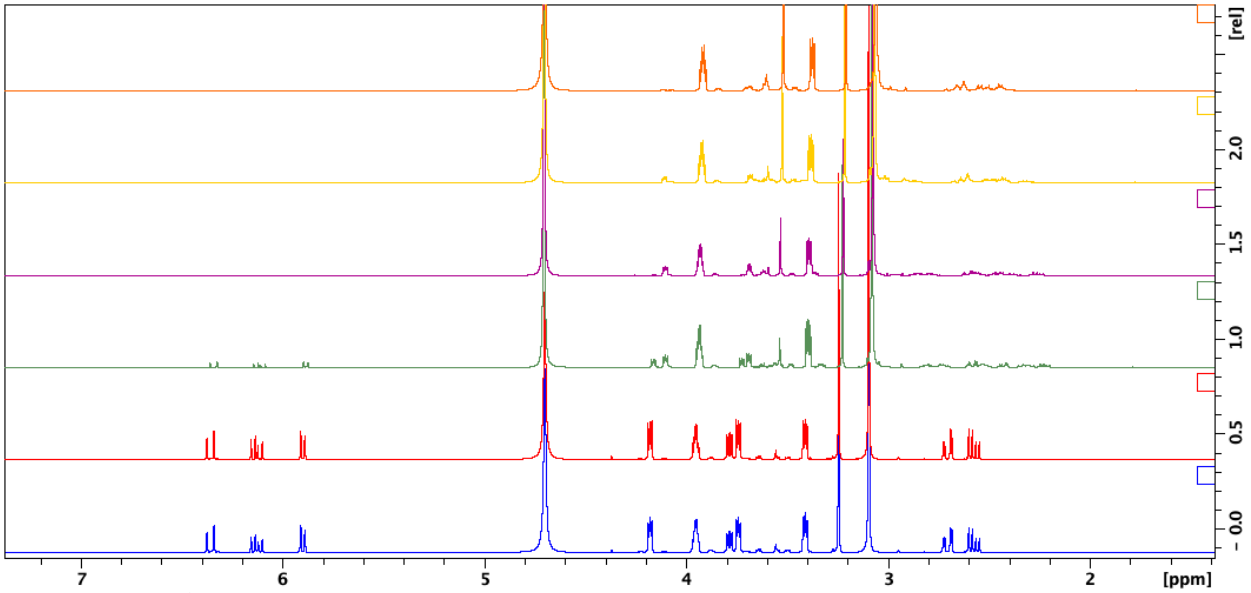

Figure S7.41. ^{1}H NMR stacking for reaction monitoring of ChAspIL with HEA, before and after 1 eq ChOH added after 24 hours. From bottom to top first two spectra represent 5 mins and 24 h after reaction before ChOH is added. 1eq ChOH added at 24 hours

timepoint, then the top four spectra representing reaction monitored at 30 min, 1h, 4h, and 24h after the addition of ChOH.

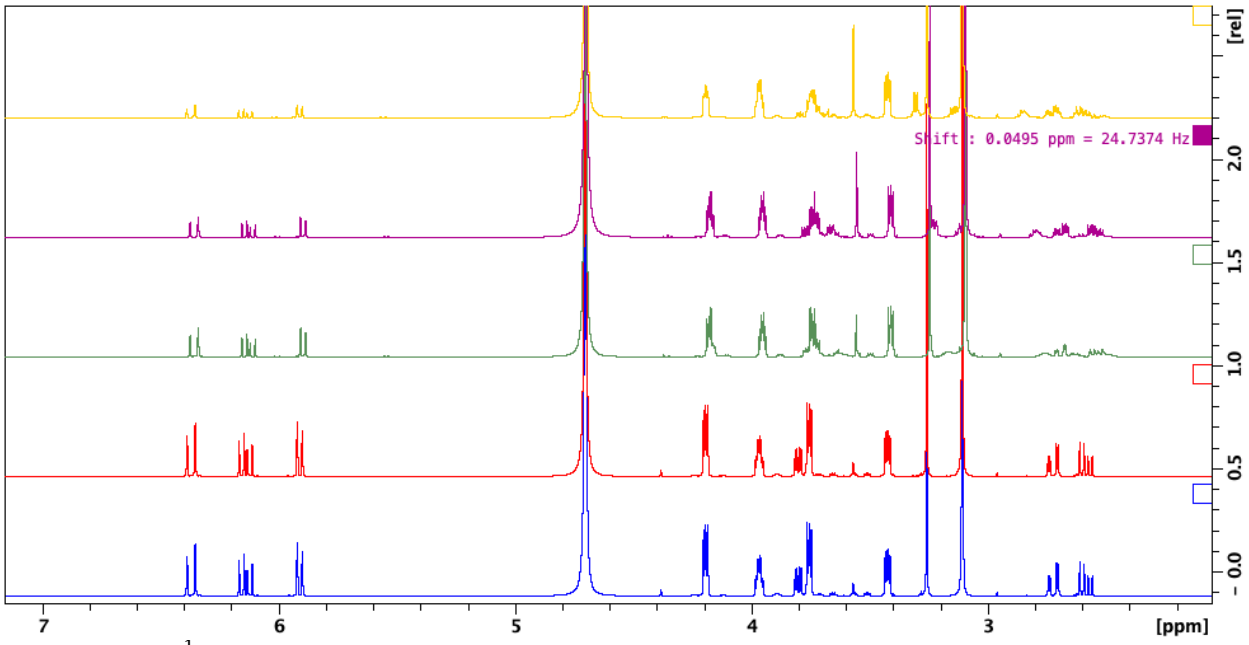

Figure S7.42. ^{1}H NMR stacked plots for reaction monitoring of ChAspIL with HEA, before and after 0.01 eq ChOH added after 24 hours. From bottom to top first two spectra represent 5 mins and 24 h after reaction before ChOH is added. 1eq ChOH added at 24 hours timepoint, then the top three spectra representing reaction monitored at 1h, 4h, and 24h after the addition of ChOH.

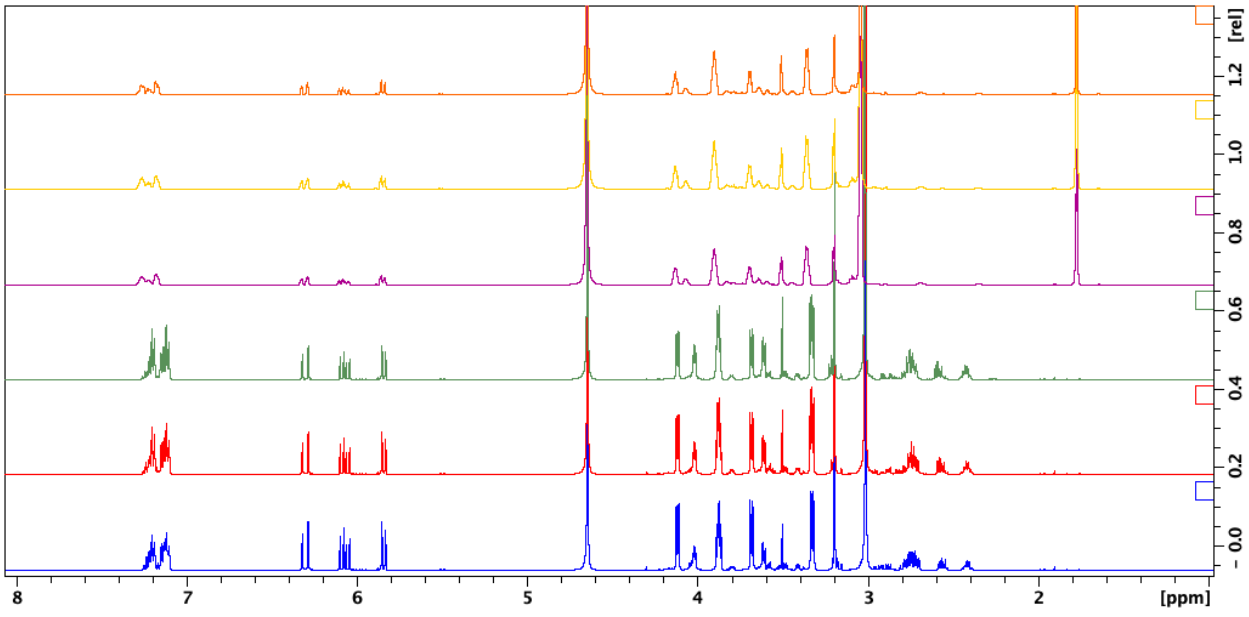

Figure S7.43. ^{1}H NMR stacked plots for reaction monitoring of ChPheIL with HEA.

From bottom to top, it is shown the reaction was let reacted and monitored at 30 min, 1h and 2h (bottom three), the reaction mixture was then quenched with 1 eq AcOH and precipitate formed was then removed before the reaction was monitored at 1h, 4h, and 24h after reaction work up (top three).

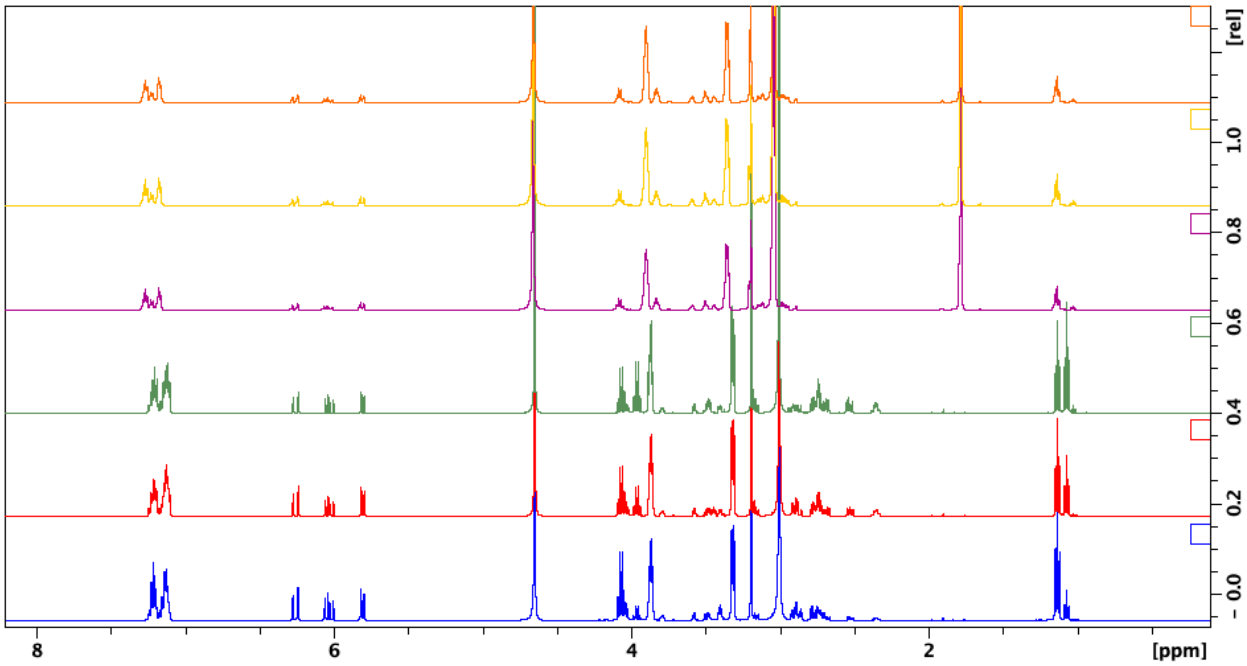

Figure S7.44. ^{1}H NMR stacked plots for reaction monitoring of ChPheIL with EA. From bottom to top, it is shown the reaction was let reacted and monitored at 30 min, 1h and 2h (bottom three), the reaction mixture was then quenched with 1 eq AcOH and precipitate formed was then removed before the reaction was monitored at 1h, 4h, and 24h after reaction work up (top three).

7.2.5 ChAAIL Reactivity with PEG

Table S7.7. Reaction summary of ChAAILs with polymer acrylates.

ChAAILs	Polymer Acrylates	Reaction Time (h)	Conversion
ChLysIL	Di10	1	26%
ChLysIL	HODi9	1	88%
ChLysIL	Di10	24	99%
ChLysIL	HODi9	24	99%
ChSerIL	Di10	1	5%
ChSerIL	HODi9	1	67%
ChSerIL	Di10	24	26%

ChSerIL	HODi9	24	88%
ChPheIL	Di10	1	1%
ChPheIL	HODi9	1	60%
ChPheIL	Di10	24	48%
ChPheIL	HODi9	24	80%
ChLeuIL	Di10	1	34%
ChLeuIL	HODi9	1	74%
ChLeuIL	Di10	24	89%
ChLeuIL	HODi9	24	88%
ChAspIL	Di10	1	0%
ChAspIL	HODi9	1	0%
ChAspIL	Di10	24	0%
ChAspIL	HODi9	24	0%
ChLysIL	PEGACR	1	97%
ChLysIL	OHGlyACR	1	99%
ChLysIL	PEGACR	24	99%
ChLysIL	OHGlyACR	24	99%
ChSerIL	PEGACR	1	23%
ChSerIL	OHGlyACR	1	72%
ChSerIL	PEGACR	24	75%
ChSerIL	OHGlyACR	24	98%
ChPheIL	PEGACR	1	57%
ChPheIL	OHGlyACR	1	24%
ChPheIL	PEGACR	24	83%
ChPheIL	OHGlyACR	24	61%
ChLeuIL	PEGACR	1	82%
ChLeuIL	OHGlyACR	1	69%
ChLeuIL	PEGACR	24	91%
ChLeuIL	OHGlyACR	24	90%
ChAspIL	PEGACR	1	0%
ChAspIL	OHGlyACR	1	26%
ChAspIL	PEGACR	24	0%
ChAspIL	OHGlyACR	24	77%

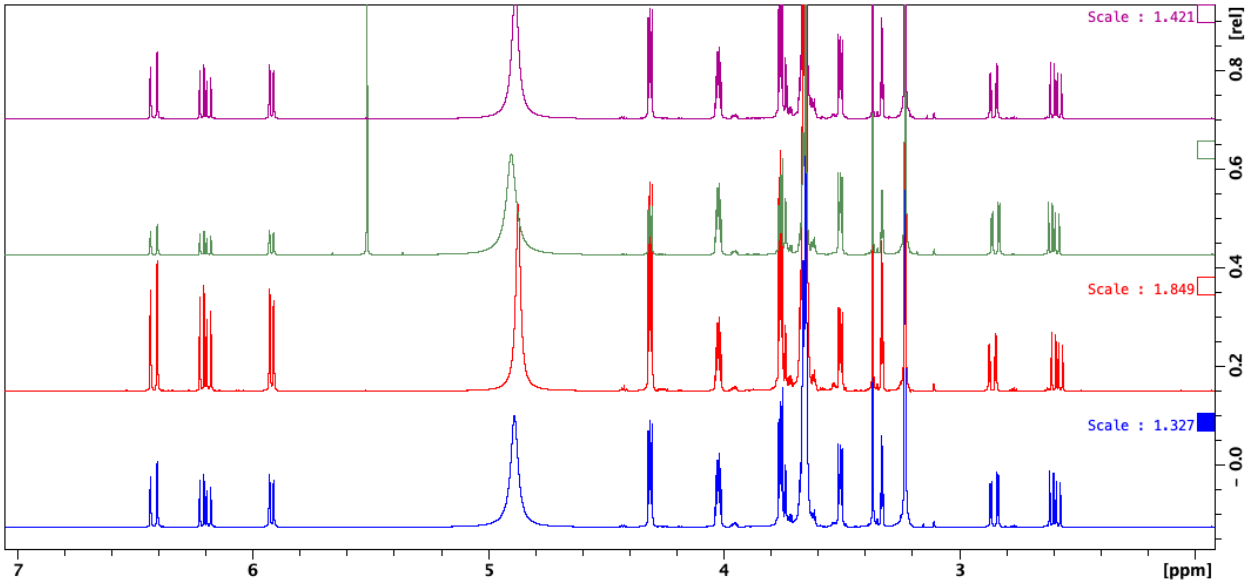

Figure S7.45. ^{1}H NMR stacked plots for reaction monitoring of ChAspIL with PEGACR, from bottom to top, reaction at 1h, 4h, 12h, 24h. The spectral window is scaled to the choline peak at ~4 ppm for better relative comparison between different time points. The mixture was inhomogeneous, therefore different aliquot had variations of amount of acrylates.

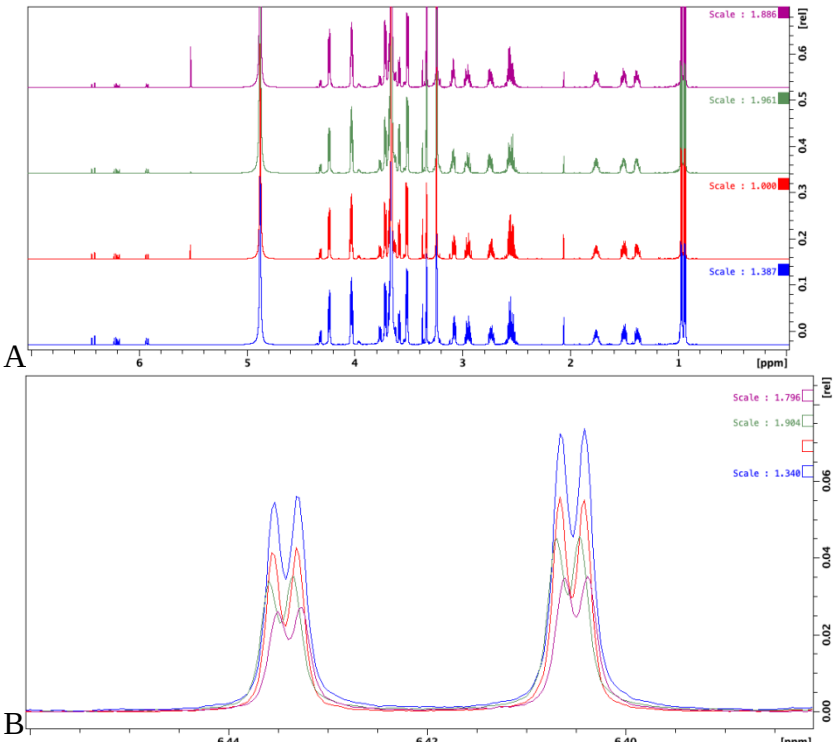

Figure S7.46. A) ^{1}H NMR stacked plots for reaction monitoring of for ChLeuIL with PEGACR, from bottom to top, reaction at 1h, 4h, 12h, 24h. B) Zoom-in image of the acrylate depletion trend over time around 6.38 – 6.46 ppm. The spectral window is scaled to the Choline peak at ~4 ppm for better relative comparison between different time points.

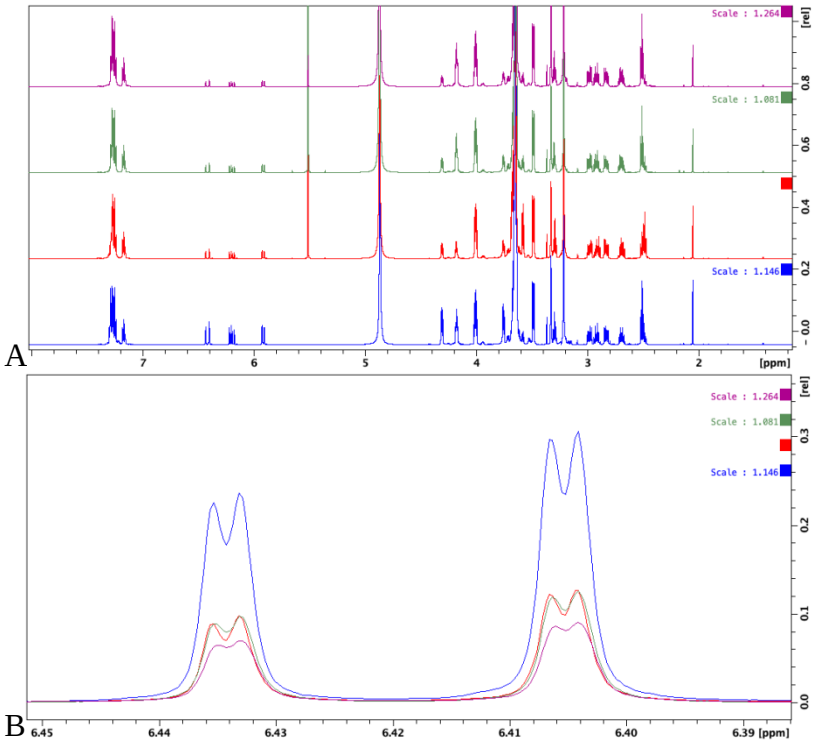

Figure S7.47. A) ^{1}H NMR stacked plots for reaction monitoring of ChPheIL with PEGACR, from bottom to top, reaction at 1h, 4h, 12h, 24h. B) Zoom-in image of acrylate depletion trend over time around 6.38 – 6.46 ppm. The spectral window is scaled to the Choline peak at ~4 ppm for better relative comparison between different time points.

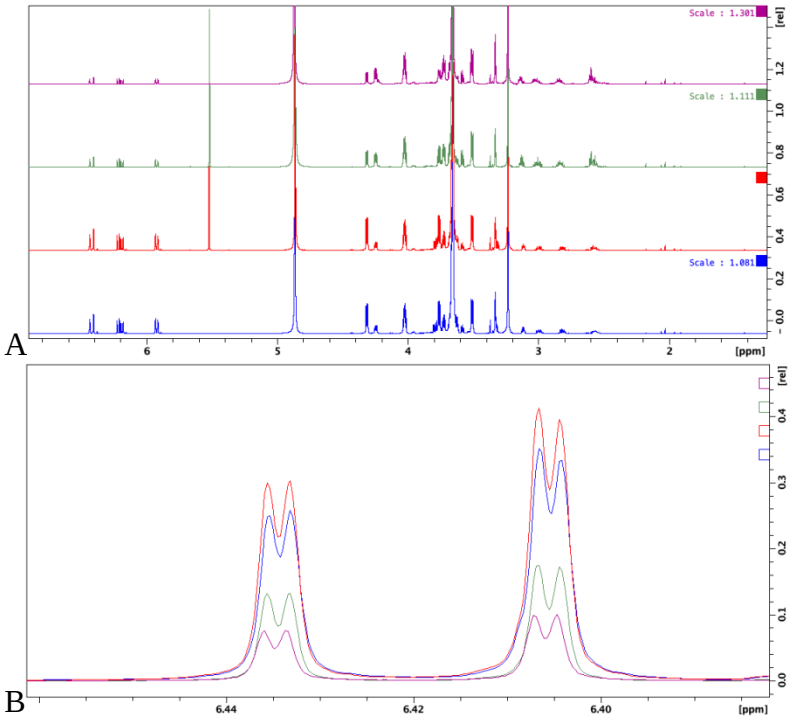

Figure S7.48. A) ^{1}H NMR stacked plots for reaction monitoring of ChSerIL with PEGACR, from bottom to top, reaction at 1h, 4h, 12h, 24h. B) Zoom-in image of acrylate depletion trend over time around 6.38 – 6.46 ppm. The spectral window is scaled to the Choline peak at ~4 ppm for better relative comparison between different time points.

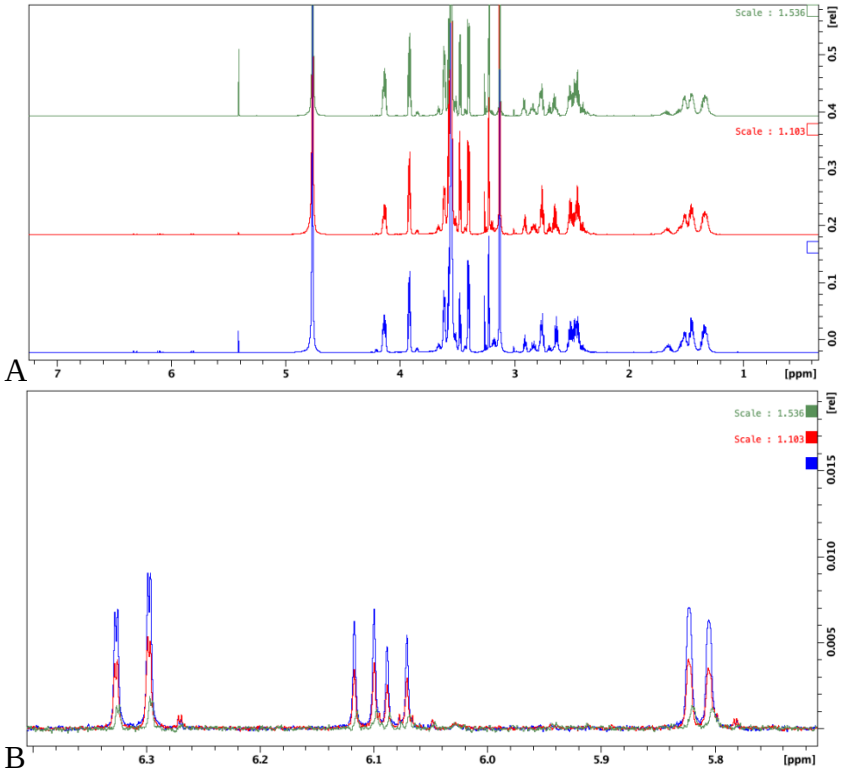

Figure S7.49. A) ^{1}H NMR stacked plots for reaction monitoring of ChLysIL with PEGACR, from bottom to top, reaction at 1h, 4h, 12h, 24h. B) Zoom-in image of acrylate depletion trend over time around 5.7 – 6.4 ppm. The spectral window is scaled to the Choline peak at ~4 ppm for better relative comparison between different time points.

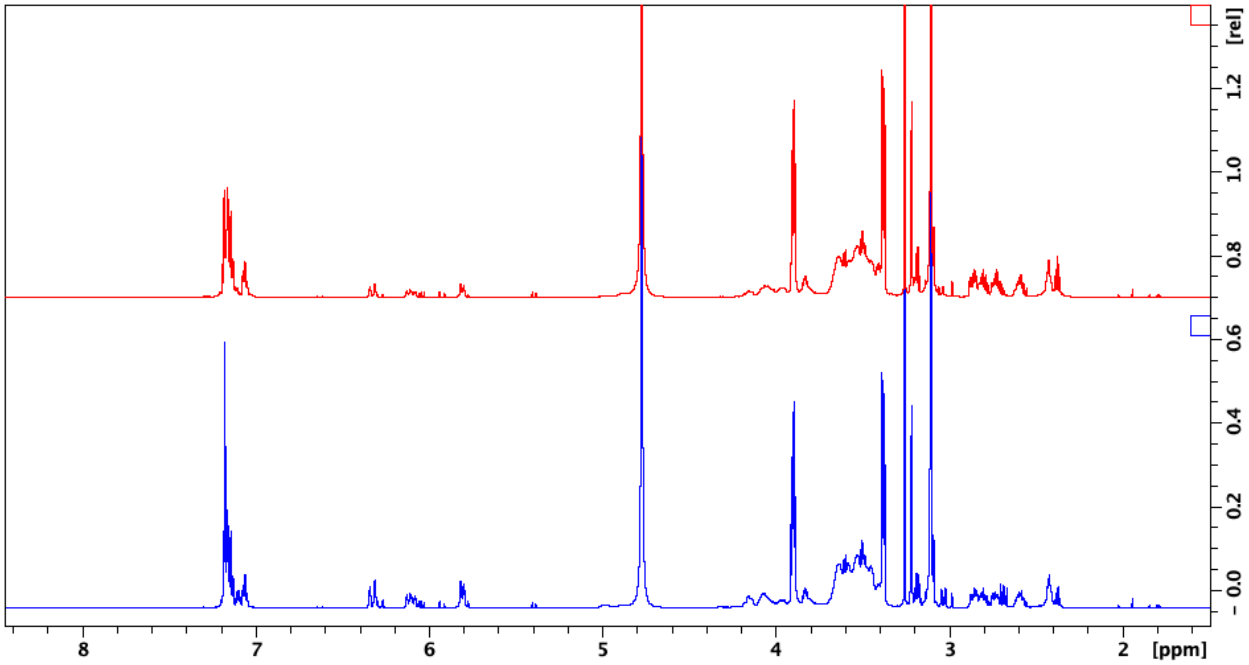

Figure S7.50. ^{1}H NMR stacked plots for reaction monitoring of ChPheIL with OHGlyACR at 1h and 24 hours.

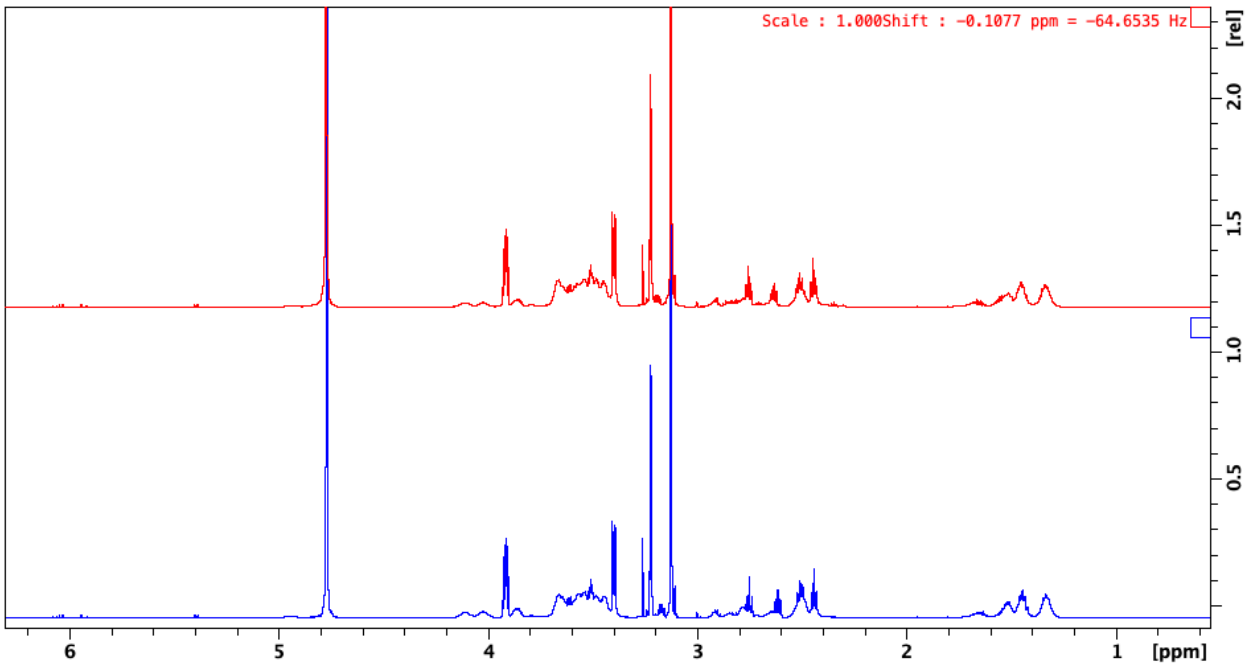

Figure S7.51. ^{1}H NMR stacked plots for reaction monitoring of ChLysIL with OHGlyACR at 1h and 24 hours.

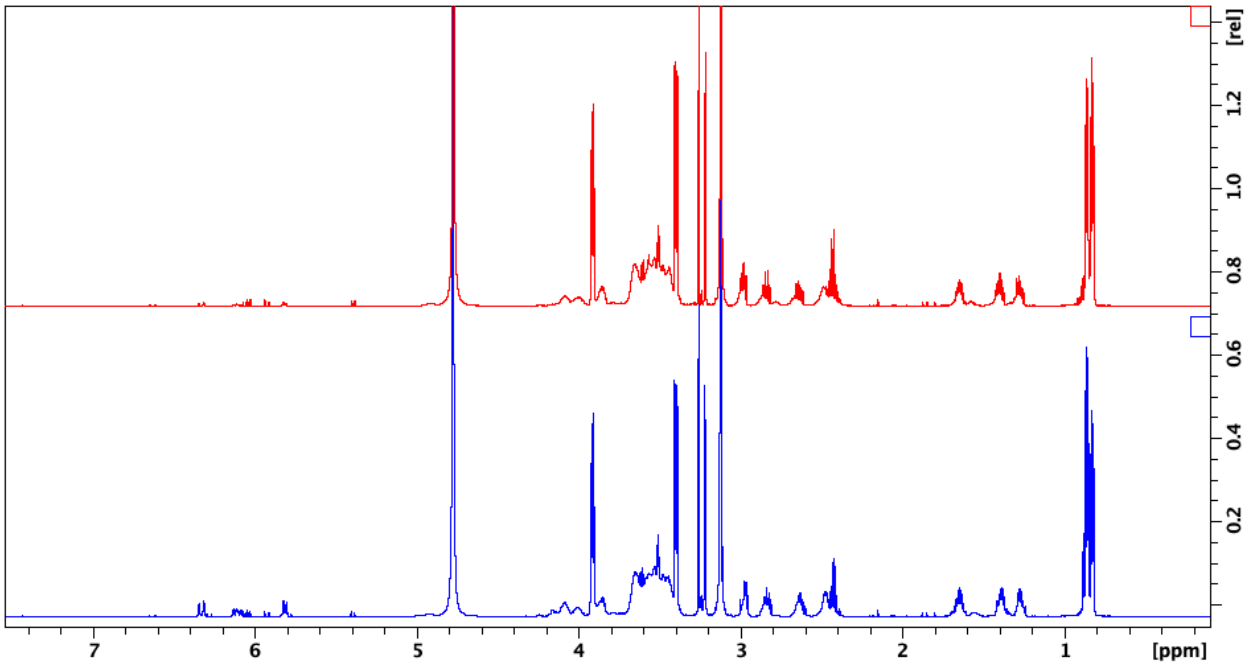

Figure S7.52. ^{1}H NMR stacked plots for reaction monitoring of ChLeuIL with OHGlyACR at 1h and 24 hours.

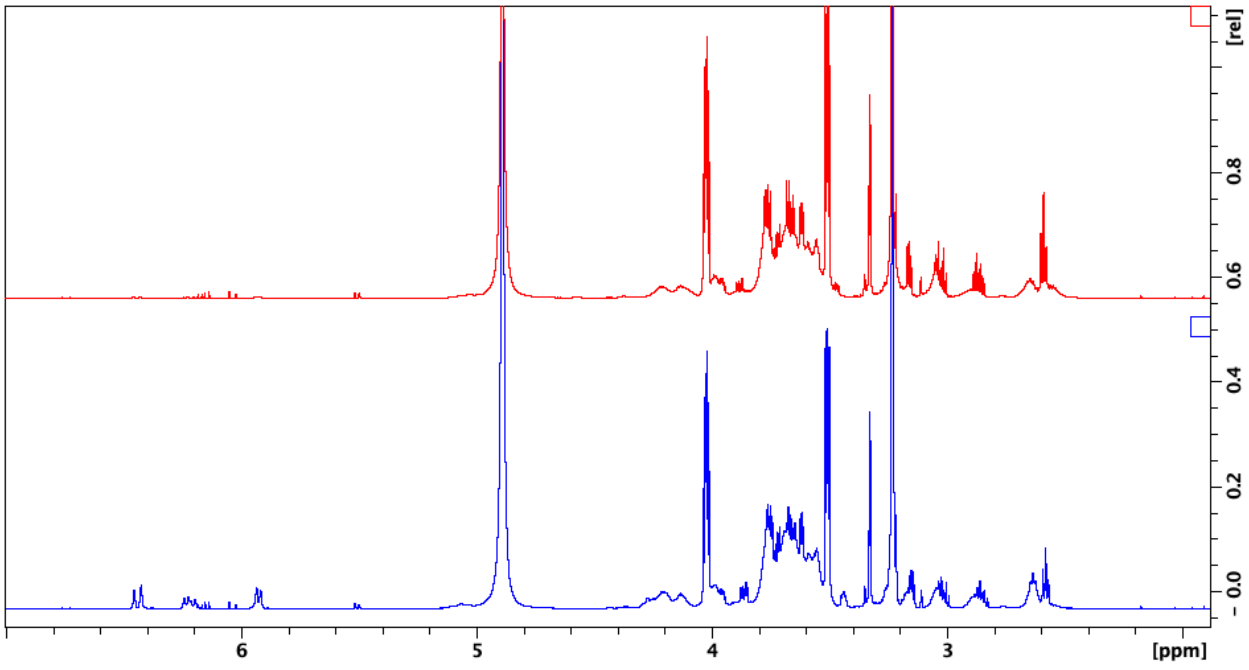

Figure S7.53. ^{1}H NMR stacked plots for reaction monitoring of ChSerIL with OHGlyACR at 1h and 24 hours.

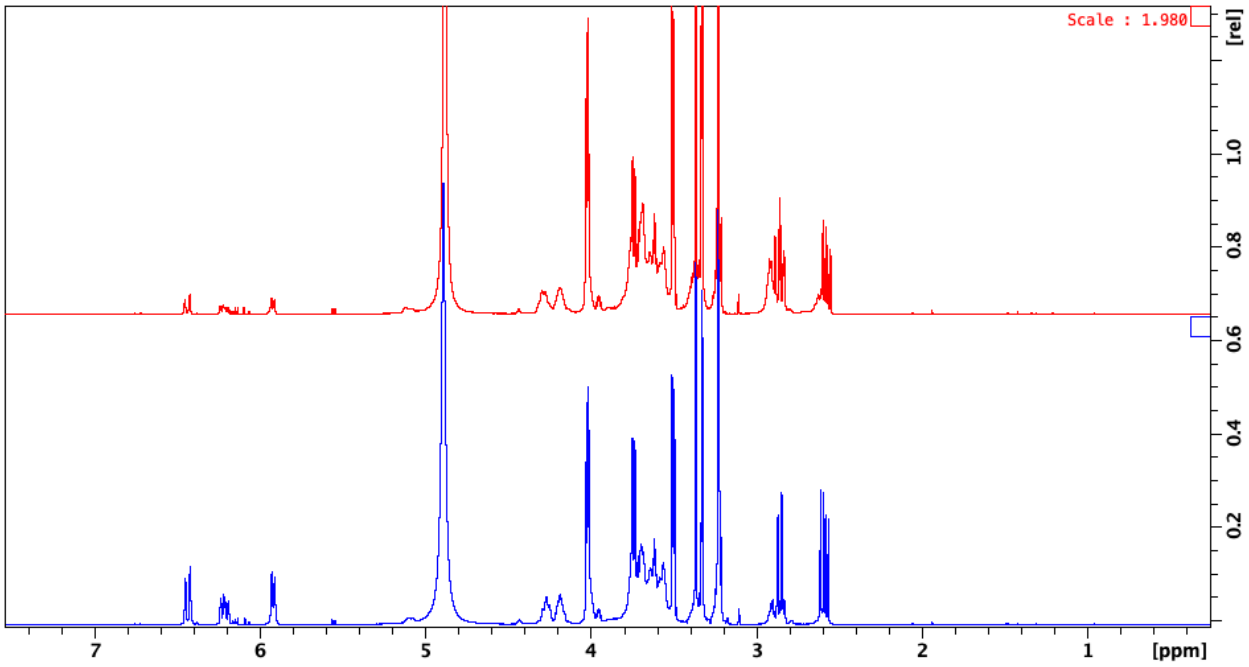

Figure S7.54. ^{1}H NMR stacked plots for reaction monitoring of ChAspIL with OHGlyACR at 1h and 24 hours.

7.2.6 ChAAIL Reactivity with Silicones

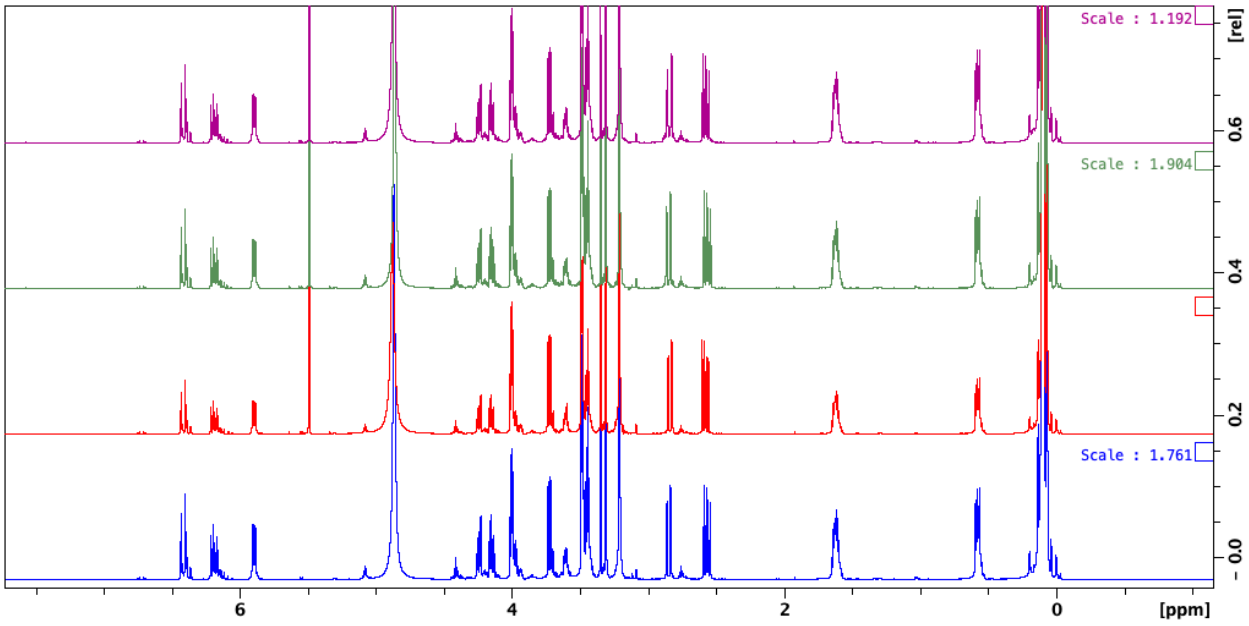

Figure S7.55. ^{1}H NMR stacked plots for reaction monitoring of ChAspIL and **HODi9** neat, at 30min, 1h, 14h, 24h from bottom to top. The spectral window is scaled to the

height of choline peak at ~3.5 ppm for better relative comparison between different time points.

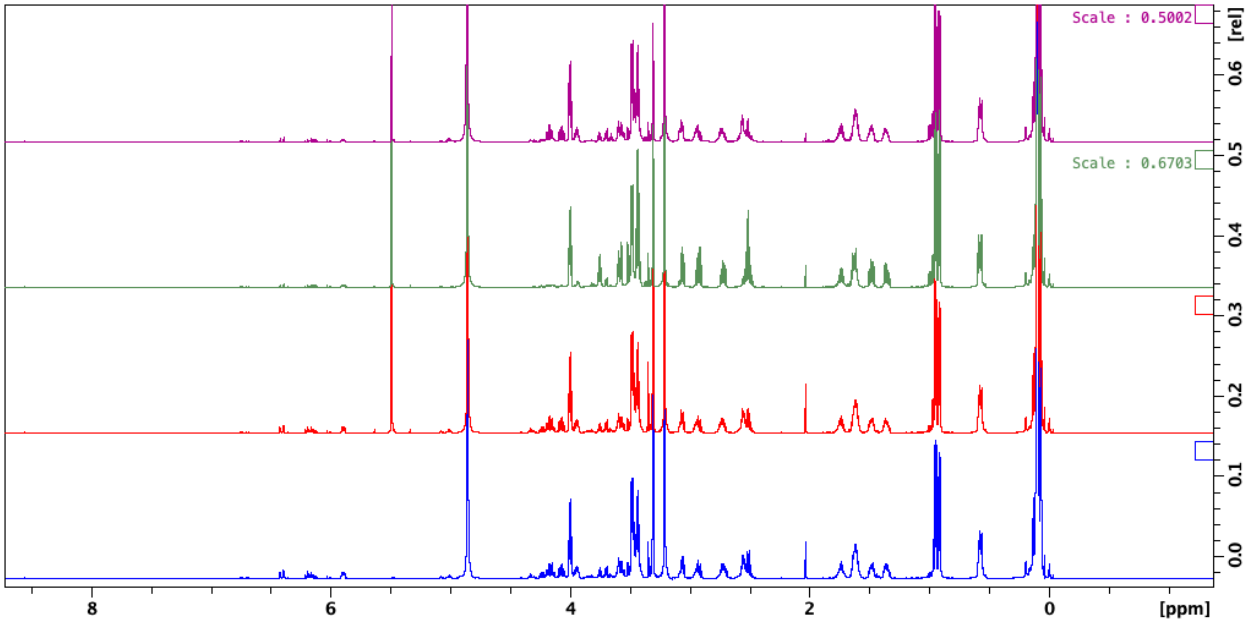

Figure S7.56. ^{1}H NMR stacked plots for reaction monitoring of ChLeuIL and **HODi9** neat, at 30min, 1h, 14h, 24h from bottom to top. The spectral window is scaled to the height of choline peak at ~3.5 ppm for better relative comparison between different time points.

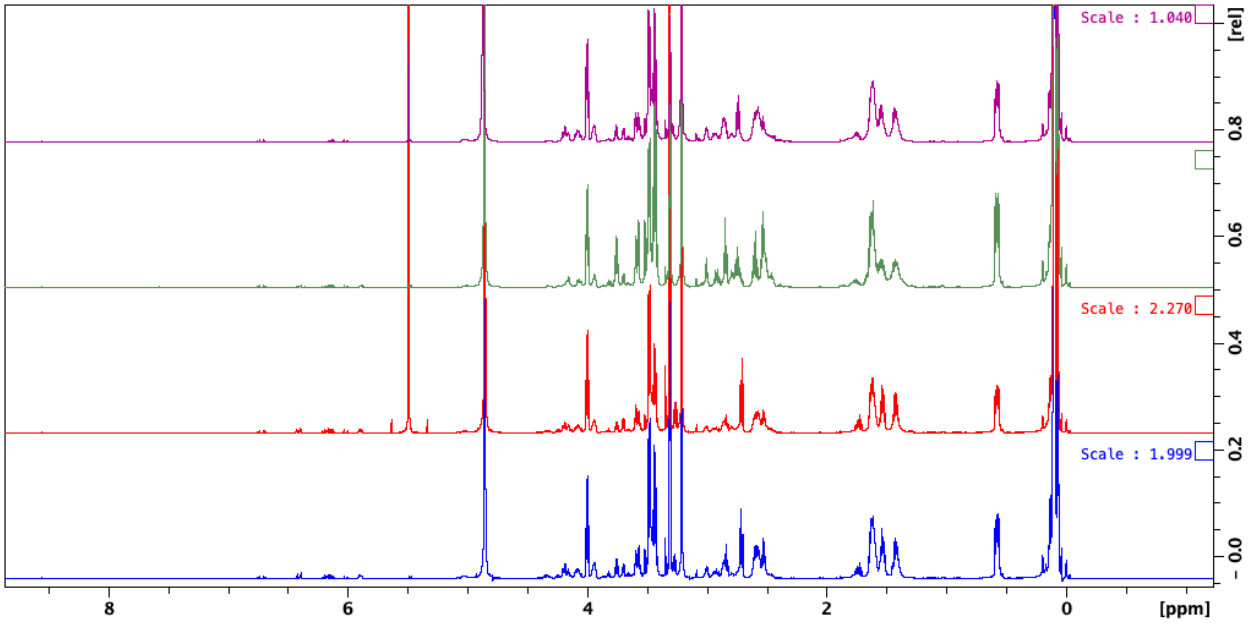

Figure S7.57. ^{1}H NMR stacked plots for reaction monitoring of ChLysIL and **HODi9** neat, at 30min, 1h, 14h, 24h from bottom to top. The spectral window is scaled to the height of choline peak at ~4ppm for better relative comparison between different time points.

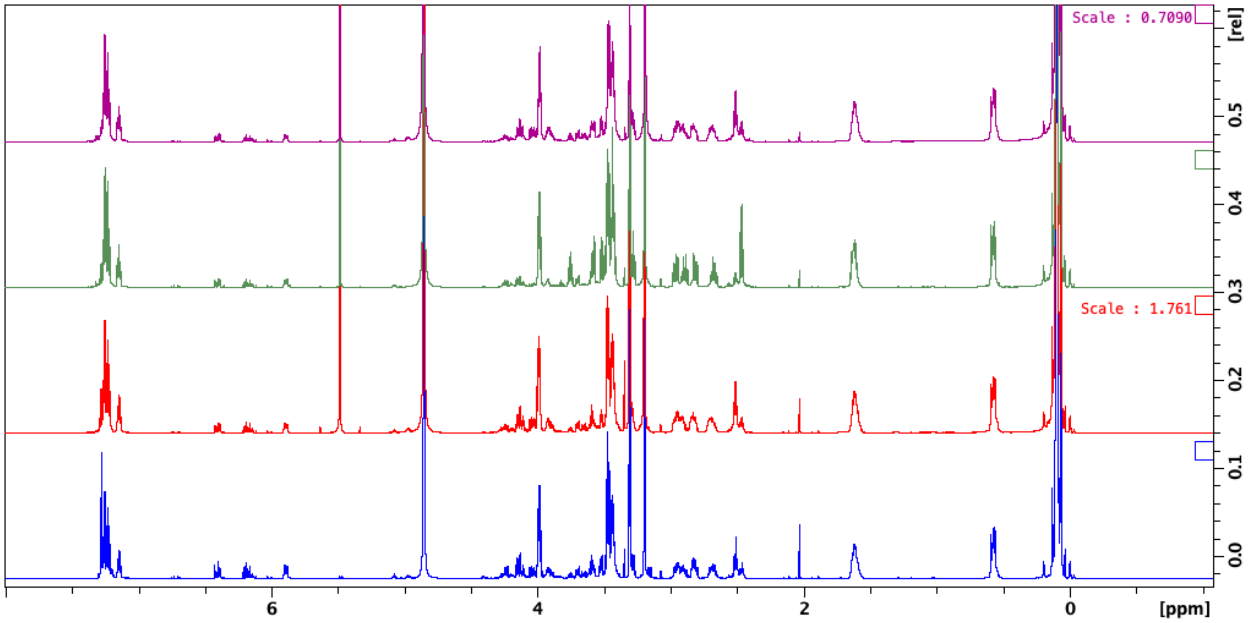

Figure S7.58. ^{1}H NMR stacking for reaction monitoring of ChPheIL and **HODi9** neat, at 30min, 1h, 14h, 24h from bottom to top. The spectral window is scaled to the height of choline peak at ~4 ppm for better relative comparison between different time points.

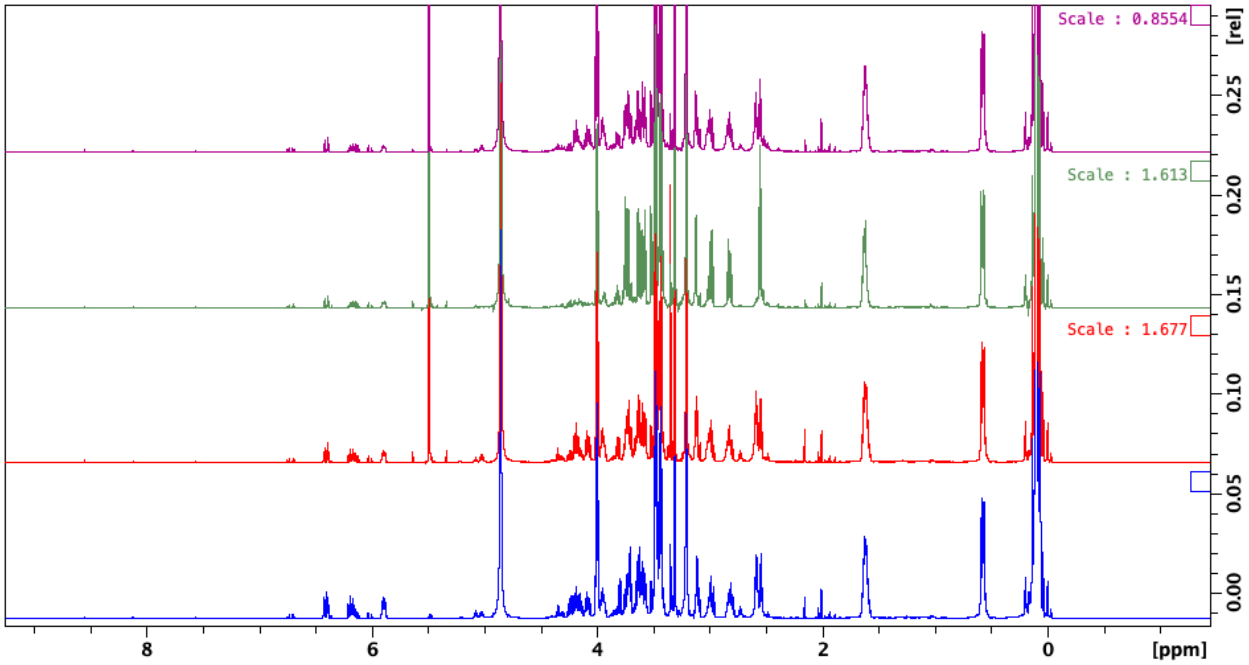

Figure S7.59. ^{1}H NMR stacked plots for reaction monitoring of ChSerIL and **HODi9** neat, at 30min, 1h, 14h, 24h from bottom to top. The spectral window is scaled to the ethylene peak at ~0.5 ppm for better relative comparison between different time points.

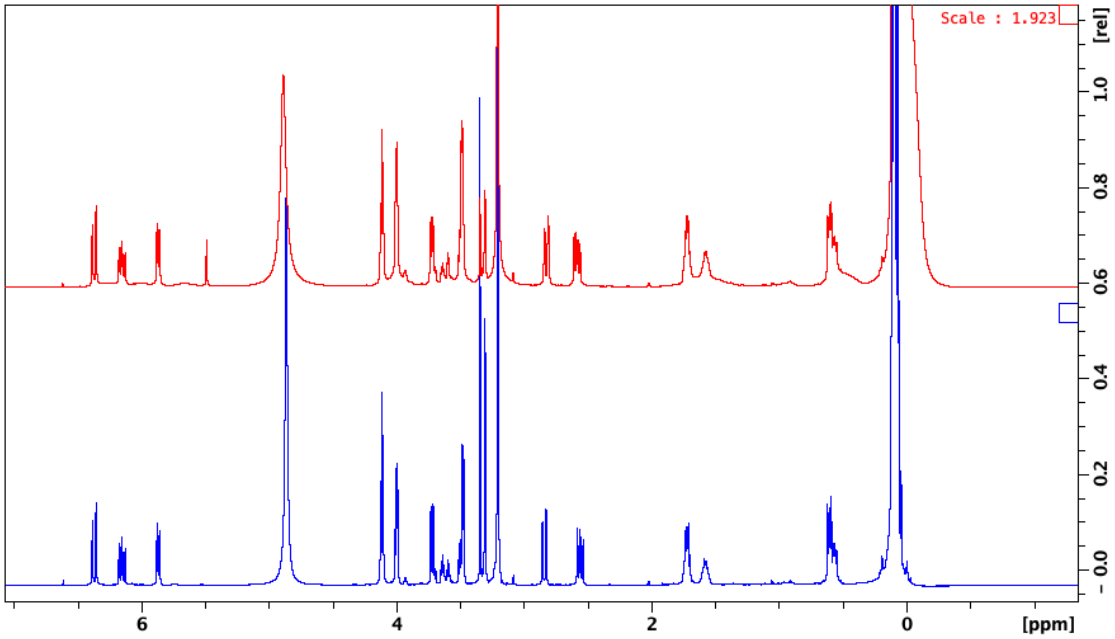

Figure S7.60. ^{1}H NMR stacked plots for reaction monitoring of ChAspIL and **Di10** neat, at 1h, and 24h from bottom to top.

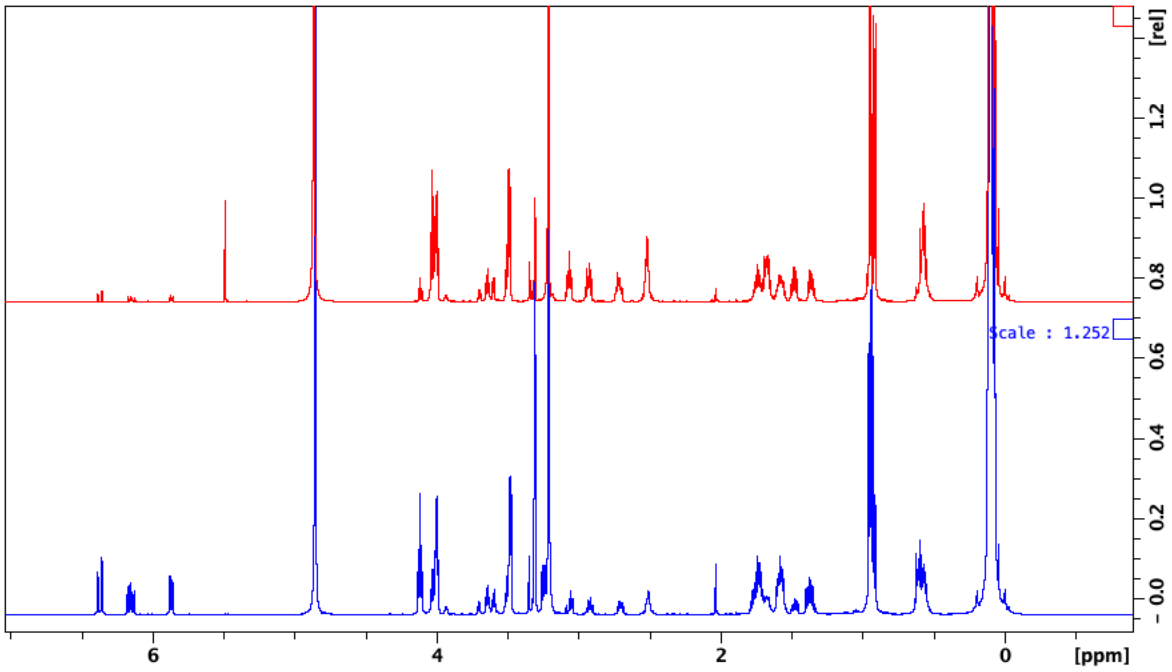

Figure S7.61. ^{1}H NMR stacked plots for reaction monitoring of ChLeuIL and **Di10** neat at 1h and 24h from bottom to top.

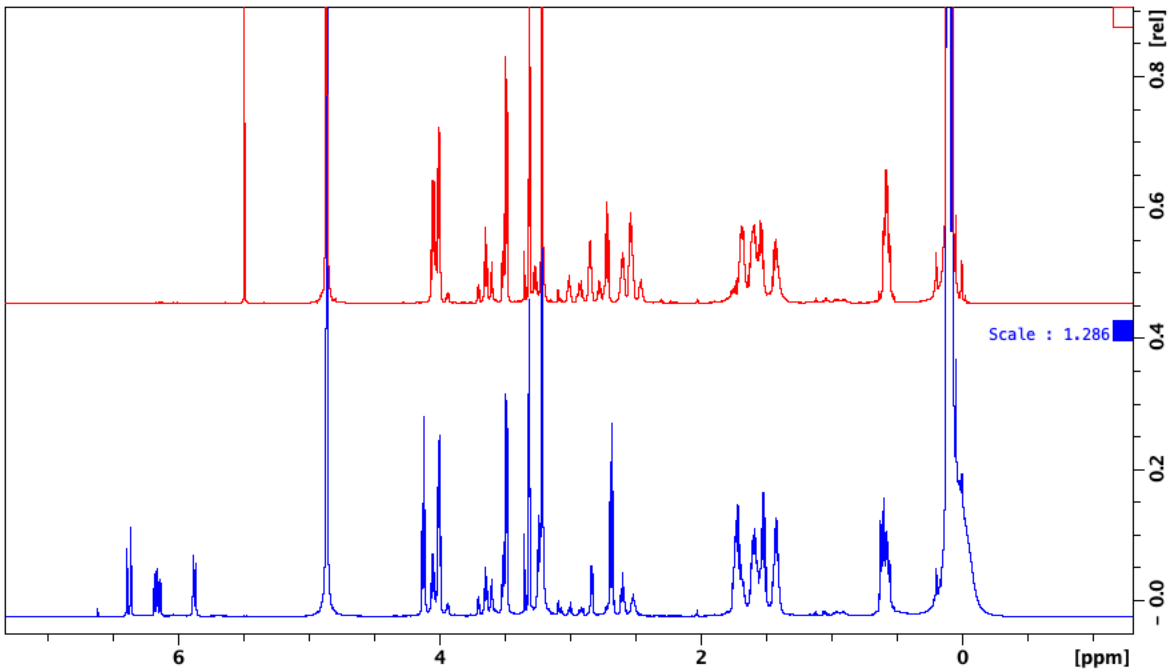

Figure S7.62. ^{1}H NMR stacked plots for reaction monitoring of ChLysIL and **Di10** neat at

1h and 24h from bottom to top.

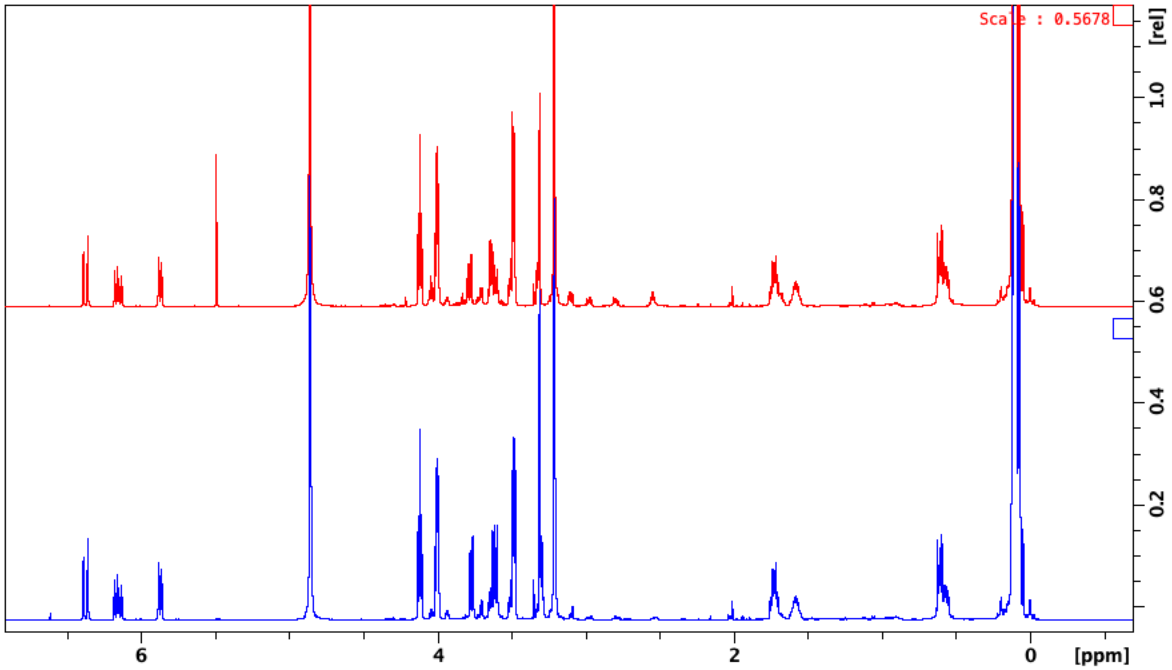

Figure S7.63. ^{1}H NMR stacked plots for reaction monitoring of ChSerIL and **Di10** at 1h and 24h from bottom to top.

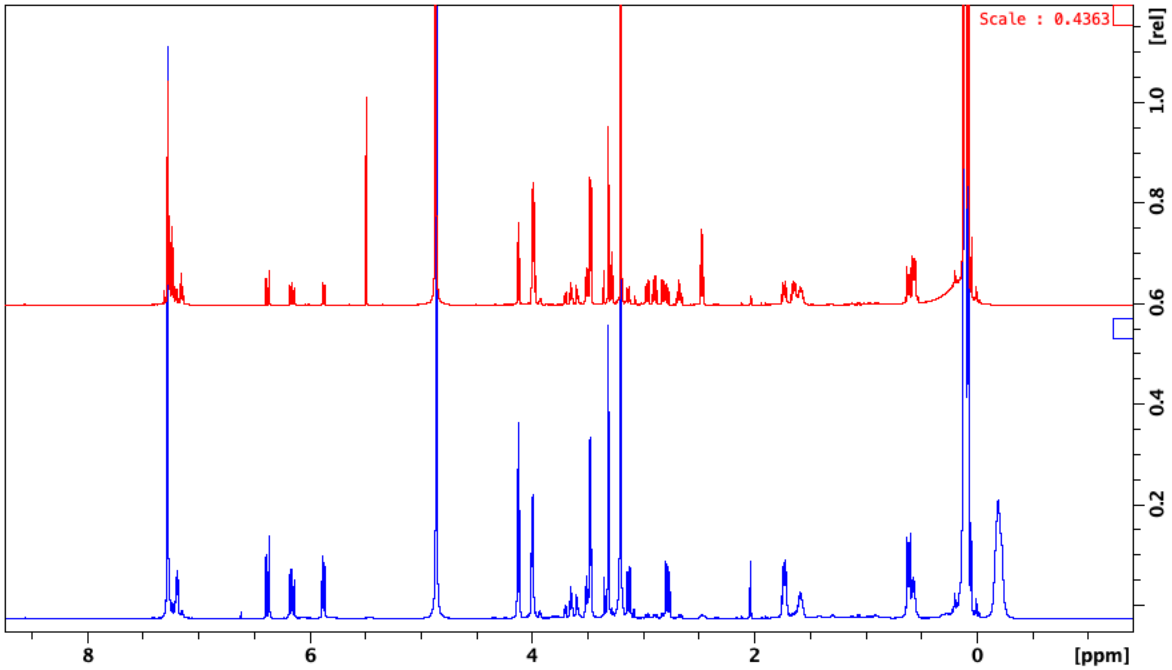

Figure S7.64. ^{1}H NMR stacked plots for reaction monitoring of ChPheIL and **Di10** neat at 1h and 24h from bottom to top.

7.3 Appendix III: Supporting Information for Chapter 5

Table S7.8. Experimental details of the synthesis of benzylated, acryl ascorbic acid - modified silicones.

Sample Name	% ACR to NH_2	mass of P-22 (g)	Volume of 0.02 g/mL Bn_2Asc stock solution
P22-2	2.00%	2.46	2.5
P22-5	5%	0.99	2.5
P22-10	10%	0.49	2.5
P22-15	15%	0.33	2.5
P22-20	20%	0.25	2.5
P22-50	50%	0.10	2.5
P22-75	75%	0.07	2.5
P22-100	100%	0.05	2.5
P21-25	25%	1.04	2.5

Table S7.9 DPPH Assay sample preparation weight

P21-25		**P22-2**		**P22-10**	
AA group concentration (M)	Elastomer Weight (g)	AA group concentration (M)	Elastomer Weight (g)	AA group concentration (M)	Elastomer Weight (g)
0.0212	0.0500	0.0212	0.0500	0.0212	0.0500
0.0106	0.0250	0.0106	0.0250	0.0106	0.0250
0.0042	0.0100	0.0042	0.0100	0.0042	0.0100
0.0021	0.0050	0.0021	0.0050	0.0021	0.0050

Table S7.10 DPPH Assay result summary

	Absorbance at 520 nm (n=3)									
	P22-10		**P22-2**		**P21-25**		**Bn2AA**		AA	
AA Conc. (M)	Average	Std Error	Average	Std Error	Average	Std Error	Average	Std Error	Average	Std Error

0.002	0.343	0.006	0.412	0.005	0.376	0.005	0.494	0.008	0.082	0.001
0.004	0.274	0.004	0.426	0.008	0.312	0.003	0.481	0.010	0.081	0.001
0.011	0.141	0.002	0.482	0.008	0.150	0.003	0.466	0.009	0.081	0.002
0.021	0.094	0.002	0.591	0.013	0.088	0.001	0.426	0.009	0.078	0.000
0.042							0.385	0.006	0.078	0.001

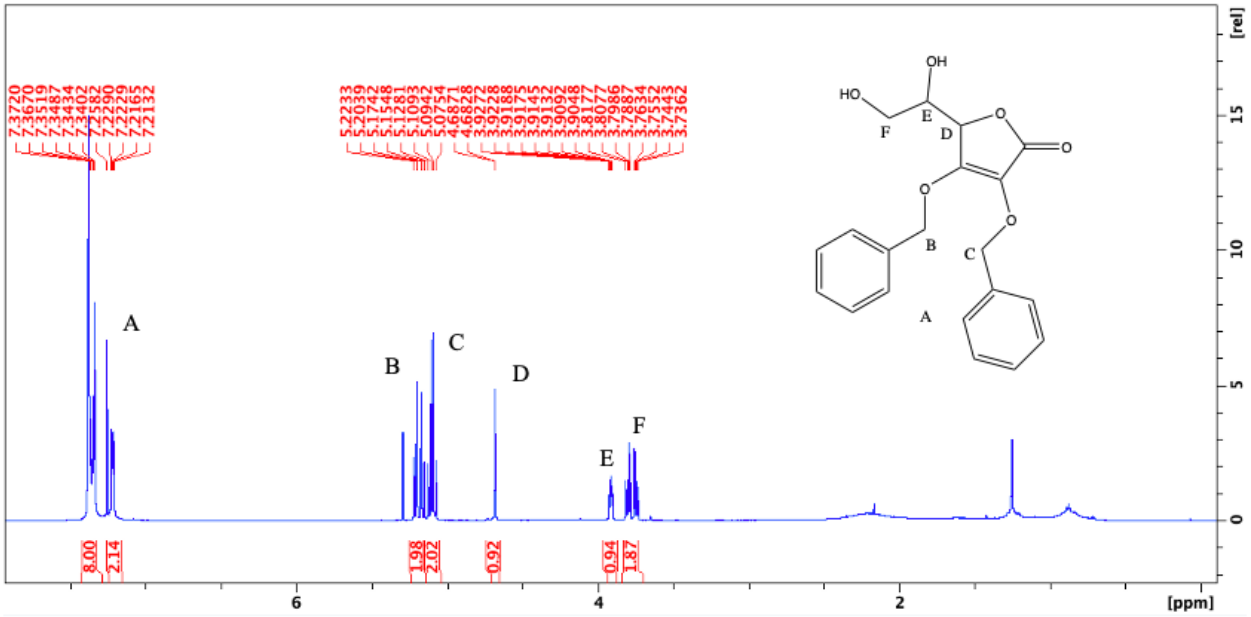

Figure S7.65. ^{1}H NMR spectrum of benzylated ascorbic acid **Bn2AA**.

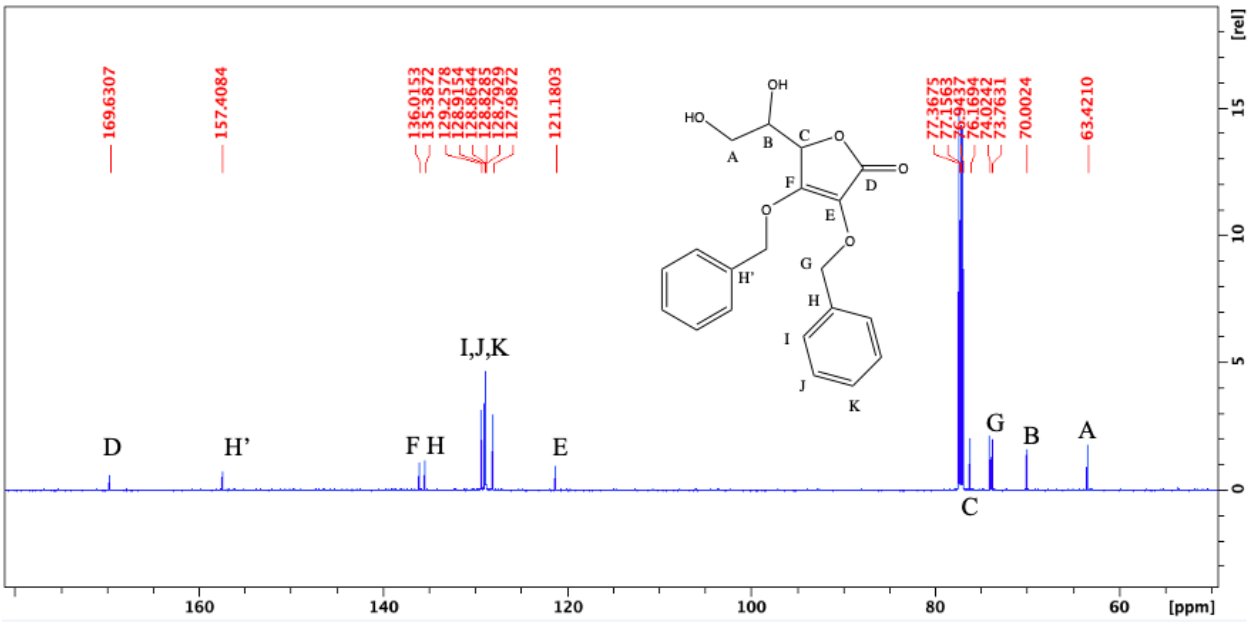

Figure S7.66. ^{13}C NMR spectrum of benzylated ascorbic acid **Bn2AA**.

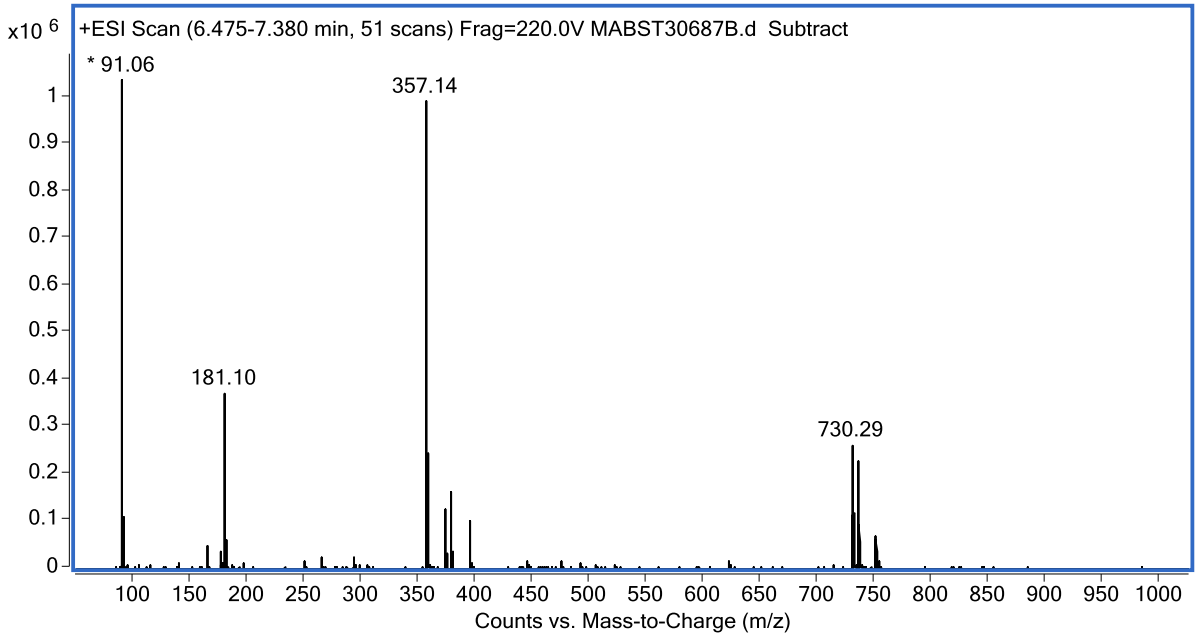

Figure S7.67. Mass spectrum (ESI, Ve+ mode) of benzylated ascorbic acid Bn2AA. Shown [M+H]+, [M+NH4]+, [M+Na]+ and [M+K]+ at m/z 357, 374, 379 and 395 respectively.

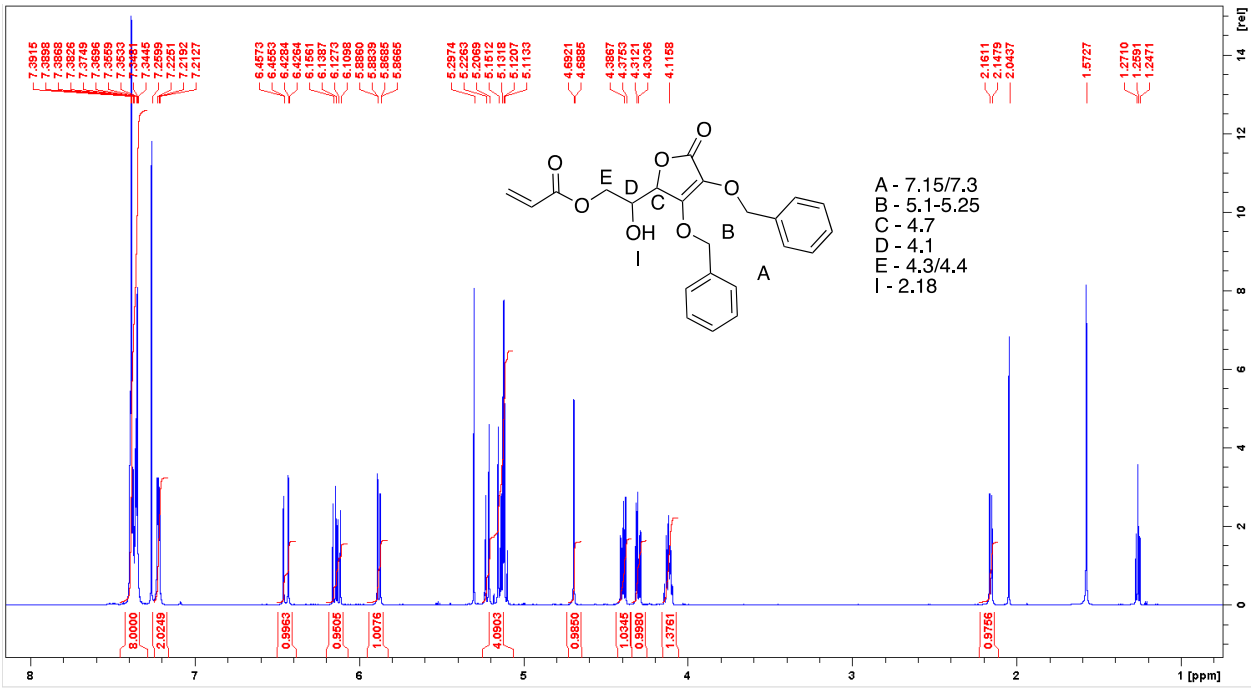

Figure S7.68. ^{1}H NMR of benzylated acryl ascorbic acid **1.**

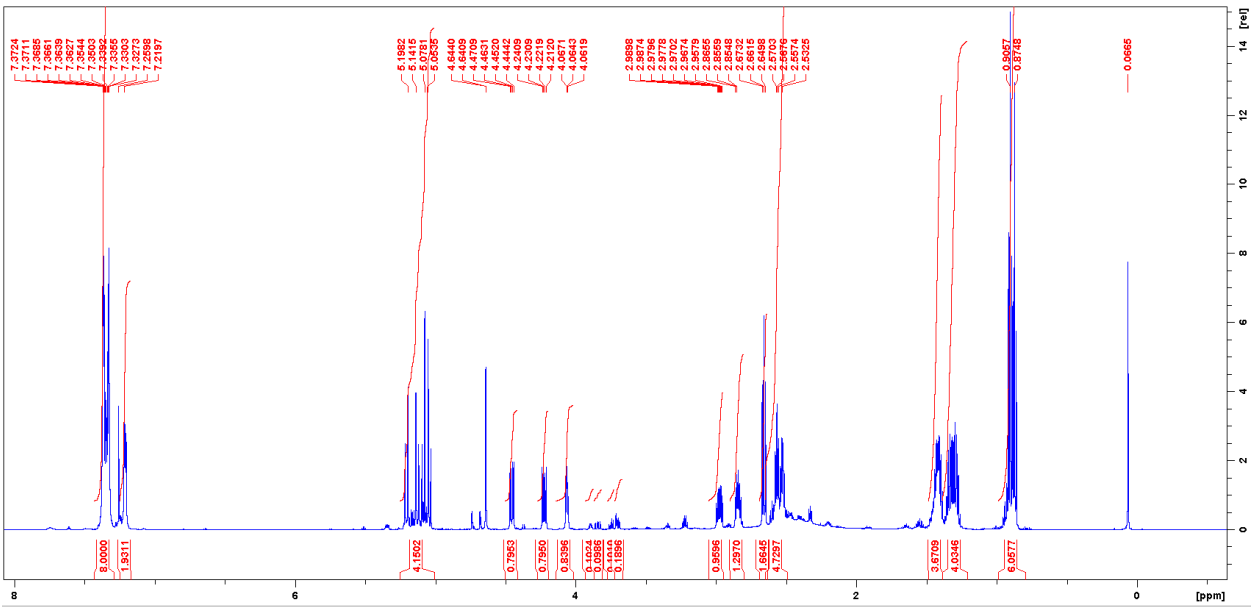

Figure S7.69. Final product of benzylated acryl ascorbic acid with over excess butyl amine, shown two eq butyl amine was reacted with benzylated acryl ascorbic acid **N2AA**.

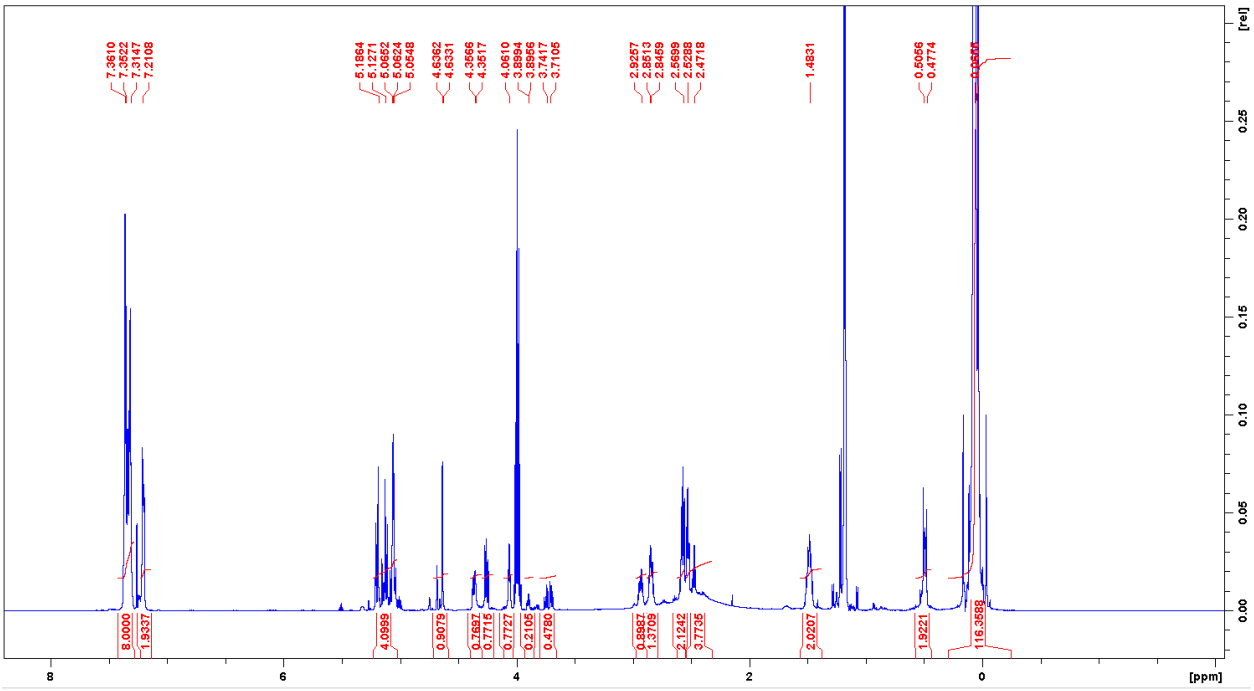

Figure S7.70. Benzylated acryl ascorbic acid **1**-modified **T334** reaction in IPA after overnight.

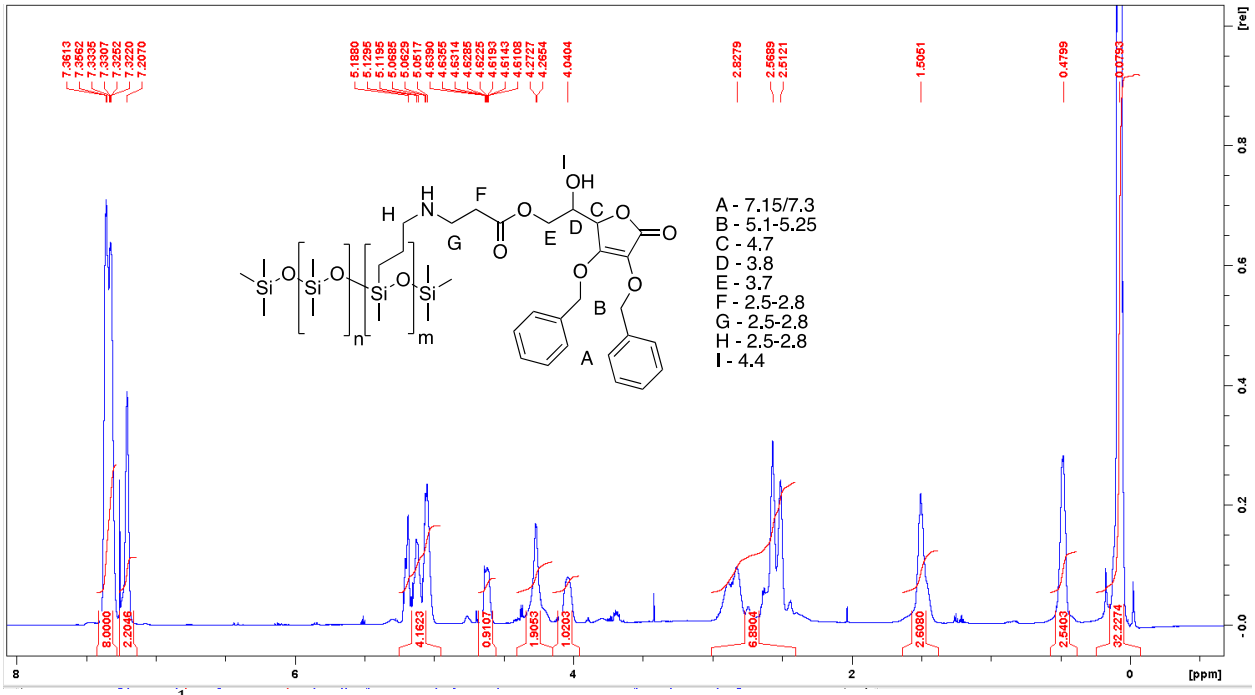

Figure S7.71 ^{1}H NMR of benzylated acryl ascorbic acid modified **P22-100** reaction in $CDCl_3$ after 24h.

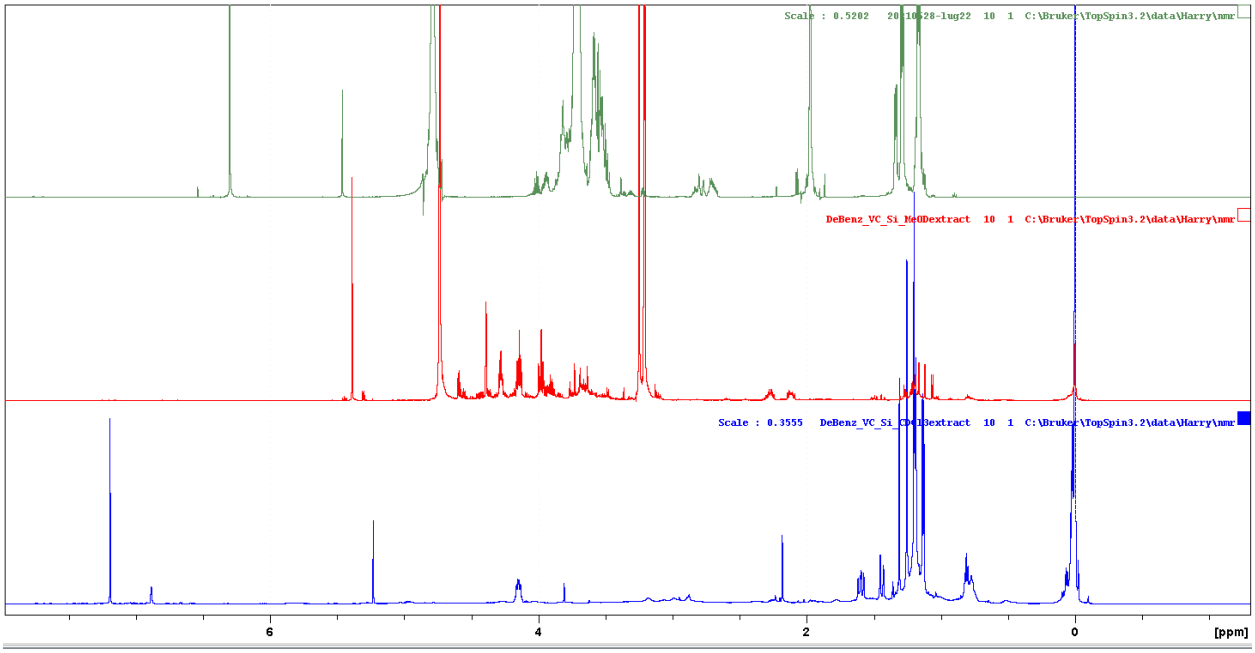

Figure S7.72. Hydrogenation product of **P22-100** from bottom to top to be $CDCl_3$ extract, MeOD-d_4 extract and D_2O extract.

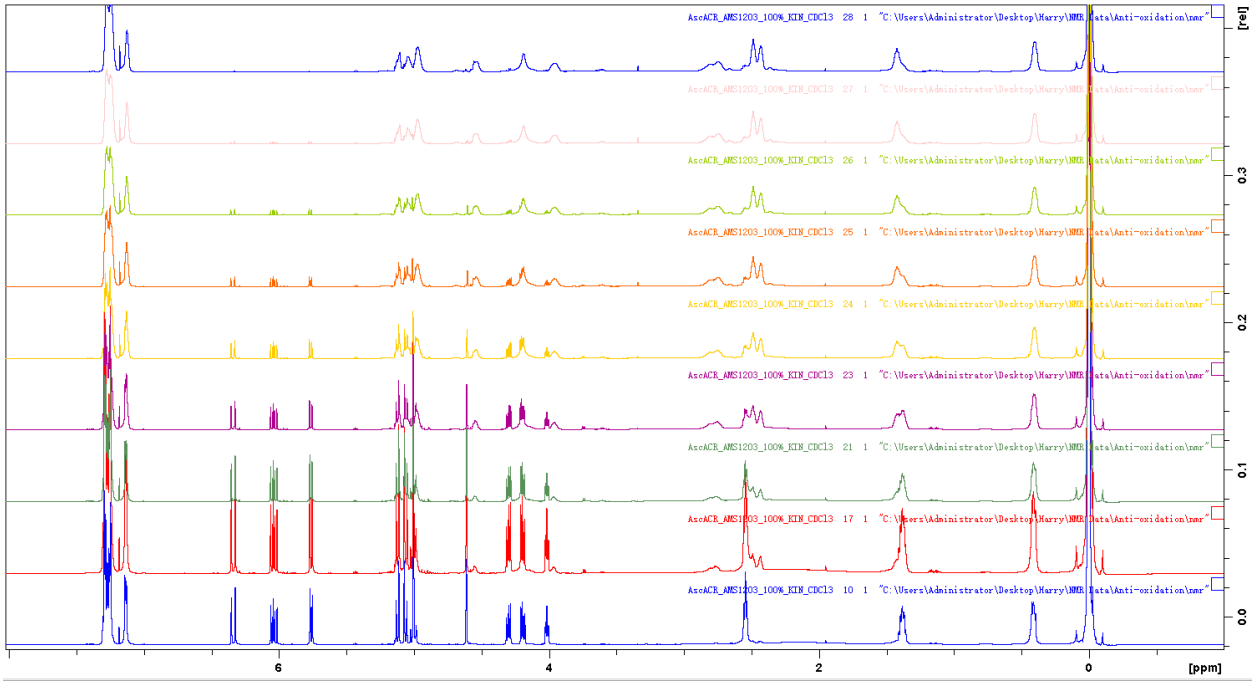

Figure S7.73. Kinetic study of benzylated acryl ascorbic acid **1** reacting with **P22** in $CDCl_3$. Reaction time 0, 15 min, 30 min, 1 h, 2 h, 4 h, 8 h, 12h, 24 h from bottom to the top.

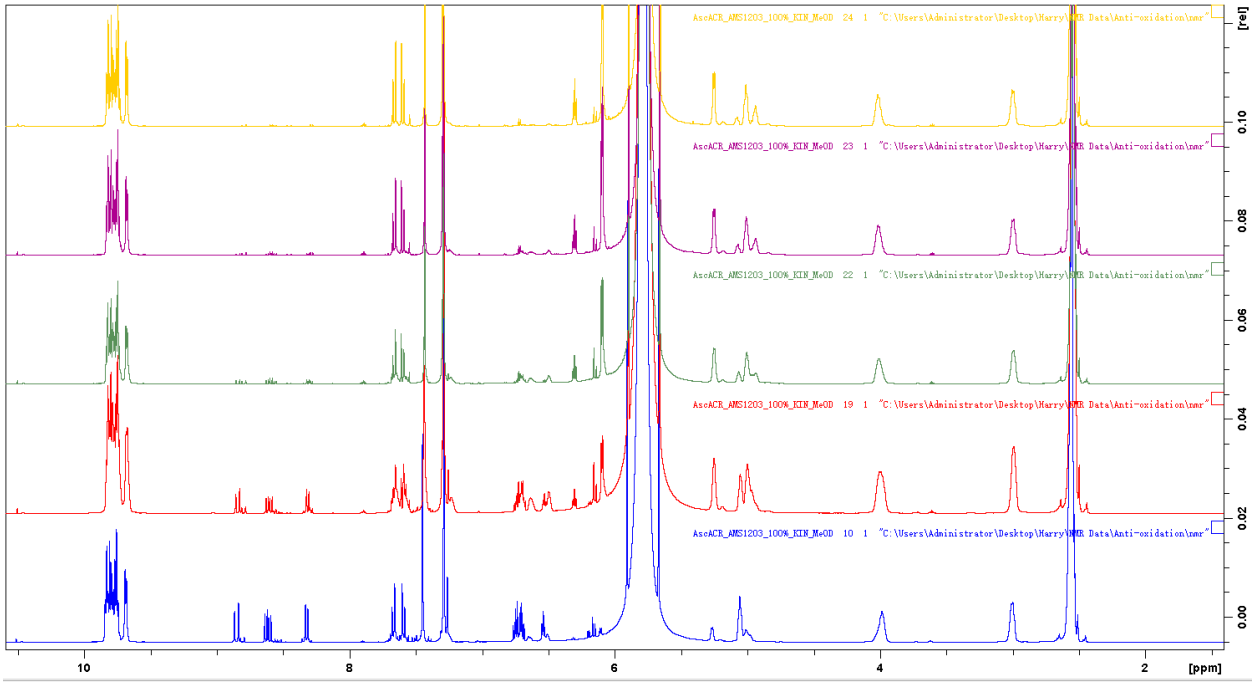

Figure S7.74. Kinetic study of benzylated acryl ascorbic acid **1** reacting with **P22** in MeOD-d_1. Reaction time 0, 15min, 30min, 1h, 2h from bottom to the top.

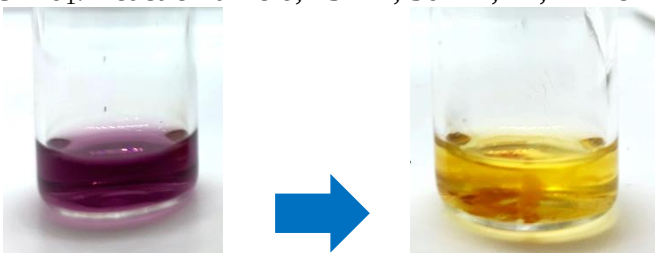

Figure S7.75. Antioxidant testing: hydrogenated product mixture of **P22-100** before and immediately after addition of DPPH.